SYNTHETIC, STRUCTURAL AND ELECTROCHEMICAL STUDIES OF SOME TRANSITION METAL CARBONYL AND NITROSYL COMPLEXES

A thesis submitted to the
UNIVERSITY OF CAPE TOWN
in fulfilment of the requirements for the degree of
DOCTOR OF PHILOSOPHY.

by

ROBERT BERTRAM ENGLISH B.A. (HONS.) (CANTAB.)

Department of Physical Chemistry,
University of Cape Town,
Rondebosch, Cape,
Republic of South Africa.

April, 1977.

A C K N O W L E D G E M E N T S

I am indebted to my supervisors Professors R. J. Haines, L.R. Nassimbeni and D.A. Thornton, for all the help and encouragement they have given me during the progress of the research described in this Thesis.

My thanks are also due to Doctors G. Gafner and M. Thackeray for performing the X-ray diffraction data collection at the C.S.I.R., Pretoria.

I would also like to thank Doctor G. Heath of Stirling University, Scotland, for performing the electrochemical reductions and measuring the polarograms, voltammograms, e.s.r., and infra-red spectra, the results of which are described in Chapter 2.

Finally, I wish to thank Miss Margaret Dreyer for typing the manuscript.

C O N T E N T S

PUBLICATIONS

Parts of this work have been published or are in press as follows:

1. R.B. English, R.J. Haines and C.R. Nolte, J. Chem. Soc. Dalton, 1030 (1975). "Reactions of Metal Carbonyl Derivatives. Part XVIII. Synthesis and Redox Properties of Some Binuclear Derivatives of Iron Bridged by Both Carbonyl and Alkylthio Groups."

2. R.B. English, L.R. Nassimbeni and R.J. Haines, Acta Crystallogr., B32, 3299 (1976). "*cis*-Dibromonitrosyl-bis(triphenylphosphite) Rhodium."

3. J.C.T.R. Burckett-St. Laurent, M.R. Caira, R.B. English, R.J. Haines and L.R. Nassimbeni, J. Chem. Soc. Dalton, in press. "Reactions of Metal Carbonyl Derivatives. Part XX. The Synthesis, Redox Behaviour and Crystal and Molecular Structure of μ-Ethylthiobis-(η-methylcyclopentadienyldicarbonylmanganese) (Mn-Mn) Perchlorate, an Unusual Monothio-Bridged Derivative of Manganese."

PART I.

THE SYNTHESIS, STRUCTURES AND ELECTROCHEMICAL BEHAVIOUR OF SOME DINUCLEAR COMPLEXES OF IRON AND MANGANESE BRIDGED BY AN ALKYLTHIO GROUP.

SUMMARY.

Previous work on dinuclear systems containing Cr, Mn, Fe, Co and Mo is reviewed, and the relevance of such systems as models for the enzyme, ferredoxin, is discussed in terms of their redox behaviour. A theory of bonding in such systems is advanced and examined in the light of X-ray crystallographic studies and Mössbauer spectra. The synthesis of the monocations $[\{Fe(cp)(CO)_2\}_2(SEt)]^+$ and $[Fe_2(cp)_2(CO)_3(SEt)]^+$ from the mononuclear species $[Fe(cp)(CO)_2(SEt)]$ is described and the reversible redox behaviour of $[Fe_2(cp)_2(CO)_3(SEt)]^+$ is discussed. The crystal and molecular structures of these three species, determined by the author, are described and compared. It is shown that conformational isomerism is possible in $[\{Fe(cp)(CO)_2\}_2(SEt)]^+$ and its molecular structure is compared with those of closely related dinuclear iron complexes. An attempt to synthesize a dinuclear manganese complex $[\{Mn(Mecp)(CO)(SEt)\}_2]$ was shown by an X-ray crystallographic analysis to result in the unusual cation $[\{Mn(Mecp)(CO)_2\}_2(SEt)]^+$ in which the two manganese atoms are joined both through a sulphur bridge and a metal-metal bond. The electrochemical behaviour of this species is described. Finally, the synthesis of the mixed iron-manganese complex $[Fe(cp)(CO)_2(SEt)(CO)_2(Mecp)Mn]$ is described. The relative instability of this complex, however, has so far precluded examination of its redox behaviour.

CHAPTER 1

THE SYNTHESIS AND REACTIONS OF SOME DINUCLEAR IRON COMPLEXES CONTAINING A BRIDGING ETHYLTHIO GROUP.

1.1 Introduction.

In recent years, a very great deal of effort has gone into research on those remarkably efficient catalysts, present in all living species, known as enzymes. They are among the smallest of proteins and take part in a plethora of biological processes, of which two important examples are the reduction of atmospheric nitrogen to give ammonia (in which the enzyme nitrogenase plays an essential role)[1.1] and electron-transfer reactions forming part of the mechanisms of nitrogen fixation and photosynthesis (for which ferredoxins are responsible)[1.2]. A common characteristic of enzymes is the presence of one or more transition metal atoms, exhibiting an unusual coordination number and/or a distorted ligand environment. Thus rubredoxin has been shown to contain an iron atom tetrahedrally coordinated by four sulphur atoms; the bond lengths Fe - S vary between 1.97(5) and 2.39(5) Å and the angles S-Fe-S vary between 101° and 118° [1.3]. One enzyme active for nitrogen fixation contains one Mo atom and forty Fe atoms in unknown coordination geometries[1.4].

Two aspects of metalloenzyme research connected with the work presented in this section are: the determination of their structure by X-ray crystallography - a technique which has grown in importance as the level of sophistication of high-speed computers has increased - and the synthesizing of low-molecular weight molecules which mimic, albeit at a far lower efficiency, the catalytic activity of these complex proteins.

Recently, the biological, structural and electronic properties of metalloproteins (including enzymes) which contain iron and sulphur, have been reviewed in detail[1.5 - 1.8]. X-ray structure determinations have been published for several such proteins[1.9-1.11]. Lyle, H. Jensen and co-workers have reported the structure, at 2.0 Å resolution, of the ferredoxin isolated from *Peptococcus aerogines*[1.11], with a total of 390 atoms, and have confirmed the presence in this molecule of two Fe_4S_4 clusters. These clusters appear to be identical, each containing 4 iron and 4 inorganic sulphur atoms with 4 cysteinic sulphur atoms coordinated to the Fe atoms. The clusters, which are separated by 12 Å, are in the form of distorted cubes with Fe and S atoms at alternate corners. The distortion is such that the clusters may be thought of as comprising two interpenetrating tetrahedra of Fe atoms and S atoms, with a common centroid (Figure 1.1)

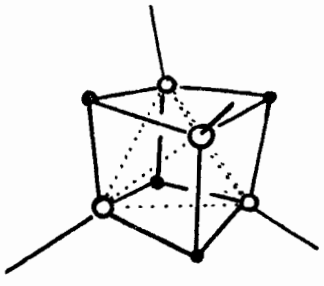

○ = Fe atoms ● = S atoms.

FIGURE 1.1

The property of ferredoxin enzymes which is germane to the subject of this Section is the ease with which they are reduced and/or oxidised, which enables them to function as electron transfer agents in some important biological reactions. Thus, bacterial ferredoxins, found in anaerobes, which contain two Fe_4S_4 clusters and have molecular

weights of about 6,000, play a key role in nitrogen fixation and fermentation metabolism. The enzyme isolated from *P.aerogenes* is a member of this class.

Although the exact nature of the reduced and oxidized forms of ferredoxins and the mechanism by which electrons are taken up or released is not clear, it is reasonable to assume that most of the activity of these enzymes is associated with their possession of metal atom clusters.

A large number of complexes which incorporate an $[L_nM_4X_4]$ (M = metal, X = bridging ligand and L = terminal ligand) nucleus with a cubane-like structure are known[1.12]. The diversity of M, X and Y components is considerable: two very dissimilar examples are $[(Et_3As)CuI]_4$ [1.13] and $[(CO)_2(NO)Mo(OH)]_4$ [1.14]. However, the closest analogue to the active site in the ferredoxin from *P.aerogenes* yet reported is the iron-sulphur complex $[(SCH_2Ph)_4Fe_4(\mu_3\text{-}S)_4]^{2-}$ [1.12]. Electronic properties of this tetrameric dianion have been partially characterized by measurement of pmr, Mössbauer, photoelectron and electronic spectra and comparison of these with corresponding properties of ferredoxin implies that the oxidation levels of the anionic tetramer and the oxidized form of ferredoxin are equivalent. The tetramer possesses the one-electron redox capacity associated with the Fe_4 centres in ferredoxin. In acetonitrile solution, polarographic and cyclic voltammetric studies reveal that the complex undergoes the reversible one-electron transfer process

$$[(SCH_2Ph)_4Fe_4(\mu_3\text{-}S)_4]^{3-} \rightleftharpoons [(SCH_2Ph)_4Fe_4(\mu_3\text{-}S)_4]^{2-} + e^-, \quad E_{\frac{1}{2}} = -1.19V.$$

This half-wave potential is somewhat more cathodic than that observed

for ferredoxin$_{(reduced)}$ $\rightleftharpoons$ ferredoxin$_{(oxidized)}$ + e^- ($E_{\frac{1}{2}}$ = -0.57V for *Cl. pasteurianum* ferredoxin)[1.15]. The bond length and angles in the Fe_4S_4 clusters are very similar[1.12] (Figure 1.2):

The Fe_4S_4 clusters in a) ferredoxin, and b) $[(SCH_2Ph)_4Fe_4\ (\mu_3\text{-}S)_4]^{3-}$:

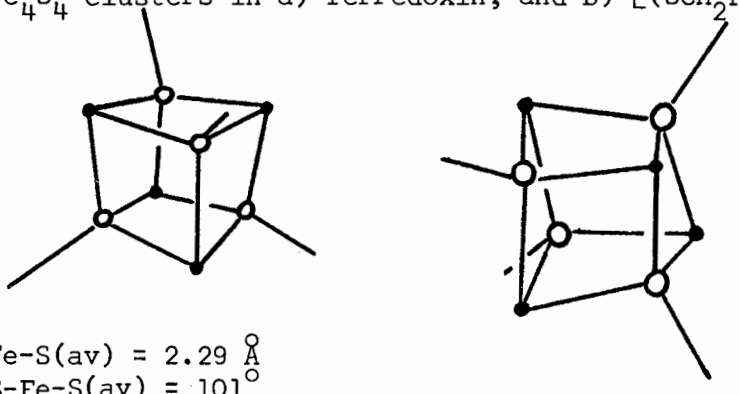

a) Fe-S(av) = 2.29 Å
S-Fe-S(av) = 101°
Fe-S-Fe(av) = 77°

b) Fe-S(av) = 2.285 Å
S-Fe-S(av) = 104.1°
Fe-S-Fe(av) = 83.8°

FIGURE 1.2

With the recognition that the Fe_4S_4 cluster in some bacterial ferredoxins can be thought of as comprising two semi-(Fe_4S_4) moieties,

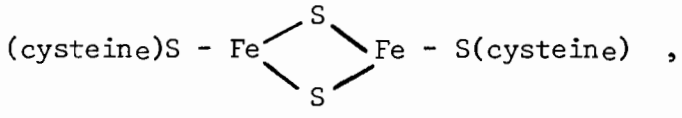

a number of complexes have been synthesized in which the essential feature is two metal atoms bridged by one or two ligands. A metal-metal bond may be present. The study of the reactions and electrochemistry of such models for ferredoxin has proved most fruitful, as many of these species exhibit reversible redox behaviour. In a considerable proportion of the model complexes studied, one or more carbonyl groups have been bound to the metal atoms. The presence of a CO group provides structural information about the complex in two ways:

1. Since the infra-red band ν(C-O) occurs in a region of the i.r. spectrum (2125 - 1650 cm^{-1})[1.16] in which other ligand vibrations do

not occur, the position and intensities of the bands observed for a complex may be determined with some accuracy and from the number of bands present, and their pattern of intensities, *ad hoc* deductions may be made about the symmetry of the complex and therefore its structure.

2. The frequency of the band ν(C-O) is extremely sensitive to the degree of population of the π^*(CO) orbital; this, in turn, is affected by the amount of back-bonding from the d-orbitals of the metal atom to which the CO group is bound. The degree of metal-to-carbon back-bonding is influenced by the electron density on the metal atom; and so the frequency of the ν(C-O) band is a measure of the charge density at the metal atom[1.16]. In short, the carbonyl ligand is a useful structural probe in these species. The related nitrosyl ligand, (NO), has also been widely employed.

As will be discussed subsequently, the nature of the bridging ligand plays an important part in the redox behaviour of dinuclear bridged species. Ligands such as RS and R_2P (R = alkyl or aryl groups) which can bridge a wide range of metal-metal distances give rise to complexes

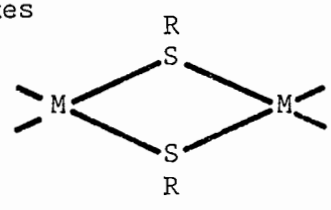

and

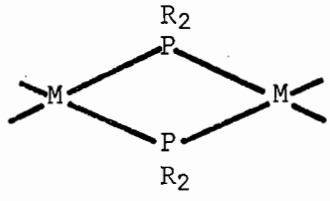

which show very similar redox behaviour to ferredoxins, while the complex

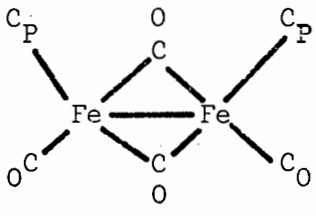

containing relatively inflexible bridging carbonyls does not exhibit reversible redox behaviour[1.17].

1.2 A Review of Dinuclear Complexes of the Type

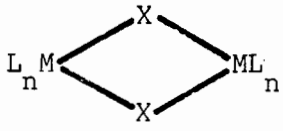

(M = metal atom, L = terminal ligand, X = bridging ligand).

The synthesis, structures and redox properties of dinuclear complexes of the above type have received considerable attention in the last decade. Dessy and co-workers[1.18-1.20], have published electrochemical, infra-red and Mössbauer spectral data for a large number of complexes and, more recently, the structures of several compounds of the above type have been determined. Although it would be outside the scope of this thesis to discuss fully the findings described in the above references, their main burden may be briefly summarized.

1.2.1 Electrochemical studies on

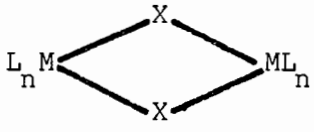 complexes.

Dessy *et al.* report electrochemical data for 22 complexes of the above type[1.18]. All have been shown, by polarography and cyclic voltammetry, to undergo reversible one-electron reduction and oxidation. In particular, the species $[(CO)_4Cr(PMe_2)]_2$, $[(cp)Mo(SMe)_2]_2$ and $[(CO)_3Mn(SPh)]_2$ yield the stable one-electron reduced and oxidized species $[(CO)_4Cr(PMe_2)]_2^-$ (which is formed by reacting the dianion

$[(CO)_4Cr(PMe_2)]_2^{2-}$, produced polarographically, with the neutral complex); $[(cp)Mo(SMe)_2]_2^+$ and $[(CO)_3Mn(SPh)]_2^-$. However, the most extensive redox chemistry is that of iron. Dessy reports the equilibrium

$$[(cp)Fe(CO)(PPh_2)]_2 \underset{+e^-}{\overset{-e^-}{\rightleftharpoons}} [(cp)Fe(CO)(PPh_2)]_2^+ \underset{+e^-}{\overset{-e^-}{\rightleftharpoons}} [(cp)Fe(CO)(PPh_2)]_2^{2+}$$

while both $[(CO)_3Fe(PMe_2)]_2$ and $[(NO)_2Fe(PPh_2)]_2$ undergo two reversible one-electron reductions to yield first radial anions and then dianions. $[(cp)Fe(CO)(SR)]_2$ (R = alkyl or aryl group) can be oxidized electrochemically to give both a radial cation and dication; these oxidations may also be effected by using chemical oxidizing agents such as $NOPF_6$ or Br_2 [1.21]. The manganese complexes $[(cp)Mn(NO)(SR)]_2$ (R = alkyl group) have been shown by voltammetry to undergo oxidation to the dication in two one-electron steps[1.22].

In the case of radical anions and cations, electron spin resonance techniques have been employed to gain information about the nature of the orbital occupied by the unpaired electron[1.18]. For instance, e.s.r. spectra of $[(CO)_3Mn(SPh)_2]^-$ [1.18] and $[(cp)Mn(NO)(SR)]^+$ [1.22] show eleven equally-spaced lines, confirming the presence in both species of two equivalent manganese atoms (^{53}Mn, $I = \frac{5}{2}$), and typical of interaction of a delocalized lone electron with two such nuclei.

Hydes, McCleverty and Orchard[1.22] point out that the half-wave potential, $E_{\frac{1}{2}}$, for the reaction

$$[compound]^+ \rightarrow [compound]^{2+} + e^-$$

is generally higher than that for oxidation of the neutral species to

TABLE 1.1

a) Oxidation couples

$$[(L)_nMX]_2 \rightarrow [(L)_nMX]_2^{+} + e^-$$

$$[(L)_nMX]_2^{+} \rightarrow [(L)_nMX]_2^{2+} + e^-$$

Compound	$E_{\frac{1}{2}}$(V)	Couple
$[(cp)Mo(SMe)_2]_2$	+0.6	0 → +1
$[(cp)Mo(SMe)_2]_2$	+3.1	+1 → +2
$[(cp)Fe(CO)(PPh_2)]_2$	+0.2	0 → +1
$[(cp)Fe(CO)(PPh_2)]_2$	+0.5	+1 → +2
cis$[(cp)Fe(CO)(SR)]_2$ when		
R = CH_3	+0.4	0 → +1
R = Bu^t	+0.24	0 → +1
R = Ph	+0.25	0 → +1
$[(cp)Mn(NO)(SR)]_2$ when		
R = Bu^t	-0.18	0 → +1
R = Bu^t	+0.55	+1 → +2
R = Pr^i	-0.33	0 → +1
R = Pr^i	+0.43	+1 +2

b) Reduction couples

$$[(L)_nMX]_2 + e^- \rightarrow [(L)_nMX]_2^-$$

$$[(L)_nMX]_2^- + e^- \rightarrow [(L)_nMX]_2^{2-}$$

Compound	$E_{\frac{1}{2}}$(V)	Couple
$[(CO)_4Cr(PMe_2)]_2$	+1.85	0 → -1
$[(CO)_3Mn(SPh)]_2$	+1.6	0 → -1
$[(CO)_3Mn(SPh)]_2$	+2.5	-1 → -2
$[(CO)_3Fe(PMe_2)]_2$	+2.1	0 → -1
$[(NO)_2Fe(PPh_2)]_2$	+1.7	0 → -1

the mono-cation. Similarly, inspection of half-wave potentials published by Dessy *et al.* show that reduction of a mono-anionic to a dianionic species is associated with a higher half-wave potential than the first reduction, from a neutral to a mono-anionic complex. $E_{\frac{1}{2}}$ values for a number of oxidations and reductions, from Dessy *et al.*[1.18] and Hydes *et al.*[1.22] are set out in Table 1.1. The ease of reduction of $[(CO)_3Fe(PR_2)]_2$ to the mono-anion may be contrasted with the relative difficulty of oxidizing the mono cations $[(cp)Mn(NO)(SR)]_2^+$ to $[(cp)Mn(NO)(SR)]_2^{2+}$. Another trend which may be observed in published $E_{\frac{1}{2}}$ values is that reduction of a neutral $[(L)_nMX]_2$ species to a mono-anion is usually associated with a higher change in free energy ($E_{\frac{1}{2}}$ values are typically around +1.5V - + 2.5V) than that observed for oxidation of neutral $[(L)_nMX]_2$ complexes to mono cations (for which $E_{\frac{1}{2}}$ values are usually around +0.2V - + 0.4V). (Note - all $E_{\frac{1}{2}}$ values are based on the European convention).

1.2.2 Infra-red and Mössbauer studies on complexes of the type $[(L)_nMX]_2$

These have been limited to those derivatives containing carbonyl or nitrosyl groups, as mentioned previously.

1.2.2.1 Symmetry and Structural Aspects.

The position, number and intensities of the bands observed in the carbonyl-stretching region of the infra-red spectrum provide, as pointed out before, a useful basis for deduction about the overall molecular symmetry and structure in a complex of the type

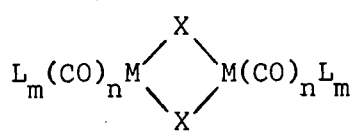

X may also be CO). Thus, terminal carbonyl groups are characterized by sharp bands in the region 1850 - 2125 cm^{-1}, while bands due to bridging carbonyl groups are found in the range 1900 - 1650 cm^{-1}. In addition, in a complex such as $[(L)_m(CO)_nMX]_2$ the terminal carbonyl groups form a coupled vibrating system, and the symmetry of a molecule may be deduced from the relative intensities of the symmetric and antisymmetric ν(C-O) bands. For instance, since only one C-O stretching band is observed in the infra-red spectrum of *cis*-$[Fe(cp)(CO)(SPh)]_2$[1.23] it may be deduced that either the symmetric or antisymmetric ν(C-O) vibration is infra-red inactive. For the symmetric mode to be inactive the two carbonyl ligands must be parallel and oppositely oriented so that the resultant change in dipole moment due to their vibration is zero. This is clearly not possible in *cis*-$[Fe(cp)(CO)(SPh)]_2$ and so the antisymmetric band is infra-red inactive. This requires the carbonyls to be oriented the same way with the C-O vectors parallel, as was actually found in the structural determination of this complex[1.24]. *Cis*$[Fe(cp)(CO)(CS)]_2$ exhibits two terminal CO bands in its infra-red spectrum while the corresponding *trans* isomer only has one[1.73]. However, deductions concerning the structure of such compounds are not generally as straightforward as in these examples, as molecular point symmetry generally tends to be low. Nevertheless, taken in conjunction with other techniques, infra-red spectroscopy provides a valuable and convenient tool for assigning tentative structures to complexes.

1.2.2.2 Electronic Aspects.

As pointed out before, the stretching frequency of the CO ligand is very sensitive to the charge density on the metal atom, overlap occurring of occupied metal d-orbitals of the correct symmetry

with the π-antibonding orbitals of the CO ligand.

Dessy and Wieczorek[1.19] have analysed the infra-red spectra of a series of octahedral systems of the types $LM(CO)_5$ (L = py, quinoline; M = Cr, Mo and W), $L_2M(CO)_4$ (L_2 = en, dipy, and $(py)_2$; M = Cr, Mo and W), $[LM(CO)_4]_2$ (L = $As(CH_3)_2$, $P(CH_3)_2$; M = Cr, Mo and W) and $[LFe(CO)_3]_2$ (L = SCH_3, $P(CH_3)_2$ and $As(CH_3)_2$) before and after electrochemical reduction. They calculated force constants using the Cotton-Kraihanzel force field [1.25, 1.26] and have discussed the results in terms of σ- and π-bonding. As expected, reduction results in a significant shift of the ν(C-O) bands to lower frequencies. The magnitudes of the shifts depend very much on the nature of the complex and the particular vibrational mode associated with the band, and can provide a means of assigning the bands to particular modes of CO vibration. The results of this work confirm that the added electron enters an orbital which is intimately associated with the metal atom or atoms. In addition, Dessy and Wieczorek deduce from their observations on $[(L)Fe(CO)_3]_2$ that this orbital must be a metal-metal antibonding orbital of σ-symmetry. This aspect of $[(L)_nMX]_2$ structure is discussed further in Section 1.2.3.

1.2.2.3 Mössbauer Studies.

A Mössbauer spectroscopic study[1.27] of the sulphido-bridged species $[Fe(cp)(CO)(SR)]_2^n$ (n = 0, +1 or +2) has revealed that the iron atoms are equivalent down to a temperature of 4K. On this basis the electrons involved in the one- and two-electron oxidation of $[Fe(cp)(CO)(SR)]_2$ must originate from a molecular orbital localised over both metal atoms. In addition, Dessy and co-workers have shown

using Mössbauer spectroscopy that transmission of charge, occurring on one- and two-electron reduction of a series of mono-nuclear iron carbonyl complexes, involves a molecular orbital, associated with the iron atom, of σ symmetry[1.19]. Very recently, a Mössbauer study[1.28] has been carried out on $[\{Fe(cp)(CO)\}_2\{(Ph_2P)_2R\}]^+$, I,

I: 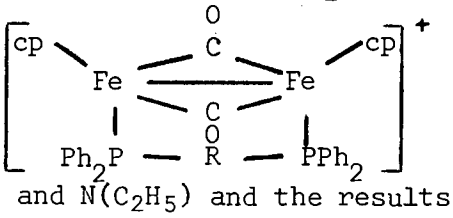

for R = CH_2, C_2H_4 and $N(C_2H_5)$ and the results show that, although the iron atoms are equivalent at ambient temperatures, at 4K a splitting of the doublet in the Mössbauer spectrum occurs, indicating that they have become magnetically non-equivalent. An X-ray structural analysis[1.29] of $[\{Fe(cp)(CO)\}_2(Ph_2P)_2CH_2]SbF_6$ at ambient temperatures reveals that the iron atoms are crystallographically equivalent, being related by a plane of symmetry. This unusual observation, that the Fe atoms are magnetically non-equivalent at low temperatures but crystallographically equivalent at ambient temperatures, may be due to localization of the unpaired electron on one Fe atom at 4K. At room temperatures such an effect would be unlikely, the electron being shared equally by the two atoms.

1.2.3 The Electronic and Molecular Structures of Complexes of the type

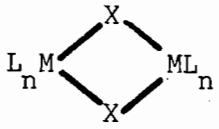

The relative ordering of the molecular orbitals in dinuclear complexes $[(L)_nMX]_2$, and the nature of the highest occupied, and lowest unoccupied, molecular orbitals, have been the subject of much debate. Dessy *et al*[1.18] remark that the radical anion $[(CO)_4Cr(PMe_2)]_2^-$ gives a well-defined e.s.r. spectrum indicating complete delocalization of the unpaired electron over the $[Cr_2P_2]$ system. This observation implies that the lowest unoccupied molecular orbital (LUMO) in $[(CO)_4Cr(PMe_2)]_2$ is delocalized over the two metal atoms. In contrast, no delocailzation of the lone electron in $[(cp)Fe(CO)(PPh_2)]_2^+$ is apparent, the e.s.r. spectrum showing a featureless resonance signal; this suggests that the iron atoms are non-equivalent in this complex, and that the highest occupied molecular orbital (HOMO) in $[(cp)Fe(CO)(PPh_2)]_2$ is localized on the metal atoms. However, $[(CO)_3Fe(PMe_2)]_2^-$ shows some unresolved hyperfine splitting in its e.s.r. spectrum, indicating partial delocalization of the lone electron[1.18].

Metal-metal interactions play an important role in determining the structure of some complexes of the type $[(L)_nMX]_2$. Dahl , de Gil and Feltham have reviewed this subject in some detail[1.30]. For instance, structural studies have confirmed the deduction, based on the noble gas formalism and the magnetic properties of the complexes, that one or two-electron metal-metal bonds must be present in $[(cp)Fe(CO)_2]_2$[1.31], [1.32], $[(cp)Fe(CO)(SR)]^+$ [1.33] and

$[(cp)Fe(CO)(PR_2)]_2^{2+}$ [1.34]. The nature of the metal-metal bond is open to speculation. Two schools of thought exist at the present time: one ascribes π-symmetry to it[1.35] and the other considers it as having σ-symmetry[1.36]. It has been shown that the metal-metal bond lengths in the two iron complexes cited above are extremely sensitive to reduction. Thus, one-electron reduction of $[(cp)Fe(CO)(PPh_2)]_2^{2+}$ to the mono-cation and neutral complex, results in an increase in the Fe-Fe distance from 2.764 Å to 3.14 Å, to 3.498 Å [1.34]. This behaviour is also observed for $[(cp)Fe(CO)(SR)]_2^+$ [1.33]. These observations confirm what might intuitively have been deduced; that is, that the metal-metal interaction is higher in energy than any metal-ligand bonds, and that oxidation of a species such as $[(cp)Fe(CO)(PPh_2)]_2$ involves removal of electrons from an orbital, the HOMO, which is antibonding with respect to the two Fe atoms. However, in the situation where a formal two-electron metal-metal bond already exists in a complex, removal of an electron has not been observed to affect the bond length. Thus one-electron oxidation of the metal-metal bonded species $[\{(cp)Fe(CO)\}_2(dppm)]$ to $[\{(cp)Fe(CO)\}_2(dppm)]^+$ [1.29] is accompanied by a slight increase in the metal-metal bond length, from 2.513 to 2.577 Å. A similar small increase is observed on oxidation of $[(cp)Mo(SMe)_2]_2$ to the mono-cation[1.37]. The observed essential invariance of the metal-metal bond length, towards oxidation, in these complexes, may be ascribed to the HOMO being primarily non-bonding with respect to the two metal atoms. However, a more plausible explanation which is still consistent with the hypothesis that the electron is being removed from an orbital which is anti-bonding with respect to the metal atoms, resulting in a metal-metal bond order

greater than one, is that steric constraints prevent the metal atoms from moving closer together. Thus, a contraction in the Mo-Mo bond length, which is 2.603 Å in the neutral species $[(cp)Mo(SMe)_2]_2$, would result in the Mo-S-Mo bond angles decreasing still further from their already acute value of 64°.

As mentioned previously, two theoretical treatments of the molecular orbital scheme in $[(L)_nMX]_2$ have been published. Their salient points may be summarized as follows:

Mason and Mingos[1.35], basing their treatment on symmetry considerations, deduce that the HOMO in, for instance, $[(cp)Fe(CO)(PPh_2)]_2$, should be of π-symmetry, and antibonding with respect to the metal atoms. The three metal atom hybrid orbitals which transform in the same sense (Figure 1.3) as d_z2, d_{xz} and d_{yz} will form the most stable bridge

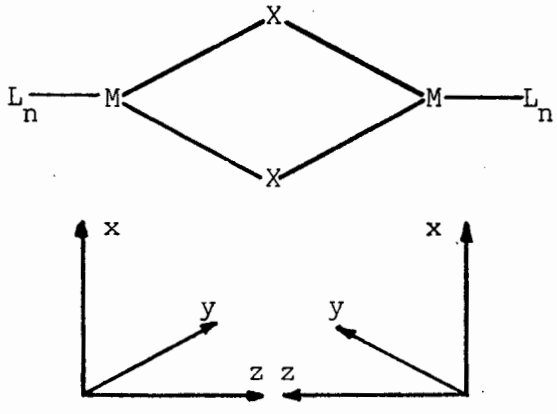

FIGURE 1.3

The coordinate system on which the molecular orbitals for $[(L)_nMX]_2$, depicted in Figure 1.4, are based.

molecular orbitals. The monodentate ligands, L_n, will form n stable molecular orbitals with the metal orbitals and the remaining [9-(n+3)] metal orbitals can be regarded as non-bonding. The d_{yz} orbital is orthogonal to the M_2X_2 plane and can form bonding and antibonding combinations with the ligand orbitals perpendicular to the M_2X_2 plane. An ordering scheme for the molecular orbitals in $[(L)_nMX]_2$ is set out in Figure 1.4 below.

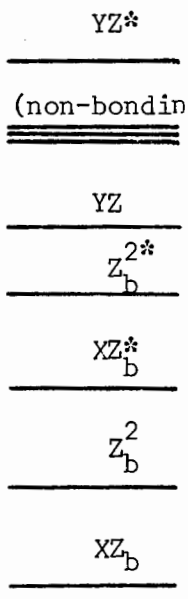

Schematic molecular orbital scheme for $[(L)_nMX]_2$ complexes :
$Z^2 = 2^{-\frac{1}{2}}[d_z2(1)+d_z2(2)]$; $Z^{2*} = 2^{-\frac{1}{2}}[d_z2(1)-d_z2(2)]$ etc.,
$Z_b^2 = Z^2$ + appropriate combination of bridging ligand orbitals etc.

FIGURE 1.4

The bis(alkylthio)-bridged complex, $[Fe(cp)(CO(SPh)]_2$, is a convenient example for treatment using the scheme of Mason and Mingos. The electronic configuration of the complex, according to them, will be $(XZ_b)^2(Z_b^2)^2(XZ_b^*)^2(Z_b^{2*})^2(YZ_b)^2$ $(\text{nonbonding})^8(YZ^*)^2$. The net metal-metal interaction, comprising the Z_b^2 and YZ molecular orbitals

correspondsto a bond order of zero. Removal of electrons from the YZ* orbital will result in a bond order of 0.5 (a configuration $..(YZ_b)^2(\text{nonbonding})^8(YZ^*)^1$) and 1.0 (a configuration $...(YZ_b)^2(\text{nonbonding})^8(YZ^*)^0$) for the mono- and dication, respectively. As mentioned previously, a corresponding contraction in the Fe-Fe distance is observed on oxidation of $[(cp)Fe(CO)(SPh)]_2$.

This treatment is, therefore, consistent with observed changes in structure on oxidation of $[(L)_nM(X)]_2$ species. However, as the authors themselves point out, it is at best only a very qualitative theory based on *ex post-facto* conclusions and the molecular orbital ordering scheme is somewhat arbitrary.

Teo, Hall, Fenske and Dahl[1.36] have published the results of some parameter-free MO calculations carried out on the complexes $[(CO)_4Cr(PR_2)]_2^n$ (n = 0,-1,-2), and $[(CO)_4Mn(PR_2)]_2^n$ (n = 0,+1,+2). The calculations clearly support the σ- rather than the π- type of metal-metal bond and the distinction between these two bonding models is made rather simple by the octahedral geometry displayed by the two metal atoms. Thus the σ- and π-molecular orbitals separate into two irreducible representations, a and b, based on the (reasonable) assumption of D_{2h} molecular point symmetry. Figure 1.5 shows the calculated molecular orbital ordering for the complexes $[(CO)_4Cr(PR_2)]_2^{0,-1,-2}$. To simplify the calculation, R was replaced by hydrogen. Examination of the scheme shows that for all species the highest MO is the antibonding dimetal combination of the $3d_{x^2-y^2}$ orbitals. With respect to the metal-metal axis, this orbital has both a σ- and a δ- component, the former being the most important for the metal-metal bond (Figure 1.5). As electrons are added to the

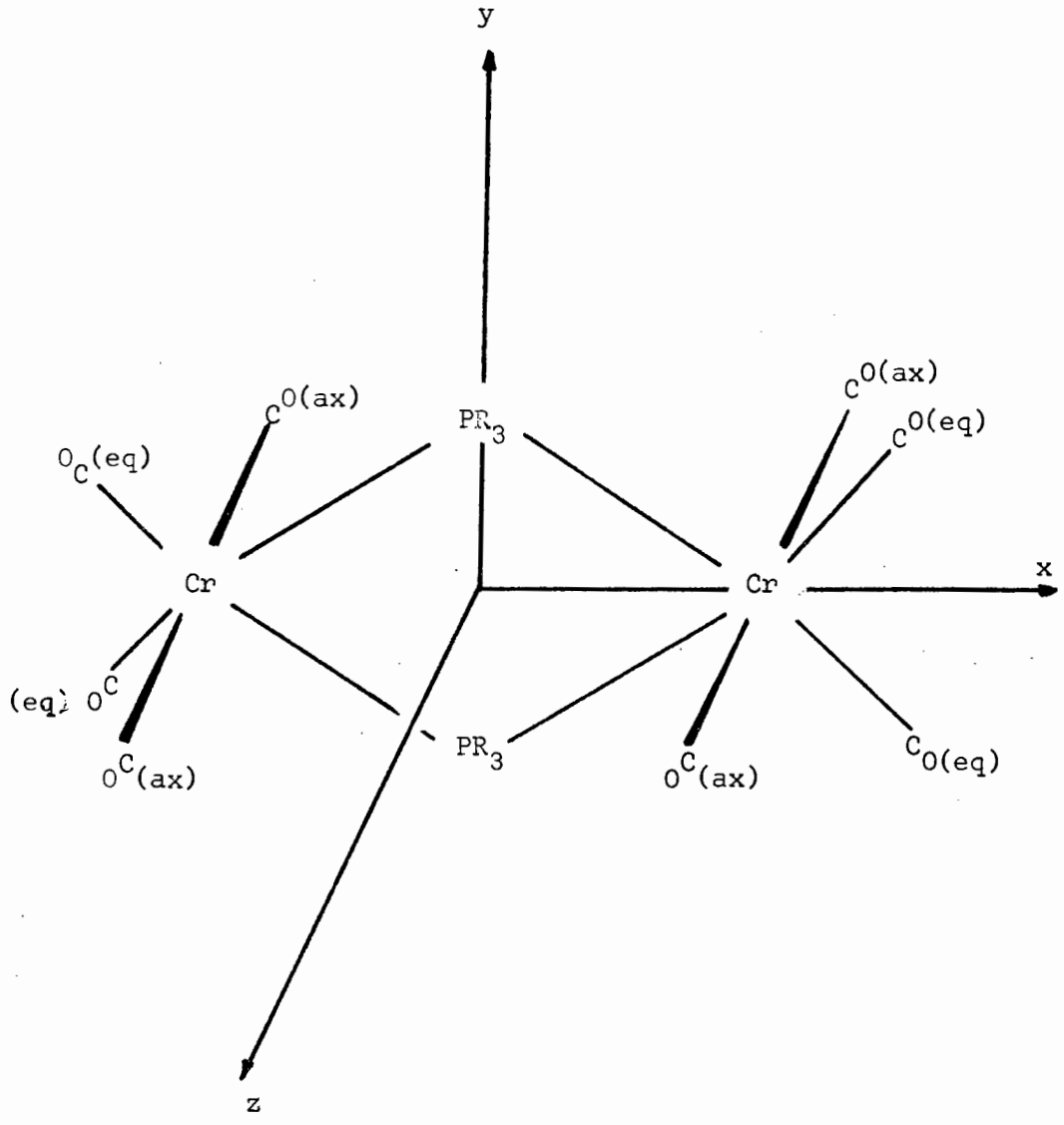

FIGURE 1.5

The coordinate system (x, y, z) used in the orbital symmetry classification of $[Cr(CO)_4(PR_2)]_2$

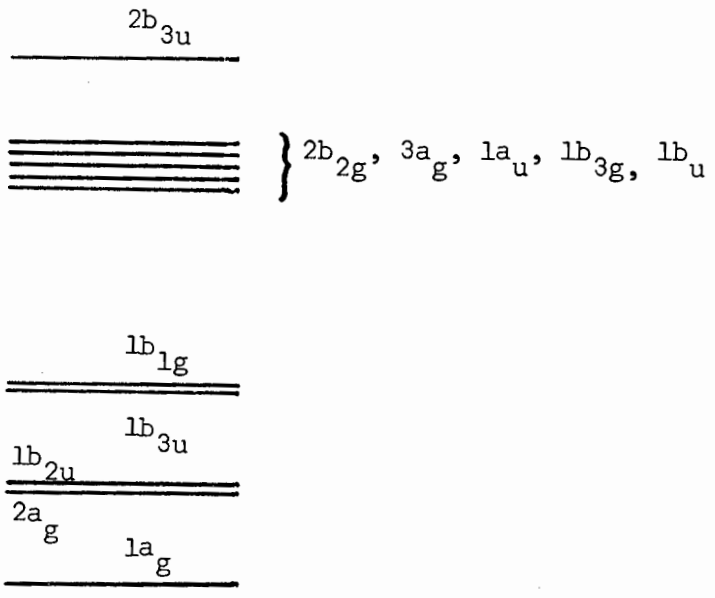

Molecular orbital energy diagram for $[Cr(CO)_4(PR_2)]_2$

FIGURE 1.6

$[(CO)_4Cr(PH_2)]_2$ system, therefore, only the antibonding $2b_{3u}$ MO will be affected drastically. Teo *et al* adduce experimental evidence to support their hypothesis: as electrons are injected into the $3d_{x^2-y^2}$ orbitals, $d\pi$-$p\pi^*$ back donation will increase and the force constant for the C-O vibration in the equatorial carbonyl ligands should decrease more than that for the axial CO's (for which only indirect π back donation is possible). Dessy *et al*[1.19] have found this to be the case: Δk^{eq} = 2.44 mdyne Å^{-1} *vs* Δk^{ax} = 1.55 mdyne Å^{-1}.

Although chemical evidence does not unequivocally favour any of these theoretical treatments, that by Teo *et al*, based on molecular orbital calculations, seems the most reliable - although a qualitative rationale for it, proposed at the end of their paper, is somewhat involved.

1.2.4 Motivation for subsequent Work on Dinuclear Iron and Manganese Complexes.

Few reports have been made of oxidation of complexes of the type 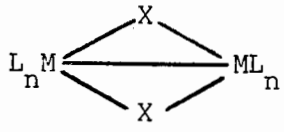 where a two-election metal-metal bond already exists.

As discussed previously, one-electron oxidation of the complex[1.29]

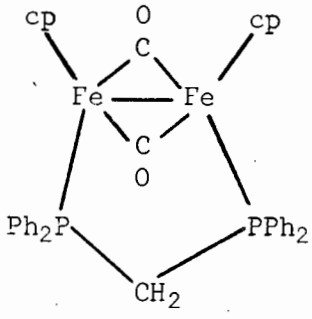

to the mono-cation results in a slight increase in the metal-metal distance of 0.05 Å, and a similar small increase from 2.603 to 2.617 Å has been observed for the oxidation of $[Mo(cp)(SMe)_2]_2$ [1.37]. However, the essential invariance of the metal-metal distance may result from steric constraints being placed on the molecule by the bridging ligands, and therefore structural characterization of these two complexes has not yielded information about the HOMO in metal-metal bonded species $[(L)_nMX]_2$.

Attempted oxidation of the formally metal-metal bonded species $[(cp)Fe(CO)(PPh_2)]_2^{2+}$ and $[(cp)Fe(CO)(SR)]_2^{2+}$ was not successful[1.34] - the half-wave potential for the reaction

$$[(cp)M(CO)(X)]_2^{2+} \rightarrow [(cp)M(CO)(X)]_2^{3+} + e^-$$

is likely to be high, and break-up of the species is expected instead.

Inspection of the molecular orbital ordering scheme of Mason and Mingos[1.35] suggests that the HOMO is non-bonding with respect to the metal atoms. However, according to Teo *et al*[1.36], the HOMO in such species is the $2b_{2g}$ orbital, with the $3a_g$ orbital very close to it in energy. The $2b_{2g}$ orbital is an antibonding combination of the metal $3d_{xz}$ orbitals, while the $3a_g$ is a bonding combination of the $3d_{x^2-y^2}$ orbitals. From this molecular orbital ordering one would predict, initially, that the next electron would be removed from the $2b_{2g}$ molecular orbital, resulting in a complex with an Fe-Fe bond order greater than one (such compounds are known - *e.g.*[1.38]).

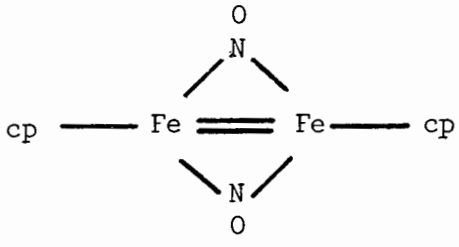

However, closer inspection of the trends in the molecular orbital ordering, as calculated by Teo *et al*, as electrons are removed from the HOMO, suggest that in complexes where the $2b_{3u}$ orbital is empty the $2b_{2g}$ and $3a_g$ orbitals cross in energy and removal of a further electron may well cause the $3a_g$ orbital to become the HOMO. Since the $3a_g$ orbital is bonding with respect to the metal atoms, a decrease in bond order will occur and the metal-metal bond length should increase.

If the cation $[Fe_2(cp)_2(CO)_3(SEt)]^+$, which contains a formal metal-metal bond and is isoelectronic with the species $[Fe(cp)(CO)(SEt)]_2^{2+}$, undergoes analogous reduction to a neutral and an anionic species (isoelectronic with $[Fe(cp)(CO)(SEt)]_2^n$, n = +1 and 0, respectively) then an Fe-Fe bond length of about 2.6 Å would be

expected for the cation, an Fe-Fe distance of about 2.9 Å for the neutral species and one of about 3.3 Å for the non-(Fe-Fe)-bonded anion.

In a recent paper, Cotton and Troup[1.39], comparing the structures of $[Fe_3(CO)_{12}]$ and a number of its substituted derivatives, *viz.* $[Fe_3(CO)_{11}(PPh_3)]$, $[Fe_3(CO)_9(PMe_2Ph)_3]$ and $[Fe_3(CO)_8(SC_4H_8)_2]$, show that in compounds containing pairs of bridging carbonyls, there is a correlation between the length of the metal-metal bond and the degree of asymmetry exhibited by the bridging carbonyl group. The [FeC(O)FeC(O)] systems for two complexes are depicted in Figure 1.7

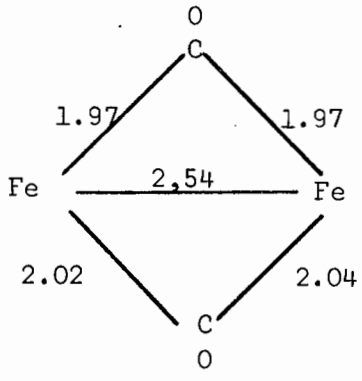

$[Fe_3(CO)_9(PMe_2Ph)_3]$

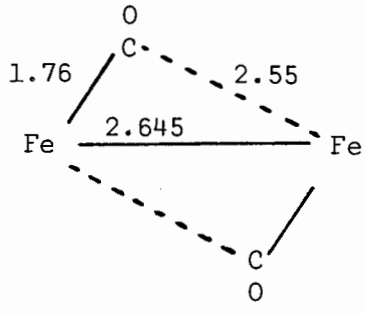

$[Fe_3(CO)_8(SC_4H_8)_2]$

FIGURE 1.7 (bond lengths in Å)

Whereas the bridging carbonyl system in $[Fe_3(CO)_9(PMe_2Ph)_3]$ does not deviate significantly from C_{2v} symmetry, the 'bridging' carbonyl groups in $[Fe_3(CO)_8(SC_4H_8)_2]$ might better be described as terminal carbonyl groups where there is some interaction of the CO entity with the other metal atom, perturbing its bonding scheme. The same type of asymmetry has been observed in complexes where only one carbonyl group is asymmetric. An example, $[Fe_2(CO)_7dipy]$ Figure 1.8 has been

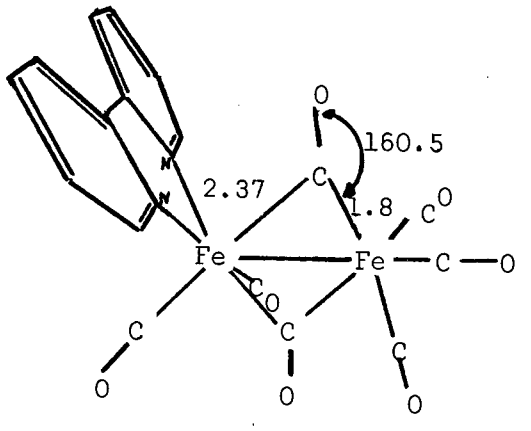

$[Fe_2(CO)_7dipy]$

FIGURE 1.8

described by Cotton and Troup[1.40]; it contains one moderately unsymmetric bridging carbonyl group and one grossly unsymmetrical CO bridging an Fe-Fe bond length of 2.611 Å. Since the *raison d'être* of the very unsymmetrical CO group is clearly not the Fe-Fe bond length, another factor must be instrumental in this case. The authors hypothesize that the relatively electron-rich Fe(2) atom in $[Fe_2(CO)_7(dipy)]$ is forming a weak d → π* dative bond to the C(1) - O(1) group, and that the unsymmetrically bridging CO group provides a mechanism for a metal atom otherwise tending to be excessively negative to transfer electron density to a CO group on a less negatively charged metal atom. Chin and Bau[1.41] in the description of the structure of $[Fe_2(CO)_6(C_{12}H_{16})]$, report an unsymmetrical carbonyl bridge (<Fe(1) - C(1) - O(1) = 162°, Fe(1) - C(1) = 1,753 Å; <Fe(2) - C(1) - O(1) = 125°, Fe(2) - C(1) = 2.321 Å) which spans a

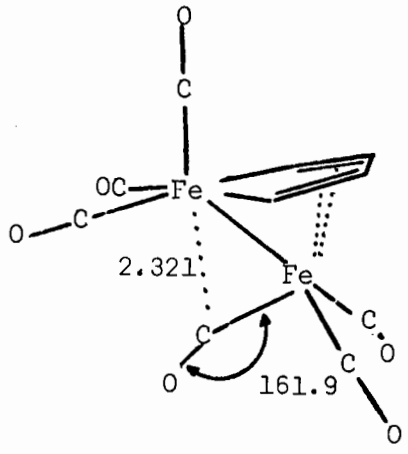

Part of the structure of $[Fe_2(CO)_6(C_{12}H_{16})]$

FIGURE 1.9

relatively short Fe-Fe bond (2.462 Å) in which the same cause may be operative (Figure 1.9).

Thus, although an unsymmetrically bridging carbonyl group is possible for a short metal-metal bond length, especially when one metal atom is more negative than the other, it is unlikely that for the Fe-Fe bond lengths of 2.9 and 3.3 Å expected for $[Fe_2(cp)_2(CO)_3(SEt)]^n$, n = 0 and -1, that the bridging carbonyl will be symmetrically disposed with respect to the two metal atoms. Therefore a further motivation exists for the synthesis and investigation of $[Fe_2(cp)_2(CO)_3(SEt)]^+$: in the neutral and anionic forms will the bridging carbonyl be asymmetrical or will it be found that the CO bridge has imposed a

steric constraint and the reduction of the parent cation has not been accompanied by the same increase in metal-metal bond length as found for $[Fe(cp)(CO)(PPh_2)]_2$ (n = +2, +1 and 0)?

The synthesis of

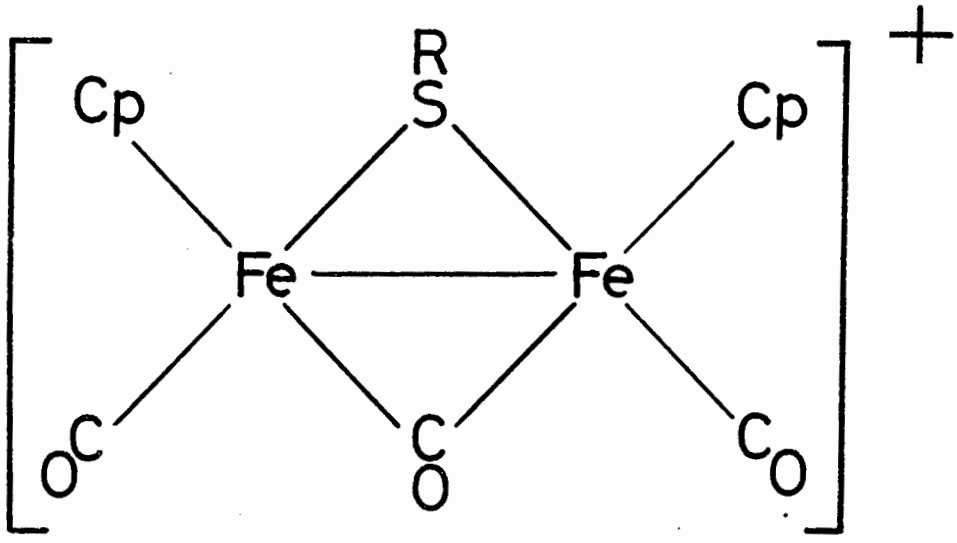

was therefore attempted. This complex should be susceptible both to oxidation to the dication $[Fe_2(cp)_2(CO)_3(SEt)]^{2+}$, isoelectronic with $[\{Fe(cp)(CO)\}_2(dppm)]^+$ [1.29], and to reduction to the neutral and anionic forms $[Fe_2(cp)_2(CO)_3(SEt)]^n$ (n = 0 and -1). X-ray crystallographic structural studies on the oxidized and reduced products, if obtained in a suitably crystalline form, should yield relevant information about the electronic structure of this class of complex.

1.3 The Synthesis of $[Fe_2(cp)_2(CO)_3(SR)]^+$, and its Redox Behaviour.

Haines, du Preez and Nolte have shown that the complex $[Fe(cp)(CO)_2(PPh_2)]$, formed by reacting, for instance, $LiPPh_2$ with $[Fe(cp)(CO)_2Cl]$, may be employed synthetically as a metal-containing 'phosphine'[1.42]. Thus reaction of this complex with $[Fe(cp)(CO)_2Cl]$ results in the chloride ligand being displaced, to give the dinuclear species

$$[\{Fe(cp)(CO)_2\}_2(PPh_2)]^+ \ [1.42].$$

A large number of complexes of the type $[\{Fe(cp)(CO)_2\}_2M]^n$ have been reported (*e.g.* M = I, n = +1[1.43]; M = $SbCl_2$, n = +1[1.44]; M = GeX_2, n = 0 for X = Cl and Me[4.4]; M = SnX_2, n = 0 for n = Cl[1.45,1.46], I[1.47], Me[1.48], (ONO)[1.49] and (σ-C_5H_5)[1.50]; M = SO_2, n = 0[1.51]; M = $(CH_2)_3$, n = 0[1.52]; M = $(CH_2)_4$, n = 0[1.53]; M = Au, n = -1[1.54]; M = Hg, n = 0[1.55]); however, in the preparation of the majority of these complexes insertion of the group M into the metal-metal bond of the dimer $[Fe(cp)(CO)_2]_2$, or reactions of the nucleophile $[Fe(cp)(CO)_2]^-$, were the methods employed.

The concept of a 'metal-containing ligand' was employed, in a manner analogous to that used in the preparation of $[\{Fe(cp)(CO)_2\}(PPh_2)]^+$ [1.42], in the synthesis of $[\{Fe(cp)(CO)_2\}_2(SR)]^+$. The alkylthio derivatives $[Fe(cp)(CO)_2(SR)]$ (R = Et, Bu^t) were prepared according to the method of Ahmad, Bruce and Knox[1.56], by reacting $[Fe(cp)(CO)_2Cl]$[1.57] with SR^- in ether. Since the metal-containing alkylthio 'ligands' $[Fe(cp)(CO)_2(SR)]$ were expected to be less nucleophilic than the corresponding metal-containing 'phosphines' $[Fe(cp)(CO)_2(PPh_2)]$, it was decided to react them with the solvated species $[Fe(cp)(CO)_2(acetone)_x]^+X^-$ [1.58], formed by stirring the dimer, $[Fe(cp)(CO)_2]_2$, with

two equivalents of a silver salt, AgX (X = ClO_4, BF_4 or SbF_6) in acetone. Although $[Fe(cp)(CO)_2(acetone)_x]^+X^-$ was not characterized during any synthesis here described, the value of x is probably 1 as iron in this type of complex is considered to be octahedrally co-ordinated. The cyclopentadienyl group, formally a five electron donor[1.59], is conventionally considered to occupy 3 coordinating positions when it coordinates as an (η^5-) ligand.

In this way the salts $[\{Fe(cp)(CO)_2\}_2(SR)]^+X^-$ (R = Bu^t, X = SbF_6; R = Et, X = ClO_4, BF_4, SbF_6) were synthesized. The salt $[\{Fe(cp)(CO)_2\}_2(SEt)]^+BPh_4^-$ was prepared from the corresponding perchlorate salt by dissolving it in methanol and adding an excess of sodium tetraphenylboron. The precipitate of $[\{Fe(cp)(CO)_2\}_2(SEt)]^+BPh_4^-$ which separated from solution did not need to be recrystallized.

The physical properties of these alkylthio-bridged dinuclear iron salts are set out in Tables 1.2, 1.3 and 1.4. It was found that their solution spectra contained four C-O stretching peaks in the terminal carbonyl region. The relative intensities of two of these peaks varied with respect to the intensities of the other two according to the counter ion employed; in the case of $[\{Fe(cp)(CO)_2\}_2(SEt)]ClO_4$ the difference was such that only two peaks were observed. This suggested the presence of more than one conformer in solution, as has been previously found for $[\{Fe(cp)(CO)_2\}_2(SnCl_2)]$ [1.60]. Not inconsistent with this suggestion is the observation that the two weaker peaks increase in intensity or irradiation of the compound in solution with ultraviolet light. This aspect of the structural properties of $[\{Fe(cp)(CO)_2\}_2(SEt)]^+$ is discussed more fully in Chapter 4.

The syntheses of the heterobridged dinuclear species $[Fe_2(cp)_2(CO)_3(SO_2)]$[1.61,1.62] and $[Fe_2(cp)_2(CO)_3(GeMe_2)]$[1.63] have been reported.

The former compound is found as a byproduct in the synthesis of the monobridged complex $[\{Fe(cp)(CO)_2\}_2(SO_2)]$ from $[Fe(cp)(CO)_2]Na$ and SO_2 at -75^oC[1.62], and also results from the decomposition of $[\{Fe(cp)(CO)_2\}_2(SO_2)]$[1.62]. Irradiation of $[\{Fe(cp)(CO)_2\}_2(SO_2)]$ with ultraviolet light in THF causes loss of SO_2 and formation of $[Fe(cp)(CO)_2]_2$ in good yields[1.61]. In contrast, $[Fe_2(cp)_2(CO)_3(GeMe_2)]$ has been synthesized by irradiating a solution of the mononuclear complex $[Fe(cp)(CO)_2(GeMe_2Cl)]$[1.63]. It is likely that the complex $[\{Fe(cp)(CO)_2\}(GeMe_2)]$ is an intermediate in this reaction.

Haines and Nolte[1.64] report that the heterobridged species

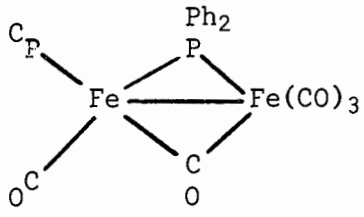

may be prepared by irradiating a solution of the mono-bridged dinuclear complex $[Fe_2(cp)(CO)_6(PPh_2)]$[1.64] with ultraviolet light to give

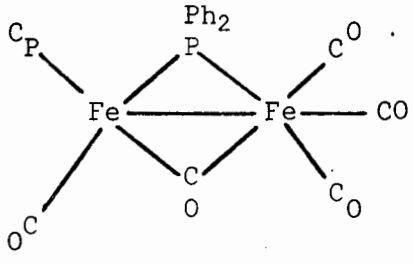

With a view, therefore, to synthesizing the corresponding ethylthio-bridged complex

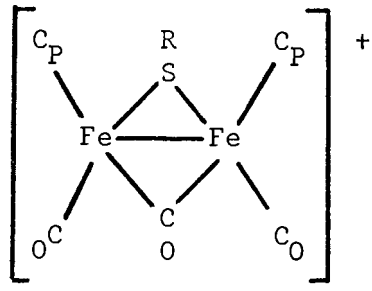

solutions of $[\{Fe(cp)(CO)_2\}_2SEt]X$ (X = BF_4 or SbF_6) in thf were irradiated for periods of two hours. Characterization of the product which separated from solution established it to be $[Fe_2(cp)_2(CO)_3(SEt)]X$ (X = BF_4 or SbF_6), Tables 1.2, 1.3 and 1.4. Its infra-red spectrum, measured using both nujol mulls and dichloromethane solutions, showed two terminal carbonyl peaks and one bridging carbonyl absorption (Table 1.3), and, in the p.m.r. spectrum (measured in d_6-acetone), the ratio of cyclopentadienyl protons to ethyl protons was 2:1. Conductance measurements (Table 1.2) established this complex to be a 1:1 electrolyte. It is insoluble in non-ligating polar solvents such as CH_2Cl_2 but very soluble in acetone. Recrystallization from acetone/petroleum ether (30° - 40° fraction) or acetone/dichloromethane solutions afforded very dark green-brown, almost black needles.

However, photolysis of $[\{Fe(cp)(CO)_2\}_2(SEt)]BPh_4$ gave $[Fe_2(cp)_2(CO)_3(SEt)]BPh_4$ as a minor product only. The major product was found to be the σ-phenyl derivative $[Fe(cp)(CO)_2(Ph)]$[1.65] formed as a result of the extraction of a phenyl group from the tetraphenylborate anion. Refluxing of a dichloromethane solution of $[Fe_2(cp)_2(CO)_3(SEt)]BPh_4$ also leads to the formation of $[Fe(cp)(CO)_2(Ph)]$, in somewhat lower yield. Phenyl transfer reactions of this type have previously been reported for *cis*-$[Pt(PEt_3)_2Cl_2]$[1.66], $[Pt(PMe_2Ph)_2(MeOH)Me]^+$ [1.67], $[Ni(cp)(PPh_3)_2]^+$ [1.68] and $[\{Ru(cp)(CO)_2\}_2X]^+$ (X = Cl, or Br)[1.69], the products of the phenylation being

trans-$[Pt(PEt_3)_2Ph_2]$, *trans*-$[Pt(PMe_2Ph)_2\ Ph_2]$, $[Ni(cp)(PPh_3)Ph]$ and $[Ru(cp)(CO)_2Ph]$, respectively.

The synthesis of $[Fe_2(cp)_2(CO)_3(SR)]BPh_4$ has been reported by Nolte[1.70]. On the basis of the corresponding reaction involving $[Fe(cp)(CO)_2(PPh_2)]$ it had been expected that treatment of the dimer $[(cod)RhCl]_2$ with $[Fe(cp)(CO)_2(SR)]$ (R = Et or Bu^t) in ethanol in the presence of $NaBPh_4$ would yield $[Rh\{Fe(cp)(CO)_2(SR)\}_2]$[1.70]. However, the product isolated from solution was established by means of X-ray fluorescence analysis not to contain rhodium, and was characterized as $[Fe_2(cp)_2(CO)_3(SR)]BPh_4$. This reaction thus provides an alternative method of obtaining $[Fe_2(cp)(CO)_3(SR)]^+$, the rhodium compound presumably functioning as an extractor of carbon monoxide from $[\{Fe(cp)(CO)_2\}_2(SR)]^+$. Nolte did not investigate $[Fe_2(cp)_2(CO)_3(SR)]\ BPh_4$ further, merely reporting its synthesis.

The Redox Behaviour of $[Fe_2(cp)_2(CO)_3(SEt)]^+$.

As expected, this complex showed well-defined reversible redox behaviour. Controlled reduction of a thf suspension of the complex using sodium amalgam (1% w/w Na/Hg, freshly prepared, in slight excess) gave an intense green neutral complex, soluble in benzene. This compound was very air-sensitive, reverting rapidly to $[Fe_2(cp)_2(CO)_3SEt]^+$ in air. In solution it was observed to decompose slowly in solution to the di-alkylthio-bridged species $[Fe(cp)(CO)(SEt)]_2$ as shown by infra-red spectroscopy. In view of its poor stability, it was not obtained analytically pure. However, the band pattern of the peaks in the C-O stretching region of its solution infra-red spectrum is

very similar to that of the cation $[Fe_2(cp)_2(CO)_3SEt]^+$ but shifted to a lower frequency (Table 1.3) while its magnetic susceptibility corresponds to a magnetic moment of approximately 1.5 B.M. Thus it can be deduced that $[Fe_2(cp)_2(CO)_3SEt]$, with a similar structure to the cation $[Fe_2(cp)_2(CO)_3SEt]^+$, has been produced by one-electron reduction of the parent cation.

Reaction of a tetrahydrofuran suspension $[Fe_2(cp)_2(CO)_3SEt]^+$ with excess of sodium amalgam resulted first in an intense green solution of the neutral species, as described above, and then in a further colour change to a red-brown solution. The green colour was restored upon admission to the reaction flask of small amounts of air. The infra-red spectrum of this species in dichloromethane in the presence of $[(Ph_3P)_2N]Cl$ showed strong, rather broad absorbances at 1928 and 1690 cm^{-1}, as well as peaks at 1970 and 1775 cm^{-1} which could be ascribed to $[Fe_2(cp)_2(CO)_3SEt]$. This infra-red evidence, coupled with the susceptibility of the red-brown species to oxidation, suggested that the anion, $[Fe_2(cp)_2(CO)_3SEt]^-$ had been prepared. However, its instability in solution prevented its isolation as the $[(Ph_3P)_2N]^+$ salt.

Thus, the following equilibrium has been demonstrated to exist:

$$[Fe_2(cp)_2(CO)_3SEt]_2^n : \quad n = +1 \rightleftharpoons n = 0 \rightleftharpoons n = -1.$$

This system is isoelectronic with that observed for the *bis*-(alkythio)-bridged species $[Fe(cp)(CO)SR]^n$ $\quad n = +2 \rightleftharpoons n = +1 \rightleftharpoons n = 0.$

While anionic complexes of transition metals in low oxidation states tend to be unstable, the instability of $[Fe_2(cp)_2(CO)_3SEt]$ is not readily explained. The isoelectronic $[Fe(cp)(CO)(SR)]_2^+$ is thermodynamically stable and does not decompose rapidly in air. It would

appear that this instability is due to the degree of strain in the Fe S Fe C(O) ring introduced, with the extra electron, on reduction of the cation. However, in the absence of X-ray crystallographic data, no *prima facie* deductions may be made about the Fe-Fe bond length and the possible existence of an unsymmetrically bridging carbonyl group, as discussed in 1.2.

Oxidation of $[Fe_2(cp)_2(CO)_3SEt]^+$ was now attempted. However, attempts to obtain $[Fe_2(cp)_2(CO)_3SEt]^{2+}$ met with no success; oxidants such as iodine, bromine and silver hexafluoroantimonate were employed but each time decomposition of the parent compound occurred. Presumably further reduction of electron density on the metal atoms lessens d-π^* overlap between the Fe and bridging C atom to such an extent that Fe S Fe C(O) ring breaks up to give, firstly

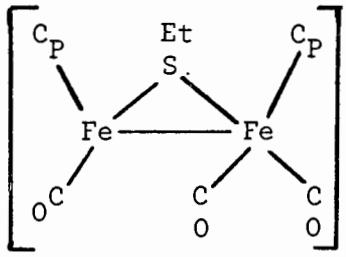

$^{2+}$

species which then decompose further to mononuclear products.

1.4 The Structure of $[Fe_2(cp)_2(CO)_3SEt]^+$.

This is described fully in Chapter 5. In the solid state, the cation has a *cis*-configuration, approximate mirror symmetry and the Fe-Fe distance of 2.58 Å corresponds to the presence of a two electron Fe-Fe bond. However, the possibility of structural isomerism may be discussed here. As Haines *et al* have pointed out[1.33], the complex $[Fe(cp)(CO)(SR)]_2^n$ can exist in five different isomeric forms[1.33,1.71]. If the Fe S Fe C(O) ring is planar, three isomers only are possible for the complex $[Fe_2(cp)_2(CO)_3SEt]^+$ (Figure 1.10).

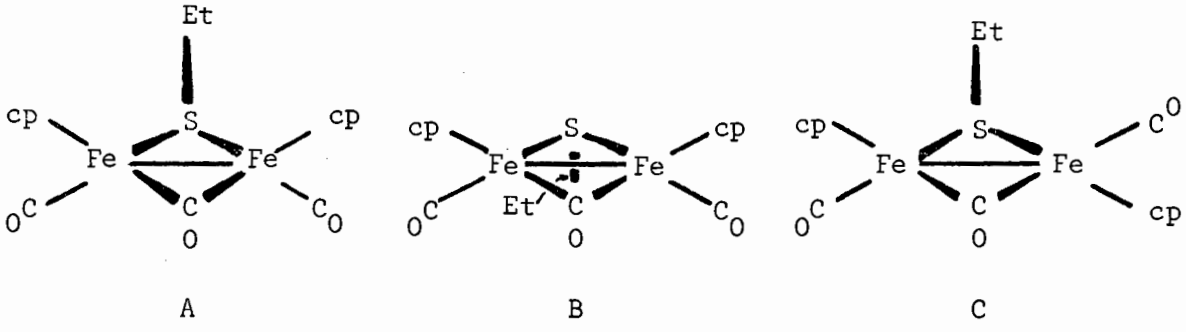

FIGURE 1.10

The *cis* isomers A and B will give rise to single cyclopentadienyl resonances in their p.m.r. spectra while the *trans* isomer should exhibit two, although they may be accidentally degenerate. Two infra-red terminal C-O stretching modes are predicted for all three isomers which belong to the molecular point groups C_s, C_s and C_i, respectively (considering the ethyl group as a 'point' group). However, inspection of a to-scale molecular model indicates that if the iron atoms show ideal octahedral coordination (with the cp groups

occupying three coordination sites) then in both *cis* and *trans* isomers the terminal carbonyl groups will be parallel. It is very likely that dipole-dipole repulsion in the *cis* isomer is the cause of the 'splaying apart', observed in the molecular structure, of the CO groups, since, for parallel vectors, their separation is equal to the Fe-Fe bond length of 2.58 Å. In a *trans* isomer dipole-dipole interaction would be negligible and the two carbonyl groups would lie parallel to each other. Thus, the infra-red spectrum of the *cis* isomer is expected to show two bands in the terminal carbonyl region, while that of the *trans* isomer should only exhibit one band, due to the asymmetric C-O stretching mode.

The infra-red spectrum of $[Fe_2(cp)_2(CO)_3SEt]^+$ measured in CH_2Cl_2 as the BF_4^- or SbF_6^- salts, contains a strong terminal carbonyl stretching peak at 2032 cm^{-1}, a band of medium intensity at 1848 cm^{-1} assigned to the bridging carbonyls and a medium to weak shoulder at 2004 cm^{-1}. In the solid state, the bands due to the bridging and terminal carbonyls are of the same intensity, while the intensity of the shoulder peak has increased. In addition, the two peaks at 2032 and 2004 cm^{-1} observed in the solution spectra are clearly resolved in the solid state. They may be assigned to the symmetric (2032 cm^{-1}) and antisymmetric (2004 cm^{-1}) modes respectively. The p.m.r. spectrum of this species exhibits single cyclopentadienyl, methylene and methyl resonances down to temperatures of 213K.

This spectroscopic evidence is interpreted in terms of the cation existing as one of the *cis* isomeric forms A or B both in solution and in the solid state. This is in contrast with $[Fe(cp)(CO)_2]_2$ which occurs as a mixture of its *cis* and *trans* isomers in solution, in rapid equilibrium with each other[1.72]. Irradiation

of $[Fe_2(cp)_2(CO)_3(SEt)]BF_4$ in thf with ultraviolet light did not appear to convert it to the *trans* isomer (the irradiation study was monitored using infra-red spectroscopy), unlike the effect on *cis*-$[Fe(cp)(CO)(SR)]_2$ of ultraviolet light under similar conditions[1.71]. However, isomerization of $[Fe_2(cp)_2(CO)_3(SEt)]^+$ in a manner analogous to that of the *bis*-(alkylthio)-bridged derivative would involve, as well as the breaking of an Fe-S bond, the breaking-up of the Fe-Fe interaction; and therefore a higher energy barrier to isomerism might be expected to exist than is present in $[Fe(cp)(CO)(SR)]_2$. The concerted breaking of metal-bridging ligand bonds, by which mechanism *cis*-$[Fe(cp)(CO)_2]_2$ isomerizes to the *trans*-form[1.72], is also an unlikely mechanism for *cis* - *trans* isomerization of $[Fe_2(cp)_2(CO)_3(SEt)]$.

It is interesting to speculate on the mechanism for formation of the dinuclear heterobridged species $[Fe_2(cp)_2(CO)_3(ML_n)]^m$ (ML_n = $GeMe_2$, SO_2, m = 0; ML_n = SEt, m = +1) from the corresponding monobridged complexes $[\{Fe(cp)(CO)_2\}_2(ML_n)]^m$, and why it should be that the above heterobridged complexes are formed very readily from their precursors, while no such reactions have been reported for $[\{Fe(cp)(CO)_2\}_2(ML_n)]^m$ where ML_n = $SbCl_2$, m = +1; ML_n = I, m = +1; ML_n = Hg, m = 0; ML_n = Au, m = -1; ML_n = SnX_2, m = 0. A plausible mechanism for the reaction is, first, loss of a CO ligand from I to give the unsymmetrical species II.

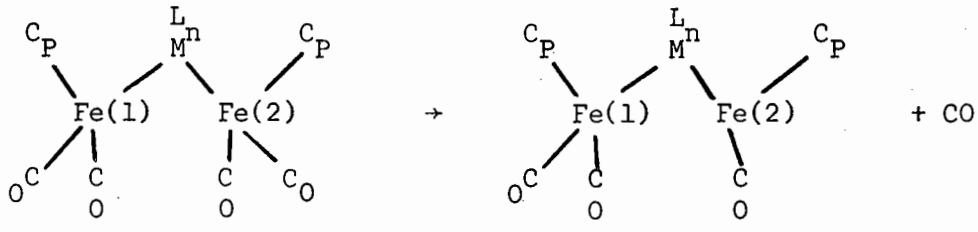

I II

Depending upon the ease with which the angle Fe(1) - M - Fe(2) can be varied, *i.e.* the flexibility of the ligand ML_n, the reaction can now follow one of three pathways

a) II can either break up to form mononuclear products *via* homo- or heterolytic fission of an Fe-M bond; one possible product is the $[Fe(cp)(CO)_2]^{\cdot}$ radical which would be expected to dimerize to give $[Fe(cp)(CO)_2]_2$, as has been observed for $[\{Fe(cp)(CO)_2\}_2(SO_2)]$[1.61,1.62]; or

b) interaction may occur between the molecular orbital systems of the two iron atoms to give, firstly, an unsymmetrical metal-metal bonded intermediate containing no bridging carbonyls, III which will further rearrange to give the symmetrically bridged product IV:

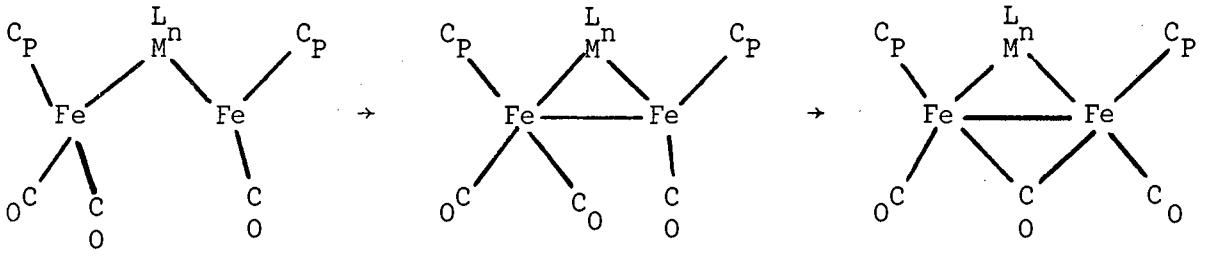

II III IV

c) overlap of a d-orbital of the coordinatively unsaturated Fe(2) atom with a π^* orbital of one of the carbonyl groups bound to Fe(1) may take place to yield an unsymmetrically bridged intermediate, V, similar to the complexes $[Fe_2(CO)_7(dipy)]$[1.40] and $[Fe_2(CO)_6(C_{12}H_{16})]$[1.41] discussed in Section 1.2.5:

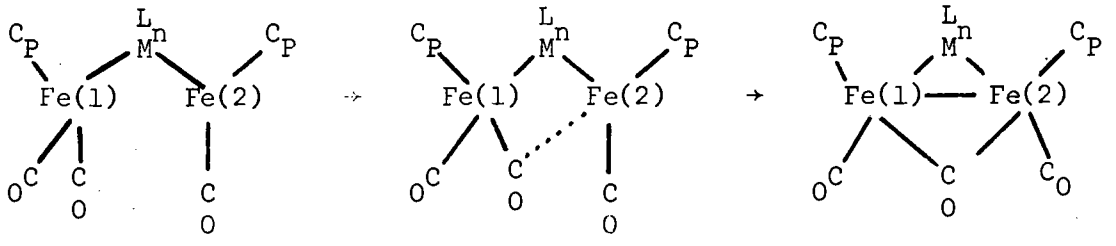

II V IV

Interaction between Fe(2) and the unsymmetrically bridging will tend to decrease the Fe(1)-Fe(2) distance and V should further condense to form the symmetrical product IV.

The actual mechanism may be a combination of pathways b) and c), involving a concerted 'closing-up' of the $Fe(1)-Fe(2)-C(O)_{(bridging)}$ triangle. In any case, it is very probable that the interaction between Fe(2) and the carbon atom of the bridging carbonyl group-to-be is an important part of the process. It is instructive, therefore, to examine the closest distance of approach, d, of this carbon atom to the iron atom Fe(2) in a number of complexes of the type

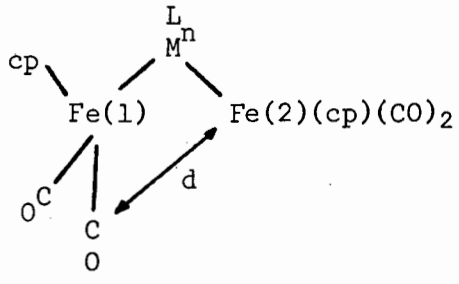

, whose structures are known, as the residue $\{Fe(1)cp(CO)_2\}$ is rotated about the Fe(1)-M bond. Values of d have been calculated, based on the Fe-M bond lengths reported in the literature, for an idealized molecular geometry in which the Fe - M - Fe angle is 109° 28'. The $\{Fecp(CO)_2\}$ moiety is assumed to be octahedral (with the cp group occupying 3 coordination sites) so that the angles M - Fe - C(O) = 90.0°.

For such a geometry the closest distance of approach of Fe(2) and C occurs when the atoms Fe(1), M, Fe(2) and C are coplanar. The values of d are set out in Table 1.5 for various complexes of the above type, together with the Fe - M - Fe bond angle associated with a hypothetical $[Fe_2(cp)_2(CO)_3(ML_n)]$ molecule with an Fe-Fe bond distance of 2.6 Å.

TABLE 1.5

Complex	M	d (Å)	Fe - M - Fe(°)	Ref.
$[\{Fe(cp)(CO)_2\}_2SEt]^+$	S	2.54	68.8	
$[\{Fe(cp)(CO)_2\}_2SO_2]$	S	2.50	69.5	1.61
$[\{Fe(cp)(CO)_2\}_2GeCl_2]$	Ge	2.61	67.0	1.74
$[\{Fe(cp)(CO)_2\}_2SnCl_2]$	Sn	2.83	62.9	1.45
$[\{Fe(cp)(CO)_2\}_2SbCl_2]^+$	Sb	2.75	63.9	1.44
$[\{Fe(cp)(CO)_2\}_2I]^+$	I	2.98	60.2	1.43

The distances between the relevant iron atom and the carbon atom of the unsymmetrically bridging carbonyl groups in $[Fe_2(CO)_7(dipy)]$ and $[Fe_2(CO)_6(C_{12}H_{16})]$ (Figures 1.8 and 1.9) are 2.37 and 2.32 Å respectively. From inspection of Table 1.5 it is apparent that only in the complexes $[\{Fe(cp)(CO)_2\}_2ML_n]$, where ML_n = SEt, SO_2 and $GeCl_2$, should any Fe-C(O) interaction of the type postulated for mechanism (c) be expected. In addition, the bond angles Fe - M - Fe for the molecules $[Fe_2(cp)_2(CO)_3ML_n]$ deviate considerably from tetrahedral, the greatest difference being shown by those species where ML_n = $SnCl_2$, $SbCl_2$ and I. Thus it would appear that $[Fe_2(cp)_2(CO)_3(ML_n)]$ (M = S and Ge) are more likely to form than when M = Sn, Sb or I.

In accordance with these somewhat speculative conclusions, heterobridged dinuclear complexes $[Fe_2(cp)_2(CO)_3ML_n]^m$ have been reported for ML_n = SEt, SO_2 and $GeMe_2$, but not for ML_n = $SnCl_2$, $SbCl_2$ or I.

1.5 Summary.

The dibridged metal-metal bonded complex $[Fe_2(cp)_2(CO)_3(SEt)]X$ ($X = BF_4$, SbF_6 and BPh_4) was synthesized, *via* the mono-alkylthio-bridged complex $[\{Fe(cp)(CO)_2\}_2(SEt)]X$, from the precursor $[Fe(cp)(CO)_2(SEt)]$. A reversible redox equilibrium has been shown to operate : $[Fe_2(cp)_2(CO)_3(SEt)]^n$:

$$n = +1 \rightleftharpoons n = 0 \rightleftharpoons n = -1;$$

the neutral and anionic forms of the complex, for reasons of instability, were not characterized beyond infra-red spectroscopy, and magnetic measurements in the case of $[Fe_2(cp)_2(CO)_3SEt]$. The dication ($n = +2$) was not obtained. Reasons for this, and the instability of the neutral and anionic species, were discussed in terms of the charge on the metal atoms, and the metal-metal distance, affecting the mode of bonding of the bridging carbonyl group. The possible isomerism of $[Fe_2(cp)_2(CO)_3SEt]^+$ was discussed in terms of its solution and solid-state infra-red spectra, and its p.m.r. spectrum. Finally, a mechanism for the formation of metal-metal bonded species such as $[Fe_2(cp)_2(CO)_3ML_n]^m$ from $[\{Fe(cp)(CO)_2\}_2ML_n]^m$ was put forward.

1.6 Experimental.

The compounds $[Fe(cp)(CO)_2SR]$ (R = Et and Bu^t) were synthesized according to literature methods[1.56]. All experiments were made under a nitrogen atmosphere. I.r. spectra were measured on either a Perkin-Elmer model 21 or a Beckmann IR 12 spectrophotometer. N.m.r. spectra were recorded using Varian HA 100 and XL 100 instruments. Conductivities were obtained by conventional methods. The magnetic susceptibility was measured on a Newport Instruments Gouy balance. Elemental analyses were obtained by the Alfred Bernhardt Microanalytical Laboratory, Elbach-uber Engelskirchen, West Germany, and by Mr. W. T. Hemsted of the University of Cape Town.

μ-Alkylthio-bis[dicarbonyl(η-cyclopentadienyl)iron] Salts: $[\{Fe(cp)(CO)_2\}_2(SR)][SbF_6]$ (R = Et or Bu^t). The compound $[Fe(cp)(CO)_2SEt]$ (0.7 g, 3 mmol) or $[Fe(cp)(CO)_2SBu^t]$ (0.8 g, 3 mmol) in acetone (50 cm^3) was added dropwise to a stirred acetone solution (60 cm^3) of $[Fe(cp)(CO)_2(OCMe_2)][SbF_6]$ (3 mmol), prepared *in situ* from $[\{Fe(cp)(CO)_2\}_2]$ and two equivalents of $Ag[SbF_6]$, and the resulting solution stirred for 30 min. The solvent was removed under reduced pressure to afford a red residue which was washed with benzene and light petroleum. The compound $[\{Fe(cp)(CO)_2\}_2(SEt)][SbF_6]$ was crystallized from dichloromethane-light petroleum (yield 90%) while $[\{Fe(cp)(CO)_2\}_2(SBu^t)][SbF_6]$ was identified by means of i.r. only. The tetrafluoroborate salts were obtained analogously employing $Ag[BF_4]$ as oxidant.

$[\{Fe(cp)(CO)_2\}_2(SEt)][BPh_4]$. A solution of $[\{Fe(cp)(CO)_2\}_2(SEt)][ClO_4]$ (3 mmol) in acetone (50 cm^3) was obtained

as above using $AgClO_4$ as oxidant. The solvent was removed under reduced pressure and the residue redissolved in methanol (30 cm^3). Excess of $Na[BPh_4]$ in methanol (20 cm^3) was added and the product which separated from solution isolated. Further recrystallization was not necessary, yield 90%.

μ-Carbonyl-μ-alkylthio-bis[carbonyl(η-cyclopentadienyl-iron] (Fe-Fe) Salts. $[Fe_2(cp)_2(CO)_3SEt][SbF_6]$. A solution of $[\{Fe(cp)(CO)_2\}_2(SEt)][SbF_6]$ (0.47 g, 2 mmol) in thf (150 cm^3) was irradiated with u.v. light for 120 min. The product which separated from solution was isolated, washed with dichloromethane, and crystallized from acetone-dichloromethane, yield 50%.

Formation of $Fe(cp)(CO)_2Ph$ from $[\{Fe(cp)(CO)_2\}_2(SEt)]$ $[BPh_4]$. a) Photochemically. The compound $[\{Fe(cp)(CO)_2\}_2(SEt)][BPh_4]$ (0.5 g, 0.8 mmol) in thf (150 cm^3) was irradiated with u.v. light for 120 min. The solvent was removed under reduced pressure and the residue extracted with benzene. Evaporation of the extract afforded a brown residue which was re-extracted with cyclohexane. Removal of the solvent gave $[Fe(cp)(CO)_2Ph]$ as a brown crystalline material. The compound was identified by means of i.r. and p.m.r. spectroscopy only, yield 20%.
b) Thermally. A dichloromethane solution (50 cm^3) of $[\{Fe(cp)(CO)_2\}_2(SEt][BPh_4]$ (0.5 g, 0.8 mmol) was heated under reflux for 60 min. The solvent was removed under reduced pressure and the residue extracted with benzene; $[Fe(cp)(CO)_2Ph]$ was isolated from this solution and purified as described above, yield 10%.

$[Fe_2(cp)_2(CO)_3SEt]$. A suspension of $[Fe_2(cp)_2(CO)_3SEt]$ $[SbF_6]$ (0.24 g, 1 mmol) in thf (50 cm^3)was stirred over a stoich iometric

amount of 1% sodium amalgam for 10 min. The solution was filtered and the solvent removed under reduced pressure to afford the product as a green crystalline material.

TABLE 1.2

Colours, Conductivity and Analytical Data

Compound	Colour	Λ_0^*, $m\Omega^{-1}\ cm^2\ mol^{-1}$	Analysis % Found C	H	S	Calculated C	H	S
$[\{Fe(cp)(CO)_2\}_2(SEt)]SbF_6$	Red-brown	140	29.5	2.4	4.8	29.5	2.3	4.9
$[\{Fe(cp)(CO)_2\}_2(SEt)]BPh_4$	Red-purple	98	65.3	4.8	5.0	65.4	4.8	4.4
$[Fe_2(cp)_2(CO)_3(SEt)]SbF_6$	Olive-green	131	28.6	2.7	5.1	28.9	2.4	5.2
$[Fe_2(cp)_2(CO)_3(SEt)]BPh_4$	Green	103	65.7	5.1		65.7	5.1	

* 1×10^{-4} - 10×10^{-4} solutions in acetone

TABLE 1.3

Infra-red Spectroscopic Data

Compound	ν(CO) cm^{-1}
$[\{Fe(cp)(CO)_2\}_2(SEt)]SbF_6$	2057vs, 2043s, 2007vs, 2002sh [a]
$[\{Fe(cp)(CO)_2\}_2(SEt)]BPh_4$	2058vs, 2041s, 2008vs, 2003sh [a]
$[\{Fe(cp)(CO)_2\}_2(SEt)]BF_4$	2053vs, 2042s, 2007vs,br [a]
$[\{Fe(cp)(CO)_2\}_2(SEt)]ClO_4$	2051s, 2008s [a]
$[\{Fe(cp)(CO)_2\}_2(SBu^t)]SbF_6$	2052s, 2008s [a]
$[Fe_2(cp)_2(CO)_3(SEt)]SbF_6$	2044s, 2005s, 1829s [b]
$[Fe_2(cp)_2(CO)_3(SEt)]BPh_4$	2034s, 2009m(sh), 1845m [a]
$[Fe_2(cp)_2(CO)_3(SEt)]$	1970ms, 1773s [a]
$[(Ph_3P)_2N][Fe_2(cp)_2(CO)_3(SEt)]$	1927ms, 1690s [a]
$[Fe(cp)(CO)_2Ph]$	2022s, 1971s [c]

[a] Measured in CH_2Cl_2. [b] Measured as Nujol mull. [c] Measured in cyclohexane

TABLE 1.4

P.m.r. Spectroscopic Data. τ at 38°C

Compound	Cp proton resonances	Other resonances
$[\{Fe(cp)(CO)_2\}_2(SEt)]SbF_6$	4.45 [a]	7.50(q), 8.50(t) [J(HH)7.3] : Et
$[\{Fe(cp)(CO)_2\}_2(SEt)]BPh_4$	4.60 [a]	3.0 (mt) : C_6H_5 7.60(q), 8.80(t) [J(HH)7.3] : Et
$[Fe_2(cp)_2(CO)_3(SEt)]SbF_6$	4.27 [a]	7.26(q), 8.30(t) [J(HH)7.4] : Et
$[Fe_2(cp)_2(CO)_3(SEt)]BPh_4$	5.08 [b]	2.78 (mt) : C_6H_5 8.83(t) [J(HH) 8.0] : CH_3
$[Fe\ (cp)\ (CO)_2Ph]$	4.70 [c]	2.5 (mt) : C_6H_5

[a] Measured in $(CD_3)_2CO$. [b] Measured in CD_2Cl_2. [c] Measured in $CDCl_3$

CHAPTER 2

SOME MONO-ALKYLTHIO-BRIDGED COMPLEXES OF IRON AND MANGANESE

2.1 Introduction.

In the previous Chapter the synthesis of a dinuclear complex of iron bridged both by an alkylthio- and a carbonyl group, $[Fe_2(cp)_2(CO)_3(SEt)]X$ (X = a monovalent anion such as BF_4) was described. This complex was shown to be easily and reversibly reduced to the neutral and anionic species $[Fe_2(cp)_2(CO)_3(SEt)]^n$ (n = 0 and -1). However, attempts to oxidise it to a dication (n = +2) proved unsuccessful, decomposition always occurring. Failure to synthesize the dicationic species was attributed to the high positive charge reducing the metal d-orbital to bridging carbonyl-π^* orbital overlap and therefore weakening the Fe-bridging-CO bond, resulting in the breakup of the species. Attention was therefore turned to the possible synthesis of a dinuclear species in which a metal-metal bond is present, the overall charge of which would be zero. Such a complex should be susceptible to oxidation to a monocation and structural characterization of both the neutral and oxidized species should yield information about the relative ordering of the molecular orbitals in species of the type

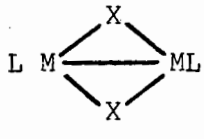

which contain a metal-metal bond.

Accordingly, the synthesis of the hypothetical dimanganese complex, I

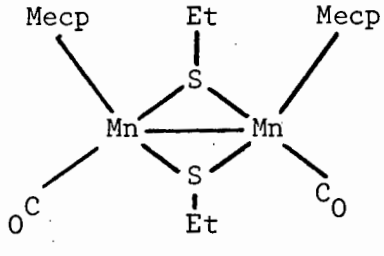

I

which is isoelectronic with $[Fe(cp)(CO)(SR)]_2^{2+}$, described previously[1.21, 1.23], was attempted.

2.2 The Attempted Synthesis of $[Mn(Mecp)(CO)(SR)]_2$.

A recognized synthesis of bridging-alkyl- or arylthio metal carbonyl derivatives involves the reaction of the parent carbonyl with R_2S, R_2S_2 or RSH (R = alkyl or aryl groups)[2.1]. The reaction is facilitated by irradiation of a solution of the reacting species in thf with ultra-violet light. Strohmeier has shown[2.2] that irradiation of $[Mn(cp)(CO)_3]$ in donor solvents such as acetone, thf and ethanol effects the replacement of one or more carbonyl groups with solvent molecules, to give, for instance, $[Mn(cp)(CO)_2(thf)]$. These solvent ligands are readily displaced by molecules of stronger ligating powers.

A solution, in thf, of $[Mn(Mecp)(CO)_3]$ and dibenzyldisulphide was irradiated with ultraviolet light for about 12 hours. The infra-red spectrum of a sample of the reaction mixture, taken after this period, indicated that the reaction was complete. The product which formed had ν(C-O) bands corresponding to those expected for $[Mn(Mecp)(CO)_2\{(PhCH_2)_2S_2\}]$. However, attempts to convert this compound to the bis(arylthio)-bridged dimer $[Mn(Mecp)(CO)(PhCH_2S)]_2$ proved unsuccessful, always resulting in decomposition of the mono-nuclear species to carbonyl-free products. Use of ethanethiol as the source of the bridging ligand also met with little success. Thus, although a second product (ν(C-O) = 1981 and 1918 cm^{-1}) as well as $[Mn(Mecp)(CO)_2(SEtH)]$ (ν(C-O) = 1934 and 1860 cm^{-1}) occurred on irradiation of a solution of $[Mn(Mecp)(CO)_3]$ and EtSH in thf with

ultraviolet light, it decomposed readily on heating. Failure to synthesize $[Mn(Mecp)(CO)(SR)]_2$ by these methods is attributed to the difficulty of removing carbonyl groups from derivatives of the type $[Mn(Mecp)(CO)_2L]$ [2.2].

A previous study has shown that the electrochemical oxidation of $[Fe(cp)(CO)(SMe)]$ results in the formation of the cationic dimer $[Fe(cp)(CO)(SMe)]_2^+$ [2.3,2.4]. It was therefore presumed that oxidation of the monomeric $[Mn(Mecp)(CO)_2(SEt)]^-$, prepared from $[Mn(Mecp)(CO)_2(thf)]$ and SEt^-, might result in the formation of the desired product.

Consequently, $[Mn(Mecp)(CO)_2(SEt)]^-$ was prepared by irradiating a thf solution of $[Mn(Mecp)(CO)_3]$ containing suspended NaSEt. Addition of 35% $HClO_4$ to the resulting red-brown reaction mixture, and exposure to the atmosphere, resulted in a colour change to deep green. The green product was isolated and characterized, by means of elemental analysis and conductivity measurements (Table 2.5), as the mono-bridged derivative

II.

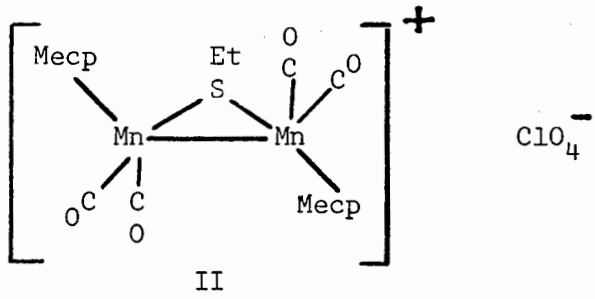

II

Confirmation of the stoichiometry and structure of this species as the *trans*-isomer, as well as the existence of a two-electron Mn-Mn bond (required by electronic book-keeping), was provided by a single crystal X-ray structural determination (described in Chapter 6). The structure of the cation is remarkably similar to that very recently

reported for the phenylacetylide 'carbene' bridged species, III, prepared from phenylacetylene and $[Mn(cp)(CO)_2thf]$[2.5]

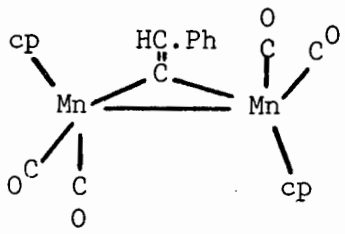

III

Relevant bond lengths and angles for the two complexes are set out in Table 2.1 for comparison.

TABLE 2.1

Comparison of Bond Lengths and Angles in the Related Complexes $[\{Mn(Mecp)(CO)_2\}_2(SEt)]^+ClO_4$, A and $[\{Mn(cp)(CO)_2\}_2(C{=}CH.PH)]$, B.

Complex	A	B
Bond Lengths:		
Mn - Mn	2.930 Å	2.734 Å
Mn - X (av)	2.26 Å	1.97 Å
(X is the bridging atom)		
Bond Angles:		
Mn - X - Mn	81°	88°
Mn(1) - Mn(2) - C(3)	108.6°	104°
Mn(1) - Mn(2) - C(4)	74.9°	79°
Mn(2) - Mn(1) - C(1)	113.2°	100°
Mn(2) - Mn(1) - C(2)	76.1°	77°
(C(1) to C(4) are carbonyl group carbon atoms)		
Angle between normals to the cyclopentadienyl rings	22°	9°

The similarity of $[\{Mn(Mecp)(CO)_2\}(SEt)]^+$ to $[\{Mn(cp)(CO)_2\}_2(C{=}CH.Ph)]$ lends weight to the description of SEt^- as a 'bridging carbenoid', put forward in the discussion of the structure of $[\{Mn(Mecp)(CO)_2\}(SEt)]^+$ in Chapter 6.

Apart from an extra peak at 1937 cm^{-1} in the former, resulting possibly from a site symmetry effect, the solid state and dichloromethane solution infra-red spectra of $[\{Mn(Mecp)(CO)_2\}_2SEt]ClO_4$ are very similar in the C-O stretching region (ν(C-O): 2015sh, 1994s, 1964s and 1937 m cm^{-1}, measured as a nujol mull; 2019sh, 1994s and 1969ms cm^{-1}, measured in CH_2Cl_2) suggesting that the solid state structure is retained, to some extent, in solution. Although the Mecp groups are magnetically non-equivalent for this molecular geometry, the room temperature p.m.r. spectrum of the complex reveals a single resonance for the methyls of the Mecp groups and a doublet for the protons bonded to the β- and γ-carbon atoms of the cyclopentadienyl rings. However, the same spectrum measured at 213K showed two doublets associated with these protons and two peaks assigned to the Mecp methyl groups. Although the resonance due to the methyl group of the SEt ligand remains unchanged on running the p.m.r. spectrum at 213K, the quadruplet due to the $-CH_2-$ group is split. As discussed in Chapter 6, this reversible temperature dependence of the p.m.r. spectrum is interpreted as being due to the presence, in solution, of two rapidly interconverting conformers of $[\{Mn(Mecp)(CO)_2\}_2SEt]^+$. Slowing down the rate of interconversion of the conformers by lowering the temperature causes the Mecp and $-CH_2-$ protons to become magnetically non-equivalent on a p.m.r. time scale, while the methyl protons of the SEt groups, which have more degrees of freedom than the other protons, still experience an average magnetic environment which is the same for the two conformers. On the infra-red time scale, however, the two conformers are distinguishable at both 213K and ambient temperatures. As pointed out in Chapter 5, the complexity of the infra-red spectrum suggests that the structures

of the two conformers should be quite dissimilar.

The mechanism for the formation of $[\{Mn(Mecp)(CO)_2\}_2SEt]ClO_4$ is not immediately clear. However, a similar monobridged dimanganese complex, $[\{Mn(Mecp)(CO)_2\}_2S]$, the structure of which has not been determined but which should, according to the 18-electron rule, contain a metal-metal bond, has been synthesized by reacting H_2S with $[Mn(Mecp)(CO)_2(thf)]$ at -79° in thf to give $[Mn(Mecp)(CO)_2(H_2S)]$ (the attempted synthesis of which was reported by Strohmeier and Guttenberger)[2.6] and allowing the solution to warm to room temperature. Treatment of $[Co(CO)_4]_2$ [2.7], $[Au(PPh_3)Cl]$ [2.8] or sodium molybdate [2.9] with H_2S also leads to the formation of sulphur-bridged dinuclear products. On this basis it is suggested that $[Mn(Mecp)(CO)_2(SEt)]^-$ is protonated to give $[Mn(Mecp)(CO)_2(H_2SEt)]^+$, and that the latter reverts to $[\{Mn(Mecp(CO)_2\}_2(SEt)]^+$ by loss of a hydrogen molecule, by a mechanism analogous to that involved in the formation of $[\{Mn(Mecp)(CO)_2\}_2S]$. $[Ru(NH_3)_5(H_2S)](BF_4)_2$ has recently been shown to decompose in the solid state, in the absence of water and atmospheric oxygen, by the loss of a hydrogen molecule[2.10].

2.3 The Redox Behaviour of $[\{Mn(Mecp)(CO)_2\}_2(SEt)]ClO_4$

This cation can be thought of as the two-electron oxidation product of the dinuclear anionic species $[\{Mn(Mecp)(CO)_2\}_2(SEt)]^-$, which is isoelectronic with the non-metal-metal-bonded species $[\{Fe(cp)(CO)_2\}_2(SEt)]^+$ the synthesis of which is described in Section 1.3. This anionic complex should result from the reaction of $[Mn(Mecp)(CO)_2(thf)]$ with the anion $[Mn(Mecp)(CO)_2(SEt)]^-$, in a manner exactly analogous to the preparation of $[\{Fe(cp)(CO)_2\}_2(SEt)]^+$ from $[Fe(cp)(CO)_2(solvent)]^+$ and $[Fe(cp)(CO)_2(SEt)]$. However, such a preparation was not performed in the course of this study. With a view to establishing whether the two species $[\{Mn(Mecp)(CO)_2\}_2SEt]^n$ (n = +1 and -1) are interconvertible according to the Scheme,

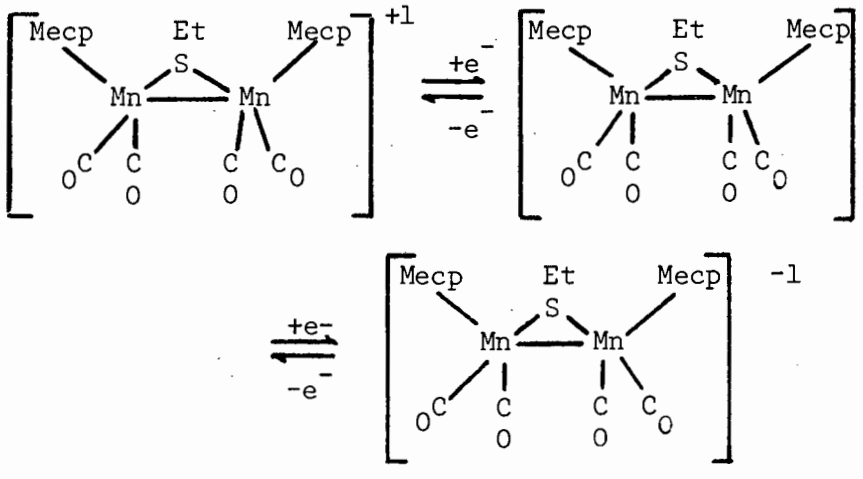

REDOX SCHEME

electrochemical studies were carried out on $[\{Mn(Mecp)(CO)_2\}_2(SEt)]ClO_4$. Using A.C. and D.C. polarography and cyclic voltammetry, it was established that the complex does, in fact, undergo two well-behaved one-electron reductions, and that these meet all the criteria for electrode reversibility at both mercury and platinum electrodes. At the dropping mercury electrode in acetone, using 0.1 M Et_4NClO_4 as

the support electrolyte, the successive reductions occur at $E_{\frac{1}{2}}$ (D.C. polarography) = +0.172V and -0.222V as measured against a silver-silver chloride electrode.

It was also found that the first reduction product, *i.e.* the neutral species $[\{Mn(Mecp)(CO)_2\}_2SEt]$ is indefinitely stable at 193K in the dark, if atmospheric oxygen is rigorously excluded. However, at room temperature it is thermally unstable and decays with a half life of approximately ten minutes. In addition, it is attacked by halide ions. Despite the difficulties caused in manipulation of the species by its photo- and thermal instability, both infra-red (in acetone) and e.s.r. (in acetone, in the presence of 0.1M $Bu^n_4NClO_4$) spectra have been recorded. The infra-red spectrum contains two peaks in the carbonyl stretching region at 1970 and 1900 cm^{-1}, while the e.s.r. spectrum shows an eleven-line signal (^{53}Mn, $I = \frac{5}{2}$) indicating that the unpaired electron in the neutral species is delocalized over two equivalent Mn atoms. The anionic species $[\{Mn(Mecp)(CO)_2\}_2(SEt)]^-$ was generated on an extremely small scale (5 mg) electrochemically and its infra-red spectrum shown to contain two peaks in the terminal carbonyl region at 1880 and 1800 cm^{-1}. It showed no e.s.r. signal.

2.4 The Electronic Structure of the Species $[\{Mn(Mecp)(CO)_2\}_2SEt]^n$ (n = +1, 0 and -1).

In the absence of structural information (save on the complexes $[\{Mn(Mecp)(CO)_2\}_2(SEt)]^+$ and $[\{Mn(Mecp)(CO)_2\}_2(C{=}CH.Ph]$) little is known for certain about the molecular orbital levels in these novel complexes. It is probable that the unpaired electron in $[\{Mn(Mecp)(CO)_2\}_2(SEt)]$ resides in an orbital which is antibonding with respect to the two Mn atoms, and the Mn - Mn distance corresponds to a bond order of 0.5, but direct proof of this supposition can only come from a complete structural analysis of this complex. Attempts are presently in progress to isolate the complex in a form suitable for X-ray crystallographic analysis.

2.5 Structural and Electrochemical Studies on $[\{Fe(cp)(CO)_2\}_2SEt]^+$.

The success of the electrochemical study described in Section 2.3 prompted further investigation of $[\{Fe(cp)(CO)_2\}_2(SEt)]^+$ whose synthesis was reported in Section 1.3. In a manner analogous to the two-electron electrochemical oxidation of $[\{Mn(Mecp)(CO)_2\}_2SEt]^-$ to the monocation, oxidation of $[\{Fe(cp)(CO)_2\}_2\ SEt]^+$ might be expected to yield $[\{Fe(cp)(CO)_2\}_2\ SEt]^{3+}$, isoelectronic with $[\{Mn(Mecp)(CO)_2\}_2(SEt)]^+$ and containing a formal Fe - Fe bond. However, the high overall charge on this hypothetical product may preclude its formation: nevertheless the study was considered worth attempting, as the intermediate dication $[\{Fe(cp)(CO)_2\}_2(SEt)]^{2+}$ might prove stable enough to be isolated.

In a preliminary study, the structures of $[Fe(cp)(CO)_2(SEt)]$ and $[\{Fe(cp)(CO)_2\}_2SEt]BF_4$ were determined. These anaylses are described in Chapters 3 and 4. As has been pointed out in Chapter 3, the compound whose structure was finally established to be that of the mono-nuclear $[Fe(cp)(CO)_2(SEt)]$ was first thought to be the mixed dinuclear complex $[Fe(cp)(CO)_2(SEt)(CO)_2(Mecp)Mn]$. However, on realization of the true nature of the complex the structure determination was continued, as interesting comparisons could be made of bond lengths and angles in the mono- and dinuclear complexes $[Fe(cp)(CO)_2(SEt)]$, $[\{Fe(cp)(CO)_2\}_2(SEt)]BF_4$ and $[Fe_2(cp)_2(CO)_3(SEt)]SbF_6$.

2.5.1 The effects of coordination, of $[Fe(cp)(CO)_2(SEt)]$ to $[Fe(cp)(CO)_2(solvent)]^+$, on bond lengths and angles in $[Fe(cp)(CO)_2SEt]$ and the further effects on these parameters of formation of the hetero-bridged species $[Fe_2(cp)_2(CO)_3(SEt)]^+$.

Relevant parameters for the three complexes, and the sulphur-bridged species $[\{Fe(cp)(CO)_2\}_2(SO_2)]$ and $[\{Fe_2(cp)_2(CO)_3(SO_2)]$ are set out in Table 2.2 for comparison.

On comparing the Fe - S bond lengths for the five complexes, it is apparent that neither coordination of $[Fe(cp)(CO)_2(SEt)]$ to give $[\{Fe(cp)(CO)_2\}_2(SEt)]^+$ nor the increase in overall charge affects the Fe - S bond to any extent. As Churchill and Kalra point out[2.11], the bond length itself is somewhat shorter than would be expected from consideration of the covalent radii of the carbon and sulphur atoms[2.12], suggesting some π-interaction between the two. The Fe - S bond in the non-metal-metal bonded $[\{Fe(cp)(CO)_2\}_2(SO_2)]$ is very slightly shorter than in the above species. However, on 'condensation' of the non-bonded species to give the metal-metal bonded dibridged species a significant decrease. of the order of 4%, occurs in the Fe - S distance: it may be surmised that π-interaction between the S p-orbitals and iron d-orbitals has increased appreciably. The S - C(ethyl) bond length increases on coordination of $[Fe(cp)(CO)_2(SEt)]$ to give the dinuclear species, reflecting a probable shift of electron density from the sulphur onto the iron atom (which, in $[\{Fe(cp)(CO)_2\}_2(SEt)]^+$ will be somewhat positively charged). The S - C(ethyl) bond length appears insensitive to condensation of $[\{Fe(cp)(CO)_2\}_2(SEt)]^+$ to the dibridged species. As expected, the Fe - C(cp) bond lengths are unaffected by either overall charge or the existence of an Fe - Fe bond. The effects on the Fe - carbonyl parameters of coordination and charge are significant and show some correlation with the infra-red spectra of these species. Thus, it is observed that coordination of neutral $[Fe(cp)(CO)_2(SEt)]$ to give

TABLE 2.2

Related Bond Lengths (Å) and Angles (°) in $[Fe(cp)(CO)_2(SEt)]$, A; $[\{Fe(cp)(CO)_2\}_2(SEt)]^+$, B; $[\{Fe(cp)(CO)_2\}_2(SO_2)]$, C; $[Fe_2(cp)_2(CO)_3(SEt)]^+$, D; and $[Fe_2(cp)_2(CO)_3(SO_2)]$, E.

Complex	A	B	C	D	E
Fe-S(av)	2.296(2)	2.300(2)	2.280(6)	2.203(3)	2.178(4)
Fe-C(O)(av)	1.751(5)	1.775(6)	1.768(2)	1.77 (1)	1.763(4)
C-O(av)	1.150(6)	1.140(5)	1.140(3)	1.135(10)	1.148(4)
Fe-C(cp)(av)	2.10 (1)	2.100(6)	2.104(2)	2.10 (1)	2.104(4)
S-C(ethyl)	1.819(7)	1.851(5)		1.84 (1)	
S-Fe-C(O)(av)	90.7	94.8	88.7	95.5	90.8
C(O)-Fe-C(O)(av)	93.9	93.5	94.2	87.9	87.1
Fe-S-Fe		117.4	118.0	71.7	73.0

the cationic dinuclear complex $[\{Fe(cp)(CO)_2\}_2(SEt)]^+$ results in an increase in the Fe - C(O) bond length of about 0.025 Å, equivalent to four standard deviations. This implies a reduction in the d - π^* overlap between the Fe and C atoms, which should lead to an increase in the C-O bond order and force constant. The former is in fact reflected by a slight decrease of about 0.01 Å in the C-O distance (equivalent to 2σ), which is also found in $[Fe_2(cp)_2(CO)_3(SEt)]^+$. However, such a slight change is not really significant in terms of the possible errors in these parameters. The latter is reflected in the increase in the terminal carbonyl stretching frequencies from 1980 and 2021 cm^{-1} in the mononuclear species, to 2007 - 2053 cm^{-1} in the mono- and dibridged cationic complexes. A similar effect is observed in the SO_2-bridged neutral complexes: here the inductive effect of the SO_2 ligand is presumably causing a drift of electron density away from the Fe - C - O system. However, the effect is not quite as marked.

The bond angles round the iron atoms do not show any systematic trends, and their mean is approximately 92°, as would be expected for octahedrally coordinated Fe atoms. Some repulsion is possible between *cis*-disposed ligands.

The bond angles Fe - S - Fe reflect the presence of an Fe - Fe bond in $[Fe_2(cp)_2(CO)_3(SO_2)]$ and $[Fe_2(cp)_2(CO)_3(SEt)]^+$, decreasing from a normal tetrahedral angle to acute angles of 71.7 and 73°. As mentioned before, it appears unlikely that further contractions in this angle are possible for such ligands. Conversely, in the non-bonded species $[\{Fe(cp)(CO)_2\}_2(SO_2)]$ and $[\{Fe(cp)(CO)_2\}_2SEt]^+$ these angles are somewhat larger than the tetrahedral angle of 109.5, suggesting some repulsion between the bulky $\{Fe(cp)(CO)_2\}$ moieties.

2.5.2 Comparison of the Structures of $[L_2SEt]^+$ (L = $\{Fe(cp)(CO)_2\}$ or $\{Mn(Mecp)(CO)_2\}$) with the Structures of other Complexes of the type $[L_2M]^n$ (M = bridging group, n = overall charge).

The molecular structures of some twelve complexes of the type $[L_2M]^n$ have been reported. For L = $\{Fe(cp)(CO)_2\}$ the complexes for which M = SO_2, $GeCl_2$, $SnCl_2$, $SnMe_2$, $Sn(ONO)_2$, $Sn(\sigma\text{-}cp)_2$, $SbCl_2$, I, $(CH_2)_3$ and $(CH_2)_4$ have been the subjects of X-ray crystallographic studies. In addition, for L = $\{Mn(cp)(CO)_2\}$, the structure of $[L_2(Ph.CH{=}C)]$, a bridging carbene species, has been described. It is instructive to compare the conformers of these species as observed in the solid state.

The configurations, values of τ (defined as the torsion angle ct(cp)-metal atom-metal atom-ct(cp) where ct(cp) means the centroid of the cyclopentadienyl group) and molecular symmetries for the complexes are set out in Table 2.3. Structures A, B, and C are depicted schematically below the Table.

TABLE 2.3

Structures and Approximate Symmetries of Complexes of the type $[L_2M]^n$

M	τ	Structure	Symmetry	Reference
a) L = $\{Fe(cp)(CO)_2\}$				
SEt	58.2	C	C_1	
SO_2	98.9	A	C_2 (approx)	1.51
$GeCl_2$	-33.2	A	C_2 (exact)	1.73
$SnCl_2$	74.2	A	C_2 (exact)	1.45
$SnMe_2$	~60	A	C_2 (approx)	1.48
$Sn(ONO)_2$	~60	A	C_2 (exact)	1.49
$Sn(\sigma\text{-cp})_2$	~60	A	C_2 (approx)	1.50
$SbCl_2$ (a)	-71.8	A	C_2 (approx)	1.44
$SbCl_2$ (b)	-76.7	A	C_2 (approx)	1.44
I	153.0	B	C_2 (approx)	1.43
b) L = $\{Mn(cp)(CO)_2\}$ or $\{Mn(mecp)(CO)_2\}$				
SEt	~150	B	C_2 (approx)	
Ph.CH=C	~150	B	C_2 (approx)	2.5

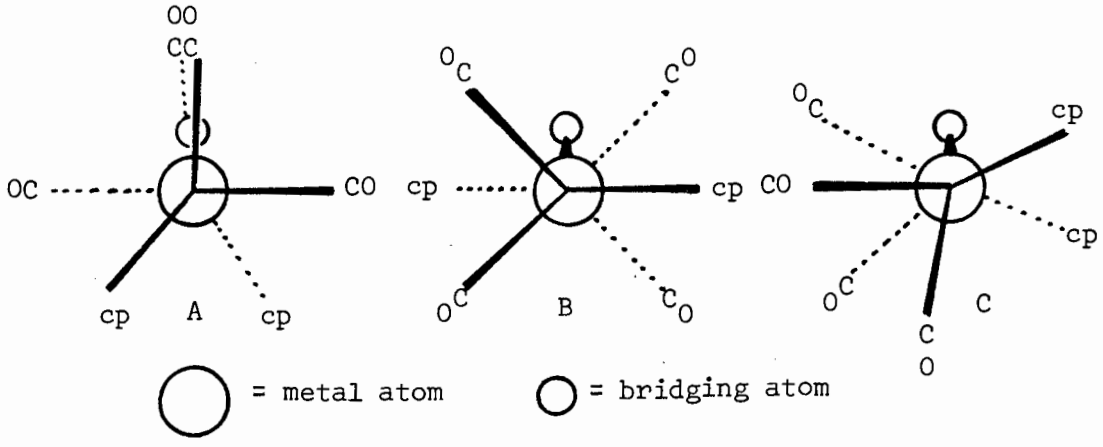

It is interesting to note that, to date, the somewhat varied family of complexes, $[L_2M]^n$, have been found to crystallize in only 3 preferred conformations - clearly, individual complexes vary somewhat but the gross features of the preferred conformation are still observed. Thus, in conformation A, two carbonyl groups are eclipsed and two are *trans* with respect to the metal-metal vector and the cyclopentadienyl groups lie on the same side of the plane defined by the metal atoms and the *trans*-carbonyl groups; the bridging ligand lies on the other side of this plane. This structure has C_2 symmetry and is that found for all $[L_2M]^n$ complexes where L is a symmetrically disubstituted ligand. In conformation B, that adopted by $[\{Fe(cp)(CO)_2\}_2I]^+$ where a single iodine atom bridges the two iron atoms, each cyclopentadienyl group is staggered with respect to the carbonyl groups on the other metal atom if the molecule is viewed down the metal-metal vector. This structure also has C_2 symmetry. If the substituents, (Et) and (Ph.CH=) of the bridging atoms S and C in the respective manganese complexes $[\{Mn(Mecp)(CO)_2\}_2(SEt)]^+$ and $[\{Mn(cp)(CO)_2\}_2(C{=}CH.Ph)]$ are disregarded, then these complexes may be considered to have molecular symmetry C_2 according to conformation B in the solid state.

The only example of an $[L_2M]^n$ complex, then, with a symmetry other than C_2, is $[\{Fe(cp)(CO)_2\}_2SEt]^+$. It is debatable whether the unsymmetrical nature of the bridging ligand SEt is instrumental in causing such a conformation to be preferred, as the two manganese complexes discussed previously crystallize in approximate C_2 symmetry and yet they both have unsymmetrical bridging groups. In the absence of further structural information about this type of complex, it can only be said that if the bridging group is symmetrically disubstituted,

a structure similar to A is likely to be adopted in the solid state. Any predictions on the possible preferred conformations of $[L_2M]^n$ complexes with an unsymmetrical bridging ligand must await the arrival of more data on these species.

2.6 The Redox Behaviour of $[\{Fe(cp)(CO)_2\}_2SEt]^+$.

Preliminary A.C. and D.C. polarographic and cyclic voltammetric studies have indicated that $[\{Fe(cp)(CO)_2\}_2SEt]^+$ undergoes one one-electron oxidation to, presumably, a dicationic species $[\{Fe(cp)(CO)_2\}_2SEt]^{2+}$. However, this oxidation is not reversible and the polarographic half-wave associated with it is very broad. The potential, $E_{\frac{1}{2}}$, for the oxidation is approximately +0.8V. It would appear that the increased charge on the oxidized species, reduces the stability of this species, causing decomposition.

2.7 The Synthesis of $[Fe(cp)(CO)_2(SEt)(CO)_2(Mecp)Mn]$.

This species was synthesized with two aims in mind:

i. Since it is a neutral complex, electrochemical oxidation may result in the isolation of a monocation $[Fe(cp)(CO)_2(SEt)(CO)_2(Mecp)Mn]^+$ in which a one-electron 'bond' between the Fe and Mn might exist; and

ii. it was desired to investigate whether the complex

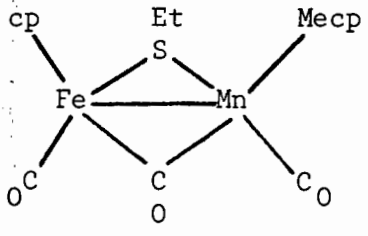

could be synthesized; the Fe - Mn bond length should be intermediate between a typical Mn - Mn bond length of 2.9 Å and an Fe - Fe bond length of 2.6 Å; *viz*, some 2.75 Å.

$[Fe(cp)(CO)_2SEt]$ was synthesized as before. A solution of $[Mn(Mecp)(CO)_2(thf)]$ was prepared by irradiation of an $[Mn(Mecp)(CO)_3]$ solution in thf for three hours. A third of a molar equivalent of $[Fe(cp)(CO)_2SEt]$ was added, and the mixture stirred under nitrogen. A colour change from deep cherry-red to an intense dark green was observed. Chromatography of the products of this reaction gave a fair yield of the required product, after crystallization from low-boiling petroleum ether, as dark green crystals, which were characterized by infra-red and p.m.r. spectroscopy and microanalysis (C, H and S) (Tables 2.4 and 2.5). The stability of the complex in air is poor, but it appears to be indefinitely stable under nitrogen.

2.7.1 The Attempted Synthesis of $[Fe(cp)(CO)_3SEt(Mecp)Mn]$.

The mono-bridged Fe - Mn species was prepared as above. A

solution of the compound in low-boiling petroleum ether was irradiated for a short time, and a red-brown crystalline precipitate was formed. Characterization of this precipitate by infra-red and p.m.r. spectroscopy and microanalysis showed it to be $[Fe(cp)(CO)_2]_2$. Decomposition of the starting compound had clearly taken place, in a manner analogous to the decomposition of $[\{Fe(cp)(CO)_2\}_2SO_2]$, upon irradiation with ultraviolet light, to yield $[Fe(cp)(CO)_2]_2$ and mononuclear manganese derivatives which were not characterized.

Further attempts to prepare the hetero-dibridged species $[Fe(cp)(CO)_3SEt(Mecp)Mn]$ were not made.

2.7.2 Electrochemical Studies on $[Fe(cp)(CO)_2SEt(CO)_2(Mecp)Mn]$.

An electrochemical study has been initiated on the complex but so far no results have been made available.

2.8 Summary.

The synthesis of an unusual mono-bridged dimanganese cation, $[\{Mn(Mecp)(CO)_2\}_2SEt]^+$, has been described. It has been shown (electrochemically) that this complex exhibits two reversible one-electron reductions, to yield a very unstable anion. The infra-red spectrum of this species, as well as the e.s.r. spectrum of the intermediate neutral species, has been measured. The e.s.r. spectrum of the neutral species may be explained in terms of an unpaired electron occupying a molecular orbital which is localized on two equivalent manganese atoms. The structures of $[Fe(cp)(CO)_2(SEt)]$ and $[\{Fe(cp)(CO)_2\}_2SEt]BF_4$ are described, and relevant bond lengths and angles are compared among these species, as well as the sulphur-bridged complexes $[\{Fe(cp)(CO)_2\}_2SO_2]$ and $[Fe_2(cp)_2(CO)_3(SO_2)]$. The conformations and molecular symmetries of a variety of dinuclear monobridged complexes of the type $[L_2M]^n$ where L = $\{Fe(cp)(CO)_2\}$, $\{Mn(cp)(CO)_2\}$ or $\{Mn(Mecp)(CO)_2\}$, M is a bridging group and n is the overall charge, are compared with those of $[\{Fe(cp)(CO)_2\}_2SEt]^+$ and $[\{Mn(Mecp)(CO)_2\}_2SEt]^+$. Finally the synthesis of the mixed iron manganese complex, $[Fe(cp)(CO)_2SEt(CO)_2(Mecp)Mn]$ is described.

2.9 Experimental.

Synthesis of $[\{Mn(Mecp)(CO)_2\}_2(SEt)]ClO_4$.

A solution of $[Mn(Mecp)(CO)_3]$ (2g, 9.2 mmol) and NaSEt (5g, 59.5 mmol) in tetrahydrofuran (100 ml) was irradiated with ultraviolet light until reaction was near complete as shown by i.r. spectroscopy (*ca.* 12 hours). An aqueous solution of 35% perchloric acid (100 ml) was then added to the solution under aerobic conditions, while stirring, whereupon the solution changed from orange-brown through red to green over 5 mins. A large volume of water was added (*ca.* 250 ml) and the product extracted with dichloromethane. The extract was dried and the solvent removed under reduced pressure. The residue was crystallized from dichloromethane/petroleum ether. Yield : 30%.

Synthesis of $[Fe(cp)(CO)_2SEt(CO)_2(Mecp)Mn]$ -

A solution of $[Mn(Mecp)(CO)_3]$ (3g, 13.8 mmol) in thf (100ml) was irradiated with ultraviolet light until evolution of CO had ceased (*ca.* 3 hours). A solution in 20 ml of thf of $[Fe(cp)(CO)_2(SEt)]$ (1gm, 4.2 mmol) was added and the mixture stirred for 1 hour. Solvent was removed under reduced pressure and the crude product was dissolved in 30 ml of a mixture of low-boiling petroleum ether and benzene (2:1 v/v), and loaded onto an alumina chromatography column (Merck, neutral, Grade III). The column was flushed once with pure petroleum ether, and then the product was eluted with a 1:1 mixture (v/v) of benzene and 60°-80°-boiling petroleum ether. The solvent was partially removed by evaporation, and the product was recrystallized from 60°-80° petroleum ether at $-15^{\circ}C$. The yield was 1.2 gm (67% of theoretical) of glossy black crystals, soluble in all common organic solvents except low-molecular weight alkanes, to give solutions which decompose rapidly, as observed by monitoring with infra-red and p.m.r. spectroscopy.

TABLE 2.4

Infra-red and P.m.r. Spectroscopic Data.

Complex	ν(CO) cm^{-1}	τ at 38°C
$[\{Mn(Mecp)(CO)_2\}_2SEt]ClO_4$		4.78 (s,4H)
		5.00 (s,4H)
	2019sh, 1994s, 1969s	6.62 (q, 2H, J = 7.5Hz)
		8.00 (t, 3H, J = 7.5Hz)
		7.87 (s, 6H)
$[Fe(cp)(CO)_2SEt(CO)_2(Mecp)Mn]$		4.99 (s, 5H)
		5.60 (s, 2H)
	1836s, 1903s, 1985s,	5.80 (s, 2H)
		7.68 (q, 2H, J = 8.0Hz)
	2031s	8.80 (t, 3H, J = 8.0Hz)
		8.15 (s, 3H)

TABLE 2.5

Colours and Conductivity Data.

Complex	Colour	Analytical : Found (%)				Calculated (%)			
		C	H	N	S	C	H	N	S
$[\{Mn(Mecp)(CO)_2\}_2SEt]ClO_4$	Green	39.8	3.6	-	5.8	40.0	3.6	-	5.9
$[Fe(cp)(CO)_2SEt(CO)_2(Mecp)Mn]$	Green	47.2	3.9	-	7.3	47.7	4.0	-	7.5

Λ_0 for $[\{Mn(Mecp)(CO)_2\}_2SEt]ClO_4$ = 138 Ω^{-1} cm^2 mol^{-1}

CHAPTER 3

3.1 INTRODUCTION. GENERAL CRYSTALLOGRAPHIC EXPERIMENTAL AND COMPUTATIONAL PROCEDURES.

The methods used for preliminary space-group determination of, and X-ray diffraction data collection from each of the complexes whose structure determinations are described in this and subsequent chapters did not vary in the main and are summarized in this Section.

3.1.1 Density Determination.

Densities of suitable crystals of the complexes were determined by flotation in a mixture of xylene and methylene iodide, except in the case of $[Fe(cp)(CO)_2SEt]$; for solubility reasons a mixture of saturated aqueous zinc bromide and sodium chloride solutions was used here.

3.1.2 Preliminary X-ray Analysis.

Based on layer-line spacing and systematic absences of reflections in single crystal oscillation, Weissenberg, cone-axis and precession photographs, unit cell dimensions and space group symmetries were determined for the five complexes. In the cases of $[Fe(cp)(CO)_2SEt]$ and $[Fe_2(cp)_2(CO)_3SEt]SbF_6$ systematic absences did not differentiate between centric and acentric space groups; the ambiguities encountered were resolved as described in the relevant Sections. Nickel-filtered CuK_α radiation (λ = 1.542 Å) was used with Stoe (Heidelberg) Weissenberg and precession goniometers. X-ray generators (Philips PW1120 and PW1008) were operated at 20mA and 40kV. X-ray films were processed in the conventional manner.

3.1.3 Diffractometer Data Collection.

Suitable crystals were cut to roughly cubic dimensions, or (in the cases of $[\{Fe(cp)(CO)_2\}_2SEt]BF_4$ and $[Fe(cp)(CO)_2(SEt)]$) ground to spheres to minimise absorption and mounted on glass fibres. Intensity data collection was carried out at the National Physical Research Laboratory, C.S.I.R. (Pretoria) on a Philips PW1100 computer-controlled four-circle diffractometer employing graphite monochromated MoK_α x-radiation (λ = 0.7107 Å). Lattice constants were obtained by a least-squares fit of the χ, ϕ and 2θ angles of 25 reflections accurately centred on the diffractometer. The ω-2θ scan mode was used for all data collections. For any one crystal, the intensities of three suitable reference reflections were measured every hour to monitor crystal and instrumental stabilities. The standard error $\sigma(I_{rel})$ in the relative integrated intensity I_{rel} was calculated by

$$\sigma(I_{rel}) = [(0.02N_o)^2 + K^2N_b + N_o]^{\frac{1}{2}} \quad 3.12$$

where N_o is the gross peak count for the reflection, N_b the background count (measured on each side of the peak) and K the ratio of scan to background times. The criterion for a reflection being considered 'observed' varied from complex to complex and is discussed separately for each. Lorentz-polarization corrections were applied automatically at the C.S.I.R. in the process of transferring intensity data to punched cards.

3.1.4 Computation.

All calculations were performed on a Univac 1106 computer at the Computer Centre, University of Cape Town. The program SHELX[3.1]

was used for data reduction and structure determination. It was found necessary, during the structure determination of $[Fe(cp)(CO)_2SEt]$, to employ the subroutine NORMSF (normalized structure factor calculation of the XRAY 72 program library[3.2] to confirm the correct choice of space group. XANADU[3.3] was used to calculate bond distances, angles, torsion angles and least square planes, while PLUTO[3.4] and ORTEP[3.5] were used to obtain molecular illustrations. GPCP[3.6] was employed to produce a contour map of the disordered cyclopentadienyl ring in $[Fe(cp)(CO)_2SEt]$ while a short program MAP (listed in Appendix) was written by the author to translate the large volume of Fourier map data output by SHELX into a format suitable for input to GPCP for this purpose.

In all cases, the agreement between observed (F_o) and calculated (F_c) structure factors is expressed by the conventional residual factors defined by

$$R = \frac{\Sigma|F_o - F_c|}{\Sigma|F_o|} = \frac{\Sigma|\Delta|}{\Sigma|F_o|}$$

and

$$R_w = \frac{\Sigma w^{\frac{1}{2}}|\,|F_o| - |F_c|\,|}{\Sigma w^{\frac{1}{2}}|F_o|}$$

where $w = \frac{k}{[\sigma^2(F) + gF^2]}$, [3.1]; the value of k was redetermined after each structure factor calculation. The value of g was chosen to give the smallest variation of $w\Delta^2$ with the magnitude of F_c, except in the cases of $[\{Fe(cp)(CO)_2\}_2SEt]BF_4$ and $[RhBr_2(NO)\{P(OPh)_3\}_2]$ where g = 0.0.

Thermal parameters are of the form:

$\exp[-2\pi^2(U_{11}h^2a^{*2} + U_{22}k^2b^{*2} + U_{33}l^2c^{*2} + 2U_{12}hka^*b^* + 2U_{13}hla^*c^* + 2U_{23}klb^*c^*) \times 10^3]$ where U_{ij} are the anisotropic temperature factors

referred to in the subsequent text. Scattering factors for all elements except hydrogen were those of Cromer and Mann[3.7]; for hydrogen the scattering factors of Stewart *et al*[3.8] were used. Values of the absorption coefficient, A*, are from Ref. 3.9.

For the sake of clarity, hydrogen atoms have been omitted from all molecular illustrations.

3.2 THE DETERMINATION OF THE CRYSTAL AND MOLECULE STRUCTURE OF ETHYLTHIO-η-CYCLOPENTADIENYLDICARBONYLIRON: $[Fe(cp)(CO)_2SEt]$

Before describing the determination of the structure of this complex it is necessary to point out that initially, the crystals that were obtained were thought to have the formula $[Fe(cp)(CO)_2SEt(CO)_2(Mecp)Mn]$, that of the mixed manganese-iron complex whose synthesis is described in Chapter 2. This error came about as follows: the crystals employed were selected by hand from the crystalline mass obtained by cooling a solution in petroleum ether of $[Fe(cp)(CO)_2SEt(CO)_2(Mecp)Mn]$ to $-25^{\circ}C$. They were lustrous black needles which had apparently grown separately from the main body of glossy black lozenges. At the same time that these crystals were selected for X-ray crystallographic analysis, a sample was removed from the remaining mass for physical and chemical characterization - the results thereof showing that the complex was indeed $[Fe(cp)(CO)_2SEt(CO)_2(Mecp)Mn]$ which has an intense dark green colour in solution. The full characterization is detailed in Chapter 2. Separate identification of the needles selected for the structure determination was not considered. However, determination of the density of the crystals and their unit cell dimensions led to a value for Z of two molecules of $[Fe(cp)(CO)_2SEt(CO)_2Mecp)Mn]$ per unit cell. Systematic absences in the reflection established the space group as either Pnma or $Pn2_1a$. It was immediately obvious that the complex under investigation could not be $[Fe(cp)(CO)_2SEt(CO)_2(Mecp)Mn]$, nor indeed any dinuclear complex of iron or manganese bridged by a tetrahedral sulphur atom. Nevertheless, it was decided to proceed with the X-ray analysis, In order to establish the nature of the complex being investigated.

For a notional Z of 2 in Pnma[3.9], the asymmetric unit must comprise half the molecule and exhibit Laue symmetry m. The constraints that would thereby be imposed upon an asymmetrical dinuclear complex such as $[Fe(cp)(CO)_2SEt(CO)_2(Mecp)Mn]$ are remarkably stringent, one of them being that each metal atom is related to the other three by the symmetry operations of Pnma which limit their closest approach to a/2 or b/2 Å, whichever is the smaller. In this case, b/2 = 4.91 Å. Since Fe - S and Mn - S bond distances vary between about 2.2 and 2.3 Å[3.10], the presence of a dinuclear complex containing iron, and/or manganese, bridged by a tetrahedral sulphur atom, can be discounted.

The space group $Pn2_1a$ has four equivalent positions: again, for Z = 2 the asymmetric unit must be one half of the molecule of $[Fe(cp)(CO)_2SEt(CO)_2(Mecp)Mn]$. Such a bisection, however, is not consistent with the symmetry operations of $Pn2_1a$ in that generation of full atoms from half-atoms is required.

Although the nature of the compound was therefore uncertain, it seemed likely that it was a mononuclear complex containing either a $Fe(cp)(CO)_2$ or $Mn(Mecp)(CO)_2$ moiety, and the elucidation of the structure was based upon this supposition.

Density Determination.

The crystal density was measured as 1.51 $gm\,cm^{-3}$ by flotation in a mixture of saturated aqueous solutions of ZnBr and NaCl.

Space group assignment

The systematic absence of reflections of the types $0k\ell$: $k+\ell$ = 2n+1 and hk0 : h = 2n+1 indicated either the centric space group Pnma or the acentric $Pn2_1a$[3.9].

Diffractometer Data Collection

Three dimensional intensity data were collected by the ω-2θ scan technique (scan width 1.2°θ, scan speed 0.04°θ sec^{-1}) in the range $6^\circ \leq 2\theta \leq 54^\circ$ from a spherical crystal of diameter 0.45 mm. During the data collection, an average decrease in intensity of 6% was observed in the three reference reflections monitored. A total of 1178 reflections were collected, 229 of which were systematically absent on space group equivalent. Of the remainder, 885 had $I_{rel} > 2\sigma(I_{rel})$ and were considered observed.

For the crystal selected, μR was 0.69 and the variation in A^* over the θ range scanned was less than 5%[3.9]; absorption corrections were therefore deemed unnecessary. Crystal data is summarized in Table 3.2.1.

TABLE 3.2.1

Molecular formula	$[Fe(C_5H_5)(CO)_2SC_2H_5]$
Molecular weight	238.1 g $mole^{-1}$
Space group	Pnma
a = 14.118(5)	Dm = 1.51 gm cm^{-3}
b = 9.822(5)	Dc = 1.53 gm cm^{-3} for Z = 4
c = 7.443(4)	$\mu(MoK_\alpha)$ = 15.43 cm^{-1}
V = 1032.10 $\AA^3$	F(000) = 488

Solution and refinement of the structure

Although at this stage the composition of the crystals was not known with certainty, it seemed reasonable to assume from density considerations that there were, indeed, four heavy atoms per unit cell. A three dimensional Patterson map was computed and searched for vectors arising from these four atoms. The expected positions of such vectors are given in Table 3.2.2. At the same time, normalized

TABLE 3.2.2

	$x, \frac{1}{4}, z$	$-x, \frac{3}{4}, -z$	$\frac{1}{2}-2x, \frac{3}{4}, \frac{1}{2}+z$	$\frac{1}{2}+x, \frac{1}{4}, \frac{1}{2}-z$
$x, \frac{1}{4}, z$	0, 0, 0	$-2x, \frac{1}{2}, -22$	$\frac{1}{2}-2x, \frac{1}{2}, \frac{1}{2}$	$\frac{1}{2}, 0, \frac{1}{2}-2z$
$-x, \frac{3}{4}, -z$	$2x, \frac{1}{2}, 2z$	0, 0, 0	$\frac{1}{2}, 0, \frac{1}{2}+2z$	$\frac{1}{2}+2x, \frac{1}{2}, \frac{1}{2}$
$\frac{1}{2}-x, \frac{3}{4}, \frac{1}{2}+z$	$\frac{1}{2}+2x, \frac{1}{2}, \frac{1}{2}$	$\frac{1}{2}, 0, \frac{1}{2}-2z$	0, 0, 0	$2x, \frac{1}{2}, -2z$
$\frac{1}{2}+x, \frac{1}{4}, \frac{1}{2}-z$	$\frac{1}{2}, 0, \frac{1}{2}+2z$	$\frac{1}{2}-2x, \frac{1}{2}, \frac{1}{2}$	$-2x, \frac{1}{2}, 2z$	0, 0, 0

structure factors, E, were calculated from the diffraction data[3.2]. E_{hkl} is defined as

$$E^2_{hkl} = \frac{U^2_{hkl}}{\overline{U^2}}$$

where U_{hkl} is a structure factor which has the same phase as F_{hkl}, but whose value ranges from -1 to +1, the extreme cases occurring when all the atoms in the unit cell scatter in phase. The distribution of the $|E|$ values, although effectively independent of the size and content of the unit cell, depends on the presence or absence of a centre of symmetry in the space group. Thus consideration of the distribution pertaining in this particular case (Table 3.2.3) showed that the space group of the crystals was very probably Pnma; this group was used in subsequent calculations.

From the Patterson map, the coordinates of a strong scattering centre were calculated as 0.773, 1/4, 0.75. An electron density map was computed phased on an iron atom with these coordinates. The residual factor R was 0.45 and several other peaks were present in the map in chemically reasonable positions for a carbonyl group and the ethylthio-group. It was now apparent that the crystals under investigation were composed of the dark brown, neutral, mononuclear iron complex $[Fe(cp)(CO)_2SEt]$ (the corresponding ethylthiomanganese complex $[Mn(Mecp)(CO)_2SEt]^-$ [3.11] is anionic and very air sensitive) formed by disproportionation of $[Fe(cp)(CO)_2SEt(CO)_2(Mecp)Mn]$ during recrystallization.

A difference electron density map phased on the iron atom, the carbonyl group and the ethyl-thio half-group of the asymmetric unit revealed the two and a half carbon atoms comprising the half cyclopentadienyl group in the asymmetric unit. Eight cycles of full-matrix least-squares refinement with anisotropic temperature factors assigned to all non-cyclopentadienyl atoms resulted in an R of 0.08 based on all non-hydrogen atoms. The constraints $U_{12} = U_{23} = 0$ were applied to all

TABLE 3.2.3

NORMALIZED STRUCTURE FACTOR STATISTICS FOR $[Fe(cp)(CO)_2SEt]^{3.2}$

Function	Theoretical		$[Fe(cp)(CO)_2SEt]$
	Centric	Acentric	
Av. $\|E\|$	0.798	0.886	0.779
Av. $\|E\|^2$	1.000	1.000	1.000
Av. $\|E^2-1\|$	0.968	0.736	1.014
Av. $\{\|E^2-1\|\}^2$	2.000	1.000	1.748
Av. $\{\|E^2-1\|\}^3$	8.000	2.000	4.845
Percentage of:			
$\|E\| > 3.0$	0.27	0.01	0.0
$\|E\| > 2.0$	4.55	1.83	4.09
$\|E\| > 1.8$	7.19	3.92	7.58
$\|E\| > 1.6$	16.15	14.09	19.78
$\|E\| > 1.0$	31.73	36.79	33.09

TABLE 3.2.4

FRACTIONAL ATOMIC COORDINATES ($\times 10^4$) AND TEMPERATURE FACTORS ($\times 10^3$) AND THEIR e.s.d's.

Atom	x/a	y/b	z/c	U_{11} or U_{iso}	U_{22}	U_{33}	U_{12}	U_{13}	U_{23}
Fe	2272(1)	7500	2573(1)	44(1)	41(1)	42(1)	0	1(0)	0
S	1970(1)	7500	-458(2)	48(1)	67(1)	42(1)	0	3(1)	0
C(1)	1443(4)	8802(6)	2900(6)	56(3)	63(3)	57(3)	-5(2)	1(2)	5(2)
O(1)	924(3)	9686(5)	3137(7)	82(3)	77(3)	116(3)	-19(3)	2(3)	36(2)
C(1)'	1443(4)	6198(6)	2900(6)	56(3)	63(3)	57(3)	5(2)	1(2)	-5(2)
O(1)'	924(3)	5314(5)	3137(7)	82(3)	77(3)	116(3)	19(3)	2(3)	-36(2)
C(2)	689(5)	7500	-724(10)	50(4)	114(7)	47(4)	0	-3(3)	0
C(3)	436(7)	7500	-2734(10)	73(5)	84(6)	58(5)	0	-17(4)	0
C(4)	3166(8)	7500	4869(7)	50(4)					
C(5)	3349(7)	8671(11)	3832(15)	56(3)					
C(5)'	3349(7)	6329(11)	3832(15)	56(3)					
C(6)	3686(7)	8191(12)	2112(13)	55(3)					
C(6)'	3686(7)	6809(12)	2112(13)	55(3)					
C(40)	3704(13)	7500	1977(25)	58(5)					
C(50)	3508(9)	8597(15)	2945(22)	62(5)					
C(50)'	3508(9)	6403(15)	2945(22)	62(5)					
C(60)	3145(9)	8221(14)	4633(19)	57(5)					
C(60)'	3145(9)	6779(14)	4633(19)	57(5)					

TABLE 3.2.5

Observed and Calculated Structure Factors for $[Fe(cp)(CO)_2SEt]$

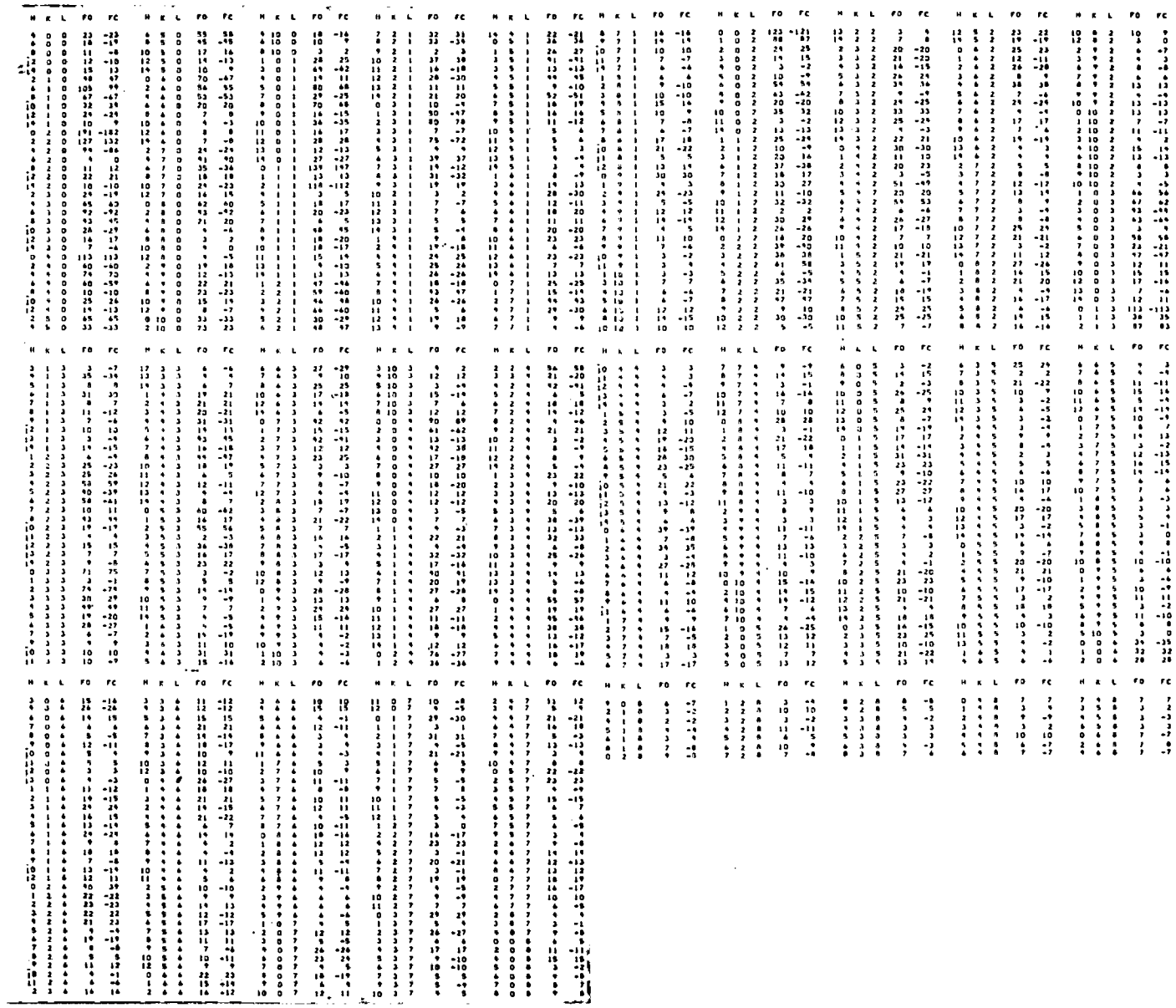

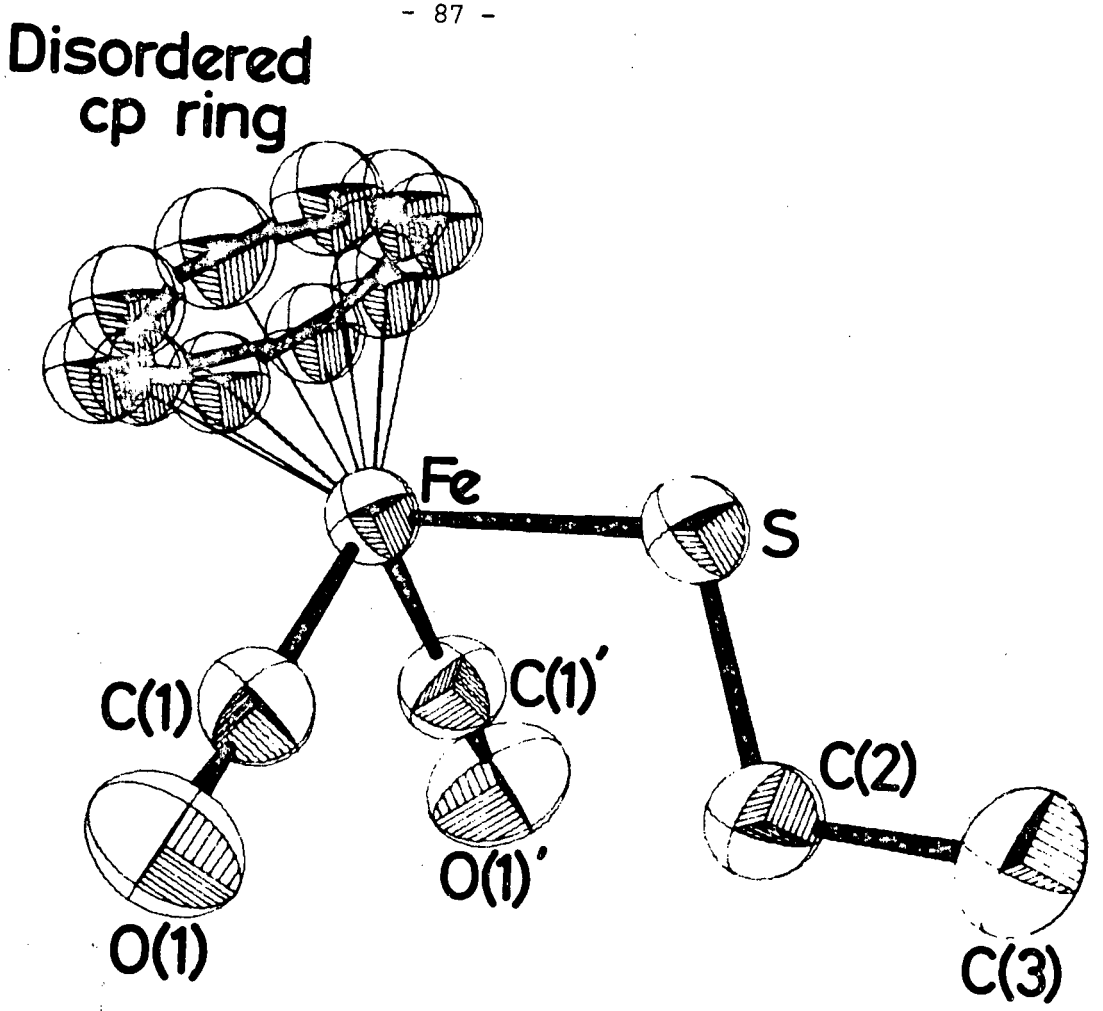

FIGURE 3.2.2

The Molecular Structure of $[Fe(cp)(CO)_2(SEt)]$.

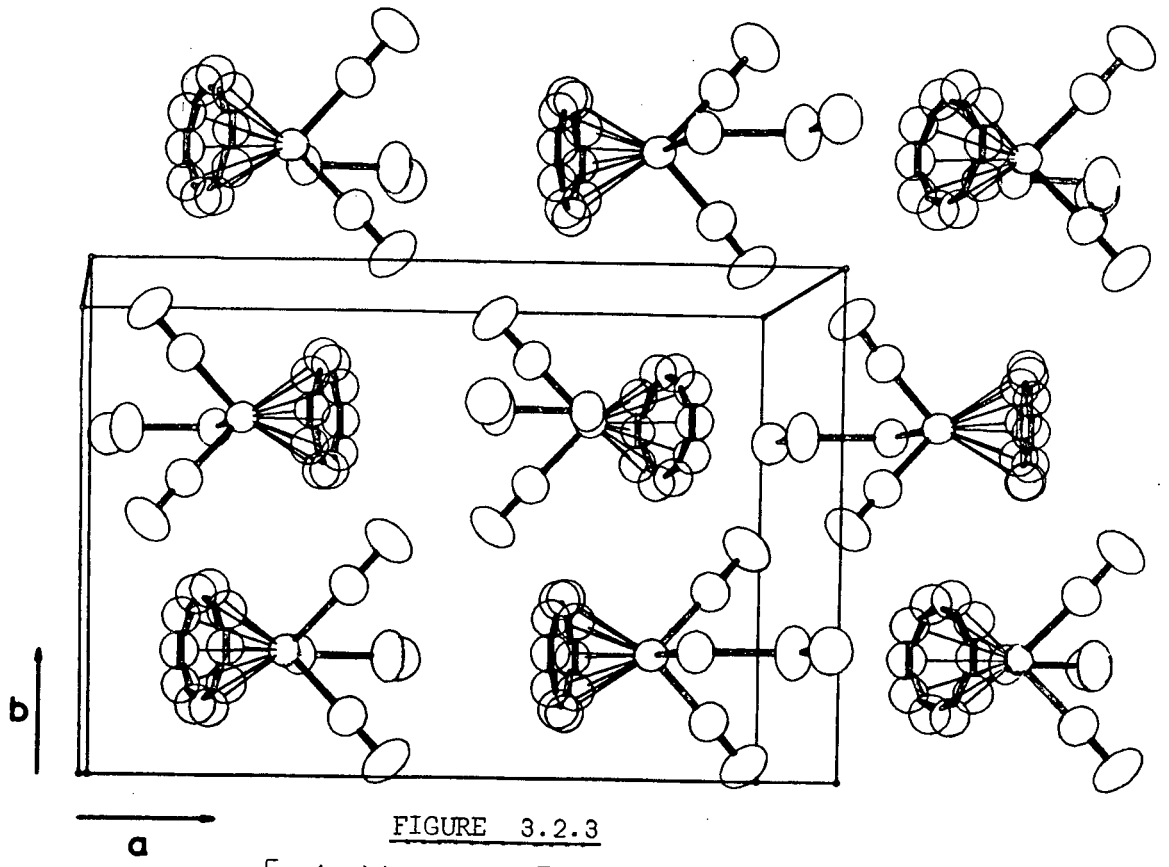

FIGURE 3.2.3

$[Fe(cp)(CO)_2(SEt)]$: Packing Diagram.

TABLE 3.2.6

INTRAMOLECULAR BOND LENGTHS AND THEIR E.s.d's. (Å)

Fe - S	2.296(2)	S - C(2)	1.819(7)
Fe - C(1)	1.751(5)	C(2) - C(3)	1.539(9)
Fe - C(4)	2.12(1)	C(1) - O(1)	1.150(6)
Fe - C(5)	2.12(1)	C(4) - C(5)	1.41(1)
Fe - C(6)	2.14(1)	C(5) - C(6)	1.45(1)
Fe - C(40)	2.07(2)	C(6) - C(6)'	1.36(2)
Fe - C(50)	2.07(1)	C(40)- C(50)	1.33(2)
Fe - C(60)	2.09(1)	C(50)- C(60)	1.41(2)
		C(60)- C(60)'	1.42(3)

TABLE 3.2.7

INTRAMOLECULAR BOND ANGLES AND THEIR E.s.d's. (DEGREES).

S - Fe - C(1)	90.7(2)	C(1) - Fe - C(1)'	93.9(2)
Fe - S - C(2)	107.0(2)	Fe - C(1) - O(1)	177.6(5)
C(5) - C(4) - C(5)'	109(2)	C(4) - C(5) - C(6)	106(2)
C(5) - C(6) - C(6)'	109(2)	C(50) - C(40) - C(50)'	109(2)
C(40) - C(50) - C(60)	110(2)	C(50) - C(60) - C(60)'	105(2)

TABLE 3.2.8

LEAST-SQUARES PLANE FOR $[Fe(cp)(CO)_2SEt]$

The equation of the plane in orthogonalized space is

$$(1.2755)I + (0.0)J + (2.5327)K = 7.9579$$

Below are distances (Å) of selected atoms from the plane (atoms marked with an asterisk were not included in the calculation)

C(4)	0.011	C(5)	-0.009	C(6)	0.003
C(5)'	-0.009	C(6)'	0.003	C(40)*	-0.007
C(50)*	-0.023	C(60)*	-0.076	C(50)'*	-0.023
C(60)'*	-0.076	Fe*	-1.757		

CHAPTER 4

THE CRYSTAL STRUCTURE OF, AND CONFORMATION STUDIES ON μ-ETHYLTHIO-BIS(η-CYCLOPENTADIENYL DICARBONYL IRON) TETRAFLUROOBORATE: $[\{Fe(cp)(CO)_2\}_2SEt]BF_4$

4.1 ELUCIDATION OF THE STRUCTURE

Crystal Preparation

The complex was prepared as described in Chapter 1. Large red-brown lozenges were grown at $-5^{\circ}C$ from an acetone-petroleum ether solution.

Density Determination

The density of the crystals was found to be 1.69 gm cm^{-3} by flotation in a m-xylene-methylene iodide mixture.

Space Group Assignment

No systematic absences were recorded on zero- and first-layer Weissenberg photographs taken about all three axes, indicating the space groups P1 or $P\bar{1}$. Consideration of the crystal density and unit cell dimensions showed that there were two formula units in the cell. The latter group was chosen after inspection of E-value statistics, and successful refinement of the structure vindicated this choice.

Diffractometer Data

Three dimensional intensity data were collected in the $\omega - 2\theta$ scan mode at a scan width of $1.4^{\circ}\theta$ and speed of $0.05^{\circ}\theta$ sec^{-1} in the range $8^{\circ} \leq 2\theta \leq 44^{\circ}$ from a spherical crystal of diameter 0.4mm. No crystal instability was detected during data collection; variation in

reference reflection intensity was within 2% of their initial value. 2341 reflections were collected of which 24 were rejected as being space group equivalent and 120 as being unobserved using the criterion $I > 2.0\sigma(I)$ for an 'observed' reflection. No absorption corrections were made; for $\mu R = 0.64$ the variation in A^* for the θ range scanned is less than 5%. Crystal data are listed in Table 4.1.1.

TABLE 4.1.1

CRYSTAL DATA

Molecular formula	$[\{Fe(C_5H_5)(CO)_2\}_2 SC_2H_5]BF_4$		
Molecular weight	501.9 gm $mole^{-1}$		
Space Group	$P\bar{1}$		
a = 9.41(1) Å			
b = 11.36(1) Å			
c = 10.04(1) Å			
α = 99.77(1)°	Dm = 1.69 gm cm^{-3}		
β = 104.40(1)°	Dc = 1.69 gm cm^{-3}	for Z = 2	
γ = 67.83(1)°	μ(MoKα) = 15.9 cm^{-1}		
V = 959.24 $Å^3$	F(000) = 504		

Solution and Refinement of Structure

Analysis of a three-dimensional Patterson map yielded the positions of the two iron atoms. Their coordinates were allowed to vary in four cycles of accelerated least-squares refinement[3.1], and a subsequent electron density map phased on the new positions revealed the coordinates of all the non-hydrogen atoms. In a further four cycles of least-squares refinement all non-hydrogen atoms were assigned anisotropic temperature factors and R fell to 0.046. For

the final five cycles of refinement idealized coordinates for the hydrogen atoms were computed, with the C-H bond lengths set at 1.08 Å and the bond geometry dictated by the type of carbon atom. Their isotropic temperature factors were varied as three parameters, one each for the methylene, methyl and cyclopentadienyl groups. The refinement converged to $R = 0.03$ ($R_w = 0.031$ with a weighting scheme $\omega = \frac{1.17}{\sigma^2(F)}$). In the last cycle, the average shift : error ratio was less than 0.05. A final difference map computed after the last cycle showed no peak hither than 0.3 $e\text{Å}^{-3}$.

The final atomic coordinates and thermal parameters for the heavy atoms and hydrogen atoms are set out in Tables 4.1.2 and 4.1.3 respectively. Observed and calculated structure factors are tabulated in Table 4.1.4.

TABLE 4.1.2 NON-HYDROGEN ATOMS

FRACTIONAL ATOMIC COORDINATES ($\times 10^4$) AND

ANISOTROPIC TEMPERATURE FACTORS ($\times 10^3$) AND THEIR E.s.d's.

	x/a	y/b	z/c	U_{11}	U_{22}	U_{33}	U_{23}	U_{13}	U_{12}
Fe(1)	7075(6)	1812(5)	1731(5)	30(3)	40(3)	32(3)	4(2)	6(2)	-8(2)
Fe(2)	4010(6)	2472(5)	4057(5)	33(3)	41(4)	43(4)	8(3)	11(3)	-10(3)
S(1)	4848(11)	3173(9)	2473(10)	32(5)	37(5)	41(6)	7(4)	9(4)	-8(4)
C(1)	6352(46)	2055(39)	-43(45)	41(25)	53(27)	47(28)	2(21)	8(20)	-14(21)
O(1)	5986(40)	2168(33)	-1197(31)	85(25)	97(26)	36(19)	13(17)	1(17)	-30(21)
C(2)	6575(43)	422(42)	1549(39)	31(22)	50(28)	44(24)	4(20)	7(18)	-3(20)
O(2)	6271(35)	-478(30)	1425(33)	63(21)	50(20)	90(24)	0(17)	15(17)	-25(18)
C(3)	3312(48)	1441(42)	2763(48)	40(26)	53(28)	67(30)	9(24)	17(22)	-17(22)
O(3)	2855(38)	775(32)	1930(37)	62(22)	76(23)	100(27)	-25(21)	24(20)	-38(20)
C(4)	5835(52)	1270(42)	4642(43)	48(28)	54(28)	53(27)	17(22)	17(22)	-12(24)
O(4)	6951(39)	485(33)	5077(35)	56(22)	75(23)	89(25)	42(20)	14(18)	3(19)
C(5)	3173(45)	3516(41)	987(42)	36(24)	62(28)	53(26)	23(22)	2(19)	-6(21)
C(6)	3138(59)	4563(45)	205(50)	66(34)	67(32)	69(32)	33(26)	8(26)	-4(27)
C(7)	8335(45)	3045(41)	2562(43)	40(24)	53(26)	60(28)	6(23)	8(21)	-22(21)
C(8)	8369(44)	2340(41)	3609(39)	39(23)	68(31)	36(23)	0(21)	0(18)	-19(22)
C(9)	9079(44)	1042(43)	3243(43)	31(23)	67(32)	55(27)	22(23)	-8(20)	-12(22)
C(10)	9490(45)	915(46)	1950(47)	29(23)	70(33)	65(30)	-5(25)	12(21)	-6(22)
C(11)	9050(47)	2168(47)	1548(44)	38(26)	91(37)	52(27)	13(26)	10(21)	-29(26)
C(12)	1900(54)	3978(47)	4262(47)	45(29)	73(33)	55(28)	10(26)	24(23)	10(25)
C(13)	3174(64)	4395(42)	4850(52)	86(39)	42(27)	77(35)	-7(25)	55(31)	-12(27)
C(14)	4134(53)	3638(45)	5924(46)	58(30)	72(33)	54(29)	-14(25)	22(24)	-27(27)
C(15)	3449(51)	2741(44)	6003(42)	60(30)	73(31)	43(26)	8(22)	17(23)	-24(25)
C(16)	2083(51)	2954(48)	4987(45)	47(27)	88(36)	54(28)	2(26)	22(23)	-26(25)
B(1)	398(65)	7255(52)	2442(56)	62(39)	55(35)	55(34)	13(28)	19(29)	0(30)
F(1)	-434(35)	8135(27)	3357(28)	100(23)	82(20)	74(19)	10(16)	44(17)	-4(17)
F(2)	91(44)	7780(34)	1250(30)	147(32)	132(30)	67(20)	43(20)	49(20)	4(25)
F(3)	-50(46)	6220(34)	2213(41)	135(32)	87(25)	148(33)	8(23)	8(25)	-46(24)
F(4)	1967(35)	6862(35)	3041(33)	62(21)	138(29)	103(25)	16(21)	14(18)	-11(20)

TABLE 4.1.3. HYDROGEN ATOMS

FRACTIONAL ATOMIC COORDINATES AND THEIR E.s.d's. AND ISOTROPIC TEMPERATURE FACTORS ($x10^3$)

	x/a	y/b	z/c	U_{iso}
H(51)	209(4)	381(4)	135(4)	74(10)
H(52)	328(4)	265(4)	29(4)	74(10)
H(61)	212(5)	459(4)	-59(4)	113(10)
H(62)	414(5)	436(4)	-23(4)	113(10)
H(63)	291(5)	546(4)	81(4)	113(10)
H(7)	784(4)	407(4)	254(4)	78(10)
H(8)	792(4)	273(4)	454(3)	78(10)
H(9)	927(4)	26(4)	384(4)	78(10)
H(10)	1003(4)	3(4)	137(4)	78(10)
H(11)	923(4)	240(4)	62(4)	78(10)
H(12)	95(5)	437(4)	341(4)	78(10)
H(13)	337(6)	516(4)	452(5)	78(10)
H(14)	520(5)	372(4)	657(4)	78(10)
H(15)	390(5)	201(4)	672(4)	78(10)
H(16)	129(5)	242(4)	478(4)	78(10)

TABLE 4.1.4

Observed and Calculated Structure Factors for $[\{Fe(cp)(CO)_2\}_2SEt]BF_4$

H	K	L	FO	FC
2	0	0	32	-31
3	0	0	175	175
4	0	0	21	-20
6	0	0	16	16
7	0	0	17	21
8	0	0	17	-21
-7	1	0	12	-7
-6	1	0	24	22
-5	1	0	35	-31
-4	1	0	90	-90
-3	1	0	179	179
-2	1	0	151	-141
-1	1	0	44	-42
2	1	0	111	109
3	1	0	27	24
4	1	0	34	35
5	1	0	43	-42
6	1	0	74	-74
7	1	0	42	42
8	1	0	9	6
9	1	0	24	-18
-7	2	0	39	-33
-5	2	0	62	-59
-4	2	0	32	-30
-1	2	0	95	-86
0	2	0	267	-288
1	2	0	172	179
2	2	0	190	-144
3	2	0	92	91
4	2	0	69	70
5	2	0	33	-32
6	2	0	21	-29
9	2	0	20	20
-7	3	0	14	-13
-6	3	0	8	8
-5	3	0	16	19
-4	3	0	38	39
-3	3	0	176	-169
-2	3	0	93	89
-1	3	0	17	15
0	3	0	14	-12
1	3	0	79	-79
2	3	0	6	2
3	3	0	26	-29
4	3	0	15	-16
5	3	0	74	74
6	3	0	79	80
7	3	0	90	-92
8	3	0	27	27
-6	4	0	60	-60
-5	4	0	60	59
-4	4	0	40	-36
-3	4	0	5	-5
-2	4	0	60	-57
-1	4	0	5	-4
0	4	0	62	64
1	4	0	106	-105
2	4	0	100	107
3	4	0	43	47
4	4	0	103	-109
5	4	0	48	48
6	4	0	35	34
7	4	0	6	5
8	4	0	9	8
9	4	0	14	-15
-5	5	0	6	-1
-4	5	0	21	-21
-3	5	0	82	81
-2	5	0	97	-98
-1	5	0	73	75
0	5	0	44	45
1	5	0	43	-43
2	5	0	68	70
3	5	0	83	87
5	5	0	4	3
6	5	0	21	-23
7	5	0	92	94
8	5	0	58	-58
9	5	0	24	24
-6	6	0	54	54
-5	6	0	51	-51
-4	6	0	23	23
-3	6	0	18	18
-2	6	0	9	9
-1	6	0	40	-39
0	6	0	11	-13
1	6	0	42	41
2	6	0	70	-74
3	6	0	56	-57
4	6	0	127	131
5	6	0	98	-99
6	6	0	12	15
7	6	0	19	20
8	6	0	27	-27
-5	7	0	10	10
-4	7	0	5	2
-3	7	0	5	-4
-2	7	0	49	48
-1	7	0	64	-65
0	7	0	33	-33
1	7	0	68	70
2	7	0	78	-79
3	7	0	56	-57
4	7	0	18	19
5	7	0	15	-14
6	7	0	8	8
7	7	0	40	-39
8	7	0	51	51
9	7	0	27	-26
-4	8	0	49	-49
-3	8	0	7	8
-2	8	0	46	47
-1	8	0	6	-4
0	8	0	34	-34
1	8	0	11	14
2	8	0	28	30
3	8	0	26	-26
4	8	0	52	-50
5	8	0	103	105
6	8	0	73	-75
7	8	0	15	13
8	8	0	26	26
-3	9	0	14	-12
-2	9	0	8	-6
-1	9	0	27	29
0	9	0	8	-7
1	9	0	55	-54
2	9	0	80	79
3	9	0	57	-56
4	9	0	16	-18
5	9	0	19	18
6	9	0	16	-15
7	9	0	6	5
8	9	0	25	-25
-1	10	0	37	36
0	10	0	11	-11
1	10	0	15	13
2	10	0	15	15
3	10	0	11	-11
4	10	0	23	22
5	10	0	45	-44
6	10	0	40	40
7	10	0	18	-18
1	11	0	39	38
2	11	0	55	-53
3	11	0	58	58
4	11	0	7	6
5	11	0	22	-23
-6	-11	1	24	23
-5	-11	1	40	-39
-4	-11	1	10	10
-3	-11	1	20	-20
-2	-11	1	15	15
-1	-11	1	20	-18
-7	-10	1	12	-11
-6	-10	1	6	6
-5	-10	1	23	23
-4	-10	1	32	-32
-3	-10	1	13	-13
-2	-10	1	58	56
-1	-10	1	51	-51
0	-10	1	28	28
-8	-9	1	21	21
-7	-9	1	38	-36
-6	-9	1	12	-12
-5	-9	1	55	54
-4	-9	1	62	-61
-3	-9	1	27	28
-2	-9	1	35	-37
-1	-9	1	28	25
0	-9	1	24	-25
1	-9	1	6	-6
2	-9	1	38	39
3	-9	1	9	-8
-8	-8	1	23	22
-7	-8	1	6	-6
-6	-8	1	23	24
-5	-8	1	33	-33
-4	-8	1	78	75
-3	-8	1	90	-39
-2	-8	1	47	-47
-1	-8	1	90	92
0	-8	1	58	-59
1	-8	1	14	-14
2	-8	1	4	5
3	-8	1	6	9
4	-8	1	5	-6
-9	-7	1	6	-5
-8	-7	1	23	-24
-7	-7	1	59	58
-6	-7	1	15	14
-5	-7	1	65	-66
-4	-7	1	124	126
-3	-7	1	47	-47
-2	-7	1	40	41
-1	-7	1	25	-23
0	-7	1	7	-4
1	-7	1	12	-12
2	-7	1	36	-38
3	-7	1	17	15
4	-7	1	11	12
5	-7	1	51	-52
-8	-6	1	66	-67
-7	-6	1	52	52
-6	-6	1	15	-14
-5	-6	1	15	-16
-4	-6	1	69	-69
-3	-6	1	80	79
-2	-6	1	61	-63
-1	-6	1	83	-85
0	-6	1	45	46
1	-6	1	12	-12
2	-6	1	97	-97
3	-6	1	10	9
-8	-5	1	6	4
-7	-5	1	48	-48
-6	-5	1	44	45
-5	-5	1	23	26
-4	-5	1	124	-125
-3	-5	1	128	129
-2	-5	1	7	-8
-1	-5	1	34	-37
0	-5	1	41	40
1	-5	1	49	50
2	-5	1	14	15
3	-5	1	65	-67
4	-5	1	22	23
5	-5	1	47	49
6	-5	1	66	-69
-9	-4	1	15	15
-8	-4	1	36	36
-7	-4	1	83	-83
-6	-4	1	74	75
-5	-4	1	20	20
-4	-4	1	27	-24
-3	-4	1	6	-4
-2	-4	1	160	162
-1	-4	1	49	-49
0	-4	1	27	-28
1	-4	1	110	107
2	-4	1	100	99
3	-4	1	98	-99
4	-4	1	68	68
5	-4	1	27	-29
7	-4	1	17	-18
-9	-3	1	36	35
-8	-3	1	22	-23
-7	-3	1	37	37
-6	-3	1	58	-61
-5	-3	1	90	90
-4	-3	1	52	50
-3	-3	1	99	-101
-2	-3	1	189	189
-1	-3	1	46	45
0	-3	1	67	-68
1	-3	1	109	100
2	-3	1	79	-77
3	-3	1	103	101
4	-3	1	26	-26
5	-3	1	31	-31
6	-3	1	49	51
7	-3	1	63	-67
-9	-2	1	23	-22
-8	-2	1	4	1
-7	-2	1	60	61
-6	-2	1	116	-118
-5	-2	1	53	53
-4	-2	1	79	77
-3	-2	1	44	-43
-2	-2	1	6	6
-1	-2	1	16	17
0	-2	1	151	152
1	-2	1	25	-25
2	-2	1	104	-104
3	-2	1	151	145
4	-2	1	133	-132
5	-2	1	43	43
6	-2	1	13	13
8	-2	1	26	-27
-9	-1	1	55	-54
-8	-1	1	30	31
-7	-1	1	25	-25
-6	-1	1	34	33
-5	-1	1	79	-76
-4	-1	1	54	-52
-3	-1	1	25	24
-2	-1	1	220	-212
1	-1	1	190	-184
2	-1	1	9	8
3	-1	1	71	-69
4	-1	1	23	21
5	-1	1	61	-61
6	-1	1	21	-20
7	-1	1	49	51
8	-1	1	26	-28
-9	0	1	20	19
-8	0	1	16	-16
-7	0	1	8	-6
-6	0	1	62	64
-5	0	1	77	-75
-4	0	1	53	-52
-3	0	1	97	90
-2	0	1	81	-77
1	0	1	90	90
2	0	1	49	49
3	0	1	61	57
4	0	1	196	196
5	0	1	81	-84
6	0	1	5	1
7	0	1	11	8
8	0	1	17	16
-8	1	1	18	-17
-7	1	1	15	-15
-6	1	1	19	-19
-5	1	1	78	77
-4	1	1	26	-24
-3	1	1	79	-72
-2	1	1	164	159
-1	1	1	64	-62
1	1	1	291	303
2	1	1	35	-35
3	1	1	124	126
4	1	1	20	21
5	1	1	112	114
6	1	1	22	21
7	1	1	42	-44
8	1	1	29	28
9	1	1	4	8
-8	2	1	35	36
-7	2	1	28	-28
-6	2	1	38	-38
-5	2	1	85	83
-4	2	1	30	-29
-3	2	1	178	-170
-2	2	1	157	149
-1	2	1	79	-76
0	2	1	47	-47
1	2	1	115	-116
2	2	1	8	9
3	2	1	90	-90
4	2	1	81	-84
5	2	1	105	108
6	2	1	38	40
7	2	1	48	-48
8	2	1	24	25
-6	3	1	38	-39
-5	3	1	71	69
-3	3	1	6	-4
-2	3	1	24	-22
-1	3	1	99	100
0	3	1	56	-55
1	3	1	207	-214
2	3	1	158	164
3	3	1	69	-70
4	3	1	81	-80
5	3	1	15	-14
6	3	1	30	31
7	3	1	20	20
8	3	1	9	-8
9	3	1	17	17
-7	4	1	7	5
-6	4	1	9	-5
-5	4	1	6	4
-4	4	1	27	27
-3	4	1	64	64
-2	4	1	149	-145
-1	4	1	100	105
0	4	1	33	-32
1	4	1	54	-53
2	4	1	19	-21
3	4	1	19	-19
4	4	1	33	-35
5	4	1	58	-60
6	4	1	6	-5
7	4	1	50	50
8	4	1	66	-65
9	4	1	39	40
-6	5	1	26	26
-5	5	1	65	-65
-4	5	1	34	33
-3	5	1	3	4
-2	5	1	26	23
-1	5	1	88	-89
0	5	1	50	51
1	5	1	26	27
2	5	1	103	-105
3	5	1	57	59
4	5	1	29	30
5	5	1	40	-40
6	5	1	16	16
7	5	1	12	-13
8	5	1	9	9
9	5	1	11	-9
-5	6	1	6	5
-4	6	1	28	-28
-3	6	1	3	-5
-2	6	1	81	81
-1	6	1	95	-102
0	6	1	81	81
1	6	1	16	17
2	6	1	14	-14
3	6	1	21	22
4	6	1	8	-8
5	6	1	54	55
6	6	1	21	-21
7	6	1	28	-29
8	6	1	74	73
9	6	1	52	-52
-5	7	1	46	47
-4	7	1	53	-52
-3	7	1	21	21
-1	7	1	34	35
0	7	1	53	-56
1	7	1	12	13
2	7	1	47	47
3	7	1	80	-83
4	7	1	33	-34
5	7	1	73	75
6	7	1	82	-83
7	7	1	13	14
8	7	1	6	3
-4	8	1	31	31
-3	8	1	8	-6
-2	8	1	14	-14
-1	8	1	70	71
0	8	1	44	-43
1	8	1	15	15
2	8	1	61	62
3	8	1	45	-46
4	8	1	11	14
5	8	1	16	-16
6	8	1	8	8
8	8	1	33	-32
-3	9	1	36	-36
-2	9	1	9	-10
-1	9	1	28	29
0	9	1	12	13
1	9	1	23	-22
2	9	1	12	13
3	9	1	25	23
4	9	1	5	7
5	9	1	39	-38
6	9	1	46	46
7	9	1	32	-31
-1	10	1	19	-20
0	10	1	18	18
1	10	1	8	-7
2	10	1	41	-41
3	10	1	47	47
4	10	1	9	-8
6	10	1	21	-21
7	10	1	26	25
2	11	1	6	-6
3	11	1	7	-5
4	11	1	22	22
5	11	1	14	13
-7	-11	2	39	-37
-6	-11	2	32	31
-5	-11	2	10	8
-4	-11	2	30	-29
-3	-11	2	10	11
-2	-11	2	5	5
-1	-11	2	32	-32
0	-11	2	13	14
-8	-10	2	21	20
-7	-10	2	48	-47
-6	-10	2	15	16
-5	-10	2	27	27
-4	-10	2	21	-20
-3	-10	2	14	14
-2	-10	2	32	-30
-1	-10	2	45	45
0	-10	2	61	-62
-8	-9	2	7	6
-7	-9	2	16	16
-5	-9	2	21	-19
-4	-9	2	35	34
-3	-9	2	22	-22
-2	-9	2	13	-13
-1	-9	2	60	59
0	-9	2	37	-38
2	-9	2	9	-13
-9	-8	2	43	-41
-8	-8	2	6	-7
-7	-8	2	43	44
-6	-8	2	40	-40
-5	-8	2	20	-22
-4	-8	2	59	58
-3	-8	2	53	-56
-2	-8	2	17	17
-1	-8	2	30	-30
0	-8	2	61	62
1	-8	2	52	-51
3	-8	2	22	21
4	-8	2	19	-21
-9	-7	2	6	-4
-8	-7	2	38	-40
-7	-7	2	30	30
-6	-7	2	8	-6
-5	-7	2	15	16
-4	-7	2	16	-16
-3	-7	2	109	108
-2	-7	2	27	-27
-1	-7	2	33	-34
0	-7	2	98	99
1	-7	2	5	-2
2	-7	2	15	-12
3	-7	2	11	-12
4	-7	2	8	9
-9	-6	2	20	21
-8	-6	2	10	-10
-7	-6	2	24	-23
-6	-6	2	58	59
-5	-6	2	49	-50
-4	-6	2	36	-36
-3	-6	2	99	101
-2	-6	2	33	-32
-1	-6	2	60	60
0	-6	2	62	-64
1	-6	2	44	44
3	-6	2	36	-36
4	-6	2	18	18
5	-6	2	6	-6
-9	-5	2	35	35
-8	-5	2	14	15
-7	-5	2	65	-64
-6	-5	2	83	83
-5	-5	2	56	-57
-4	-5	2	8	10
-3	-5	2	110	-112
-2	-5	2	76	75
-1	-5	2	21	-20
0	-5	2	92	-93
1	-5	2	70	70
2	-5	2	6	-9
3	-5	2	45	-45
4	-5	2	28	27
5	-5	2	18	-19
6	-5	2	18	20
-9	-4	2	25	23
-7	-4	2	42	42
-6	-4	2	83	-83
-5	-4	2	66	69
-4	-4	2	67	65
-3	-4	2	107	-110
-2	-4	2	16	18
-1	-4	2	13	-12
0	-4	2	65	63
1	-4	2	27	-26
2	-4	2	16	16
3	-4	2	85	85
4	-4	2	60	-60
5	-4	2	22	21
6	-4	2	57	59
-9	-3	2	53	-54
-8	-3	2	30	28
-7	-3	2	52	52
-6	-3	2	126	-128
-5	-3	2	54	53
-4	-3	2	5	6
-3	-3	2	29	30
-2	-3	2	119	-118
-1	-3	2	65	62
0	-3	2	36	35
1	-3	2	111	-110
2	-3	2	26	26
3	-3	2	113	113
4	-3	2	65	-67
5	-3	2	22	21
6	-3	2	4	2
7	-3	2	36	37
-9	-2	2	69	-69
-8	-2	2	15	14
-7	-2	2	6	-6
-6	-2	2	59	59
-5	-2	2	132	-131
-4	-2	2	96	93
-3	-2	2	8	6
-2	-2	2	135	-131
-1	-2	2	186	183
0	-2	2	98	93
1	-2	2	48	-49
2	-2	2	3	3
3	-2	2	23	23
4	-2	2	110	109
5	-2	2	79	-80
6	-2	2	24	25
7	-2	2	46	47
-9	-1	2	42	42
-8	-1	2	52	-51
-6	-1	2	39	41
-5	-1	2	80	-78
-4	-1	2	65	63
-3	-1	2	4	5
-2	-1	2	13	13
-1	-1	2	120	-114
0	-1	2	64	-60
1	-1	2	174	170
2	-1	2	82	-80
3	-1	2	39	-41
4	-1	2	111	113
5	-1	2	95	-94
6	-1	2	31	31
8	-1	2	24	23
-9	0	2	45	45
-8	0	2	36	-33
-7	0	2	29	29
-6	0	2	40	-39
-5	0	2	81	79
-4	0	2	99	-95
-3	0	2	36	35
-2	0	2	13	10
-1	0	2	194	-190
0	0	2	98	-96
1	0	2	7	-1
2	0	2	127	-126
3	0	2	22	20
4	0	2	74	-76
5	0	2	63	63
6	0	2	36	-34
7	0	2	13	-13
8	0	2	28	27
-8	1	2	65	65
-7	1	2	22	-22
-6	1	2	7	-7
-5	1	2	145	143
-4	1	2	97	-92
-3	1	2	118	-107
-2	1	2	283	266
-1	1	2	25	25
0	1	2	46	-44
1	1	2	100	-100
2	1	2	57	60
3	1	2	64	-63
4	1	2	24	-26
5	1	2	121	.119
6	1	2	36	-37
8	1	2	10	11
-8	2	2	29	29
-7	2	2	43	-43
-6	2	2	14	-14
-5	2	2	27	27
-4	2	2	18	19
-3	2	2	36	-36
-2	2	2	10	8
-1	2	2	72	-69
0	2	2	46	45
1	2	2	4	-5
2	2	2	30	30
3	2	2	58	-55
4	2	2	14	-13
5	2	2	75	-74
6	2	2	76	79
7	2	2	17	17
8	2	2	29	-29
-7	3	2	23	27
-6	3	2	40	-39
-5	3	2	64	-63
-4	3	2	73	71
-3	3	2	3	-2
-2	3	2	117	-112
-1	3	2	85	83
0	3	2	82	-83
1	3	2	94	98
2	3	2	92	-97
3	3	2	85	88
4	3	2	36	-34
5	3	2	95	-96
6	3	2	47	47
7	3	2	8	-8
8	3	2	23	-23
-7	4	2	36	37
-6	4	2	25	25
-5	4	2	56	-55
-4	4	2	5	4
-3	4	2	30	30
-2	4	2	96	92
-1	4	2	65	-67
0	4	2	77	80
1	4	2	62	65

TABLE 4.1.4 CONTINUED

H	K	L	FO	FC	H	K	L	FO	FC	H	K	L	FO	FC	H	K	L	FO	FC	H	K	L	FO	FC	H	K	L	FO	FC	H	K	L	FO	FC
2	4	2	138	-139	7	6	2	12	12	5	9	2	8	8	2	-9	3	5	-2	-1	-6	3	36	-36	6	-9	3	9	2	7	-2	3	7	-9	8	0	3	19	-18	-7	3	3	53	54	-9	5	3	13	-12
3	4	2	90	94	8	6	2	6	9	6	9	2	11	-12	-9	-8	3	20	-20	0	-6	3	9	-9	-9	-3	3	18	-19	-9	-1	3	31	32	-8	1	3	47	49	-6	3	3	39	-35	-3	5	3	6	6
4	4	2	39	32	-5	7	2	11	-11	7	9	2	38	38	-8	-8	3	6	-7	1	-6	3	73	72	-8	-3	3	5	-9	-8	-1	3	35	-35	-7	1	3	41	-40	-5	3	3	26	-29	-1	5	3	54	56
5	4	2	17	-17	-9	7	2	30	30	8	10	2	9	6	-7	-8	3	9	-9	4	-6	3	7	-8	-7	-3	3	7	7	-7	-1	3	6	-3	-6	1	3	12	11	-4	3	3	33	-31	0	5	3	91	-92
6	4	2	56	-55	-3	7	2	50	-49	2	10	2	10	-9	-6	-8	3	29	29	5	-6	3	24	24	-6	-3	3	37	36	-6	-1	3	22	-22	-5	1	3	6	9	-3	3	3	10	-7	1	5	3	59	60
7	4	2	11	-11	-2	7	2	6	6	3	10	2	10	-10	-5	-8	3	16	-17	-9	-5	3	23	-22	-5	-3	3	98	-98	-5	-1	3	96	96	-4	1	3	125	120	-2	3	3	7	6	2	5	3	25	26
8	4	2	20	19	-1	7	2	91	91	4	10	2	16	16	-4	-8	3	29	-29	-8	-5	3	33	34	-4	-3	3	192	139	-4	-1	3	180	-175	-3	1	3	29	-30	-1	3	3	90	-93	3	5	3	38	-40
-4	5	2	32	33	0	7	2	78	-80	5	10	2	9	10	-3	-8	3	79	78	-7	-5	3	4	-5	-3	-3	3	21	-21	-3	-1	3	94	-91	-2	1	3	19	13	0	3	3	56	58	4	5	3	38	38
-5	5	2	29	29	1	7	2	22	23	6	10	2	33	-31	-2	-8	3	49	-51	-6	-5	3	60	-59	-2	-3	3	90	-92	-2	-1	3	129	128	-1	1	3	48	49	1	3	3	21	-22	8	5	3	16	23
-4	5	2	59	-56	2	7	2	5	6	3	11	2	30	-30	-1	-8	3	19	-22	-5	-5	3	94	95	-1	-3	3	38	36	-1	-1	3	20	-19	0	1	3	101	-101	2	3	3	96	-98	-5	6	3	26	25
-3	5	2	50	50	3	7	2	22	21	4	11	2	22	22	0	-8	3	47	46	-4	-5	3	91	-90	0	-3	3	17	-16	0	-1	3	86	-87	1	1	3	16	16	3	3	3	51	52	-4	6	3	44	42
-2	5	2	39	40	4	7	2	14	-12	-7	-11	3	19	-19	1	-8	3	8	-10	-3	-5	3	71	-69	1	-3	3	16	17	1	-1	3	152	149	2	1	3	126	123	4	3	3	7	-7	-3	6	3	50	-46
-1	5	2	109	-108	6	7	2	20	19	-6	-11	3	4	4	3	-8	3	18	-19	-2	-5	3	34	34	2	-3	3	53	-53	2	-1	3	42	-40	3	1	3	93	-95	5	3	3	31	33	-2	6	3	55	56
0	5	2	118	123	7	7	2	26	-26	-3	-11	3	10	-11	-9	-7	3	49	48	-1	-5	3	16	-18	3	-3	3	8	-9	3	-1	3	27	-26	4	1	3	8	-10	6	3	3	71	-72	-1	6	3	32	32
1	5	2	30	-32	8	7	2	5	-3	-2	-11	3	11	9	-8	-7	3	34	-33	0	-5	3	10	9	4	-3	3	90	91	5	-1	3	17	16	5	1	3	84	-86	7	3	3	29	28	0	6	3	36	-36
2	5	2	26	27	-4	8	2	32	32	-1	-11	3	24	23	-7	-7	3	29	-27	1	-5	3	88	-90	5	-3	3	50	-48	5	-1	3	88	87	6	1	3	74	73	8	3	3	11	-11	1	6	3	11	12
3	5	2	99	-103	-3	8	2	54	-54	-7	-10	3	32	32	-6	-7	3	57	56	2	-5	3	81	80	6	-3	3	26	26	6	-1	3	69	-70	7	1	3	32	-31	-7	4	3	32	-33	2	6	3	26	-25
4	5	2	23	24	-2	8	2	15	16	-6	-10	3	37	-35	-5	-7	3	61	-63	3	-5	3	15	-16	7	-3	3	32	34	7	-1	3	4	5	8	1	3	11	-10	-6	4	3	93	93	3	6	3	70	71
5	5	2	37	38	-1	8	2	7	-6	-5	-10	3	6	6	-4	-7	3	64	-64	4	-5	3	27	-25	-9	-2	3	37	37	-9	0	3	20	-21	-8	2	3	39	-41	-5	4	3	25	-25	4	6	3	69	-71
6	5	2	65	-67	0	8	2	36	37	-4	-10	3	6	6	-3	-7	3	68	68	5	-5	3	28	29	-8	-2	3	57	-58	-8	0	3	64	66	-7	2	3	92	93	-4	4	3	52	-52	5	6	3	34	33
8	5	2	27	26	1	8	2	55	-55	-3	-10	3	26	-29	-2	-7	3	16	-18	-9	-4	3	48	-48	-7	-2	3	94	92	-7	0	3	80	-79	-6	2	3	47	-45	-3	4	3	45	45	6	6	3	14	13
-4	6	2	8	9	3	8	2	28	29	-2	-10	3	4	4	0	-7	3	59	-59	-8	-4	3	44	44	-6	-2	3	36	-34	-6	0	3	24	22	-5	2	3	5	-4	-2	4	3	44	-48	8	6	3	14	7
-5	6	2	46	46	4	8	2	17	-16	-1	-10	3	19	19	1	-7	3	97	98	-7	-4	3	11	-10	-5	-2	3	71	-70	-5	0	3	58	58	-4	2	3	110	107	-1	4	3	94	-97	-4	7	3	27	27
-4	6	2	58	-58	5	8	2	13	-14	0	-10	3	13	-12	2	-7	3	53	-53	-4	-4	3	41	-39	-4	-2	3	43	44	-4	0	3	78	-75	-3	2	3	29	-27	0	4	3	56	55	-3	7	3	34	-36
-3	6	2	48	47	6	8	2	30	29	1	-10	3	6	-6	3	-7	3	4	6	-5	-4	3	85	83	-3	-2	3	135	-132	-3	0	3	79	-75	-1	2	3	131	130	1	4	3	11	11	-2	7	3	26	26
-2	6	2	11	-12	7	8	2	23	-22	-8	-9	3	26	25	4	-7	3	47	48	-4	-4	3	25	-24	-2	-2	3	165	159	-2	0	3	37	36	0	2	3	10	10	2	4	3	81	83	-1	7	3	12	-11
-1	6	2	29	29	8	8	2	7	4	-7	-9	3	21	21	-9	-6	3	42	42	-3	-4	3	112	110	-1	-2	3	171	-172	-1	0	3	80	80	1	2	3	35	36	3	4	3	110	-114	0	7	3	79	80
0	6	2	74	-78	-2	9	2	34	-33	-6	-9	3	9	-8	-8	-6	3	6	-5	-2	-4	3	146	-148	0	-2	3	60	-60	0	0	3	141	-138	2	2	3	108	-108	4	4	3	90	93	1	7	3	70	-73
1	6	2	74	75	-1	9	2	6	-2	-4	-9	3	34	33	-7	-6	3	26	-26	-1	-4	3	144	145	1	-2	3	82	80	1	0	3	9	-9	3	2	3	131	136	5	4	3	12	10	2	7	3	15	15
2	6	2	41	42	0	9	2	55	56	-3	-9	3	12	10	-6	-6	3	39	40	0	-4	3	27	-23	2	-2	3	63	-63	2	0	3	107	106	4	2	3	25	-25	6	4	3	26	-25	3	7	3	51	51
3	6	2	82	-84	1	9	2	28	-27	-2	-9	3	12	-11	-5	-6	3	30	-28	1	-4	3	85	-85	3	-2	3	35	-32	3	0	3	118	-119	5	2	3	57	-57	7	4	3	39	36	4	7	3	40	-39
4	6	2	28	27	2	9	2	4	4	-1	-9	3	33	-32	-4	-6	3	32	32	2	-4	3	44	45	4	-2	3	40	39	4	0	3	31	-30	6	2	3	28	27	8	4	3	8	3	6	7	3	40	40
5	6	2	43	42	3	9	2	40	41	0	-9	3	80	80	-3	-6	3	77	-77	3	-4	3	15	11	5	-2	3	39	-39	5	0	3	60	63	7	2	3	32	-33	-6	5	3	20	20	-3	8	3	40	40
6	6	2	31	-31	4	9	2	7	-8	1	-9	3	46	-46	-2	-6	3	79	83	4	-4	3	4	-3	6	-2	3	9	-9	6	0	3	23	-23	8	2	3	7	-7	-5	5	3	17	18	-2	8	3	71	-72

H	K	L	FO	FC	H	K	L	FO	FC	H	K	L	FO	FC	H	K	L	FO	FC	H	K	L	FO	FC	H	K	L	FO	FC	H	K	L	FO	FC
0	8	3	40	40	-6	-9	4	48	48	-9	-6	4	16	-15	1	-9	4	9	-6	4	-2	4	5	2	7	0	4	50	-50	-5	3	4	52	-50	0	5	4	55	-55	1	8	4	61	61	-8	-8	5	19	19
1	8	3	53	-53	-5	-9	4	44	-44	-3	-6	4	77	-76	2	-9	4	84	-84	5	-2	4	33	33	-8	1	4	41	-41	-9	3	4	44	43	1	5	4	18	-18	2	8	4	41	-41	-7	-8	5	39	-38
2	8	3	14	-13	-4	-9	4	5	7	-2	-6	4	19	-17	3	-9	4	64	64	6	-2	4	55	-56	-7	1	4	77	76	-3	3	4	16	17	2	5	4	5	-1	3	8	4	27	26	-5	-8	5	60	60
3	8	3	18	18	-3	-9	4	44	45	-1	-6	4	43	41	4	-9	4	9	-9	-9	-1	4	24	24	-6	1	4	93	-93	-2	3	4	4	-1	3	5	4	72	72	4	8	4	13	13	-4	-8	5	41	-42
4	8	3	5	-3	-2	-9	4	48	-48	0	-6	4	14	15	5	-9	4	35	-36	-8	-1	4	43	43	-5	1	4	19	18	-1	3	4	16	15	4	5	4	84	-84	5	8	4	15	-15	-3	-8	5	8	-7
5	8	3	35	-34	-1	-9	4	10	-10	1	-6	4	113	-111	6	-9	4	18	18	-7	-1	4	47	-46	-4	1	4	29	27	0	3	4	11	9	5	5	4	44	43	6	8	4	8	-9	-2	-8	5	38	39
6	8	3	10	11	0	-9	4	22	22	2	-6	4	109	106	-9	-3	4	14	-13	-6	-1	4	72	71	-3	1	4	34	-35	1	3	4	65	67	6	5	4	17	17	-1	9	4	51	-52	-1	-8	5	22	-22
7	8	3	28	27	1	-9	4	10	-9	3	-6	4	32	-33	-8	-3	4	28	-26	-5	-1	4	24	-23	-2	1	4	16	15	2	3	4	16	15	7	5	4	17	-16	2	9	4	18	-18	0	-8	5	6	6
-2	9	3	43	-44	2	-9	4	8	-7	4	-6	4	19	-20	-7	-3	4	28	29	-4	-1	4	36	-34	-1	1	4	22	-23	3	3	4	112	-113	-5	6	4	4	2	4	9	4	13	-11	1	-8	5	11	11
-1	9	3	15	16	-4	-8	4	46	44	-9	-5	4	4	5	-6	-3	4	12	12	-3	-1	4	12	12	0	1	4	75	76	4	3	4	99	101	-4	6	4	5	-4	5	9	4	26	25	-9	-7	5	19	-19
0	9	3	18	-18	-8	-8	4	34	-34	-8	-5	4	22	21	-5	-3	4	6	4	-2	-1	4	59	-56	1	1	4	49	-51	5	3	4	19	-17	-3	6	4	19	-19	1	10	4	29	-23	-8	-7	5	57	56
1	9	3	21	21	-7	-8	4	22	21	-7	-6	4	23	-23	-4	-3	4	19	-18	-1	-1	4	63	63	2	1	4	66	-68	6	3	4	23	-22	-2	6	4	12	-11	2	10	4	38	36	-7	-7	5	63	-62
2	9	3	25	-24	-4	-8	4	4	-5	-6	-5	4	35	-34	-3	-3	4	7	-4	0	-1	4	194	-199	3	1	4	74	72	7	3	4	14	13	-1	6	4	15	16	3	10	4	30	-29	-6	-7	5	36	34
4	9	3	17	16	-3	-8	4	42	41	-5	-5	4	29	-28	-2	-3	4	147	146	1	-1	4	11	10	4	1	4	27	-28	-7	4	4	14	-15	0	6	4	57	59	-6	-11	5	15	15	-5	-7	5	7	6
5	9	3	7	-7	-2	-8	4	34	34	-4	-5	4	52	51	-1	-3	4	50	-49	2	-1	4	71	70	5	1	4	6	-6	-6	4	4	17	18	1	6	4	92	-94	-4	-11	5	14	14	-4	-7	5	15	14
6	9	3	15	-15	0	-8	4	44	-47	-3	-5	4	16	16	0	-3	4	130	131	3	-1	4	41	-42	6	1	4	11	8	-5	4	4	6	5	2	6	4	39	39	-3	-11	5	16	16	-3	-7	5	9	-11
1	10	3	22	21	1	-8	4	68	67	-2	-5	4	134	-136	1	-3	4	29	29	4	-1	4	6	-5	7	1	4	6	1	-4	4	4	4	0	4	6	4	29	-29	-2	-11	5	34	-33	-2	-7	5	5	-2
2	10	3	5	-5	2	-8	4	35	-35	-1	-5	4	88	89	2	-3	4	21	-20	5	-1	4	15	17	-7	2	4	43	44	-3	4	4	67	-65	5	6	4	4	-6	-7	-10	5	11	10	-1	-7	5	48	48
3	10	3	8	-8	3	-8	4	8	8	0	-5	4	100	-99	3	-3	4	17	-17	6	-1	4	21	-21	-6	2	4	6	-3	-2	4	4	54	54	6	6	4	28	29	-6	-10	5	32	32	0	-7	5	7	-8
4	10	3	12	13	-7	-7	4	5	-6	1	-5	4	13	-15	4	-3	4	46	47	7	-1	4	5	-4	-5	2	4	26	-25	-1	4	4	29	-30	-4	7	4	13	13	-5	-10	5	52	-51	1	-7	5	23	-25
-6	-11	4	54	-51	-6	-7	4	13	-15	2	-5	4	15	14	5	-3	4	8	-9	-9	0	4	5	2	-4	2	4	36	-36	0	4	4	109	-111	-3	7	4	29	27	-4	-10	5	47	46	2	-7	5	72	74
-5	-11	4	37	35	-5	-7	4	53	52	3	-5	4	13	13	6	-3	4	21	-23	-6	0	4	12	11	-3	2	4	200	198	1	4	4	99	101	-2	7	4	55	-56	-3	-10	5	8	9	3	-7	5	38	-40
-4	-11	4	8	-7	-4	-7	4	43	-43	4	-5	4	18	-18	-9	-2	4	33	33	-5	0	4	65	-64	-2	2	4	23	-24	2	4	4	65	-67	-1	7	4	31	31	-1	-10	5	24	-24	-9	-6	5	22	24
-3	-11	4	14	-12	-3	-7	4	43	-43	5	-5	4	24	-26	-7	-2	4	19	-18	-4	0	4	141	137	-1	2	4	33	-33	3	4	4	30	-30	0	7	4	49	49	0	-10	5	21	21	-8	-6	5	4	-2
-2	-11	4	4	4	-2	-7	4	85	86	-9	-4	4	11	-10	-6	-2	4	36	36	-3	0	4	135	-135	0	2	4	143	145	4	4	4	32	32	1	7	4	17	-18	-8	-9	5	53	-53	-7	-6	5	24	23
-1	-11	4	19	19	-1	-7	4	58	-57	-8	-4	4	36	-36	-5	-2	4	78	79	-2	0	4	52	-50	1	2	4	17	-17	5	4	4	10	-10	2	7	4	11	11	-7	-9	5	34	34	-6	-6	5	45	-45
-8	-10	4	44	43	0	-7	4	24	26	-7	-4	4	44	45	-9	-2	4	133	-130	-1	0	4	60	60	2	2	4	12	-14	6	4	4	16	17	3	7	4	6	5	-6	-9	5	39	-39	-5	-6	5	10	-10
-7	-10	4	14	-16	3	-7	4	5	1	-6	-4	4	21	-20	-3	-2	4	114	113	0	0	4	93	-92	3	2	4	60	59	7	4	4	38	-36	4	7	4	30	29	-5	-9	5	4	2	-4	-6	5	84	83
-5	-10	4	6	4	4	-7	4	23	-23	-5	-4	4	134	-135	-2	-2	4	36	-35	1	0	4	99	-99	4	2	4	16	15	-6	5	4	57	-57	5	7	4	52	-52	-4	-9	5	33	-31	-3	-6	5	23	-23
-2	-10	4	29	-29	-9	-6	4	44	-44	-4	-4	4	116	117	-1	-2	4	59	-59	2	0	4	27	27	5	2	4	8	6	-5	5	4	32	31	6	7	4	26	24	-2	-9	5	35	34	-2	-6	5	25	-23
-1	-10	4	6	-5	-8	-6	4	57	56	-3	-4	4	38	-38	0	-2	4	5	2	3	0	4	4	3	6	2	4	43	-44	-4	5	4	13	-12	7	7	4	16	16	-1	-9	5	50	-48	-1	-6	5	79	80
0	-10	4	31	32	-7	-6	4	33	-31	-2	-4	4	49	-48	1	-2	4	53	51	4	0	4	5	4	7	2	4	77	76	-3	5	4	27	-26	-3	8	4	16	15	0	-9	5	12	-9	0	-6	5	64	-63
-8	-9	4	8	-6	-6	-6	4	30	-29	-1	-4	4	51	50	2	-2	4	29	28	5	0	4	35	-35	-7	3	4	90	90	-2	5	4	20	20	-2	8	4	11	-12	1	-9	5	30	31	1	-6	5	18	18
-7	-9	4	20	-19	-5	-6	4	77	76	0	-4	4	3	-5	3	-2	4	79	-81	6	0	4	71	71	-6	3	4	90	90	-1	5	4	6	4	0	8	4	26	-28	-9	-8	5	13	-13	2	-6	5	19	19

TABLE 4.1.4 CONTINUED

4.2 DESCRIPTION OF THE STRUCTURE AND DISCUSSION

Intramolecular bond lengths and angles for the complex are listed in Tables 4.2.1 and 4.2.2 respectively. Least-squares planes and torsion angles are set out in Table 4.2.3.

The cation, comprising two $\{Fe(cp)(CO)_2\}$ moieties linked *via* an ethylthio group, is depicted in Figure 4.2.1 together with the atomic nomenclature employed in the structure analysis. The conformation of the complex, which is discussed in greater detail in Section 4.3, is such that, if viewed along the Fe(1) - Fe(2) vector, the cyclopentadienyl groups are seen to be approximately *cis* to each other (Figure 4.3.1(6)). The two $\{Fe(cp)(CO)_2\}$ residues show but slight deviations from an ideal octahedral geometry, with the convention that the cyclopentadienyl group occupies three coordinating sites of the Fe atom. The coordination round the sulphur atom is almost exactly tetrahedral. In the cyclopentadienyl group comprising C(7) - C(11), C(11) appears to deviate significantly from the least-squares plane through the atoms. However, no close contact less than 3.6 Å is observed. Otherwise the cyclopentadienyl groups are essentially regular plane pentagons symmetrically bound to the two iron atoms. A projection of the molecular packing in the unit cell on to (001) is shown in Figure 4.2.3; although no intermolecular close contacts are observed, it is interesting to note that this complex packs more tightly (the average volume occupied by a non-hydrogen atom is 17.1 $Å^3$) than the neutral mononuclear $[Fe(cp)(CO)_2SEt]$ (for which the average non-hydrogen atom volume is 19.9 $Å^3$).

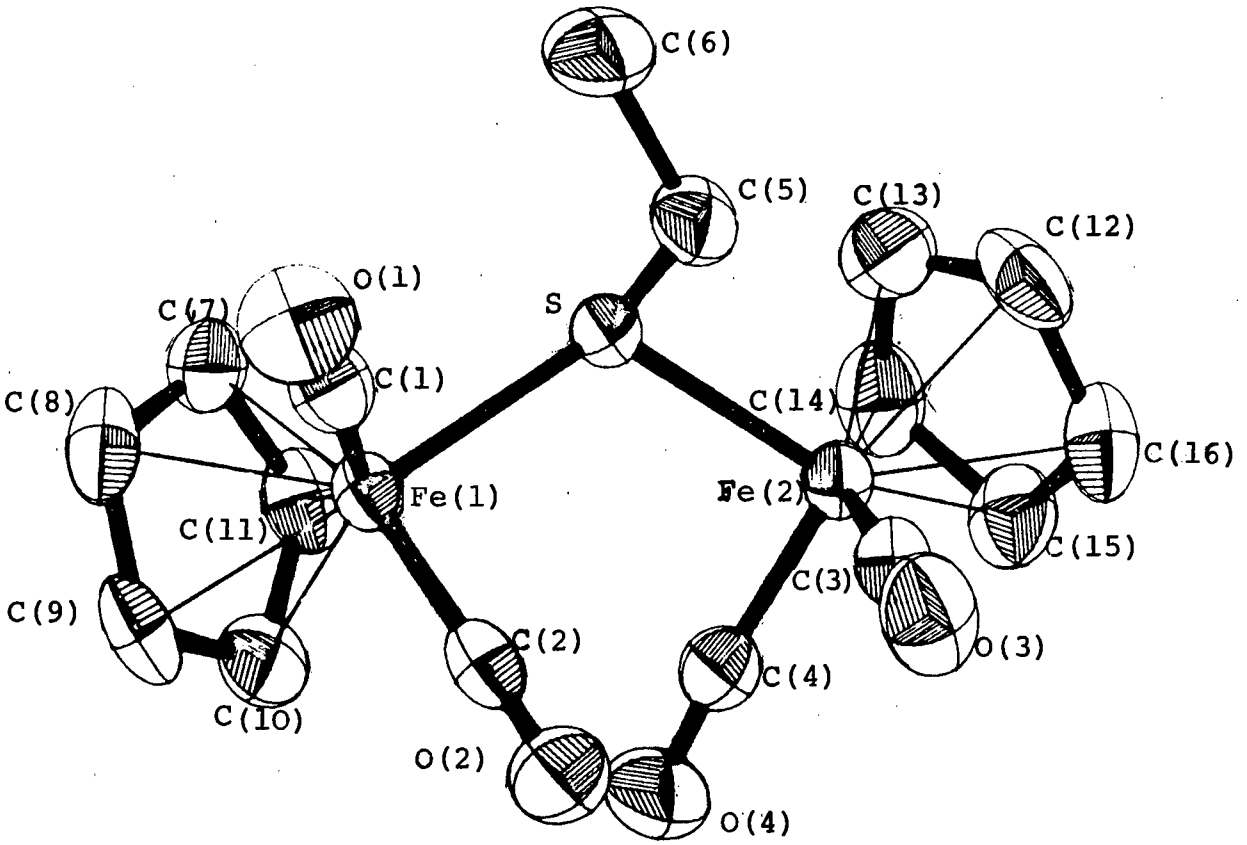

FIGURE 4.2.1

Molecular Structure of the Cation in $[\{Fe(cp)(CO)_2\}_2(SEt)]BF_4$

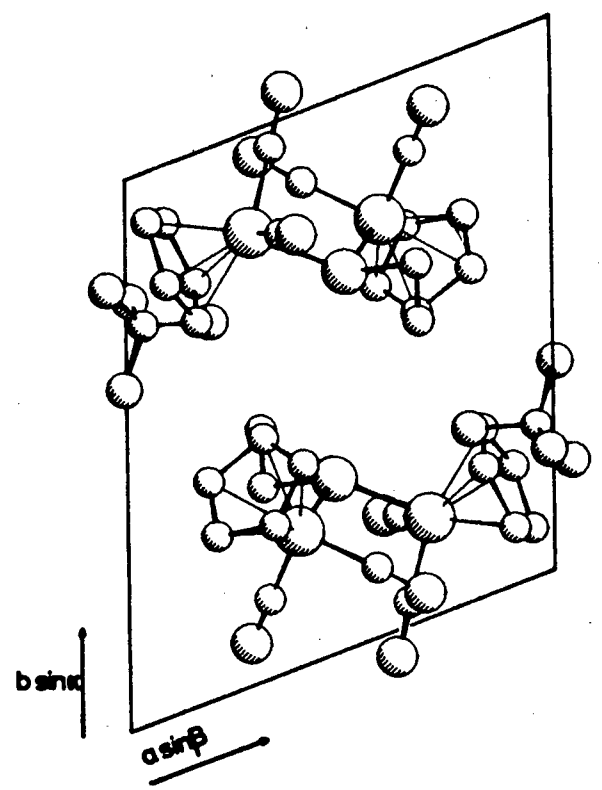

FIGURE 4.2.3

$[\{Fe(cp)(CO)_2\}_2SEt]BF_4$: Contents of the Unit Cell.

TABLE 4.2.1

INTRAMOLECULAR BOND LENGTHS AND THEIR E.s.d's (Å)

Fe(1)	-	S(1)	2.297(2)	Fe(2)	-	S(1)	2.304(2)
Fe(1)	-	C(1)	1.770(6)	Fe(2)	-	C(3)	1.770(6)
Fe(1)	-	C(2)	1.780(6)	Fe(2)	-	C(4)	1.778(6)
Fe(1)	-	C(7)	2.104(6)	Fe(2)	-	C(12)	2.105(6)
Fe(1)	-	C(8)	2.103(6)	Fe(2)	-	C(13)	2.109(6)
Fe(1)	-	C(9)	2.100(6)	Fe(2)	-	C(14)	2.108(6)
Fe(1)	-	C(10)	2.081(6)	Fe(2)	-	C(15)	2.093(6)
Fe(1)	-	C(11)	2.101(6)	Fe(2)	-	C(16)	2.093(6)
S(1)	-	C(5)	1.851(5)	C(5)	-	C(6)	1.520(7)
C(1)	-	O(1)	1.139(5)	C(3)	-	O(3)	1.144(6)
C(2)	-	O(2)	1.142(5)	C(4)	-	O(4)	1.134(6)
C(7)	-	C(8)	1.413(7)	C(12)	-	C(13)	1.411(8)
C(7)	-	C(11)	1.405(7)	C(12)	-	C(16)	1.410(7)
C(8)	-	C(9)	1.397(7)	C(13)	-	C(14)	1.400(8)
C(9)	-	C(10)	1.414(7)	C(14)	-	C(15)	1.417(7)
C(10)	-	C(11)	1.424(7)	C(15)	-	C(16)	1.397(7)
B	-	F(1)	1.383(7)	B	-	F(2)	1.347(7)
B	-	F(3)	1.360(8)	B	-	F(4)	1.376(7)

TABLE 4.2.2

INTRAMOLECULAR BOND ANGLES AND THEIR E.s.d's IN DEGREES

Fe(1) - S(1) - Fe(2)	117.4(2)	F - B - F (mean)	109.5(5)
C(2) - Fe(1) - C(1)	92.6(2)	C(4) - Fe(2) - C(3)	94.4(2)
C(2) - Fe(1) - S(1)	95.3(2)	C(4) - Fe(2) - S(1)	96.2(2)
C(1) - Fe(1) - S(1)	96.4(2)	C(3) - Fe(2) - S(1)	91.1(2)
O(1) - C(1) - Fe(1)	175.3(2)	O(3) - C(3) - Fe(2)	179.7(2)
O(2) - C(2) - Fe(1)	179.1(4)	O(4) - C(4) - Fe(2)	175.3(4)
C(5) - S(1) - Fe(1)	109.5(2)	C(5) - S(1) - Fe(2)	104.4(2)
C(6) - C(5) - S(1)	111.0(4)	C(cp) - C(cp) - C(cp) (ring bound	
C(cp) - C(cp) - C(cp) (ring bound		to Fe(2))	108.0(5) (mean)
to Fe(1))	108.0(7) (mean)		

TABLE 4.2.3

LEAST-SQUARES PLANES AND TORSION ANGLES

The equations of the planes are expressed in orthogonalized space as $PI + QJ + RK = S$

Plane 1. Through C(7), C(8), C(9), C(10) and C(11)

Equation: $(8.334)I + (3.866)J + (2.283)K = 5.777$

Atoms included in calculation	Distance from plane, Å	Atoms not included in calculation	Distance from plane, Å
C(7)	-0.004	Fe(1)	1.714
C(8)	0.002		
C(9)	-0.003		
C(10)	-0.001		
C(11)	-0.029		

Plane 2. Through C(12), C(13), C(14), C(15) and C(16)

Equation: $(-4.598)I + (4.079)J + (6.994)K = 2.747$

Atoms included in calculation	Distance from plane, Å	Atoms not included in calculation	Distance from plane, Å
C(12)	-0.001	Fe(2)	1.726
C(13)	0.003		
C(14)	0.002		
C(15)	-0.003		
C(16)	-0.005		

Angle between plane 1 and plane 2 97.4°

Torsion Angles.

(Torsion angles are positive if the rotation is clockwise when viewed along vector joining the two central atoms reading from left to right)

C(1) - Fe(1) - Fe(2) - C(3)	-52.0	C(1) - Fe(1) - Fe(2) - C(4)	-150.1
C(2) - Fe(1) - Fe(2) - C(3)	31.4	C(2) - Fe(1) - Fe(2) - C(4)	-66.7

4.3 CONFORMATIONAL STUDIES ON $[\{Fe(cp)(CO)_2\}_2SEt]BF_4$

4.3.1 INTRODUCTION.

It has already been remarked in Chapter 1 that the solution infra-red spectrum of $[\{Fe(cp)(CO)_2\}_2SEt]^+$, which exhibits four peaks in the terminal carbonyl stretching region, is sensitive to both the nature of the anion present in solution and irradiation with ultra-violet light, insofar as the intensities of the bands are concerned. The pattern of intensities is such that the bands can be grouped in two pairs, the highest frequency band with the third highest, and the lowest energy band with the second highest. The intensity of one pair of bands appears to increase at the expense of the other; indeed, the solution (CH_2Cl_2) infra-red spectrum of $[\{Fe(cp)(CO)_2\}_2SEt]ClO_4$, appears to contain only two peaks in the terminal carbonyl region. The separation of the bands in each pair is between 40 and 50 cm^{-1} while the frequency difference between the centroids of the pairs of bands is usually about 10 cm^{-1}. The lowest two bands are often poorly resolved.

A survey of other complexes of the type $[\{Fe(cp)(CO)_2\}_2M]$ where M is a bridging group reveals that these features, with some variation, are common to complexes of this type. For instance, two bands only (2010 vs, 1947 vs) occur in the terminal carbonyl region of the solution (CCl_4 and CS_2) i.r. spectrum of $[\{Fe(cp)(CO)_2\}_2SnEt_2]$[4.1] while four bands are reported for the halide derivative $[\{Fe(cp)(CO)_2\}_2SnCl_2]$[4.2] dissolved in cyclohexane or carbon disulphide (2026 vs, 200 x, 1975s, 1956 m). In the cases where three bands are reported the lowest frequency band is reported as being asymmetric, *e.g.*, $[\{Fe(cp)(CO)_2\}_2I]PF_6$[4.3] ($CH_2Cl_2$ solution); this band is probably an unresolved doublet.

Flitcroft, Harbourne, Paul, Tucker, and Stone[4.4] have discussed the appearance of the peaks in the terminal carbonyl region of the infra-red spectra of a number of complexes of the type $[\{Fe(cp)(CO)_2\}_2MX_2]$ where M is either Ge or Sn and X is a halide or an alkyl radical. Their approach is based on point group symmetry and the four carbonyl groups are considered as two coupled vibrating systems. They deduce that a molecule with Cs symmetry will give rise to a four band spectrum in which there is an alternation in intensity of bands with decreasing energy, while one with C_1 symmetry will exhibit a four band spectrum whose characteristic feature is a regular decrease in band intensity with decreasing energy. A molecule with C_{2v} symmetry will only have three bands in the terminal carbonyl region.

However, it seems unlikely that, in solution, a non-rigid molecule like $[\{Fe(cp)(CO)_2\}_2MX_2]$ will have any given conformation. In addition, this treatment does not explain the sensitivity of the infra-red spectra to irradiation, and, in the case of $[\{Fe(cp)(CO)_2\}SEt]^+$ to the nature of the anion present.

Other authors, in order to explain the multiplicity of bands in the terminal carbonyl region of such complexes, invoke the existence of conformationally distinct species in solution. For instance, Cotton and Peachey[4.5] report no less than six such bands for $[\{Fe(cp)(CO)_2\}_2GeCl_2]$ and deduce the presence of at least two conformers: this finding is in contrast with that of Flitcroft *et al.*[4.4], who only published four bands for this complex. Herber and Goscinny[4.6], *via* ^{57}Fe and ^{119}Sn Mössbauer studies, report the presence in frozen poly(methylmethacrylate) solutions of $[\{Fe(cp)(CO)_2\}_2SnCl_2]$ of two

distinct types of Sn atom, and adduce the presence of more than one rotational isomer of the molecule to explain this finding.

It, therefore, seems more likely that, far from preserving a definite symmetry in solution, the species $[\{Fe(cp)(CO)_2\}_2M]$ exists as a rapidly equilibrating mixture of two or more distinct conformers; there is little or no vibrational coupling between the two pairs of carbonyl groups and the intensities of the bands arising from them depends on the populations of the various conformers.

A study was initiated on $[\{Fe(cp)(CO)_2\}_2SEt]BF_4$ in order to ascertain whether the cation could exist in conformationally distinct forms, using the coordinates for the atoms determined in the Xray crystallographic study, and a computer program, EENY.[3.4]

4.3.2 THE FUNCTION OF EENY, AND RESULTS.

EENY is a program which calculates the non-bonded potential energy of molecules using empirical atom-pair potential curves. The energy summation may be made for both inter- and intra-molecular interactions. The program calculates atomic coordinates from parameters (rotation angles and translations) supplied and computes all interatomic distances. The non-bonded potential energy for a particular atom pair is determined using the equation

$$U(r) = \frac{a \exp(-br)}{r^d} - \frac{c}{r^6}$$

where r is the interatomic distance in Å. The values for the empirical constants a, b, c and d for all interactions involving C, H, N, O and CH_3 are those of Giglio[4.7]; U(v) is in kcal mol^{-1}. As corresponding constants were not available for iron and sulphur,

these atoms were treated as carbon atoms. The greatest variation in intramolecular potential energy will arise from changes in non-bonded atom-pair separations, and since the positions of the iron and sulphur atoms remained fixed in all rotations of the various residues comprising the cation, this approximation does not have a significant effect.

Accordingly, the total intramolecular potential energy of $[\{Fe(cp)(CO)_2\}_2SEt]^+$ was calculated in terms of three torsion angles $\tau 1$, $\tau 2$ and $\tau 3$, defined as in Figure 4.3.1. The $\{Fe(cp)(CO)_2\}$ and ethyl residues were treated as rigid groups. No allowance is made for bond binding or stretching by EENY and so not much reliance can be placed in the absolute values of the potential energy calculated.

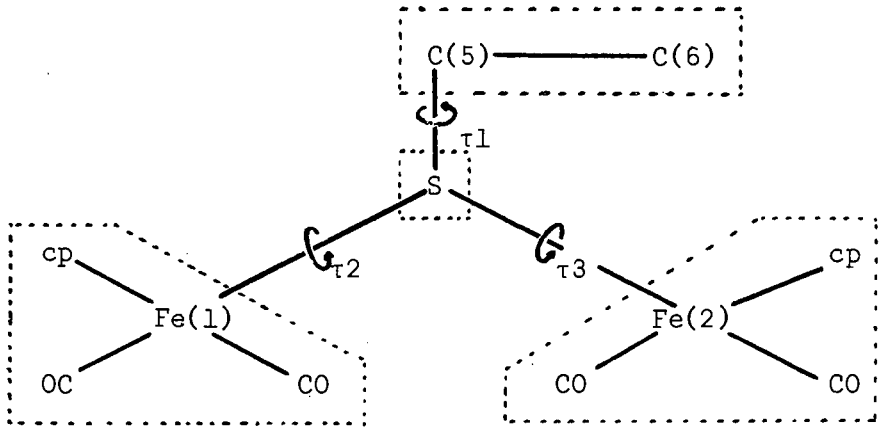

FIGURE 4.3.1

However, a good qualitative picture may be obtained of the way the energy varies as the different residues comprising the molecule are rotated about the bonds joining them. The potential energy was mapped from $\tau_1 = \tau_2 = \tau_3 = 0^\circ$ to $\tau_1 = \tau_2 = \tau_3 = 360^\circ$ in increments of

20°, and the three-dimensional map obtained scanned for energy minima, indicating the presence of possible stable conformers.

Five minima were located in the energy map: the positions of the minima were ascertained accurately from expanded maps of the region round each followed by simultaneous variation of the three torsion angles until a small change ($\Delta\tau = 0.25^{\circ}$) produced no further decrease in the intra-molecular potential energy. The positions of the energy minima (labelled 1 - 5) are set out in terms of the corresponding torsion angles τ, in Table 4.3.1 which also gives the torsion angles obtaining in the solid state, and the calculated intramolecular energy, U, in kcal $mole^{-1}$, for each energy minimum. Figure 4.3.2 depicts in schematic form the molecular configuration corresponding to each energy minimum. The molecules are viewed along the Fe(1) to Fe(2) vector with the plane defined by the iron and sulphur atoms perpendicular and vertical to the page.

TABLE 4.3.1

Energy minimum:	1	2	3	4	5	Solid State
$\tau 1$	251.46	260.29	237.13	226.81	270.00	277.45
$\tau 2$	306.95	282.39	338.61	350.75	16.75	16.98
$\tau 3$	189.75	38.15	68.27	326.10	44.75	46.88
U	-4.487	-2.779	-3.126	-2.299	-5.866	-5.632

4.3.3 DISCUSSION OF RESULTS.

It is readily apparent, both from the Table and the Figure, that configuration (5) is almost exactly that found for $[\{Fe(cp)(CO)_2\}_2SEt]^+$ in the crystalline state, providing some confirmation for the validity of this approach, since it would be expected that the complex should

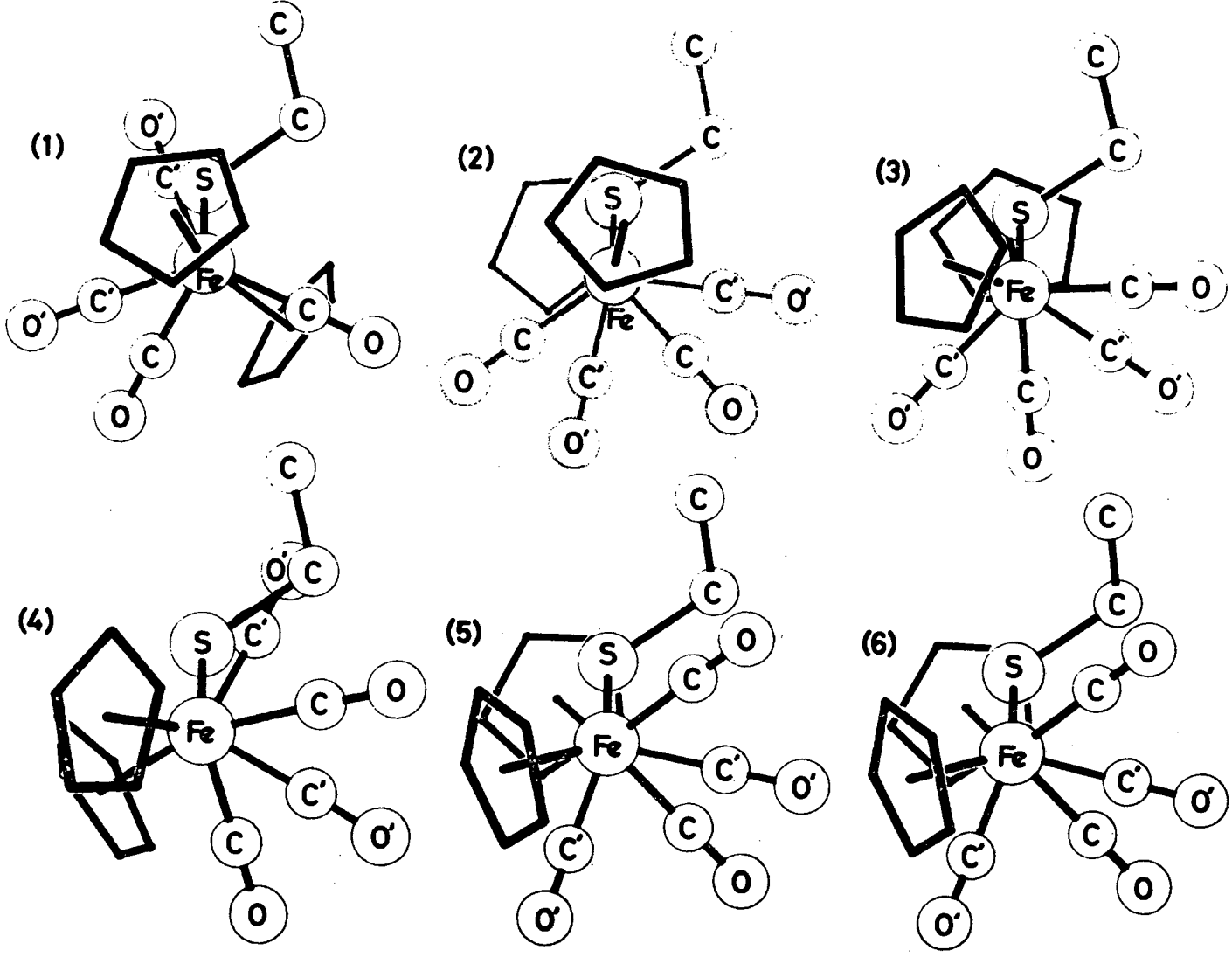

FIGURE 4.3.2

Preferred Conformations of $[\{Fe(cp)(CO)_2\}_2SEt]^+$

as calculated by EENY.

crystallize in an energetically preferred conformation.

Of the four other theoretical configurations, three are rather similar, *viz.* (2), (3) and (4); the torsion angles defined by ct(cp) - Fe(1) - Fe(2) - ct(cp) (ct(cp) denotes the centroid of the cyclopentadienyl group) are all somewhat less than 90°, the two pairs of carbonyl groups are staggered, and the calculated intramolecular energies are of the same order. If the ethyl groups are disregarded and the cyclopentadienyl groups treated as free rotators, then configurations (2) and (3) are seen to be approximate mirror images. Interestingly, conformation (1) is different from the others in that the cyclopentadienyl (and carbonyl) groups are *trans* with respect to the Fe - Fe vector. Inspection of a molecular model of $[\{Fe(cp)(CO)_2\}_2SEt]^+$ suggests that there should be energy barriers to interconversion of the five configurations described.

Thus it would seem that more than one conformer of $[\{Fe(cp)(CO)_2\}_2SEt]^+$ might exist in solution. Of the five conformers found only one is sufficiently different from that observed in the solid state to be likely to give a markedly different infra-red spectrum: the *trans* configuration 1. However, as pointed our previously EENY does not indicate reliably which configurations should correspond to the lowest potential energy minima, and therefore be the most thermodynamically stable.

In order independently to investigate the existence of several conformers of $[\{Fe(cp)(CO)_2\}_2SEt]^+$, low temperature (down to 213 K) N.M.R. spectra were run of the BF_4^- salt of the complex in d^6-acetone solution. If structurally distinct forms of the cation were present,

such low temperatures would be expected to slow interconversion between them and thus cause splitting of the sharp cyclopentadienyl resonance in a manner analogous to that observed for $[\{Mn(Mecp)(CO)_2\}_2SEt]^+$ (see Chapter 6). However, no such splitting is observed.

In conclusion, it is suggested that in order to explain the infra-red spectral behaviour of $[\{Fe(cp)(CO)_2\}_2SEt]^+$ in solution, the existence of more than one conformer of the species be invoked. As well as the configuration observed in the solid state structure, one or more of four conformations determined by the program EENY to correspond to intra-molecular potential energy minima may be present. A *trans* conformer, (1), has been shown to be an energetically favourable configuration of $[\{Fe(cp)(CO)_2\}_2SEt]^+$ and is likely to give a somewhat different infra-red spectrum from the solid state configuration. However, interconversion between such conformers appears to be rapid on an N.M.R. time scale, at least down to 213K, arguing a very low energy barrier to the interconversion.

CHAPTER 5

THE DETERMINATION OF THE CRYSTAL STRUCTURE OF μ-ETHYLTHIO-μ'-CARBONYL-BIS(η-CYCLOPENTADIENYLCARBONYLIRON) (Fe - Fe) HEXAFLUOROANTIMONATE: $[Fe_2(cp)_2(CO)_3SEt]SbF_6$

5.1 DETERMINATION OF THE STRUCTURE

Crystal Preparation

The complex was prepared as described in Chapter 1. Dark green needles were grown from an acetone-petroleum ether solution at -5°C.

Density Determination

The density of the crystals was found to be 2.10 gm cm^{-1} by flotation in an m-xylene/methylene iodide mixture.

Space Group Assignment

Zero- and first-layer Weissenberg photographs revealed that the crystals were monoclinic. The systematic absences $hk\ell$; h + k = 2n +1 and $h0\ell$ (h = 2n + 1), together with a value for Z of eight formula units per unit cell, indicated either the space group C2/c or the group Cc. The structure was successfully refined in the former after inspection of the Patterson map and the E-value statistics.

Diffractometer Data Collection

The intensities of 1929 reflections were measured in the ω-2θ scan mode up to 2θ=40° (scan width $1^{\circ}\theta$, scan speed $0.03^{\circ}\theta sec^{-1}$) using a cuboid crystal of dimensions 0.1 x 0.15 x 0.15 mm. No crystal decomposition was observed during data collection; no decay was observed in the intensities of the reference reflections, which showed

a random variation of about 4% about their initial values. 306 reflections were rejected as being systematically absent or space group equivalent. With the criterion $I_{rel} > 2\sigma(I_{rel})$ for an observed reflection, a further 118 reflections were discarded as unobserved, leaving 1505 unique reflections to be employed in the determination of the structure. No absorption corrections were made although μR varied from 0.28 to 0.66, corresponding to a change in A^* from 1.5 to 2.5 over the θ range scanned. Attempts to grind the crystals into spheres resulted in their shattering. Crystal data are listed in Table 5.1.1.

TABLE 5.1.1

CRYSTAL DATA

Molecular Formula	$[Fe_2(cp)_2(CO)_3SEt]SbF_6$
Molecular Weight	622.8 gm mole^{-1}
Space Group	C2/c
a = 18.111(9) Å	
b = 16.450(7) Å	Dm = 2.10 gm cm^{-3}
c = 13.292(6) Å	Dc = 2.09 gm cm^{-3} for Z=8
β = 92.2(3)°	μ(MoKα) = 28.0 cm^{-1}
V = 3957.13 Å^3	F(000) = 2416

Solution and Refinement of Structure

The Sb atom and the two Fe atoms were located with some difficulty using both Patterson and direct methods. The position of the Sb atom at approximately (0, $\frac{1}{4}$, 0) resulted in a number of ambiguities in the Patterson map, and its solution was not straightforward. Several E-maps were computed, and from one of the maps an equivalent position for the Sb atom, (0.5, 0.25, 0) was chosen which permitted self-consistent coordinates to be calculated for the two

iron atoms from Sb - Fe interaction peaks in the Patterson map. The iron atoms were separated by 2.6 Å, a chemically reasonable distance for an Fe - Fe bond[5.1]. A difference map based on the coordinates of these atoms, and assuming the space group C2/c, yielded the positions of the sulphur atom and six other light atoms; R was 0.48. After eight cycles of full-matrix least-squares refinement of the positions of these atoms, all non-hydrogen atoms were located in a difference map and R had fallen to 0.11. A further four cycles of refinement based on all non-hydrogen atoms with Sb and Fe assigned anisotropic temperature factors reduced R to 0.07, and all but three hydrogen atoms appeared as peaks in a subsequent difference electron density map. In a final four cycles of refinement all non-hydrogen atoms were allowed to refine anisotropically; the hydrogen atoms were constrained to ride on their parent carbon atoms with C - H set at 1.08 Å, their positions being dictated by the hybridization of the parent carbon atom. The refinement converged to R = 0.044 and R_w = 0.040 with a weighting scheme $w = \frac{0.579}{\sigma^2 F + 0.000965F^2}$; the average shift:error ratio in the final cycle was less than 0.1 for all parameters. A final difference map showed no peaks higher than 0.3eÅ^{-3}.

The final atomic coordinates and thermal parameters for the heavy atoms and hydrogen atoms are set out in Tables 5.1.2 and 5.1.3 respectively. Observed and calculated structure factors are listed in Table 5.1.4.

TABLE 5.1.2 NON-HYDROGEN ATOMS

FRACTIONAL ATOMIC COORDINATES AND THEIR E.s.d's ($\times 10^4$) AND ANISOTROPIC TEMPERATURE FACTORS AND THEIR E.s.d's. ($\times 10^3$).

Atom	x/a	y/b	z/c	U_{11}	U_{22}	U_{33}	U_{23}	U_{13}	U_{12}
Sb	-182(0)	2564(1)	10196(1)	40(1)	61(1)	41(1)	13(0)	6(0)	4(0)
Fe(1)	1893(1)	4983(1)	7991(1)	32(1)	38(1)	36(1)	-1(1)	3(1)	1(1)
Fe(2)	2828(1)	3802(1)	7953(1)	36(1)	38(1)	33(1)	-1(1)	0(1)	2(1)
F(1)	761(4)	2197(6)	9549(6)	56(5)	140(7)	109(6)	4(5)	20(4)	18(5)
F(2)	-10(4)	2419(6)	11183(5)	96(6)	235(12)	51(5)	38(6)	-10(4)	37(7)
F(3)	-1125(4)	2970(5)	10053(5)	60(5)	123(7)	70(5)	4(5)	9(4)	31(5)
F(4)	-368(5)	2761(6)	8448(5)	128(7)	168(9)	46(5)	24(5)	11(5)	43(6)
F(5)	-556(5)	1542(5)	9664(8)	109(7)	89(7)	198(10)	9(7)	17(6)	-26(6)
F(6)	178(5)	3622(5)	9953(7)	137(8)	94(7)	139(8)	-13(6)	20(6)	-36(6)
S(1)	2753(2)	4824(2)	6881(2)	44(2)	54(2)	38(2)	8(2)	9(1)	7(2)
O(1)	2653(5)	6193(5)	9244(7)	92(7)	54(6)	87(7)	-12(5)	-17(5)	-10(6)
O(2)	4096(5)	4444(6)	9087(7)	65(7)	89(7)	81(7)	7(6)	-22(5)	-19(6)
O(3)	2042(4)	4006(5)	9823(6)	79(6)	82(7)	28(5)	6(5)	13(4)	5(5)
C(1)	2370(6)	5716(8)	8746(9)	45(8)	45(8)	69(9)	-3(7)	15(7)	3(6)
C(2)	3590(7)	4216(7)	8651(8)	45(8)	56(8)	37(7)	21(6)	12(6)	9(6)
C(3)	2192(6)	4174(7)	9009(8)	40(7)	53(8)	29(7)	-4(6)	6(6)	5(6)
C(4)	3550(6)	5515(8)	7002(10)	53(9)	65(9)	85(10)	45(8)	20(7)	2(7)
C(5)	4207(7)	5150(9)	6545(11)	46(9)	123(14)	101(12)	48(10)	20(8)	12(9)
C(6)	1072(6)	4659(9)	6911(10)	43(8)	72(11)	61(10)	-25(8)	-11(7)	7(7)
C(7)	1122(6)	5523(9)	6945(10)	41(8)	73(11)	55(9)	9(8)	3(6)	10(7)
C(8)	971(6)	5760(8)	7931(11)	48(8)	48(9)	80(10)	-2(8)	-7(7)	4(7)
C(9)	813(5)	5061(9)	8489(9)	30(7)	88(11)	55(8)	-1(9)	14(6)	2(7)
C(10)	865(6)	4381(7)	7849(11)	28(7)	49(9)	86(10)	-10(9)	-11(7)	10(6)
C(11)	2247(10)	2925(9)	7083(14)	84(13)	61(10)	106(14)	-41(10)	-44(11)	25(9)
C(12)	2291(10)	2686(8)	8100(15)	93(13)	41(9)	124(15)	-29(9)	52(11)	-15(8)
C(13)	3029(9)	2605(7)	8388(10)	79(10)	32(8)	81(10)	7(7)	-13(9)	13(7)
C(14)	3449(7)	2797(7)	7553(11)	62(9)	45(8)	80(10)	-10(7)	10(9)	10(7)
C(15)	2970(11)	2981(8)	6758(9)	142(15)	48(9)	37(8)	-7(7)	-9(10)	36(10)

TABLE 5.1.3 HYDROGEN ATOMS

FRACTIONAL ATOMIC COORDINATES OF THE HYDROGEN ATOMS AND THEIR E.s.d's. ($x10^4$)
AND ISOTROPIC TEMPERATURE FACTORS AND THEIR E.s.d's. ($x10^3$).

Atom	x/a	y/b	x/c	U_{iso}	Atom	x/a	y/b	z/c	U_{iso}
H(41)	3674(6)	5646(8)	7786(10)	73(10)	H(9)	668(5)	5037(9)	9269(9)	95(11)
H(42)	3417(6)	6073(8)	6607(10)	73(10)	H(10)	767(6)	3753(7)	8040(11)	95(11)
H(51)	4642(7)	5596(9)	6497(11)	89(11)	H(11)	1753(10)	3035(9)	6622(14)	95(11)
H(52)	4028(7)	4964(9)	5795(11)	89(11)	H(12)	1823(10)	2590(8)	8567(15)	95(11)
H(53)	4412(7)	4628(9)	6962(11)	89(11)	H(13)	3236(9)	2427(7)	9129(10)	95(11)
H(6)	1181(6)	4291(9)	6260(10)	95(11)	H(14)	4045(7)	2800(7)	7532(11)	95(11)
H(7)	1256(6)	5924(9)	6335(10)	95(11)	H(15)	3127(11)	3145(8)	6009(9)	95(11)
H(8)	972(6)	6375(8)	8216(11)	95(11)					

TABLE 5.1.4

Observed and Calculated Structure Factors for $[Fe_2(cp)_2(CO)_3SEt]SbF_6$

TABLE 5.1.4 CONTINUED

H	K	L	FO	FC
7	7	6	38	-43
9	7	6	83	89
11	7	6	62	-60
-10	8	6	194	190
-8	8	6	56	59
-6	8	6	113	115
-4	8	6	242	236
-2	8	6	110	111
0	8	6	191	189
2	8	6	70	65
6	8	6	33	31
10	8	6	61	-59
-9	9	6	65	-59
-7	9	6	26	-5
-5	9	6	84	-85
-3	9	6	142	-140
-1	9	6	74	76
1	9	6	223	-226
3	9	6	57	57
5	9	6	28	-35
7	9	6	86	-86
9	9	6	55	59
11	9	6	62	-73
-8	10	6	130	-129
-6	10	6	159	-159
-4	10	6	65	-63
-2	10	6	179	-181
0	10	6	38	-42
2	10	6	36	-41
4	10	6	95	-101
6	10	6	38	25
10	10	6	26	28
-7	11	6	135	110
-3	11	6	92	94

H	K	L	FO	FC
-1	11	6	91	92
1	11	6	26	31
3	11	6	39	38
5	11	6	67	60
9	11	6	76	72
-8	12	6	111	111
-4	12	6	186	186
-2	12	6	25	-9
0	12	6	84	78
2	12	6	36	38
4	12	6	88	-80
6	12	6	92	85
-5	13	6	105	-101
-1	13	6	66	-60
3	13	6	70	-65
-13	1	7	33	-30
-11	1	7	73	-67
-9	1	7	65	-61
-7	1	7	69	69
-3	1	7	161	165
-1	1	7	169	169
1	1	7	337	335
3	1	7	282	283
5	1	7	213	211
7	1	7	211	206
9	1	7	103	96
11	1	7	167	163
13	1	7	70	64
-12	2	7	52	58
-10	2	7	62	-61
-8	2	7	73	78
-6	2	7	99	-98
-4	2	7	20	-15
-2	2	7	71	67

H	K	L	FO	FC
0	2	7	36	-47
2	2	7	118	116
4	2	7	162	-162
6	2	7	85	84
8	2	7	98	-86
10	2	7	25	15
14	2	7	29	-15
-13	3	7	63	63
-11	3	7	73	72
-7	3	7	35	36
-5	3	7	126	-127
-3	3	7	40	-40
-1	3	7	241	-232
1	3	7	169	-171
3	3	7	288	-291
5	3	7	204	-202
7	3	7	153	-159
9	3	7	222	-221
11	3	7	93	-53
13	3	7	134	-134
-12	4	7	40	-46
-6	4	7	24	16
-4	4	7	28	-29
2	4	7	41	50
6	4	7	30	18
10	4	7	39	33
12	4	7	55	44
-13	5	7	88	-87
-9	5	7	41	-47
-5	5	7	55	58
-3	5	7	33	30
-1	5	7	211	208
1	5	7	172	170
3	5	7	233	240

H	K	L	FO	FC
5	5	7	161	159
7	5	7	161	162
9	5	7	142	144
11	5	7	87	78
13	5	7	114	112
-10	6	7	109	106
-8	6	7	64	-66
-6	6	7	94	95
-4	6	7	93	-91
-2	6	7	57	62
2	6	7	67	-71
4	6	7	34	-9
6	6	7	120	-119
8	6	7	28	28
10	6	7	84	-74
-11	7	7	65	64
-9	7	7	32	6
-7	7	7	35	-23
-3	7	7	166	-164
-1	7	7	81	-83
1	7	7	173	-175
3	7	7	105	-106
5	7	7	195	-195
7	7	7	140	-138
9	7	7	93	-102
11	7	7	94	-98
-10	8	7	26	-25
-8	8	7	65	-73
-6	8	7	46	36
-4	8	7	39	-29
2	8	7	35	44
4	8	7	61	62
8	8	7	56	53
10	8	7	37	36

H	K	L	FO	FC
-9	9	7	27	-28
-7	9	7	28	35
-5	9	7	35	22
-3	9	7	107	106
-1	9	7	90	89
1	9	7	149	144
3	9	7	121	120
5	9	7	78	77
7	9	7	137	139
9	9	7	34	48
-8	10	7	43	42
-6	10	7	40	4
0	10	7	100	-99
2	10	7	45	45
4	10	7	126	-118
8	10	7	83	-77
-5	11	7	59	-69
-3	11	7	35	-25
-1	11	7	108	-111
1	11	7	65	-59
3	11	7	92	-94
5	11	7	119	-120
-6	12	7	27	-13
-2	12	7	46	45
0	12	7	37	-34
2	12	7	65	69
-3	13	7	40	35
-1	13	7	84	88
1	13	7	23	25
-14	0	8	29	30
-12	0	8	231	229
-10	0	8	43	38
-8	0	8	357	363
-6	0	8	228	229

H	K	L	FO	FC
-4	0	8	102	100
-2	0	8	349	345
0	0	8	73	-68
2	0	8	282	281
4	0	8	44	-36
6	0	8	56	57
8	0	8	70	-69
10	0	8	78	-72
12	0	8	30	-88
-13	1	8	90	-36
-11	1	8	71	72
-9	1	8	37	-33
-7	1	8	43	44
-5	1	8	102	-93
-3	1	8	41	31
-1	1	8	125	-125
1	1	8	129	129
3	1	8	80	-85
7	1	8	85	84
9	1	8	160	-156
11	1	8	147	142
13	1	8	85	-86
-12	2	8	68	-69
-10	2	8	234	-235
-8	2	8	155	-160
-6	2	8	208	-206
-4	2	8	263	-266
-2	2	8	61	-62
0	2	8	277	-281
2	2	8	55	-45
4	2	8	52	54
6	2	8	45	-42
8	2	8	67	65
12	2	8	67	63

H	K	L	FO	FC
-13	3	8	136	-102
-11	3	8	84	77
-9	3	8	60	58
-7	3	8	70	-60
-5	3	8	124	124
-3	3	8	62	-69
-1	3	8	83	80
1	3	8	94	94
3	3	8	40	-35
9	3	8	29	-38
11	3	8	45	56
-12	4	8	171	133
-10	4	8	152	149
-8	4	8	156	164
-6	4	8	262	260
-4	4	8	37	16
-2	4	8	237	241
0	4	8	22	29
2	4	8	63	62
4	4	9	168	164
6	4	8	159	-168
8	4	8	61	59
10	4	8	111	-118
12	4	8	78	-82
-7	5	8	158	-157
-5	5	8	134	132
-3	5	8	134	-140
3	5	8	61	-62
5	5	8	42	39
7	5	8	33	21
9	5	8	24	-18
11	5	8	27	26
-12	6	8	29	-46
-10	6	8	165	-161

H	K	L	FO	FC
-8	6	8	108	-107
-6	6	8	133	-135
-4	6	8	240	-237
[illegible]	6	8	196	-197
6	6	8	79	-73
8	6	8	73	77
10	6	8	37	39
-11	7	8	66	65
-9	7	8	83	90
-7	7	8	93	88
-1	7	8	76	-20
1	7	8	100	107
3	7	8	81	-81
7	7	8	38	42
9	7	8	76	-66
-8	8	8	133	131
-6	8	8	104	110
-4	8	8	46	41
-2	8	8	278	225
0	8	8	60	-60
2	8	8	165	166
4	8	8	33	-35
6	8	8	38	1
8	8	8	48	-40
-9	9	8	90	-82
-7	9	8	44	-40
-5	9	8	41	-41
-1	9	8	129	-120
1	9	8	41	38
3	9	8	87	-87
7	9	8	54	60
-8	10	8	33	-26
-6	10	8	110	-115
-4	10	8	153	-156

H	K	L	FO	FC
0	10	8	103	-108
4	10	8	27	-34
-5	11	8	110	110
-1	11	8	50	50
1	11	8	64	63
5	11	8	38	33
-2	12	8	94	94
0	12	8	41	47
2	12	8	47	-46
-11	1	9	24	-14
-9	1	9	38	43
-7	1	9	35	8
-5	1	9	164	159
-3	1	9	74	69
-1	1	9	213	212
1	1	9	152	147
3	1	9	187	131
5	1	9	150	154
7	1	9	36	44
9	1	9	127	123
11	1	9	47	41
-12	2	9	46	-43
-10	2	9	70	69
-8	2	9	49	-54
-6	2	9	48	-38
-4	2	9	37	23
-2	2	9	52	-50
0	2	9	58	60
2	2	9	96	-99
4	2	9	81	84
6	2	9	77	-80
8	2	9	35	22
-9	3	9	33	28
-7	3	9	126	-131

H	K	L	FO	FC
-3	3	9	190	-197
-1	3	9	31	-45
1	3	9	213	-218
3	3	9	151	-151
5	3	9	119	-115
7	3	9	160	-156
11	3	9	103	-107
-10	4	9	24	2
-4	4	9	40	57
4	4	9	45	42
-9	5	9	31	8
-7	5	9	38	49
-3	5	9	156	158
-1	5	9	94	96
1	5	9	146	148
3	5	9	139	142
5	5	9	100	96
7	5	9	106	112
9	5	9	60	65
-8	6	9	38	30
-6	6	9	58	-60
4	6	9	45	-38
8	6	9	29	-38
-5	7	9	109	-110
-3	7	9	46	-45
-1	7	9	144	-142
1	7	9	104	-103
3	7	9	105	-107
5	7	9	119	-118
7	7	9	65	-64
9	7	9	80	-86
-6	8	9	33	21
0	8	9	66	59
4	8	9	34	28

H	K	L	FO	FC
6	8	9	42	24
-5	9	9	38	103
-3	9	9	54	51
-1	9	9	114	108
1	9	9	84	88
3	9	9	75	78
5	9	9	98	98
-2	10	9	77	-75
0	10	9	50	49
2	10	9	95	-91
4	10	9	28	30
-3	11	9	135	-139
1	11	9	112	-108
-10	0	10	256	263
-8	0	10	84	90
-6	0	10	145	147
-4	0	10	151	150
-2	0	10	99	-101
0	0	10	272	275
2	0	10	145	-154
4	0	10	91	88
6	0	10	75	-81
8	0	10	71	-74
-11	1	10	73	-79
-9	1	10	54	48
-7	1	10	61	-50
-1	1	10	36	42
1	1	10	115	-112
3	1	10	71	71

H	K	L	FO	FC
5	1	10	31	-21
9	1	10	67	60
-10	2	10	52	-53
-8	2	10	133	-135
-6	2	10	84	-78
-4	2	10	81	-85
-2	2	10	165	-166
0	2	10	35	33
2	2	10	103	-98
4	2	10	37	36
6	2	10	52	53
10	2	10	97	97
-9	3	10	46	32
-7	3	10	40	38
-5	3	10	60	-61
-3	3	10	71	73
1	3	10	25	-24
3	3	10	89	85
5	3	10	93	-93
7	3	10	54	56
-10	4	10	132	135
-8	4	10	80	78
-6	4	10	175	184
-4	4	10	50	48
-2	4	10	51	47
0	4	10	48	43
4	4	10	42	-36
8	4	10	69	-68
-5	5	10	90	-91

H	K	L	FO	FC
-3	5	10	67	63
-1	5	10	52	-43
1	5	10	33	-47
3	5	10	81	79
5	5	10	80	-76
7	5	10	57	58
-8	6	10	164	-167
-4	6	10	72	-78
-2	6	10	108	-104
2	6	10	65	-72
4	6	10	27	32
6	6	10	61	60
-5	7	10	33	18
-3	7	10	26	12
-1	7	10	26	29
7	7	10	37	-34
-6	8	10	127	125
-4	8	10	129	137
-2	8	10	52	-52
0	8	10	114	119
2	8	10	105	-104
4	8	10	52	51
-3	9	10	43	-22
1	9	10	67	-49
3	9	10	40	31
-7	1	11	98	98
-5	1	11	75	73
-3	1	11	91	90
-1	1	11	98	84

H	K	L	FO	FC
1	1	11	108	113
3	1	11	126	118
5	1	11	73	65
7	1	11	90	95
-8	2	11	38	23
-4	2	11	48	-44
-2	2	11	60	64
0	2	11	87	-93
2	2	11	85	83
4	2	11	91	-101
-5	3	11	107	-106
-3	3	11	50	-52
-1	3	11	101	-99
1	3	11	117	-120
3	3	11	75	-78
5	3	11	123	-127
7	3	11	35	-26
-2	4	11	36	19
6	4	11	40	23
-7	5	11	27	24
-5	5	11	94	104
-3	5	11	57	55
-1	5	11	95	37
1	5	11	109	110
3	5	11	67	59
5	5	11	114	117
-6	6	11	45	-39
-4	6	11	41	41
-2	6	11	79	-74

H	K	L	FO	FC
0	6	11	51	49
2	6	11	81	-80
4	6	11	27	-11
-5	7	11	53	-67
-3	7	11	74	-71
-1	7	11	101	-107
1	7	11	50	-57
3	7	11	129	-128
-4	0	12	93	98
-2	0	12	80	80
0	0	12	80	-88
2	0	12	99	97
4	0	12	135	-140
-3	1	12	51	-35
3	1	12	27	-5
5	1	12	29	7
-6	2	12	143	-157
0	2	12	79	-79
2	2	12	75	74
-5	3	12	47	34
-3	3	12	47	-31
-1	3	12	27	26
1	3	12	59	62
3	3	12	43	-49
-4	4	12	117	121
0	4	12	27	17
2	4	12	27	-10
-3	5	12	53	-60
-1	5	12	28	-27

5.2 DESCRIPTION OF STRUCTURE AND DISCUSSION.

Interatomic distances and bond angles in $[Fe_2(cp)_2(CO)_3SEt]SbF_6$ are listed in Tables 5.2.1 and 5.2.2 respectively. Least-squares planes are set out in Table 5.2.3.

Figure 5.2.1 shows the structure of the cation and the atomic nomenclature employed. The structure is highly symmetrical with an approximate mirror plane through the bridging sulphur and carbon atoms and the methylene carbon of the $-SC_2H_5$ ligand. The Fe(1)C(3)Fe(2)S(1) ring is slightly puckered with the dihedral angles between the planes defined by Fe(1)Fe(2)C(3) and Fe(1)Fe(2)S, and by Fe(1)C(3)S and Fe(2)C(3)S being 15.6° and 19.2° respectively. The essentially planar cyclopentadienyl rings are cis-disposed with respect to the Fe - Fe vector, but trans to the ethyl of the ethylthio group and are both symmetrically bound to the iron atoms. The coordination of each iron atom is approximately octahedral, assuming the convention that a cyclopentadienyl group occupies three coordination positions. The cation can thus be considered as two octahedra sharing an edge defined by the two vertices occupied by the bridging sulphur and carbon atoms. The Fe - Fe distance of 2.580 Å and the Fe - S - Fe bond angle of 71.7° are consistent with the presence of an Fe - Fe two-electron bond, in accordance with the magnetic properties of this complex[5.1]. The two terminal carbonyls show considerable deviation from a possible parallel configuration as revealed by the C(1) - Fe(1) - Fe(2) and C(2) - Fe(2) - Fe(1) bond angles of 102.6° and 101.5° respectively. This will explain the moderate intensity of the asymmetric C - O stretching mode in the solid state infra-red spectrum. In comparison no such vibration is observed in the spectrum of

cis-$[\{Fe(cp)(CO)(SPh)\}_2]$ in which the carbonyl groups are found to be parallel to within experimental error[5.2]. Consistent with this finding, cis-$[\{Fe(cp)(CO)(SPh)\}_2]$ exhibits a single C - O stretching band in its infra-red spectrum.

A value of 82.6° for the Fe - C - Fe bond angle is worthy of comment. As discussed in Chapter 1, considerable evidence is now available to suggest that bridging carbonyls will only span metal atoms which are separated by relatively short distances. For instance while $[\{Co(CO)_4\}_2]$ with a Co - Co distance of 2.524 Å contains two symmetrically bridging carbonyls[5.3], $[FeCo(CO)_8]^-$ with an Fe - Co distance of 2.585 Å contains a single asymmetrically bridging CO group[5.4] and $[\{Fe(CO)_4\}_2]^{2-}$ with an Fe - Fe bond of 2.787 Å has only terminal carbonyls. An Mn - Mn distance of 2.923 Å in $[\{Mn(CO)_5\}_2]$ would also explain the absence of bridging carbonyls in this derivative. In contrast, the thio-ligands in both $[Fe_2(cp)_2(CO)_3SEt]^+$ and the non-metal-metal bonded $[\{Fe(cp)(CO)(SPh)\}_2]$[5.2] bridge the two atoms symmetrically, although the Fe - Fe distances are 2.580 and 3.39 Å and the Fe - S - Fe angles are 71.7 and 98° respectively.

Table 5.2.4 sets out values for these and other parameters of interest for a number of dinuclear dibridged iron complexes. Inspection of the table shows that the longest Fe - Fe bond spanned by a symmetrically bridging carbonyl group is that in $[Fe_2(cp)_2(CO)_3GeMe_2]$ (Fe - Fe = 2.628 Å) in which the Fe - C - Fe angle is 86.8°. This value is far short of that expected for an sp^2-hybridized carbon atom, and it may be argued that, similar to terminal carbonyl groups, bridging carbonyls form stable bonds with transition metals by virtue of a strong

TABLE 5.2.4

Comparison of bond lengths (Å) and angles (°) in $[Fe_2(cp)_2(CO)_3(SEt)]SbF_6$ and structurally related compounds[a]

Compound	Fe-Fe	Fe-S (av.)	Fe-C_{bridg} (av.)	Fe-C_{term} (av.)	Fe-ct(cp) (av.)	Fe-S-Fe (av.)	Fe-C_{bridg}-Fe (av.)	X-Fe-X'[b] (av.)
$[Fe_2(cp)_2(CO)_3(SEt)]SbF_6$	2.580(2)	2.204(3)	1.96(1)	1.77(1)	1.73(1)	71.7(1)	82.6(5)	101.5(3)
$[Fe_2(cp)_2(CO)_3SO_2]$ [c,d]	2.597(1)	2.184(1)	1.932(4)	1.761(4)	1.736(1)	72.93(04)	84.45(15)	98.9(1)
$[Fe_2(cp)_2(CO)_3GeMe_2]$ [e]	2.628(1)		1.913(6)	1.731(7)	1.758(8)		86.8(2)	85.9(2)
$[\{Fe(cp)(CO)_2\}_2]$ (*cis*) [f]	2.531(2)		1.917(7)	1.745(8)	1.746(5)		82.6(3)	96.0(3)
$[\{Fe(cp)(CO)_2\}_2]$ (*trans*) [g]	2.534(2)		1.914(5)	1.748(6)	1.754(6)		82.9(2)	97.1(4)
$[\{Fe(cp)(CO)(\mu\text{-}CNCH_3)\}_2]$ [h]	2.538(1)		1.942(7)	1.714(8)	1.754(7)		81.9(3)	88.0(3)
$[\{Fe(cp)(CO)(SMe)\}_2]BF_4$ [i]	2.925(4)	2.234(4)		1.79(2)		81.8(1)		95.4(1)
$[\{Fe(cp)(CO)(SPh)\}_2]$ [j,k]	3.39	2.262(6)		1.71(3)	1.71	98		81

[a] Ct(cp) signifies the centroid of the cyclopentadienyl group. [b] X,X' = bridging atoms. [c] Data are for molecule A of the asymmetric unit. [d] Ref. 1.62 [e] Ref. 5.6 [f] Ref. 1.31 [g] Ref. 1.32 [h] Ref. 5.5 [i] Ref. 1.33 [j] Average values for the two independent molecules in the asymmetric unit. [k] Ref. 5.2.

π-interaction between the metal and the carbon atom and that this interaction decreases considerably on widening of the M - C - M bond angle

The molecular packing in the crystal is depicted in Figure 5.2.2. No intermolecular close contacts less than 3.5 Å were observed. The average volume occupied by a non-hydrogen atom is 17.7 Å, which is very similar to corresponding figures for $[\{Fe(cp)(CO)_2\}_2SEt]BF_4$ and $[\{Mn(Mecp)(CO)_2\}_2SEt]ClO_4$ (see Chapters 4 and 6).

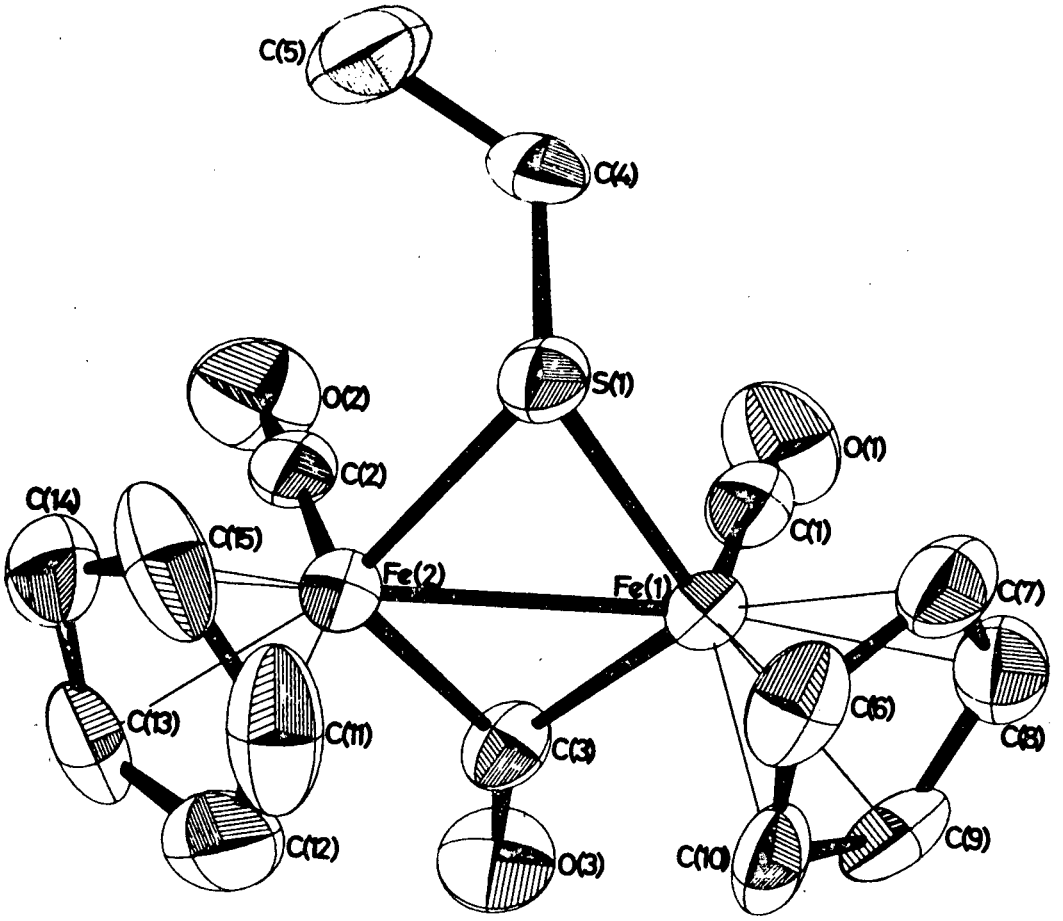

FIGURE 5.2.1. Molecular Structure of the Cation in $[Fe_2(cp)_2(CO)_3(SEt)]SbF_6$

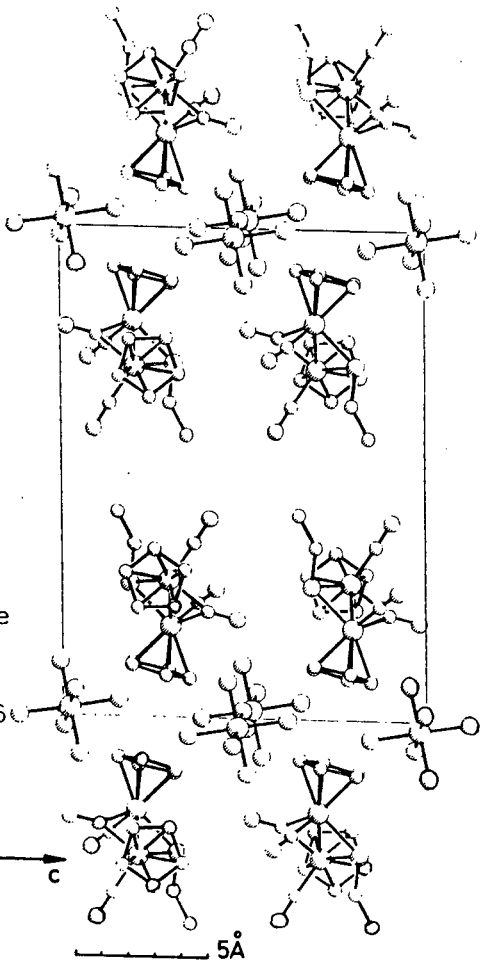

FIGURE 5.2.2

Molecular Packing in the Unit Cell of $[Fe_2(cp)_2(CO)_3(SEt)]SBf_6$

TABLE 5.2.1

BOND LENGTHS (Å) WITH E.s.d's. IN PARENTHESES

Fe(1)	- Fe(2)	2.580(2)			
Fe(1)	- S(1)	2.202(3)	Fe(2)	- S(1)	2.205(3)
Fe(1)	- C(1)	1.77 (1)	Fe(2)	- C(2)	1.77 (1)
Fe(1)	- C(3)	1.96 (1)	Fe(2)	- C(3)	1.95 (1)
Fe(1)	- C(6)	2.10 (1)	Fe(2)	- C(11)	2.11 (1)
Fe(1)	- C(7)	2.13 (1)	Fe(2)	- C(12)	2.09 (1)
Fe(1)	- C(8)	2.10 (1)	Fe(2)	- C(13)	2.08 (1)
Fe(1)	- C(9)	2.09 (1)	Fe(2)	- C(14)	2.08 (1)
Fe(1)	- C(10)	2.11 (1)	Fe(2)	- C(15)	2.11 (1)
S(1)	- C(4)	1.84 (1)	C(4)	- C(5)	1.48 (2)
C(1)	- O(1)	1.14 (1)	C(2)	- O(2)	1.13 (1)
C(3)	- O(3)	1.16 (1)			
C(6)	- C(7)	1.43 (2)	C(11)	- C(12)	1.41 (2)
C(6)	- C(10)	1.39 (2)	C(11)	- C(15)	1.40 (2)
C(7)	- C(8)	1.40 (2)	C(12)	- C(13)	1.38 (2)
C(8)	- C(9)	1.40 (2)	C(13)	- C(14)	1.41 (2)
C(9)	- C(10)	1.41 (2)	C(14)	- C(15)	1.38 (2)
Sb - F (mean)		1.855(20)			

TABLE 5.2.2

BOND ANGLES (°) WITH E.s.d's IN PARENTHESES

Fe(1)	-	S(1)	-	Fe(2)	71.7(1)		
Fe(1)	-	C(3)	-	Fe(2)	82.6(5)		
S(1)	-	Fe(1)	-	Fe(2)	54.2(1)	S(1) - Fe(2) - Fe(1)	54.1(1)
C(3)	-	Fe(1)	-	Fe(2)	48.5(3)	C(3) - Fe(2) - Fe(1)	48.9(3)
C(1)	-	Fe(1)	-	Fe(2)	102.6(4)	C(2) - Fe(2) - Fe(1)	101.5(4)
C(1)	-	Fe(1)	-	S(1)	96.8(4)	C(2) - Fe(2) - S(1)	94.2(3)
C(1)	-	Fe(1)	-	C(3)	87.4(5)	C(2) - Fe(2) - C(3)	88.4(5)
C(cp)	-	Fe(1)	-	C(cp)	(mean) 39.0(4)	C(cp) - Fe(2) - C(cp)	(mean) 38.9(4)
Fe(1)	-	C(1)	-	O(1)	178(1)	Fe(2) - C(2) - O(2)	176(1)
Fe(1)	-	C(3)	-	O(3)	138(1)	Fe(2) - C(3) - O(3)	140(1)
Mean internal angle of cp ring bound to Fe(1)					108(1)	Mean internal angle of cp ring bound to Fe(2)	108(1)
Fe(1)	-	S(1)	-	C(4)	116.1(4)	Fe(2) - S(1) - C(4)	112.7(4)
S(1)	-	C(4)	-	C(5)	111(1)		
F	-	Sb	-	F(mean)	90.0(1)		

Torsion angles

C(1)	-	Fe(1)	-	Fe(2)	-	C(2)	2.5
C(1)	-	Fe(1)	-	C(3)	-	O(3)	72.2
C(2)	-	Fe(2)	-	C(3)	-	O(3)	74.8

TABLE 5.2.3

LEAST-SQUARES PLANES.

The equationsof the planes are expressed in orthogonalized space as PI + QJ + RK = S

Plane 1. Through C(6) - C(10) inclusive

Equation (17.349)I + (-1.408)J + (3.152)K = 3.369

Atoms included in calculation	Distance from plane, Å	Atoms not included in calculation	Distance from plane, Å
C(6)	0.014	Fe(1)	1.733
C(7)	-0.012		
C(8)	0.005		
C(9)	0.004		
C(10)	-0.011		

Plane 2. Through C(11) - C(15) inclusive

Equation (0.267)I + (15.811)J + (3.653)K = 7.267

Atoms included in calculation	Distance from plane, Å	Atoms not included in calculation	Distance from plane, Å
C(11)	0.004	Fe(2)	1.724
C(12)	0.000		
C(13)	-0.004		
C(14)	0.006		
C(15)	-0.007		

TABLE 5.2.3 (CONTD.)

LEAST-SQUARES PLANES.

Plane 3. Through Fe(1), Fe(2), C(3) and O(3).

Equation (12.863)I + (10.040)J + (4.298)K = 10.875

Atoms included in calculation	Distance from plane, Å	Atoms not included in calculation	Distance from plane, Å
Fe(1)	-0.002	S(1)	0.467
Fe(2)	-0.002		
C(3)	0.008		
O(3)	-0.005		

Angles between normals to planes

Plane 1	Plane 2	89.6

CHAPTER 6

THE CRYSTAL STRUCTURE OF μ-ETHYLTHIOBIS(η-METHYLCYCLOPENTADIENYL-DICARBONYLMANGANESE)(Mn - Mn) PERCHLORATE: $[\{Mn(Mecp)(CO)_2\}_2SEt]ClO_4$

6.1 DETERMINATION OF THE STRUCTURE

Crystal Preparation

The complex was prepared as described in Chapter 2. Dark green crystals were grown from an acetone-petroleum ether solution at $-5^{\circ}C$.

Density Determination

The density of the crystals was found to be 1.64 gm cm^{-3} by flotation in m-xylene-methylene iodide mixtures.

Space Group Assignment

Unit cell dimensions determined from oscillation photographs, together with the experimentally observed crystal density, indicated that there were four formula units per unit cell. Inspection of zero- and first-order Weissenberg photographs revealed systematic absences of the form hOl : l = 2n+1 and OkO : k = 2n. The space group $P2_1/c$ was thus uniquely indicated.

Diffractometer Data Collection

A crystal of dimensions 0.12 x 0.22 x 0.38 mm was used. 2237 reflections were scanned in the ω - 2θ mode at a scan width of $1.1^{\circ}\theta$ and speed of $0.04^{\circ}\theta sec^{-1}$ in the range $6^{\circ} \leq 2\theta \leq 50^{\circ}$. No crystal decomposition was detected during data collection; variations in the

reference reflection intensities were limited to 4% about their initial values; 108 reflections of those collected were space group equivalent or systematically absent, while of the remainder, 1785 were considered observed according to the criterion $I_{rel} > 2\sigma(I_{rel})$ and were used in the structure determination. No absorption corrections were applied, although variation in A^* over the θ range scanned, corresponding to a change in μR from a minimum of 0.18 to a maximum of 0.68 was from 1.3 to 2.7. The small quantity of material available, and its friability, precluded the grinding of spheres to minimize absorption. Crystal data are presented in Table 6.1.1

TABLE 6.1.1

CRYSTAL DATA

Molecular formula	$[\{Mn(Mecp)(CO)_2\}_2SEt]ClO_4$
Molecular Weight	540.8 gm $mole^{-1}$
Space group	$P2_1/n$
a = 8.676(5)	
b = 16.062(5)	Dm = 1.64 gm cm^{-3}
c = 15.872(5)	Dc = 1.68 gm cm^{-3} for Z = 4
β = 104.45(20)	μ(MoKα) = 15.01 cm^{-1}
V = 2141.8 $Å^3$	F(000) = 1096

Structure Determination and Refinement

Inspection of the diffractometer intensity data revealed that the reflections $hO\ell$: $h+\ell$ = 2n and $0k0$: k = 2n were systematically absent. These absences uniquely determine the space group $P2_1/n$, and therefore the Miller indices of the reflections collected referred to a different unit cell from that chosen during preliminary photography. Fortuitously, however, the dimensions of the cells were very similar. Figure 6.1.1 shows the relation between the cells (drawn to scale) and

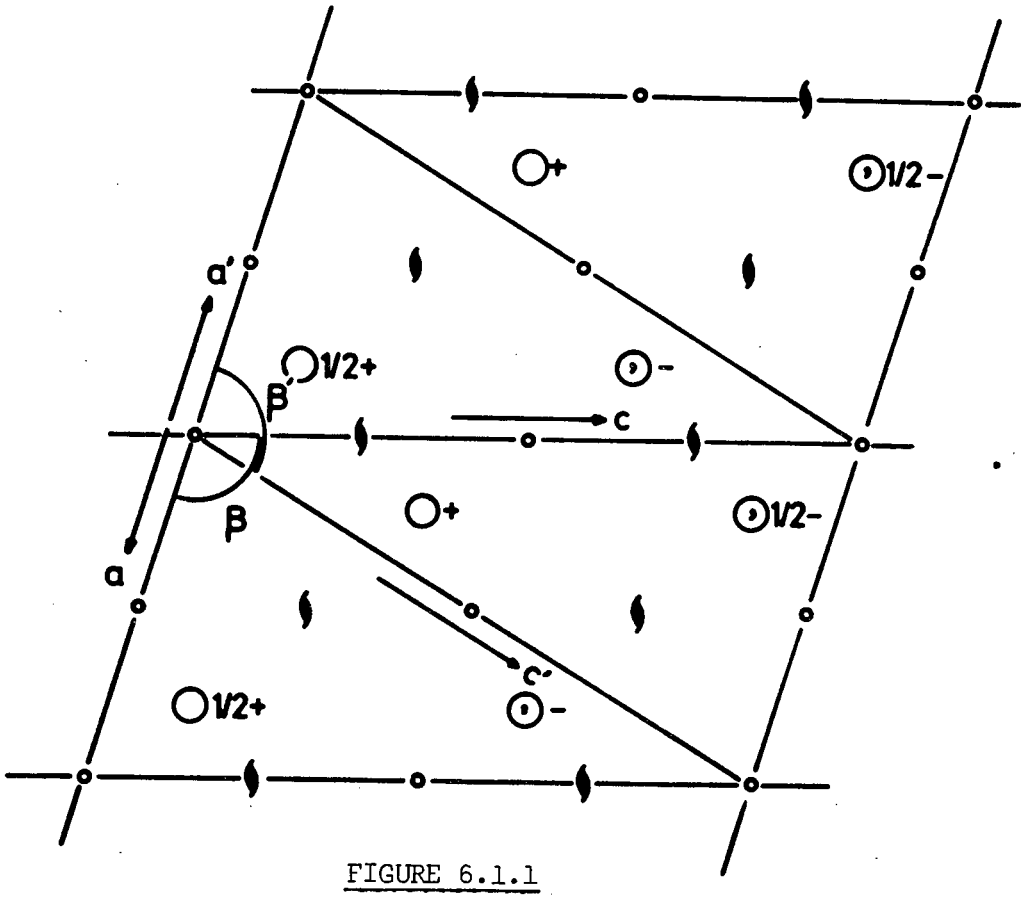

FIGURE 6.1.1

The relationship between the unit cell (bounded by a, b and c) corresponding to space group $P2_1/c$, and the unit cell (bounded by a', b' and c') corresponding to the space group $P2_1/n$, for $[\{Mn(Mecp)(CO)_2\}_2SEt]ClO_4$.

Cell dimensions and equivalent positions are:

$P2_1/c$	$P2_1/n$
a = 8.676 Å	a = 8.676 Å
b = 16.062 Å	b = 16.062 Å
c = 16.076 Å	c = 15.872 Å
β = 107.05°	β = 104.46°
x,y,z ; -x,-y,-z ;	x,y,z ; -x,-y,-z ;
$x,\frac{1}{2}-y,\frac{1}{2}+z$; $-x,\frac{1}{2}+y,\frac{1}{2}-z$	$\frac{1}{2}+x,\frac{1}{2}-y,\frac{1}{2}+z$; $\frac{1}{2}-x,\frac{1}{2}+y,\frac{1}{2}-z$

The two cells are projected onto (010). Symmetry operation symbols are taken from Ref. 3.9

sets out the equivalent positions for the two space groups. In the subsequent structure determination the equivalent positions for $P2_1/n$ were used.

Analysis of a three-dimensional Patterson map yielded the positions of the two manganese atoms. The atoms were separated by about 3 Å; this seemed a reasonable approximate value for a manganese-manganese bond (cf Mn - Mn for $[\{Mn(CO)_5\}_2]$ = 2.923 Å [6.1]). A Fourier map phased on these two atoms revealed the positions of the sulphur and carbon atoms of the ethylthio group; R was 0.42. Six other light atoms were also apparent; from interatomic distances and bonding angles it was deduced that these were three carbonyl groups. After two cycles of full matrix least squares refinement of the co-ordinates of the eleven atoms so far revealed, with anisotropic temperature factors assigned to the Mn and S atoms, a difference electron density map was computed which revealed all remaining non-hydrogen atoms. At this stage R was 0.11. Considerable thermal motion was detected in the ClO_4^- group, more than four peaks being present round the central Cl peak. Four peaks were chosen which had an approximately tetrahedral arrangement, and assigned to the oxygen atoms. A further six cycles of refinement caused R to fall to 0.08 and all hydrogen atoms were located in a subsequent difference map. During the final four cycles of refinement with anisotropic temperature factors assigned to all non-hydrogen atoms, the H atoms were constrained to ride on their parent carbon atoms with C - H distances maintained at 1.08 Å and bond angles set according to the hybridization of the carbon atoms. The refinement converged to R = 0.051 and Rw = 0.056 with a weighting scheme $w = \frac{1.691}{\sigma^2 F + 0.00066F^2}$. In the final cycle of refinement,

the average shift : error ratio for all parameters except those associated with the hydrogen atoms and the perchlorate group was less than 0.1 and a final difference map computed after the refinement showed no peak higher than 0.5e $\mathring{A}^{-3}$.

The final atomic coordinates and thermal parameters for the heavy atoms and hydrogen atoms are set out in Tables 6.1.2 and 6.1.3, observed and calculated structure factors are given in Table 6.1.4.

TABLE 6.1.2 NON-HYDROGEN ATOMS

FRACTIONAL ATOMIC COORDINATES ($\times 10^4$) AND

THERMAL PARAMETERS ($\times 10^3$) AND THEIR E.s.d's

	x/a	y/b	z/c	U_{11}	U_{22}	U_{33}	U_{23}	U_{13}	U_{12}
Mn(1)	2455(1)	546(1)	3053(1)	33(1)	38(1)	51(1)	3(1)	12(1)	2(1)
Mn(2)	3221(1)	1181(1)	1475(1)	44(1)	41(1)	44(1)	-1(1)	12(1)	4(1)
S(1)	4275(2)	1486(1)	2899(1)	42(1)	36(2)	46(1)	-3(1)	15(1)	-3(1)
Cl(1)	2541(4)	1707(2)	-3087(2)	91(2)	76(3)	101(2)	13(2)	36(2)	-2(2)
O(5)	3461(22)	2201(11)	-3422(10)	372(22)	258(19)	252(16)	-71(13)	157(16)	-224(17)
O(6)	3099(22)	1015(12)	-2785(10)	404(23)	317(20)	251(17)	187(15)	181(16)	285(19)
O(7)	1722(25)	2026(10)	-2600(10)	508(29)	232(17)	210(13)	19(12)	242(18)	164(18)
O(8)	1570(22)	1444(13)	-3887(10)	305(20)	397(29)	191(13)	-98(16)	88(14)	-214(21)
C(1)	4017(9)	-83(6)	3712(5)	51(5)	34(7)	50(5)	-4(4)	23(4)	-5(4)
O(1)	4940(7)	-504(4)	4159(4)	62(4)	53(5)	65(4)	12(3)	9(3)	19(3)
C(2)	2152(10)	-342(7)	2329(6)	52(5)	54(10)	59(6)	3(5)	9(4)	-2(5)
O(2)	1909(8)	-938(5)	1923(5)	105(5)	47(6)	79(5)	-10(4)	12(4)	-12(4)
C(3)	2823(10)	2300(8)	1400(5)	70(6)	38(12)	54(5)	8(5)	19(4)	3(6)
O(3)	2566(9)	2991(6)	1325(4)	122(6)	31(7)	91(5)	12(4)	19(4)	18(5)
C(4)	1064(11)	1073(6)	1192(5)	62(6)	55(8)	50(5)	2(4)	8(4)	9(5)
O(4)	-269(7)	1011(5)	912(4)	45(4)	105(7)	84(4)	5(4)	-4(3)	4(4)
C(5)	6364(8)	1137(6)	3276(5)	34(4)	71(8)	57(5)	-8(5)	9(4)	-10(4)
C(6)	6970(11)	1351(7)	4241(6)	58(5)	87(9)	63(6)	-5(6)	2(5)	-17(5)
C(7)	1515(11)	1528(8)	3793(7)	71(6)	46(11)	93(8)	-1(7)	59(6)	13(6)
C(8)	1682(9)	749(7)	4228(6)	47(5)	55(9)	65(6)	5(6)	28(4)	1(5)
C(9)	701(10)	154(7)	3696(6)	48(5)	72(9)	83(7)	16(6)	31(5)	-3(6)
C(10)	-44(9)	551(9)	2905(7)	32(5)	93(12)	96(8)	-8(7)	21(5)	6(6)
C(11)	464(12)	1387(9)	2964(7)	71(7)	79(11)	78(7)	33(6)	41(6)	53(7)
C(12)	2242(16)	2333(8)	4175(9)	152(12)	38(11)	152(12)	-29(9)	103(10)	-5(8)
C(13)	3195(11)	882(7)	148(5)	70(6)	71(9)	45(5)	11(5)	17(4)	7(6)
C(14)	4502(12)	1384(7)	498(6)	85(7)	66(9)	69(6)	-1(6)	47(6)	1(6)
C(15)	5500(11)	957(9)	1205(7)	53(6)	110(12)	77(7)	-25(7)	34(6)	10(7)
C(16)	4798(12)	184(8)	1300(6)	80(7)	73(10)	58(6)	-5(5)	26(5)	35(7)
C(17)	3371(11)	138(7)	652(6)	81(7)	48(9)	56(6)	-14(5)	24(5)	6(5)
C(18)	1896(15)	1071(9)	-644(6)	139(11)	114(12)	47(6)	1(6)	9(6)	16(9)

TABLE 6.1.3 HYDROGEN ATOMS

FRACTIONAL ATOMIC COORDINATES ($\times 10^4$) AND

ISOTROPIC TEMPERATURE FACTORS ($\times 10^3$) AND THEIR E.s.d's

	x	y	z	U_{iso}		x	y	z	U_{iso}
H (8)	2446(9)	628(7)	4866(6)	84(10)	H(16)	5275(12)	-283(8)	1784(6)	84(10)
H (9)	543(10)	-486(7)	3865(6)	84(10)	H(17)	2548(11)	-379(7)	551(6)	84(10)
H(10)	-847(9)	259(9)	2354(7)	84(10)	H(181)	1103(15)	542(9)	-772(6)	154(15)
H(11)	99(12)	1852(9)	2462(7)	84(10)	H(182)	2290(15)	1216(9)	-1221(6)	154(15)
H(121)	2226(16)	2827(8)	3711(9)	154(15)	H(183)	1277(15)	1600(9)	-467(6)	154(15)
H(122)	3459(16)	2178(8)	4494(9)	154(15)	H(51)	7086(8)	1453(6)	2911(5)	154(15)
H(123)	1631(16)	2536(8)	4654(9)	154(15)	H(52)	6428(8)	473(6)	3182(5)	154(15)
H(14)	4728(12)	1993(7)	267(6)	84(10)	H(61)	8210(11)	1199(7)	4504(6)	154(15)
H(15)	6611(11)	1187(9)	1607(7)	84(10)	H(62)	6245(11)	962(7)	4543(6)	154(15)
					H(63)	6772(11)	1997(7)	4371(6)	154(15)

TABLE 6.1.4

Observed and Calculated Structure Factors for $[\{Mn(Mecp)(CO)_2\}_2SEt]ClO_4$

TABLE 6.1.4 CONTINUED

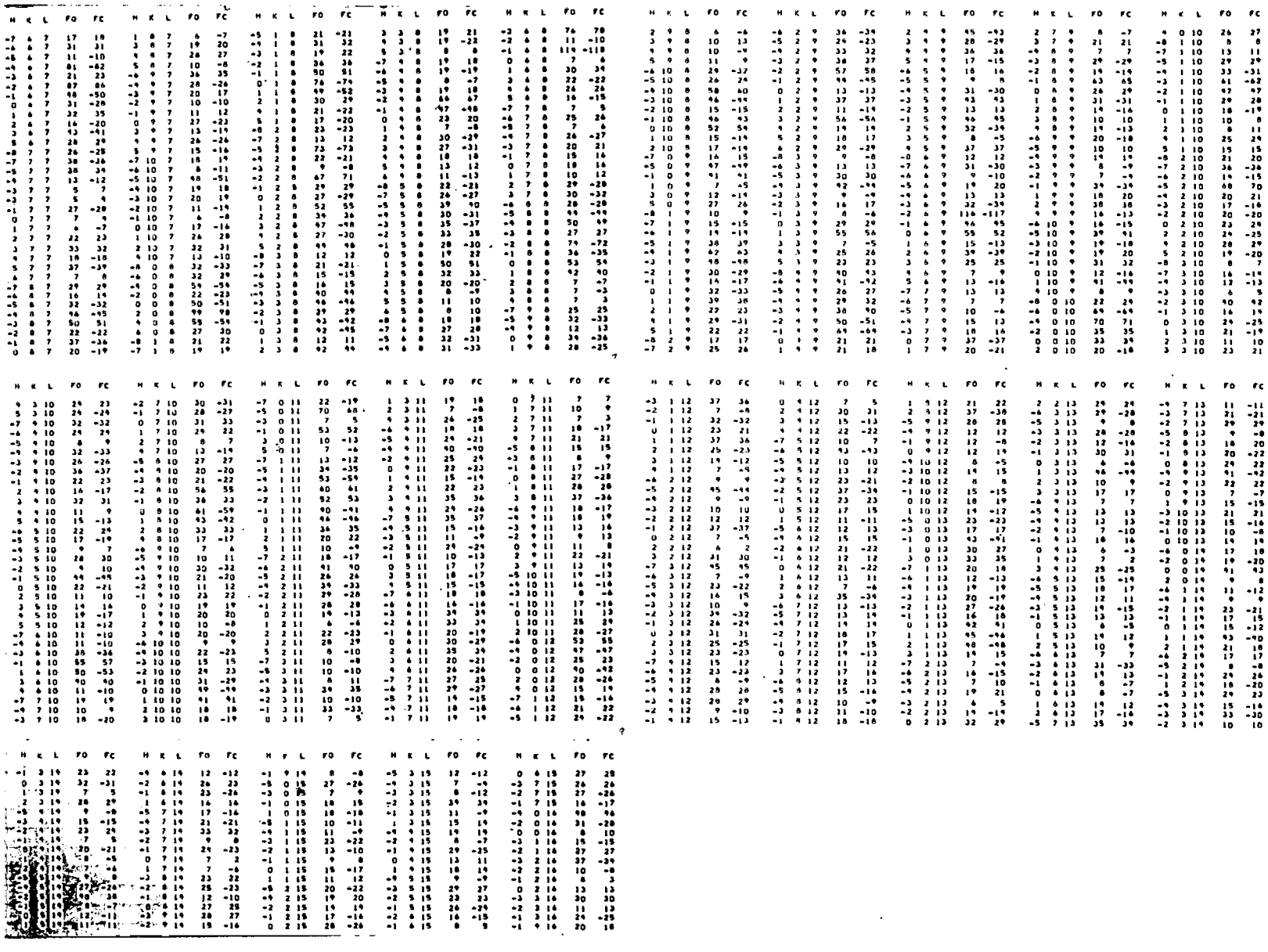

6.2 DESCRIPTION OF STRUCTURE AND DISCUSSION

Interatomic distances and bond angles for $[\{Mn(Mecp)(CO)_2\}_2SEt]ClO_4$ are listed in Tables 6.2.1 and 6.2.2 respectively. Least-squares planes and torsion angles are presented in Table 6.2.3.

The molecular geometry of $[\{Mn(Mecp)(CO)_2\}_2SEt]ClO_4$ and the atomic nomenclature utilised in its description are shown in Figure 6.2.1. The compound consists of two $Mn(\eta\text{-Mecp})(CO)_2$ moieties bridged symmetrically by an ethylthio group. The methyl cyclopentadienyl groups are *trans* with respect to the Mn - Mn vector but not quite parallel to each other, the angle between the normals to the planes being 22°. The groups are essentially planar, with the ring carbon atoms defining regular pentagons, and are symmetrically bound to the manganese atoms.

The environment of the sulphur atom is distorted tetrahedral with the Mn - S distances (2.24 and 2.27 Å) being intermediate between those for $[\{Mn(CO)_3[\mu\text{-SC(SMe)NMe}]\}_2]$ (2.41 - 2.43 Å)[6.2] and that for $[Mn(cp)(CO)_2SO_2]$ (2.04 Å)[6.3]. The Mn - S - Mn bond angle of 81° as well as the Mn - Mn distance of 2.930 Å is consistent with the presence of a manganese-manganese bond. This distance is comparable with those found for $[\{Mn(CO)_4\}_2(H)(PPh_2)]$ (2.937 Å)[6.4] and the non-bridged species $[\{Mn(CO)_5\}_2]$ (2.923 Å)[6.1] and $[\{Mn(CO)_4PEt_3\}_2]$ (2.913 Å)[6.5] but longer than those for the dibridged species $[\{Mn(CO)_4(SiPh_2)\}_2]$ (2.871 Å)[6.6], $[\{Mn(CO)_4\}_2(CO)(GeMe_2)]$ (2,854 Å)[6.7] and $[\{Mn(cp)(CO)(NO)\}_2]$ (2.571 Å)[6.8]. The shorter Mn - Mn distances for the latter have been rationalised in terms of the bridging groups functioning as bridging 'carbenoids'[6.7]. Employing a molecular orbital scheme based on that proposed by Teo *et al* for $[\{Mn(CO)_4(PH_2)\}_2]^{n+}$ (n = 0, 1 or 2)[1,36] it was suggested that the bridging 'carbenoid'

groups effect a strengthening of the manganese-manganese bond by delocalizing the Mn - Mn bonding orbitals of a_g and b_{1u} symmetry and by providing some bonding character to the b_{2g} and $1b_{3u}$ orbitals which are antibonding with respect to the two manganese atoms[6.7]. The longer Mn - Mn bond for $[\{Mn(CO)_4\}_2(H)(PPh_2)]$ was ascribed to this compound containing only one bridging group capable of behaving as a carbenoid[6.7]; the hydride ligand's lack of p orbitals precluding its function as such. By analogy, $[\{Mn(Mecp)(CO)_2\}_2SEt]^+$ which also contains only one bridging carbenoid group would be expected to have a longer Mn - Mn bond. A similar explanation would account for the Mn - Mn distance of 2.912 Å in $[Mn_2(cp)(CO)_6AsMe_2]$, also a mono-bridged species[6.9].

The molecular packing along the x-axis of the unit cell, projected onto the (010) plane, is illustrated in Figure 6.2.2. No intermolecular close contacts less than 3.5 Å are observed. However, the centrosymmetrically related methyl cyclopentadienyl rings in molecules I and III are separated by 3.75 Å. Since the van der Waals radius of carbon is approximately 1.7 Å[2.12] some π - π interaction may exist between these two groups. The average volume occupied by a non-hydrogen atom is 17.8 $Å^3$, comparable to the equivalent figures for the complexes $[\{Fe(cp)(CO)_2\}_2SEt]BF_4$ and $[Fe_2(cp)_2(CO)_3SEt]SbF_6$ (see preceding chapters).

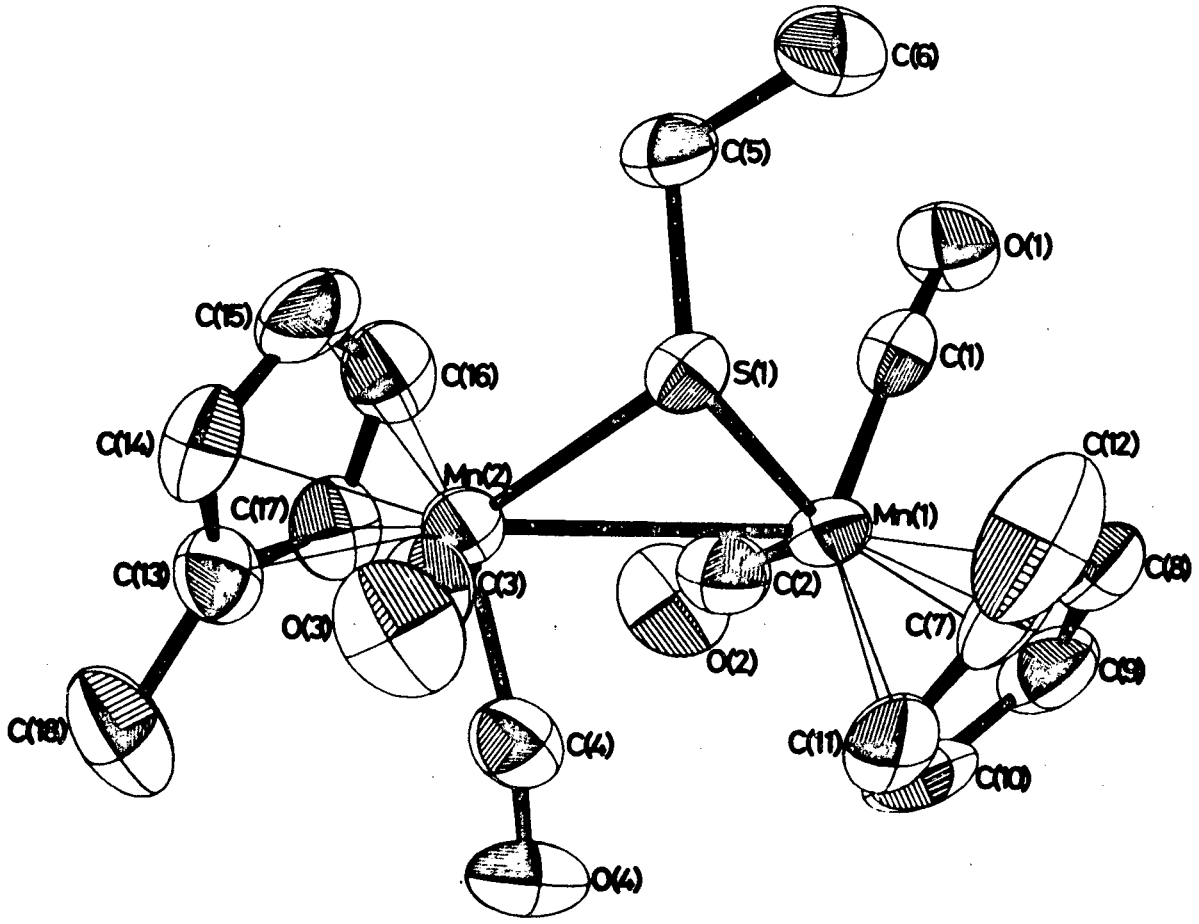

FIGURE 6.2.1

The Molecular Structure of the Cation in $[\{Mn(Mecp)(CO)_2\}_2(SEt)]ClO_4$.

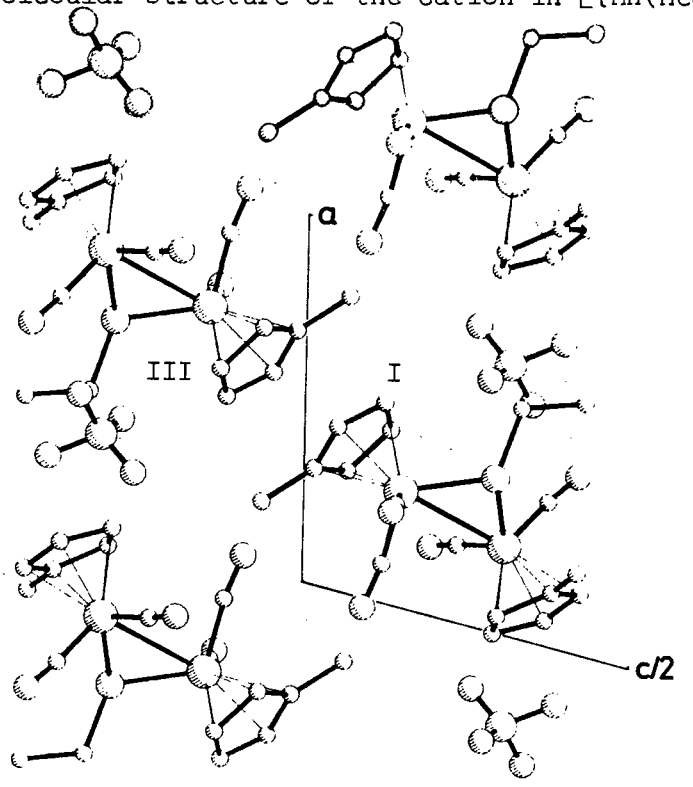

FIGURE 6.2.2

Molecular Packing along the a axis : Molecules I and III correspond to the equivalent positions (x, y, z) and (1-x, -y, -z) respectively.

TABLE 6.2.1

INTRAMOLECULAR BOND LENGTHS AND THEIR E.s.d's (Å)

Mn(1) - Mn(2)	2.930(1)		
Mn(1) - S(1)	2.242(2)	Mn(2) - S(1)	2.270(2)
Mn(1) - C(1)	1.800(7)	Mn(2) - C(3)	1.829(11)
Mn(1) - C(2)	1.809(9)	Mn(2) - C(4)	1.821(7)
Mn(1) - C(7)	2.239(8)	Mn(2) - C(13)	2.155(6)
Mn(1) - C(8)	2.159(6)	Mn(2) - C(14)	2.146(6)
Mn(1) - C(9)	2.128(6)	Mn(2) - C(15)	2.156(7)
Mn(1) - C(10)	2.122(6)	Mn(2) - C(16)	2.169(7)
Mn(1) - C(11)	2.170(7)	Mn(2) - C(17)	2.149(7)
S(1) - C(5)	1.848(6)	C(5) - C(6)	1.529(12)
C(1) - O(1)	1.148(10)	C(3) - O(3)	1.133(16)
C(2) - O(2)	1.144(13)	C(4) - O(4)	1.135(11)
C(7) - C(8)	1.419(17)	C(13) - C(14)	1.389(14)
C(8) - C(9)	1.411(14)	C(14) - C(15)	1.412(14)
C(9) - C(10)	1.413(14)	C(15) - C(16)	1.408(19)
C(10) - C(11)	1.409(20)	C(16) - C(17)	1.400(12)
C(11) - C(7)	1.420(14)	C(17) - C(13)	1.425(15)
C(7) - C(12)	1.499(18)	C(13) - C(18)	1.495(13)
Cl(1) - O(5)	1.327(20)	Cl(1) - O(6)	1.258(19)
Cl(1) - O(7)	1.280(21)	Cl(1) - O(8)	1.402(16)

TABLE 6.2.2

INTRAMOLECULAR BOND ANGLES AND THEIR E.s.d's (DEGREES)

S(1) - Mn(1) - Mn(2)	49.9(0)	S(1) - Mn(2) - Mn(1)	49.1(0)
Mn(1) - S(1) - Mn(2)	81.0(1)	O(1) - C(1) - Mn(1)	175.5(5)
O(2) - C(2) - Mn(1)	174.1(7)	C(1) - Mn(1) - C(2)	84.0(3)
C(1) - Mn(1) - S(1)	89.6(2)	C(2) - Mn(1) - S(1)	117.2(3)
C(1) - Mn(1) - Mn(2)	113.2(2)	C(2) - Mn(1) - Mn(2)	76.1(2)
O(3) - C(3) - Mn(2)	177.7(6)	O(4) - C(4) - Mn(2)	171.5(6)
C(3) - Mn(2) - C(4)	84.9(3)	C(3) - Mn(2) - S(1)	82.8(2)
C(4) - Mn(2) - S(1)	113.6(2)	C(3) - Mn(2) - Mn(1)	108.6(2)
C(4) - Mn(2) - Mn(1)	74.9(2)		
C(7) - C(8) - C(9)	109.5(1.0)	C(13) - C(14) - C(15)	108.5(1.0)
C(8) - C(9) - C(10)	107.5(1.0)	C(14) - C(15) - C(16)	108.5(1.0)
C(9) - C(10) - C(11)	108.0(1.0)	C(15) - C(16) - C(17)	107.0(1.0)
C(10) - C(11) - C(7)	109.5(1.0)	C(16) - C(17) - C(13)	108.5(1.0)
C(11) - C(7) - C(8)	106.0(1.0)	C(17) - C(13) - C(14)	107.5(1.0)
C(11) - C(7) - C(12)	128.5(1.0)	C(17) - C(13) - C(18)	126.5(1.0)
C(8) - C(7) - C(12)	125.5(1.0)	C(14) - C(13) - C(18)	126.0(1.0)

TABLE 6.2.3

Least squares planes.

The equations of the planes are expressed in direct space as

$$Px + Qy + Rz = S$$

Plane 1: Through atoms C(7), C(8), C(9), C(10), C(11) and C(12)

Equation : $-7.8273x + 3.5380y + 9.2758z = 2.9039$

Atoms included in the calculation	Distance from plane (Å)	Atoms not included in the calculation	Distance from plane (Å)
C(7)	-0.030	Mn(1)	-1.801
C(8)	-0.034	C(1)	-2.634
C(9)	0.030	O(1)	-3.091
C(10)	0.020	C(2)	-2.549
C(11)	-0.026	O(2)	-2.946
C(12)	0.040		

Plane 2: Through atoms C(13), C(14), C(15), C(16), C(17), and C(18)

Equation : $-5.8739x + 6.8022y + 11.9340z = -1.1260$

Atoms included in the calculation	Distance in Å from plane	Atoms not included in the calculation	Distance from plane, Å
C(13)	0.026	Mn(2)	1.798
C(14)	0.017	C(3)	2.704
C(15)	-0.016	O(3)	3.234
C(16)	-0.016	C(4)	2.654
C(17)	0.017	O(4)	3.060
C(18)	-0.028		

The angle between the normals to plane 1 and plane 2 is 21.98°.

The angle between the normal to plane and the Mn(1)-Mn(2) vector is 128.86°.

The angle between the normal to plane 2 and the Mn(1)-Mn(2) vector is 130.45°.

6.3 CONFORMATIONAL BEHAVIOUR OF $[\{Mn(Mecp)(CO)_2\}_2SEt]^+$

In contrast with $[\{Fe(cp)(CO)_2\}_2SEt]^+$ (see Chapter 4), the low temperature p.m.r. spectrum of $[\{Mn(Mecp)(CO)_2\}_2SEt]^+$ (213K, measured in d^2-dichloromethane) exhibited two sets of resonances associated with the cyclopentadienyl protons (which form an AB system), two singlets assigned to the cyclopentadienyl methyls, but a single triplet arising from the methyl of the ethylthio group. These features were reversibly temperature dependent, the double resonances coalescing to a pattern corresponding to one methyl cyclopentadienyl group on warming the solution to room temperature. The temperature dependence of the cyclopentadienyl resonance can be interpreted in terms of the presence of more than one conformer of $[\{Mn(Mecp)(CO)_2\}_2SEt]^+$ in solution - interconversion is rapid at room temperature but at lower temperatures becomes slow on an N.M.R. time scale and magnetically non-equivalent methylcyclopentadienyl groups can be distinguished. Indirect evidence is thus provided for like behaviour on the part of the structurally similar $[\{Fe(cp)(CO)_2\}_2SEt]^+$; however, no metal-metal interaction is present in this complex and so the energy barrier to interconversion of different conformers will be correspondingly lower.

P A R T II

THE SYNTHESIS OF A SERIES OF FIVE-COORDINATE RHODIUM NITROSYL COMPLEXES, AND THE CRYSTAL AND MOLECULAR STRUCTURE OF *CIS*-DIBROMONITROSYLBIS-TRIPHENYLPHOSPHITE RHODIUM

SUMMARY

The synthesis of a series of rhodium nitrosyl complexes $[RhBr_2(NO)\{P(OPh)_xPh_{(3-x)}\}_2]$, in which x is varied from 3 to 1, and which is complemented by the known complex $[RhBr_2(NO)(PPh_3)_2]$ is described. The change in frequency of the infra-red absorption band ν(NO) along the series is discussed. A single crystal structure determination of $[RhBr_2(NO)\{P(OPh)_3\}_2]$ shows that this complex adopts a *cis* square-pyramidal configuration with respect to the basal ligands, in contrast to the *trans* configuration observed in $[RhBr_2(NO)(PPh_3)_2]$: the implications of this are discussed. The attempted syntheses of $[RhBr(NO)\{P(OPh)_3\}_3]^+$ and $[RhBr(NO)\{P(OPh)_3\}_4]^{2+}$ are described. The mode of bonding of the nitrosyl group in, and the structures of these complexes are discussed.

CHAPTER 1

A synthetic study of the series of Neutral Five-coordinate Rhodium Nitrosyl Complexes $[RhBr_2(NO)\{P(OPh)_xPh_{(3-x)}\}_2]$ (x = 1, 2 and 3) and the Crystal and Molecular Structure of $[RhBr_2(NO)\{P(OPh)_3\}_2]$

1.1 Introduction.

The mode of coordination of the nitrosyl group in transition metal nitrosyls, and their stereochemistry, has recently been the subject of much argument[1,2]. In particular, penta-coordinate complexes containing this ligand have been discussed at length[2,3]. Interest has been further heightened by the discovery that certain transition metal nitrosyl complexes, among them $[\{Rh(NO)_2Cl\}_2]$, $[RhCl_2(NO)(PPh_3)_2]$ and $[IrCl_2(NO)(PPh_3)_2]$, have been shown to be active homogeneous catalysts, in the presence of $[Me_3Al_2Cl_3]$, for olefin metathesis[4,5,6]. The exact mechanism for the methathesis reaction has been the subject of much speculation[7,41,42] and various structures have been proposed for the intermediates in these processes. Very recently, Katz and co-workers have shown that the species $[Ph_2C = W(CO)_5]$ prepared by Casey[43] can act as a methathesis catalyst[44]. The mechanism proposed for this reaction involves a four-membered metallocycle of tungsten, I.

I.

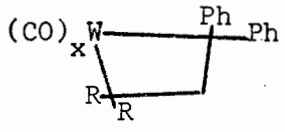

Other metallocyclic species have been postulated as intermediates in methathesis reactions[7]. Some metallocyclic species have been isolated and their reactions investigated; *e.g.* the structure and thermal decomposition of $(PPh_3)_2Pt(CH_2)_n$ (n = 4 - 6) have been studied[8,9] and the preparation of the six and seven-membered rhodacycloalkanes

$[(Me_5cp)(PPh_3)Rh(CH_2)_n]$ (n = 5 and 6) reported[45].

As part of a general study of the olefin metathesis reaction, an investigation was initiated into the five-coordinate rhodium nitrosyls $[RhX_2(NO)L_2]$ where X is a halide ligand and L is a phosphorus ligand with a view to synthesizing metallocycles of the form $[L_2(NO)Rh(CH_2)_n]$. In such a molecule, the stereochemistry and the electron density at the metal atom could be studied using the nitrosyl ligand as an infra-red probe. The subsequent Sections describe the preliminary progress of this work and the results obtained.

in ether to yield the desired metallocycle derivatives. Consequently, several reactions were performed in which the rhodium nitrosyl complex was stirred with a 2x molar excess of the dilithio-alkanes $Li_2(CH_2)_4$ and $Li_2(CH_2)_5$ in dry ether for periods of up to an hour. Dissolution of the ether-insoluble $[RhCl_2(NO)(PPh_3)_2]$ was observed in all cases to give dark brown solutions, but no ν(N–O) band was observed in the infra-red spectrum of any of the solids obtained after removal of solvent, indicating that the desired product had not formed.

It was noted that, in the solid state, the halide ligands in $[IrCl_2(NO)(PPh_3)_2]$ are *trans*-disposed[12]. Unlike $[(PPh_3)_2PtCl_2]$ for which both *cis* and *trans* isomers are known[13], no *cis* isomer of $[RhCl_2(NO)(PPh_3)_2]$ has been reported. The platinum complexes are labilised by the addition of free triphenylphosphine, and, by changing the conditions for isolation of the solid complex, either the *trans* or the *cis* isomer may be obtained[13]. However, this behaviour is not observed for $[RhCl_2(NO)(PPh_3)_2]$. The *cis-trans* isomerism of $[(PPh_3)_2PtCl_2]$ in the presence of PPh_3 proceeds via a penta-coordinate intermediate $[(PPh_3)_3PtCl_2]$ together with a Berry pseudorotation[14,39];

such an isomerization mechanism would not be possible for the rhodium complex.

The solvated species $[Rh(NO)(PPh_3)_2(solvent)_x]^{2+}$ (solvent = Me_2CO or EtOH) was then formed by reaction of $[RhCl_2(NO)(PPh_3)_2]$ with two equivalents of $AgClO_4$ in the solvent concerned. The deep brown solutions obtained gave $[RhBr_2(NO)(PPh_3)_2]$ and $[RhI_2(NO)(PPh_3)_2]$ on reaction with LiBr/acetone and Bu^t_4NI/acetone, respectively, in fair yields. However, attempted reactions using $LiCH_3$/ether and LiPh/benzene gave poorly characterized solids which did not have a ν(N-O) band in their infra-red spectra. Inability to prepare $[Rh(CH_3)_2(NO)(PPh_3)_2]$ and $[Rh(Ph)_2(NO)(PPh_3)_2]$ is attributed in the first instance to the strong nucleophilicity of CH_3^- and in the second instance, to steric overcrowding in the hypothetical product.

Predictably, reaction of $[Rh(NO)(PPh_3)_2(solvent)_2]^{2+}$ with the dilithioalkane $Li_2(CH_2)_4$ in ether, followed by removal of solvent, yielded an amorphous solid which exhibited no N-O infra-red stretching band. It appears then, that in all reactions between $[Rh(NO)(PPh_3)_2(solvent)_2]^{2+}$ and species such as RCH_2^-, the nitrosyl group is attacked by the nucleophile. No reaction was therefore attempted using $Li_2(CH_2)_5$.

Attention was now turned to a means of forcing a *cis*-disposition of the two halide ligands in $[RhX_2(NO)(PPh_3)_2]$. One method is to use a ditertiary phosphine such as dppe or dppm. The two phosphorus atoms must bind in a *cis* configuration, thus forcing all the other three ligands to be *cis* to one another, in both tbp (trigonal bipyramidal) and sp (square pyramidal) molecular geometries.

Accordingly, an attempt was made to synthesize $[RhCl_2(NO)(dppe)]$ using the method adapted by the author from those of Collman, Hoffman and Morris[15], and Heiber and Heinecke[16]. It may be noted here that Blanco, Rossi and Uva report the synthesis of $[CoCl_2(NO)(dppe)]$ from $[Co(NO)_2(dppe)]Cl$ and dppe; the former compound is, in turn, synthesized from the dimer $[CoCl(NO)_2]_2$ and dppe[17].

Nitric oxide was passed into a refluxing thf solution of $RhCl_3.3H_2O$ and dppe containing granulated zinc over a period of about four hours. The amorphous solid that was obtained gave only a broad infra-red spectrum with no sharp bands in the nitrosyl stretching frequency region and contained only a trace of nitrogen. This result is in great contrast to the outcome of the preparation when PPh_3 is employed, *viz.* 75% of the theoretical yield of red-brown crystals exhibiting a very sharp nitrosyl stretching band at 1630 cm^{-1} and analysing correctly for C, H and N. The nature of the product of the reaction employing dppe does not seem to be affected by changes in the order of addition of reagents.

Crookes and Johnson have prepared $[RhCl_2(NO)(EPh_3)_2]$ (where E = P or As) by refluxing an acetone/ethanol solution of polymeric $[Rh(NO)Cl_2]_n$ with the appropriate ligand[18]. Upon repeating this process with dppe, however, it was found that $[Rh(dppe)_2]Cl$ was formed in almost quantitative yield (based on dppe); no nitrosyl-containing species as observed by infra-red spectroscopy could be obtained by reactions between $[Rh(NO)Cl_2]_n$ solutions and dppe.

Recently, Connelly, Green and Kuc have described a facile synthesis of the cationic species $[Rh(NO)(MeCN)_4]^{2+}$ from the dimer,

$[(cod)RhCl]_2$, and nitrosyl salts such as $NOPF_6$ in acetonitrile[19]. The MeCN ligand is readily displaceable, and from this dicationic species a range of rhodium nitrosyls may be prepared. The preparation of $[RhBr_2(NO)dppe]$ was therefore attempted using this method. $[Rh(NO)(MeCN)_4]^{2+}$ was synthesized and stirred with dppe in acetonitrile. The required amount of LiBr was added and the solution evaporated to dryness. The residue gave a band in the infra-red spectrum at 1750 cm^{-1} (Nujol). After extracting with CH_2Cl_2 and recrystallizing from CH_2Cl_2/ether, green crystals were obtained. However, analysis (Table II.1) showed them to be $[Rh(NO)(dppe)_2](SbF_6)_2$. This reaction was repeated with a slight variation: $[Rh(NO)(MeCN)_4]^{2+}$ was stirred in acetonitrile with a two-fold molar excess of LiBr, and a molar equivalent of dppe was added. However, the same product was obtained.

Finally, it was noted that the complex $[(cod)Rh(dppe)]SbF_6$ had been reported[20] and contained a labile diene. A reaction of the form

$$[(cod)Rh(dppe)]SbF_6 \xrightarrow[CH_2CL_2]{NOBr} [(NO)Rh(dppe)Br]SbF_6 \xrightarrow[ether]{LiBr}$$

$[RhBr_2(NO)(dppe)] + LiSbF_6$ was envisaged; The NOBr molecule should readily displace the weakly bound cyclo-octadiene group to give the pentacoordinate cationic intermediate (in itself an interesting complex) which on further treatment with Br^- was expected to yield the desired product.

However, although this reaction was investigated under various conditions, the only pure nitrosyl-containing complex produced was $[Rh(NO)(dppe)_2](SbF_6)_2$.

It appeared, then, that for some reason which is still unclear,

$[RhX_2(NO)(dppe)]$ cannot be prepared *via* any of the syntheses by which $[RhX_2(NO)(PPh_3)_2]$ may be obtained. This remarkable observation will be discussed in Section 1.4. A survey of structures of nitrosyl complexes described in recent reviews[1,2] shows that no pentacoordinate nitrosyl complex of rhodium, $[Rh(NO)L_2L'_2]$ which has a square pyramidal structure and in which the basal ligands adopt a *cis* configuration, has yet been reported.

It now seemed desirable to investigate the effects of the ligand, L, in complexes of the type $[RhX_2(NO)L_2]$, on the stereochemistry of these compounds: hopefully, by doing so, an avenue would be indicated whereby $[Rh(NO)\ L_2(CH_2)_n]$ metallocycles could be synthesized.

The ligand PMe_2Ph was the first to be chosen: its 'cone angle'[21] is only 127° as opposed to 145° [21] for PPh_3 and therefore the probability of synthesizing *cis*-$[RhX_2(NO)(PMe_2Ph)_2]$ would be correspondingly greater. However, employing the method of Crookes and Johnson[18] only $[Rh(PMe_2Ph)_2Br]_2$ could be isolated. This complex was identified by means of its NMR spectrum and microanalysis (Tables II.1, II.2). No other synthetic routes were examined and therefore the possibility that $[RhX_2(NO)(PMe_2Ph)_2]$ may be synthesized cannot be ruled out.

Using the same method, the synthesis of $[RhBr_2(NO)\{P(OMe)_3\}_2]$ was attempted. On addition of trimethyl phosphite to the deep red-brown solution of $[Rh(NO)Br_2]_x$, the colour changed rapidly to light green and then yellow. Removal of solvents under vacuum yielded a yellow solid which exhibited no ν(N-O) bands in its infra-red spectrum. This solid was not characterized, but was probably $[Rh\{P(OMe)_3\}_3Br]$. Again, the possibility that $[RhX_2(NO)\{P(OMe_3\}_2]$ may be synthesized

cannot be discounted on this basis.

Further reactions employing other tertiary alkyl phosphites were not investigated.

The 'cone angle' of triphenyl phosphite, $P(OPh)_3$, 121±10°, is somewhat less than that of PPh_3, 145° [21]; in addition, $P(OPh)_3$ is electron withdrawing. Since these two effects vary regularly along the series $P(OPh)_3$ - $P(OPh)_2Ph$ - $P(OPh)Ph_2$ - PPh_3, the synthesis of the series $[RhX_2(NO)L_2]$ where L = $P(OPh)_xPh_{3-x}$ (x=1, 2 or 3), if possible, should yield information about the influence of (i) the 'cone angle', and (ii) the electron withdrawing power of L on the stereochemistry of the complex $[RhX_2(NO)L_2]$.

Consequently, $[Rh(NO)Br_2]_x$ was prepared[18] and stirred with two equivalents of $P(OPh)_3$ in 1 : 1 acetone/ethanol. Upon removal of acetone from the solvent mixture by evaporation, a green solid formed which gave well-formed green lozenges on recrystallization from dichloromethane/methanol. This neutral (Λ_o = 0.14 $m\Omega^{-1}$ cm^{-1} mol^{-1} dm^3) complex was characterized as $[RhBr_2(NO)\{P(OPh)_3\}_2]$ by infra-red spectroscopy (ν(N-O) = 1750 cm^{-1}) and microanalysis (Tables II.1 and II.2).

The properties of $[RhBr_2(NO)\{P(OPh)_3\}_2]$ are markedly different from those of the triphenylphosphine analogue. It is soluble in acetone and dichloromethane, it is green (in contrast with the red-brown $[RhBr_2(NO)(PPh_3)_2]$) and, most significantly, the nitrosyl stretching band occurs at a frequency 120 cm^{-1} higher than that of the triphenylphosphine complex. These observations suggested that $[RhBr_2(NO)\{P(OPh)_3\}_2]$ has a markedly different structure from the

square pyramidal $[RhBr_2(NO)(PPh_3)_2]$. The structure of $[RhBr_2(NO)(PPh_3)_2]$ has not been eludicated: however, $[RhCl_2(NO)(PPh_3)_2]$ has been reported to be isomorphous[18] with $[IrCl_2(NO)(PPh_3)_2]$, whose structure is known[12]. It is safe to assume, therefore, that $[RhBr_2(NO)(PPh_3)_2]$ will have a square pyramidal structure with *trans*-disposed basal ligands. A survey of references quoted in Molecular Structures and Dimensions[23] showed that, in five-coordinate metal nitrosyl complexes in which the metal atom has a square pyramidal environment with a bent, apical nitrosyl group, as found for $[RhBr_2(NO)(PPh_3)_2]$, the infra-red band ν(N-O) occurs in the range 1630 - 1654 cm^{-1} for neutral complexes and 1680 - 1720 cm^{-1} for cationic complexes. It therefore seemed likely that substitution of $P(OPh)_3$ for PPh_3 in $[RhBr_2(NO)(PPh_3)_2]$ had effected a change from a square pyramidal to a trigonal bipyramidal geometry - the nitrosyl stretching band in complexes with this structure occurs in the range 1770 - 1640 cm^{-1} [1,2].

An unambiguous determination of the configuration of $[RhBr_2(NO)\{P(OPh)_3\}_2]$ was not possible using conventional spectroscopic methods (the infra-red bands ν(Rh-Br) were broad and poorly defined, and no ^{31}P n.m.r. facility was available). As crystals of good quality were easily prepared, it was decided to determine the structure of $[RhBr_2(NO)\{P(OPh)_3\}_2]$ by a single crystal X-ray diffraction study. This is described in Section 1.3.

Employing the ligands $P(OPh)_2Ph$ and $P(OPh)Ph_2$, the complexes $[RhBr_2(NO)\{P(OPh)_2Ph\}_2]$ and $[RhBr_2(NO)\{P(OPh)Ph_2\}_2]$ were synthesized in a manner analogous to that used for $[RhBr_2(NO)\{P(OPh)_3\}_2]$. Their properties are set out in Tables II.1,2. As expected, the nitrosyl

stretching frequency shows a regular variation across the series. Interestingly, a colour change from green to brown is observed in the two intermediate members of the series $[RhBr_2(NO)L_2]$, L = $P(OPh)_2Ph$ and $P(OPh)Ph_2$ and it is surmised that a change takes place in the stereochemistry of the complex from a *cis* to a *trans* configuration. However, confirmation of this supposition can only come from full X-ray crystallographic analyses of the two compounds. These were not within the scope of this thesis.

The infra-red spectrum of $[RhBr_2(NO)\{P(OPh)Ph_2\}_2]$[24] and its colour merit a word of discussion. In the nitrosyl stretching frequency region of the spectrum, this complex does not exhibit the single, sharp absorption which characterizes the other members of the series. The ν(N-O) band is of medium intensity and rather broad: in the solid state two ill-defined maxima are observed at 1630 and 1665 cm^{-1}, while in solution these bands occur at 1630 and 1670 cm^{-1} and are slightly sharper. In addition, the complex is red-brown in colour (like the triphenylphosphine derivative). These observations suggest that the structure of the molecule is intermediate between that of $[RhBr_2(NO)\{P(OPh)_3\}_2]$ and that of $[RhBr_2(NO)(PPh_3)_2]$ and indeed more than one isomer may be present in the solid: this would account for the difficulty experienced in recrystallizing the complex. Crystals large enough for an X-ray crystallographic study have not, as yet, been obtained.

It is also interesting to note that the green complexes $[RhBr_2(NO)L_2]$ (L = $P(OPh)_3$ and $P(OPh)_2Ph$) are air-sensitive, decomposing to yellow-brown nitrosyl-free products over a period of several weeks. $[RhBr_2(NO)L_2]$ (L = $P(OPh)Ph_2$) appears to be air-stable

and, of course, the known complex $[RhBr_2(NO)(PPh_3)_2]$ is extremely stable.

Haines[24] has reported the synthesis of a series of rhodium triphenylphosphite complexes, prepared by stirring the dimer $[(cod)RhCl]_2$ with varying amounts of the tertiary phosphites, $P(OR)_3$. Depending on the quantities of tertiary phosphite used, the compounds $[(cod)Rh_2Cl_2\{P(OR_3\}_2]$, $[Rh\{P(OR)_3\}_3Cl]$, $[Rh\{P(OR)_3\}_4]X$ and $[Rh\{P(OR)\}_5]X$ may be prepared ($X = BPh_4^-$ or ClO_4^-).

It was considered relevant to this study to attempt the synthesis of the complexes $[RhBr(NO)\{P(OPh)_3\}_3]X$ and $[Rh(NO)\{P(OPh)_3\}_4]X_2$. Comparison of the latter complex with the known compound $[Rh(NO)(dppe)_2](SbF_6)_2$ should yield information on how the nitrosyl stretching frequency is affected by overall charge, while $[Rh(NO)\{P(OPh)_3\}_3]X$ is intermediate between the tetrakis-triphenylphosphite nitrosyl complex and $[RhBr_2(NO)\{P(OPh)_3\}_2]$. The effect of increasing coordination of triphenylphosphite ligands on the mode of coordination of the nitrosyl group could this be investigated.

Accordingly, the syntheses of the complexes $[RhBr(NO)\{P(OPh)_3\}_3]X$ and $[Rh(NO\{P(OPh)_3\}_4]X_2$ ($X = BPh_4^-$) were attempted. $[Rh\{P(OPh)_3\}_3Br]$ and $[Rh\{P(OPh)_3\}_4]X$ were prepared[24]. To a solution of each in dichloromethane at room temperature was added one equivalent of NOBr dissolved in dichloromethane. The solutions turned a deep green. This colour was transitory, and after about 30 seconds both solutions had assumed a yellow-brown colour. A four-fold molar excess of sodium tetraphenylboron dissolved in ethanol was added to each solution, and dichloromethane removed under high vacuum. In each case

a yellow precipitate was formed which exhibited no bands in the nitrosyl stretching frequency region of the infra-red spectrum.

The two reactions were repeated; it was found that a greenish oil could be isolated from the reaction

$$[Rh\{P(OPh)_3\}_4]^+ + NOBr \rightarrow$$

if addition of sodium tetraphenylboron and removal of solvents were done very quickly. Attempts to recrystallize this oil proved unsuccessful, nitrosyl-free products always resulting. The infra-red spectrum of the oil showed a weak, broad band, attributable to ν(N-O), centred on 1670 cm^{-1}. This band may, however, be due to a nitrosyl-containing impurity. Judging from the effect, on the ν(N-O) frequency, of substituting triphenylphosphite ligands for triphenylphosphine ligands[33,34] and the observed frequency of the ν(N-O) absorption in $[Rh(NO)(dppe)_2]^{2+}$ of 1750 cm^{-1}, the band in $[Rh(NO)\{P(OPh)_3\}_4]^{2+}$ should occur at a higher frequency than 1750 cm^{-1}.

Invariably, evaporation of solvents from the reaction products of

$$[RhBr\{P(OPh)_3\}_3] + NOBr \rightarrow$$

resulted in yellow-brown oily products which exhibited no ν(N-O) band in their infra-red spectrum.

TABLE II.1

COLOUR AND ANALYTICAL DATA

Compound	Colour	Analysis, % Calculated C	H	N	Found C	H	N
$[RhCl_2(NO)(PPh_3)_2]$	Light Brown	59.3	4.1	1.9	59.1	4.3	1.9
$[RhBr_2(NO)(PPh_3)_2]$	Red-brown	52.9	3.7	1.7	52.7	3.7	1.7
$[RhI_2(NO)(PPh_3)_2]$	Violet-brown	47.4	3.3	1.55	47.1	3.4	1.6
$[Rh(dppe)_2]Cl$ [a]	Yellow	66.7	5.1	-	66.7	4.9	~0.3
$[Rh(NO)(dppe)_2](SbF_6)_2$	Green	44.5	3.4	1.0	44.0	3.4	1.0
$[Rh(PMe_2Ph)_2Br]_2$ [b]	Orange-red	41.9	4.8	-	40.0	4.4	-
$[RhBr_2(NO)\{P(OPh)_3\}_2]$ [c]	Green	47.3	3.3	1.5	47.2	3.4	1.4
$[RhBr_2(NO)\{P(OPh)_2Ph\}_2]$	Green	49.1	3.4	1.6	50.3	3.8	1.3
$[RhBr_2(NO)\{P(OPh)Ph_2\}_2]$	Brown	50.9	3.6	1.7	50.6	3.2	1.9

(a) Λ_o = 43.8 $(m\Omega)^{-1}$ cm^{-1} mol^{-1} dm^3

(b) Λ_o = 0.27 $(m\Omega)^{-1}$ cm^{-1} mol^{-1} dm^3

(c) Λ_o = 0.14 $(m\Omega)^{-1}$ cm^{-1} mol^{-1} dm^3

TABLE II.2

SPECTROSCOPIC DATA

a. Infra-red Bands.

Compound		
$[RhCl_2(NO)(PPh_3)_2]$	1630vs [a]	343s ν(Rh-Cl) [a]
$[RhBr_2(NO)(PPh_3)_2]$	1631vs [a]	-
$[RhI_2(NO)(PPh_3)_2]$	1623vs [a]	-
$[Rh(NO)(dppe)_2](SbF_6)_2$	1750vs [a]	660vs ν(Sb-F) [a]
$[RhBr_2(NO)\{P(OPh)_3\}_2]$	1750vs [a]	-
$[RhBr_2(NO)\{P(OPh)_2Ph\}_2]$	1714vs [a]	
$[RhBr_2(NO)\{P(OPh)Ph_2\}_2]$	1670 m,br [a] 1665 w,br [b] 1630 w,br [b]	
$[Rh(NO)\{P(OPh)_3\}_4](BPh_4)_2$	1670 s,br [a,c]	

(a) Measured in Nujol mulls

(b) Measured in CH_2Cl_2 solution

(c) This band is suspect (see text)

b. NMR data for $[Rh(PMe_2Ph)_2Br]_2$

(τ scale; coupling constants in Hz; measured in $CDCl_3$ at 25°C)

Aromatic Protons	Methyl Protons
2.45 m	8.62d J_{P-H} = 11.0
	7.82t J = 8.0

Integration: aromatic : methyl protons = 1 : 1.2

The complexity of the methyl resonances suggests some dislocation of this species in solution to species with PMe_2Ph ligands *trans* to each other.

Abbreviations : m = multiplet d = doublet t = triplet.

1.3 Experimental.

The ligands PPh_3, PMe_2Ph, $P(OMe)_3$, $P(OPh)_3$ and C_8H_{12} (cyclo-octa - 1,5-diene or cod) were from commercial sources and were not purified further. The ligands $P(OPh)_2Ph$ and $P(OPh)Ph_2$ were prepared by standard literature methods. $[(cod)RhCl]_2$ was synthesized by the method of Chatt and Venanzi[40]. Nitric oxide was either supplied (Matheson Gases) or prepared by reacting solutions of sodium nitrite and ferrous sulphate and drying the gas by passing it over silica gel. Nitrosyl bromide was prepared as required by passing NO gas into a CH_2Cl_2 solution of bromine at -79°C until excess NO was seen to condense on the walls of the container and no further colour change was observed in the solution.

1.3.1 $[RhCl_2(NO)(PPh_3)_2]$. 2.63 gm (10 m mol) of $RhCl_3.3H_2O$ and 10.5 gm(40 m mol) of PPh_3 were refluxed in thf (100 ml) in the presence of 0.8 gm (125 m mol) of granulated zinc for 30 minutes, during which NO was bubbled through the solution. A precipitate of light red-brown crystals formed which was washed with thf. The insolubility of the produce precluded recrystallization. Yield: 5.25 gm (72%). Note: $Rh(NO)(PPh_3)_3$ may also be prepared in this way by refluxing and passing NO for 4 hours, concentrating the THF solution to 50 ml, adding 50 ml methanol and storing at -15°C. Deep red crystals of the product are formed. Typical yields are 85-90%[15].

1.3.2 $[RhX_2(NO)(PPh_3)_2]$ (X = Br, I). a) 0.73 gm (1 mmol) of $[RhCl_2(NO)(PPh_3)_2]$ was stirred in 20 ml of dry acetone with 0.17 gm (0.8 m mol) $AgClO_4$ for 30 minutes at room temperature. The dark

brown solution was filtered and to it was added 0.5 gm (6 m mol) of LiBr dissolved in 10 ml of dry acetone. A crystalline precipitate of $[RhBr_2(NO)(PPh_3)_2]$ slowly formed. The crystals were filtered and washed with methanol. Yield : 0.60 gm (75%)

b) The above preparation was repeated, with the substitution of 2.0 gm (6 m mol) of Bu^t_4NI for LiBr. Dark red-purple crystals of $[RhI_2(NO)(PPh_3)]$ formed. The crystals were filtered and washed with methanol. Yield: 0.72 gm (80%).

1.3.3 $[RhBr_2(NO)L_2]$ L = $P(OPh)_3$, $P(OPh)_2Ph$, $P(OPh)Ph_2$

These complexes were prepared by the method of Crookes and Johnson, except that the acetone/ethanol solutions of $[Rh(NO)Br_2]_x$ and L were not refluxed. Removal of the more volatile acetone under high vacuum sufficed to precipitate the products, which were then recrystallized from CH_2Cl_2/CH_3OH. Typical yields were:

$[RhBr_2(NO)\{P(OPh)_3\}_2]$	70%
$[RhBr_2(NO)\{P(OPh)_2Ph\}_2]$	63%
$[RhBr_2(NO)\{P(OPh)Ph_2\}_2]$	45%

1.3.4 $[Rh(PMe_2Ph)Br]_2$. Addition of PMe_2Ph (2 moles PMe_2Ph to 1 mole Rh) to a solution of $[Rh(NO)Br_2]_x$ in acetone/ethanol, followed by removal of acetone under high vacuum, gave a deep red solution. The solution was concentrated to half its initial volume and an equal volume of methanol added. After storing the solution at -15°C overnight, a precipitate of red crystalline $[Rh(PMe_2Ph)Br]_2$ had formed.

The yield was calculated as 90%.

1.3.5 $[Rh(NO)\{P(OPh)_3\}_4](BPh_4)$. To a solution of 0.55 gm (0.3 m mol) of $[Rh\{P(OPh)_3\}_4](BPh_4)$ in 30 ml of CH_2Cl_2 was added 0.5 m mol (calculated as Br) of NOBr dissolved in 10 ml of CH_2CL_2. The reaction mixture turned a deep green colour, and a solution of $NaBPh_4$ (0.5 gm, 1.5 m mol) in 20 ml of methanol was added. A green precipitate formed which coalesced into an oily mass. Attempts to recrystallize this oil invariably resulted in nitrosyl-free products.

1.4 ELUCIDATION OF THE CRYSTAL AND MOLECULAR STRUCTURE OF $[RhBr_2(NO)\{P(OPh)_3\}_2]$

Crystal Preparation

The complex was prepared as described in Section 1.2. Pale green lozenges were grown from a dichloromethane-methanol mixture at $-5^{\circ}C$.

Density Determination

A density of 1.60 gm cm^{-3} was recorded for the crystals by flotation in a m-xylene-methylene iodide mixture.

Space Group Assignment

A survey of zero- and first-layer Weissenberg photographs showed that reflections of the type $h0l$: l = 2n+1 and $0k0$: k = 2n+1 were systematically absent, characteristic of the monoclinic space group $P2_1/c$. Some crystal decomposition was apparent from the preliminary X-ray investigation, indicating that the complex was either air-sensitive or X-ray-sensitive or both. In fact, crystals of the complex are observed to decompose in air - the decomposition is slow, however, no noticeable change in the infrared spectrum occurring within ten days of their isolation.

Difractometer Data Collection

1788 reflections were collected in the ω-2θ scan mode (scan width $1.0^{\circ}\theta$, scan speed $0.03^{\circ}\theta$ sec^{-1}) in the range $6^{\circ} \leqslant 2\theta \leqslant 36^{\circ}$ from a crystal of dimensions 0.20 x 0.20 x 0.16 mm. A substantial decrease in intensity of the reference reflections monitored was observed, indicating extensive crystal decomposition. The rate of decomposition appeared

to be independent of whether the crystals used for data collection were mounted in Lindemann capillary tubes or were coated with a film of epoxy resin to exclude air, and it appeared that the complex was X-ray- as well as air-sensitive. The intensities measured were, on the whole, rather weak and broad, indicating strong absorption and a high degree of crystal mosaicity.

The intensities of the reference reflections were plotted on a graph versus their sequence numbers in the main body of data, in order to investigate the type of decay. Each set of reflections was multiplied by a constant factor, so that the maximum intensity in each was 1000; *i.e.* all reflections were scaled down to a common origin. From inspection of the graph it was observed that the reflections did not decay at equal rates; the maximum intensity fall-off was 50% and the minimum 11%. The decay appeared to be exponential, as expected, but could be approximated fairly well by a straight line. At least-squares straight line was duly fitted to the reference reflections intensity plot, and its gradient, $\frac{d(\text{intensity})}{dn}$ where n is the sequence number of the reference reflection was found to be -0.25.

Correction of Data

A set of corrected data was prepared from the primary intensities by applying the algorithm

$$I'_{rel} = \left[\frac{1000}{(1000 - 0.25n)}\right] I_{rel}$$

where n has the same significance as above. It was recognised that such a correction has little validity, as it presumes an isotropic decay in the crystal, and also magnifies errors in high-angle reflections.

were present in the vicinities of the oxygen atoms, no further groups of peaks, clearly recognizable as phenyl rings, appeared. At this stage R was 0.24. Repeated insertion of likely candidates for phenyl ring carbon atoms into subsequent cycles of refinement resulted in no fall in the value of R, and no further detail visible in difference syntheses. It was decided then to "synthesize" the remaining four phenyl rings, using a molecular model and a rigid-group facility available in SHELX.

A large (1" = 1Å) scale model was erected of $[RhBr_2(NO)\{P(OPh)_3\}_2]$. Coordinates for the atoms were from the last cycle of least squares refinement. For three of the four phenyl rings remaining to be located peaks were present on the previous electron density map in chemically reasonable positions for carbon atoms bonded to the oxygen atoms. Thus these rings were approximately located. The fourth ring was not placed at this stage.

Approximate coordinates for the carbon atoms $R_{ij}C(1)$ ($R_{ij}C(1)$ denotes the phenyl ring carbon atom bound to oxygen atom O_{ij}) were inserted into a difference electron density synthesis in an attempt to find peaks ascribable to $R_{ij}C(2)$ atoms, and so fix the positions of the phenyl rings and hence all the atoms comprising them. The difference map revealed the positions of two likely peaks. Employing the model, coordinates were measured for the remaining eight carbon atoms in the relevant phenyl rings, and these new positions inserted into four cycles of full-matrix least-squares refinement (in which the Rh, Br and P atoms were assigned anisotropic temperature factors). In this refinement, all four phenyl rings so far located were refined as rigid groups in which the six carbon atoms were constrained to occupy the vertices of a

regular planar hexagon of side 1.395 Å. R fell to 0.17 and inspection of the temperature factors of the phenyl carbon atoms after the final cycle indicated that so far, no atom had been wrongly located. A difference map now yielded the positions of $R_{ij}C(2)$ for the third ring and $R_{ij}C(1)$ for the fourth, and so far unlocated, ring. Using the same approach for the third ring, approximate positions for the atoms were measured. A series of difference maps were now computed based on the known atomic coordinates, and coordinates measured on the model for the fourth ring. The ring was rotated in steps of about 20° about the O(ij) - $R_{ij}C(1)$ axis, which should also pass through the $R_{ij}C(4)$ position (see Figure II.1) and for each orientation, carbon

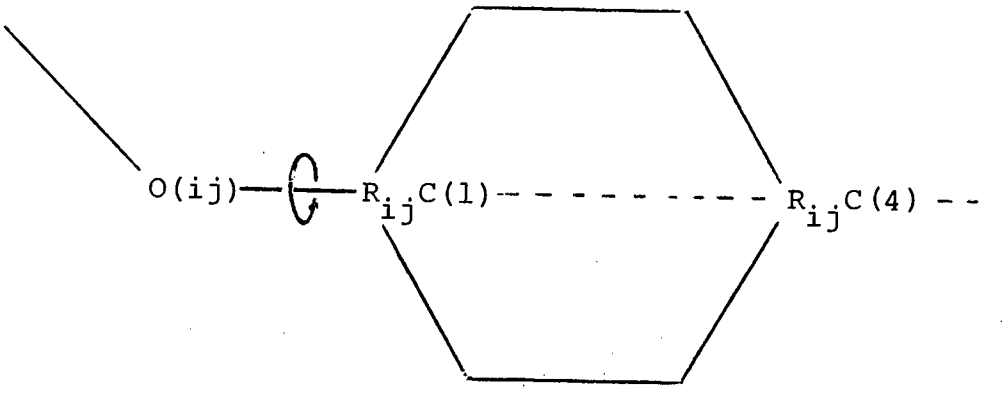

FIGURE II.1

atom positions were measured. It was found that one particular orientation resulted in a significant decrease in R to 0.14. The temperature factors of the ring carbon atoms were somewhat high, but not unreasonably so. The oxygen atom of the nitrosyl group was also located from this map.

Six cycles of full-matrix least-squares refinement based on all atoms caused R to fall to its final value of 0.116. R_w was 0.114 with a weighting scheme $w = \frac{4.268}{\sigma^2 F}$. In the final cycle of refinement the average shift : error ratio was less than 0.1. A final difference map showed only two peaks greater than 0.5e $\AA^{-3}$; 1.0 and 0.8e $\AA^{-3}$ respectively, both closely associated with the rhodium atom and ascribable to anistropic thermal motion. Peaks due to the hydrogen atoms did not show up in this map and it is conjectured that the large temperature factors of the carbon atoms were responsible for this non-appearance. In any case, the poor quality of the intensity data did not warrant location and refinement of the hydrogen atoms.

The final atomic coordinates and thermal parameters are set out in Table II.4. Observed and calculated structure factors are listed in Table II.5.

Description of the Structure

Interatomic distances and bond angles for $[RhBr_2(NO)\{P(OPh)_3\}_2]$ are set out in Tables II.6 and II.7 respectively. The least-squares plane through the four basal ligand atoms, together with relevant torsion angles, is given in Table II.8

The molecular geometry of $[RhBr_2(NO)\{P(OPh)_3\}_2]$ and the atomic nomenclature used in the structure analysis are depicted in Figure II.2 The inner coordination round the rhodium atom is shown in Figure II.3. The molecule is square pyramidal in configuration with the nitrosyl ligand occupying the apical position and coordinating in a markedly bent fashion. The basal ligands are *cis*-disposed. The N-O vector is staggered with respect to the two Rh-P

vectors. The arrangement of the phenoxy groups in the triphenyl-phosphite ligands is such as to minimise close contacts.

The apparent thermal vibration of the heavy atoms is very much greater parallel to the z axis than in the other directions; however, this is probably an artifact of the poor quality of the data. Temperature factors of the carbon atoms in the phenyl rings are very variable, but in all six rings the carbon atom bound to oxygen, RijC(1) has the lowest temperature factor, as would be expected; and RijC(3), RijC(4) and RijC(5) in general exhibit the greatest thermal activity.

The uncertainty in the position of the nitrosyl oxygen atom is considerable, due to a high e.s.d and very large temperature factor. However, its mean position corresponds to a bent Rh - N - O bond. The Rh -N bond length is among the longest so far observed in a nitrosyl complex and is in accordance with the instability of the complex with respect to decomposition products not exhibiting a ν(N-O) bond in their infrared spectra.

Large variations are observed in the phosphorus to oxygen and oxygen to phenyl ring bond lengths; however, these are also probably due to the poor quality of the intensity data. The angles P - O - R_{ij}C(1) are all greater than expected for tetrahedrally surrounded oxygen atoms: this may be a steric effect due to crowding of the large triphenyl phosphite ligands. Significantly, no 'opening up' of the P - Rh - P bond angle to accommodate the six -OPh groups is apparent - the square planar arrangement of the basal ligand atoms is clearly a fairly rigid one.

Figure II.4 depicts the molecular packing in the crystal structure of this complex.

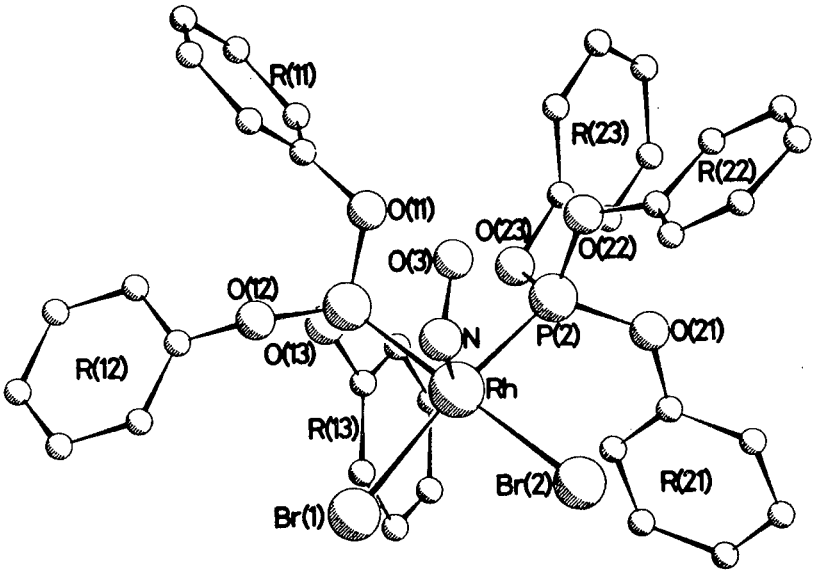

FIGURE II.2

The Molecular Geometry of $[RhBr_2(NO)\{P(OPh)_3\}_2]$

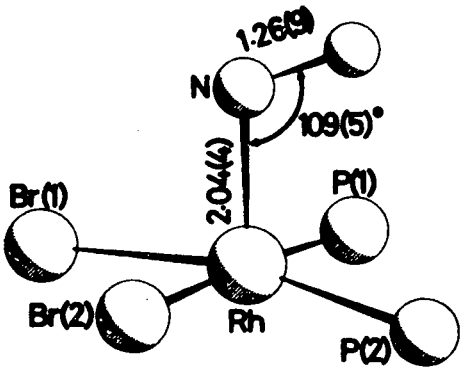

FIGURE II.3

Inner Coordination round the Rhodium Atom in

$[RhBr_2(NO)\{P(OPh)_3\}_2]$

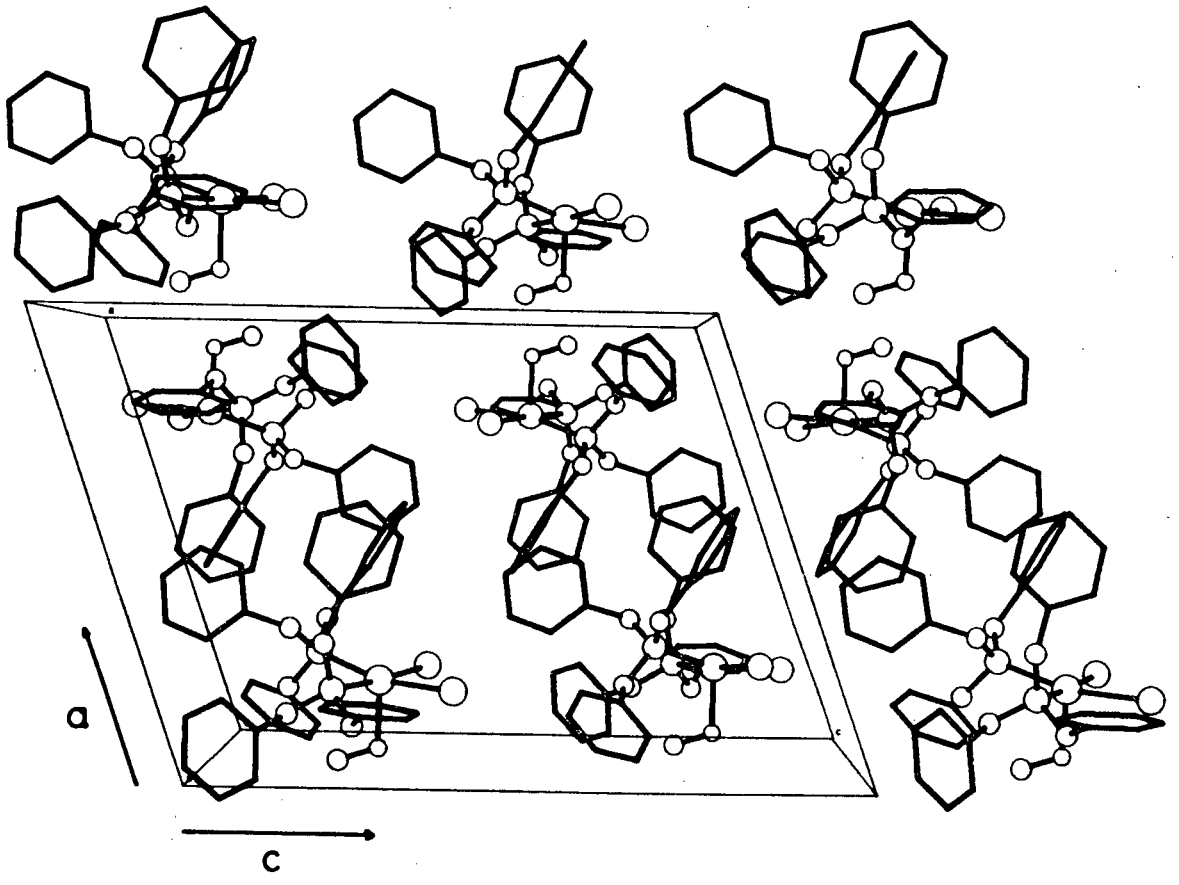

FIGURE II.4

Molecular Packing Diagram for $[RhBr_2(NO)\{P(OPh)_3\}_2]$

TABLE II.4

FRACTIONAL ATOMIC COORDINATES ($\times 10^4$) AND

TEMPERATURE FACTORS ($\times 10^3$) AND THEIR E.s.d's

Atom	x/a	y/b	z/c	U_{iso} or U_{11}	U_{22}	U_{33}	U_{23}	U_{13}	U_{12}
Rh1	2221(2)	5483(3)	8311(4)	57(2)	42(2)	334(12)	-10(3)	32(3)	-8(2)
Br1	2099(4)	4589(4)	9376(6)	92(3)	72(3)	407(19)	0(6)	43(5)	-18(3)
Br2	2401(4)	7086(4)	8995(6)	100(3)	58(2)	402(18)	-35(5)	73(5)	-17(2)
P1	2155(10)	4017(8)	7695(16)	62(7)	46(5)	235(42)	17(12)	13(13)	-12(5)
P2	2728(8)	6246(9)	7502(14)	47(6)	63(6)	190(35)	-12(11)	15(10)	-7(5)
N1	772(39)	5693(41)	7941(46)	115(8)					
O3	499(42)	5753(44)	7287(43)	172(22)					
O11	1628(20)	4221(19)	6916(28)	67(9)					
O12	1516(18)	3181(19)	7870(25)	74(8)					
O13	3140(18)	3450(19)	7837(22)	75(8)					
O21	3366(18)	7235(19)	7707(23)	68(7)					
O22	1914(20)	6699(20)	6828(25)	87(9)					
O23	3285(17)	5523(19)	7253(25)	61(7)					
R11C1	1365(26)	3423(21)	6488(20)	68(14)					
R11C2	430(21)	3050(18)	6289(18)	103(15)					
R11C3	144(21)	2292(18)	5795(18)	112(16)					
R11C4	794(21)	1907(18)	5500(18)	115(16)					
R11C5	1729(21)	2280(18)	5699(18)	113(16)					
R11C6	2015(21)	3038(18)	6193(18)	108(16)					
R12C1	1807(15)	2205(17)	8092(30)	79(14)					
R12C2	2028(15)	1501(17)	7661(30)	87(13)					
R12C3	2262(15)	531(17)	7897(30)	121(19)					
R12C4	2264(15)	267(17)	8564(30)	152(24)					
R12C5	2042(15)	957(17)	8986(30)	187(27)					
R12C6	1808(15)	1927(17)	8750(30)	139(22)					
R13C1	4072(12)	3705(14)	8273(21)	60(12)					
R13C2	4759(12)	3787(14)	7944(21)	63(11)					
R13C3	5721(12)	3971(14)	8344(21)	61(12)					
R13C4	5986(12)	4063(14)	9064(21)	88(15)					
R13C5	5299(12)	3980(14)	9394(21)	75(12)					

TABLE II.4 (CONTD.)

Atom	x/a	y/b	z/c	U_{iso} or U_{11}	U_{22}	U_{33}	U_{23}	U_{13}	U_{12}
R13C6	4347(12)	3797(14)	8994(21)	76(14)					
R21C1	4181(14)	7354(18)	8313(15)	61(11)					
R21C2	4432(14)	8323(18)	8523(15)	89(13)					
R21C3	5266(14)	8523(18)	9078(15)	94(14)					
R21C4	5857(14)	7742(18)	9423(15)	75(12)					
R21C5	5615(14)	6772(18)	9212(15)	110(16)					
R21C6	4772(14)	6573(18)	8658(15)	76(12)					
R22C1	1635(19)	7638(16)	6712(20)	61(11)					
R22C2	1880(19)	8064(16)	6170(20)	93(14)					
R22C3	1468(19)	8962(16)	5881(20)	123(17)					
R22C4	811(19)	9433(16)	6133(20)	125(18)					
R22C5	565(19)	9006(16)	6675(20)	134(19)					
R22C6	977(19)	8109(16)	6964(20)	137(19)					
R23C1	3588(23)	5797(17)	6647(21)	63(12)					
R23C2	2979(23)	5757(17)	5957(21)	87(14)					
R23C3	3328(23)	5986(17)	5413(21)	99(15)					
R23C4	4287(23)	6255(17)	5569(21)	134(20)					
R23C5	4895(23)	6304(17)	6259(21)	91(14)					
R23C6	4546(23)	6076(17)	6793(21)	89(14)					

TABLE II.5

Observed and Calculated Structure Factors for $[RhBr_2(NO)\{P(OPh)_3\}_2]$

H	K	L	FO	FC
3	0	0	362	-379
4	0	0	294	273
5	0	0	290	272
6	0	0	86	-90
7	0	0	174	-181
8	0	0	55	-57
9	0	0	124	125
11	0	0	79	-73
12	0	0	21	-19
13	0	0	25	24
14	0	0	30	38
2	1	0	113	-114
3	1	0	78	-78
4	1	0	70	67
5	1	0	108	113
7	1	0	80	-75
8	1	0	37	-41
9	1	0	49	45
11	1	0	33	-32
2	2	0	119	-132
3	2	0	15	-21
4	2	0	106	89
5	2	0	77	68
6	2	0	36	-34
7	2	0	145	-138
8	2	0	18	-23
9	2	0	79	77
10	2	0	54	49
11	2	0	43	-39
12	2	0	62	-55
14	2	0	39	35
1	3	0	26	5
2	3	0	51	-49
3	3	0	163	147
4	3	0	121	118
5	3	0	25	24
6	3	0	23	-36
7	3	0	23	22
8	3	0	29	24
0	4	0	97	-73
2	4	0	184	-159
4	4	0	24	26
5	4	0	116	112
6	4	0	15	-16
7	4	0	82	-76
9	4	0	56	50
11	4	0	27	-30
13	4	0	18	16
1	5	0	112	97
2	5	0	29	-23
3	5	0	13	6
4	5	0	55	45
5	5	0	27	17
6	5	0	22	25
7	5	0	26	-23
8	5	0	63	-57
9	5	0	15	14
10	5	0	66	64
11	5	0	15	-14
12	5	0	50	-51
0	6	0	114	-104
2	6	0	31	36
3	6	0	29	-19
5	6	0	46	-52
6	6	0	23	17
7	6	0	35	36
9	6	0	24	-26
11	6	0	28	20
2	7	0	18	14
3	7	0	69	-69
4	7	0	27	-20
5	7	0	43	45
6	7	0	47	45
7	7	0	40	-39
8	7	0	54	-53
9	7	0	17	14
10	7	0	37	37
12	7	0	20	-29
0	8	0	133	-122
1	8	0	103	-81
2	8	0	127	124
3	8	0	53	47
4	8	0	48	-47
5	8	0	67	-64
6	8	0	21	23
7	8	0	92	85
9	8	0	57	-55
11	8	0	25	32
1	9	0	24	-25
2	9	0	22	16
11	9	0	15	-4
0	10	0	43	-39
2	10	0	40	43
3	10	0	29	29
4	10	0	23	-21
5	10	0	34	-36
7	10	0	39	45
9	10	0	37	-36
10	10	0	29	-23
2	11	0	15	-12
3	11	0	30	-27
4	11	0	27	20
6	11	0	34	-27
7	11	0	30	-29
8	11	0	16	16
9	11	0	32	28
0	12	0	109	-97
2	12	0	99	89
3	12	0	22	28
4	12	0	85	-79
5	12	0	44	-40
6	12	0	53	49
7	12	0	51	43
1	13	0	71	-62
2	13	0	25	-22
3	13	0	69	61
5	13	0	34	-28
0	14	0	23	-19
2	14	0	16	11
-13	1	1	42	-41
-12	1	1	18	-14
-11	1	1	71	60
-10	1	1	32	25
-9	1	1	58	-60
-8	1	1	84	-87
-7	1	1	109	107
-6	1	1	181	168
-5	1	1	22	-39
-4	1	1	193	-161
-3	1	1	26	-40
3	1	1	309	267
5	1	1	190	-188
7	1	1	73	77
8	1	1	86	87
9	1	1	62	-59
10	1	1	71	-71
12	1	1	50	52
13	1	1	21	10
-12	2	1	22	-20
-10	2	1	22	-11
-9	2	1	42	48
-8	2	1	27	28
-7	2	1	96	-98
-6	2	1	39	-26
-5	2	1	26	29
-4	2	1	115	111
-2	2	1	39	-44
-1	2	1	59	51
0	2	1	86	75
1	2	1	59	-58
2	2	1	252	-241
3	2	1	98	96
4	2	1	162	149
5	2	1	36	-36
6	2	1	39	-56
7	2	1	30	-18
8	2	1	33	30
9	2	1	26	-23
11	2	1	24	20
-12	3	1	26	25
-11	3	1	28	25
-9	3	1	67	-66
-8	3	1	22	-18
-7	3	1	61	67
-6	3	1	53	54
-5	3	1	77	-81
-4	3	1	58	-62
-3	3	1	92	69
-2	3	1	131	111
-1	3	1	41	-54
0	3	1	27	-38
3	3	1	88	75
4	3	1	37	28
5	3	1	61	-60
6	3	1	105	-105
7	3	1	53	47
8	3	1	74	81
10	3	1	63	-62
12	3	1	36	34
13	3	1	22	17
14	3	1	35	-29
-14	4	1	29	25
-12	4	1	19	-24
-11	4	1	39	-35
-9	4	1	16	27
-7	4	1	15	-20
-6	4	1	33	-38
-5	4	1	44	-43
-4	4	1	13	17
-3	4	1	154	149
-1	4	1	74	-72
0	4	1	83	72
1	4	1	136	121
3	4	1	56	-55
4	4	1	14	-21
6	4	1	41	24
7	4	1	21	-20
8	4	1	20	-15
9	4	1	37	40
11	4	1	29	-25
13	4	1	21	22
-12	5	1	24	-26
-11	5	1	23	-18
-10	5	1	39	43
-8	5	1	27	-27
-6	5	1	34	37
-5	5	1	17	-6
-4	5	1	59	-59
-2	5	1	104	103
-1	5	1	32	-28
0	5	1	102	-97
1	5	1	20	-13
2	5	1	117	110
3	5	1	28	24
4	5	1	70	-63
5	5	1	13	-9
7	5	1	48	51
8	5	1	21	-18
9	5	1	25	-34
-13	6	1	41	45
-11	6	1	93	-90
-9	6	1	113	114
-7	6	1	136	-135
-6	6	1	35	-37
-5	6	1	137	140
-4	6	1	54	58
-3	6	1	51	-65
-2	6	1	126	-121
-1	6	1	63	56
0	6	1	170	162
1	6	1	100	-89
2	6	1	74	-79
3	6	1	37	29
4	6	1	81	75
5	6	1	18	7
6	6	1	57	-56
7	6	1	24	-28
8	6	1	27	25
9	6	1	55	54
10	6	1	25	-29
11	6	1	35	-35
12	6	1	20	19
13	6	1	25	22
-13	7	1	22	28
-12	7	1	24	21
-10	7	1	64	-58
-9	7	1	17	32
-8	7	1	87	91
-7	7	1	22	-26
-6	7	1	131	-130
-5	7	1	17	5
-4	7	1	91	100
-2	7	1	80	-94
-1	7	1	67	-69
0	7	1	100	101
1	7	1	100	115
2	7	1	55	-46
3	7	1	116	-110
4	7	1	37	45
5	7	1	56	62
6	7	1	26	29
7	7	1	55	-54
8	7	1	30	-30
9	7	1	37	31
10	7	1	32	37
11	7	1	22	-20
-9	8	1	27	30
-7	8	1	26	-25
-6	8	1	41	-43
-5	8	1	29	17
-4	8	1	78	76
-3	8	1	26	-18
-2	8	1	40	-35
-1	8	1	51	-56
0	8	1	20	16
1	8	1	97	77
3	8	1	77	-72
4	8	1	22	-20
5	8	1	68	62
6	8	1	20	12
7	8	1	35	-34
10	8	1	22	13
11	8	1	19	-18
-11	9	1	29	-22
-9	9	1	34	32
-8	9	1	17	13
-7	9	1	59	-55
-6	9	1	46	-42
-5	9	1	38	43
-4	9	1	34	43
-2	9	1	80	-72
-1	9	1	37	-30
1	9	1	38	47
2	9	1	18	18
3	9	1	33	-36
4	9	1	16	-13
6	9	1	33	30
7	9	1	18	-16
8	9	1	31	-32
10	9	1	35	36
-9	10	1	20	12
-6	10	1	18	-15
-4	10	1	31	31
-2	10	1	59	-51
-1	10	1	17	15
0	10	1	44	37
2	10	1	35	-26
4	10	1	17	11
7	10	1	21	27
8	10	1	17	17
10	10	1	19	-20
-9	11	1	34	30
-8	11	1	28	31
-7	11	1	18	-18
-6	11	1	31	-33
-4	11	1	47	55
-2	11	1	47	-47
-1	11	1	50	-41
0	11	1	59	59
1	11	1	87	77
2	11	1	84	-72
3	11	1	61	-62
4	11	1	18	15
5	11	1	87	84
6	11	1	22	10
7	11	1	54	-56
8	11	1	35	-30
9	11	1	29	28
-8	12	1	21	17
-7	12	1	31	26
-5	12	1	33	-31
-4	12	1	21	-3
-2	12	1	29	22
-1	12	1	23	-18
0	12	1	62	-51
2	12	1	36	37
4	12	1	30	-33
5	12	1	34	-31
7	12	1	30	34
-6	13	1	37	-31
-4	13	1	38	40
-3	13	1	23	19
-2	13	1	47	-45
-1	13	1	36	-32
0	13	1	43	42
1	13	1	41	38
2	13	1	22	-21
3	13	1	61	-54
5	13	1	49	45
-2	14	1	38	35
0	14	1	40	-40
2	14	1	52	48
-15	0	2	29	-22
-14	0	2	38	-37
-13	0	2	20	18
-12	0	2	59	57
-10	0	2	94	-94
-8	0	2	178	173
-7	0	2	135	143
-6	0	2	189	-195
-5	0	2	161	-169
-4	0	2	185	174
-3	0	2	424	408
2	0	2	186	168
3	0	2	315	-340
4	0	2	159	-166
5	0	2	177	170
6	0	2	108	118
7	0	2	72	-71
8	0	2	106	-107
10	0	2	82	87
11	0	2	26	28
12	0	2	35	-35
13	0	2	22	-21
-12	1	2	19	15
-11	1	2	22	26
-10	1	2	25	29
-9	1	2	59	-62
-8	1	2	60	-72
-7	1	2	27	25
-6	1	2	114	111
-5	1	2	18	25
-4	1	2	100	-86
-3	1	2	36	35
-2	1	2	22	3
1	1	2	51	-43
2	1	2	51	49
3	1	2	86	-84
4	1	2	148	-144
5	1	2	46	-50
6	1	2	65	74
7	1	2	20	18
8	1	2	39	-49
9	1	2	16	-20
10	1	2	29	33
12	1	2	23	-26
-13	2	2	19	17
-12	2	2	18	8
-11	2	2	28	-31
-10	2	2	19	-19
-9	2	2	28	26
-8	2	2	31	36
-6	2	2	49	-49
-5	2	2	43	-40
-4	2	2	62	46
-3	2	2	74	52
-2	2	2	144	-155
-1	2	2	102	-122
0	2	2	29	-47
2	2	2	146	126
3	2	2	90	-99
4	2	2	160	-166
5	2	2	18	17
6	2	2	152	162
7	2	2	38	40
8	2	2	75	-80
9	2	2	48	-52
10	2	2	35	43
11	2	2	47	55
12	2	2	19	-13
13	2	2	38	-39
-13	3	2	32	-34
-12	3	2	17	14
-9	3	2	20	18
-8	3	2	36	-36
-7	3	2	30	-25
-5	3	2	117	119
-4	3	2	58	59
-3	3	2	46	-47
-2	3	2	81	81
-1	3	2	35	-39
1	3	2	140	-147
2	3	2	19	-13
3	3	2	138	126
4	3	2	31	12
5	3	2	41	-56
6	3	2	80	-80
7	3	2	35	33
8	3	2	26	18
11	3	2	21	-5
-10	4	2	17	-11
-9	4	2	24	-30
-8	4	2	43	48
-7	4	2	24	24
-6	4	2	72	-76
-5	4	2	25	-33
-4	4	2	141	133
-3	4	2	42	40
-2	4	2	82	-86
-1	4	2	105	-107
0	4	2	129	119
1	4	2	180	167
2	4	2	32	-36
3	4	2	103	-96
5	4	2	65	71
6	4	2	20	15
7	4	2	15	-21
8	4	2	48	-44
10	4	2	33	40
-13	5	2	34	-31
-12	5	2	37	-41
-11	5	2	50	55
-10	5	2	57	62
-9	5	2	55	-59
-8	5	2	82	-91
-7	5	2	42	45
-6	5	2	123	133
-5	5	2	57	-56
-4	5	2	87	-94
-2	5	2	73	74
-1	5	2	158	140
1	5	2	119	-136
2	5	2	48	41
3	5	2	49	52
5	5	2	55	-59
6	5	2	25	-32
8	5	2	43	45
10	5	2	48	-53
12	5	2	19	24
-11	6	2	26	13
-10	6	2	29	23
-9	6	2	16	1
-8	6	2	42	-47
-7	6	2	58	-56
-6	6	2	26	24
-5	6	2	41	53
-4	6	2	15	-3
-3	6	2	56	-56
-2	6	2	32	28
0	6	2	33	46
2	6	2	40	-50
3	6	2	32	28
4	6	2	37	36
6	6	2	49	-48
8	6	2	23	20
9	6	2	24	22
-13	7	2	36	-34
-11	7	2	57	56
-10	7	2	65	66
-9	7	2	47	-50
-8	7	2	107	-111
-7	7	2	17	21
-6	7	2	127	133
-5	7	2	29	23
-4	7	2	118	-124
-3	7	2	29	-32
-2	7	2	25	33
-1	7	2	122	118
0	7	2	86	-88
1	7	2	27	-29
2	7	2	45	-43
3	7	2	65	65
4	7	2	25	22
5	7	2	27	-29
6	7	2	20	-29
8	7	2	48	50
-12	8	2	22	-24
-10	8	2	33	32
-9	8	2	38	37
-8	8	2	47	-58
-7	8	2	47	-47
-6	8	2	65	68
-5	8	2	62	71
-4	8	2	88	-82
-3	8	2	105	-101
-2	8	2	39	44
-1	8	2	88	96
1	8	2	50	-48
2	8	2	27	-19
3	8	2	67	64
4	8	2	16	16
5	8	2	25	-28
8	8	2	32	25
10	8	2	21	-22
-6	9	2	17	12
-5	9	2	24	26
-4	9	2	16	-20
-3	9	2	79	-79
-1	9	2	80	83
0	9	2	23	18
1	9	2	70	-69
2	9	2	47	-41
3	9	2	55	52
4	9	2	52	55
6	9	2	37	-27
7	9	2	17	6
9	9	2	20	-11
-10	10	2	18	18
-8	10	2	32	-28
-6	10	2	34	34
-4	10	2	32	-33
-1	10	2	33	35
0	10	2	27	25
1	10	2	47	-49
2	10	2	32	-29
3	10	2	22	24
4	10	2	40	48
5	10	2	31	-26
6	10	2	47	-47
8	10	2	32	39
-8	11	2	17	-5
-3	11	2	23	-21
-2	11	2	35	33
-1	11	2	25	-20
1	11	2	22	-2
2	11	2	38	37
3	11	2	30	-31
4	11	2	35	-32
6	11	2	30	34
8	11	2	30	-37
-8	12	2	23	-23
-7	12	2	19	-19
-6	12	2	42	34
-4	12	2	29	-32
-3	12	2	50	-46
-2	12	2	28	21
-1	12	2	82	72
1	12	2	99	-93
2	12	2	32	-19
3	12	2	79	73
4	12	2	55	46
5	12	2	46	-49
6	12	2	47	-44
7	12	2	24	27
-6	13	2	25	-32
-5	13	2	21	18
-4	13	2	28	38
-2	13	2	59	-50
-1	13	2	19	-20
0	13	2	40	46
1	13	2	44	39
2	13	2	37	-36
3	13	2	42	-40
4	13	2	21	22
5	13	2	29	31
-15	1	3	19	-15
-14	1	3	26	23
-13	1	3	19	17
-11	1	3	32	-36
-10	1	3	36	41
-9	1	3	51	46
-8	1	3	28	-27
-7	1	3	73	-69
-6	1	3	48	-51
-5	1	3	66	62
-4	1	3	24	-30
-3	1	3	98	-81
-2	1	3	45	-45
-1	1	3	28	-23
1	1	3	49	28
2	1	3	28	-25
3	1	3	78	69
4	1	3	132	118
5	1	3	24	13
6	1	3	112	-116
7	1	3	31	-34
8	1	3	42	39
9	1	3	49	51
11	1	3	45	-49
-15	2	3	31	-31
-13	2	3	42	38
-12	2	3	26	37
-11	2	3	25	-24
-10	2	3	40	-47
-9	2	3	24	26
-8	2	3	65	67
-7	2	3	33	30
-6	2	3	71	-67
-5	2	3	75	-66
-4	2	3	52	52
-3	2	3	78	59
-2	2	3	163	-177
-1	2	3	153	-158
0	2	3	37	-44
1	2	3	129	113
2	2	3	114	111
3	2	3	55	-63
4	2	3	29	-28
5	2	3	40	28
6	2	3	61	75
7	2	3	27	-30
-13	3	3	20	-10
-11	3	3	21	19
-9	3	3	16	-18
-8	3	3	15	11
-5	3	3	12	-13
-3	3	3	86	-86
-2	3	3	21	5
-1	3	3	126	117
0	3	3	24	13
2	3	3	40	-46
4	3	3	72	64
5	3	3	67	65
6	3	3	25	-18
7	3	3	64	-63
9	3	3	43	42
11	3	3	19	-20
12	3	3	18	-22
-10	4	3	30	-36
-8	4	3	28	28
-7	4	3	61	61
-5	4	3	54	-70
-4	4	3	33	29
-3	4	3	131	124
-2	4	3	19	3
0	4	3	160	-178
1	4	3	86	67
2	4	3	117	102
3	4	3	43	-60
4	4	3	124	-129
5	4	3	31	36
6	4	3	99	106
8	4	3	53	-54
9	4	3	35	-37
10	4	3	40	45
11	4	3	21	22
-10	5	3	26	-19
-9	5	3	22	22
-8	5	3	23	19
-7	5	3	46	-47

TABLE II.5 CONTINUED

H	K	L	FO	FC
-6	5	3	55	60
-5	5	3	69	76
-4	5	3	50	-47
-3	5	3	101	-101
-2	5	3	30	29
-1	5	3	100	110
0	5	3	17	-13
1	5	3	136	-137
2	5	3	53	-63
3	5	3	92	89
4	5	3	45	41
5	5	3	95	-104
6	5	3	20	-29
7	5	3	46	48
8	5	3	36	45
9	5	3	19	-15
10	5	3	21	-19
-13	6	3	18	18
-12	6	3	60	58
-10	6	3	88	-95
-9	6	3	25	-34
-8	6	3	141	148
-7	6	3	95	99
-6	6	3	146	-159
-5	6	3	124	-137
-4	6	3	135	140
-3	6	3	123	120
-2	6	3	72	-75
-1	6	3	157	-175
1	6	3	171	171
2	6	3	59	54
3	6	3	75	-85
4	6	3	45	-58
5	6	3	35	35
6	6	3	31	30
7	6	3	31	43
8	6	3	17	-19
9	6	3	28	-35
-11	7	3	22	32
-10	7	3	31	-16
-9	7	3	52	-59
-8	7	3	26	-13
-7	7	3	79	95
-6	7	3	39	42
-5	7	3	89	-95
-4	7	3	44	-45
-3	7	3	116	131
-2	7	3	62	64
-1	7	3	61	-67
0	7	3	48	-50
1	7	3	23	28
2	7	3	36	33
3	7	3	41	-48
4	7	3	27	-30
5	7	3	24	22
6	7	3	28	29
-12	8	3	27	30
-10	8	3	24	-31
-9	8	3	37	-45
-8	8	3	36	42
-7	8	3	70	76
-5	8	3	90	-97
-4	8	3	35	-41
-3	8	3	95	100
-2	8	3	89	86
-1	8	3	65	-63
0	8	3	87	-86
1	8	3	20	-19
2	8	3	108	112
4	8	3	88	-90
5	8	3	21	-23
6	8	3	49	50
7	8	3	19	27
8	8	3	37	-45
9	8	3	17	-18
-11	9	3	20	-13
-9	9	3	18	-16
-8	9	3	18	1
-7	9	3	22	26
-3	9	3	38	39
-1	9	3	34	-29
2	9	3	35	32
4	9	3	42	-40
7	9	3	30	34
8	9	3	23	-12
-8	10	3	24	29
-7	10	3	18	-14
-6	10	3	29	-31
-3	10	3	18	29
-2	10	3	26	14
-1	10	3	31	-27
0	10	3	22	-21
1	10	3	39	41
2	10	3	31	21
3	10	3	27	-28
4	10	3	19	-3
7	10	3	17	-17
-9	11	3	20	-12
-8	11	3	22	15
-7	11	3	23	24
-5	11	3	48	-47
-4	11	3	36	30
-3	11	3	27	31
-1	11	3	27	-31
0	11	3	53	-51
1	11	3	32	34
2	11	3	57	58
4	11	3	77	-75
5	11	3	18	-13
6	11	3	47	49
-7	12	3	19	-13
-6	12	3	17	6
-4	12	3	24	-21
-3	12	3	22	-22
-1	12	3	36	30
0	12	3	30	19
1	12	3	31	-27
2	12	3	41	-33
4	12	3	29	31
6	12	3	20	-23
-6	13	3	25	-6
-3	13	3	28	19
-2	13	3	22	11
-1	13	3	27	-16
0	13	3	26	-18
2	13	3	23	23
-1	14	3	31	31
-13	0	4	25	-26
-12	0	4	35	-46
-11	0	4	52	52
-10	0	4	49	47
-9	0	4	60	-49
-8	0	4	57	-58
-7	0	4	38	32
-6	0	4	60	52
-5	0	4	74	-72
-4	0	4	137	-128
-3	0	4	237	250
-1	0	4	113	114
0	0	4	195	-204
1	0	4	42	-50
3	0	4	115	94
4	0	4	32	-31
5	0	4	128	-127
6	0	4	54	54
7	0	4	24	27
9	0	4	19	-8
10	0	4	19	-19
12	0	4	19	26
-14	1	4	36	37
-12	1	4	61	-58
-11	1	4	17	-15
-10	1	4	45	38
-9	1	4	31	33
-8	1	4	52	-49
-7	1	4	52	-51
-6	1	4	37	29
-5	1	4	53	43
-4	1	4	113	-122
-3	1	4	40	-32
-2	1	4	24	35
-1	1	4	48	36
1	1	4	120	-117
2	1	4	31	-19
3	1	4	88	80
4	1	4	66	66
5	1	4	45	-46
6	1	4	26	-30
8	1	4	30	33
9	1	4	17	14
-12	2	4	31	-24
-9	2	4	33	35
-8	2	4	43	-42
-7	2	4	84	-84
-5	2	4	102	106
-4	2	4	82	82
-3	2	4	142	-156
-2	2	4	47	47
-1	2	4	32	27
0	2	4	76	72
1	2	4	20	7
2	2	4	31	-39
3	2	4	76	70
4	2	4	20	22
5	2	4	49	-41
6	2	4	23	-19
7	2	4	67	62
8	2	4	29	33
9	2	4	35	-31
10	2	4	25	-21
-12	3	4	20	-24
-10	3	4	37	36
-9	3	4	18	15
-8	3	4	33	-41
-7	3	4	26	-21
-5	3	4	83	78
-4	3	4	43	29
-3	3	4	112	-130
-2	3	4	138	-146
-1	3	4	110	110
0	3	4	226	219
1	3	4	99	82
2	3	4	148	-154
3	3	4	113	-127
4	3	4	94	80
5	3	4	101	90
6	3	4	51	-55
7	3	4	53	-51
8	3	4	36	38
9	3	4	32	30
11	3	4	27	-33
-11	4	4	19	-16
-6	4	4	57	66
-5	4	4	39	-37
-4	4	4	75	-87
-3	4	4	28	25
-2	4	4	199	157
-1	4	4	79	-88
0	4	4	65	-65
1	4	4	21	-44
2	4	4	122	115
3	4	4	23	-17
4	4	4	82	-77
5	4	4	30	-27
6	4	4	32	29
7	4	4	31	29
8	4	4	23	-25
11	4	4	29	19
-12	5	4	37	-35
-11	5	4	29	-38
-10	5	4	47	50
-9	5	4	67	66
-8	5	4	20	-20
-7	5	4	132	-155
-5	5	4	125	122
-4	5	4	39	33
-3	5	4	136	-138
-2	5	4	92	-93
-1	5	4	88	71
0	5	4	155	160
1	5	4	34	-39
2	5	4	127	-134
3	5	4	18	-26
4	5	4	109	100
5	5	4	27	16
6	5	4	46	-47
7	5	4	27	-22
9	5	4	31	34
11	5	4	25	-27
-12	6	4	18	4
-11	6	4	28	-23
-10	6	4	21	-7
-9	6	4	20	12
-8	6	4	22	23
-7	6	4	40	35
-6	6	4	37	-45
-5	6	4	23	-12
-3	6	4	44	52
-2	6	4	30	-29
-1	6	4	24	-24
0	6	4	15	-19
1	6	4	35	35
2	6	4	15	4
3	6	4	19	-17
4	6	4	28	-31
5	6	4	15	19
6	6	4	19	20
8	6	4	20	-13
9	6	4	22	-19
-11	7	4	33	-33
-9	7	4	53	56
-7	7	4	82	-88
-6	7	4	32	-32
-5	7	4	99	111
-4	7	4	67	72
-3	7	4	82	-96
-2	7	4	58	-61
-1	7	4	48	54
0	7	4	55	62
2	7	4	45	-52
3	7	4	15	-19
4	7	4	50	49
5	7	4	37	48
6	7	4	18	-11
7	7	4	35	-40
9	7	4	32	26
-8	8	4	22	28
-6	8	4	36	-40
-4	8	4	51	60
-2	8	4	82	-92
-1	8	4	21	12
0	8	4	53	50
1	8	4	15	6
2	8	4	43	-37
4	8	4	39	36
5	8	4	33	17
6	8	4	21	-15
7	8	4	29	-10
9	8	4	23	-4
-9	9	4	16	25
-7	9	4	22	-20
-6	9	4	35	-29
-5	9	4	16	31
-4	9	4	35	42
-2	9	4	49	-48
0	9	4	57	56
1	9	4	40	43
2	9	4	55	-55
3	9	4	44	-40
4	9	4	40	31
5	9	4	41	40
6	9	4	31	-34
7	9	4	45	-41
-8	10	4	20	15
-7	10	4	22	10
-5	10	4	36	-34
-2	10	4	18	7
-1	10	4	28	-27
1	10	4	25	32
3	10	4	42	-45
5	10	4	39	44
7	10	4	33	-33
-6	11	4	40	38
-4	11	4	22	-29
-2	11	4	25	23
0	11	4	30	-22
-5	12	4	33	32
-4	12	4	36	30
-3	12	4	30	-29
-2	12	4	38	-32
-1	12	4	21	12
0	12	4	25	24
2	12	4	20	-20
3	12	4	24	-15
-14	1	5	35	-36
-13	1	5	19	-15
-12	1	5	47	46
-11	1	5	20	22
-10	1	5	38	-32
-9	1	5	59	-55

H	K	L	FO	FC
-8	1	5	17	19
-7	1	5	62	59
-6	1	5	26	18
-5	1	5	30	36
-2	1	5	13	-8
-1	1	5	47	61
1	1	5	47	-51
2	1	5	24	20
3	1	5	27	15
4	1	5	65	-76
6	1	5	28	25
8	1	5	26	-21
11	1	5	18	18
-13	2	5	54	-51
-12	2	5	48	43
-11	2	5	42	31
-10	2	5	20	-19
-9	2	5	100	-89
-8	2	5	15	-19
-7	2	5	96	86
-6	2	5	19	-31
-5	2	5	64	-57
-4	2	5	65	-62
-3	2	5	127	127
-2	2	5	83	81
-1	2	5	25	-32
0	2	5	16	8
1	2	5	83	82
3	2	5	102	89
4	2	5	56	-59
5	2	5	59	-56
6	2	5	31	-27
7	2	5	74	82
9	2	5	29	-22
10	2	5	26	-24
11	2	5	22	27
-13	3	5	17	-4
-11	3	5	28	20
-9	3	5	49	-39
-8	3	5	38	-38
-7	3	5	56	46
-6	3	5	83	88
-5	3	5	76	-80
-4	3	5	81	-88
-3	3	5	57	76
-2	3	5	113	115
-1	3	5	17	-26
2	3	5	23	10
3	3	5	18	-18
4	3	5	30	-34
5	3	5	17	-24
6	3	5	28	24
7	3	5	27	-11
-11	4	5	25	24
-10	4	5	16	10
-9	4	5	52	-58
-8	4	5	33	-36
-7	4	5	59	69
-6	4	5	87	95
-5	4	5	40	-40
-4	4	5	144	-159
-3	4	5	39	-47
-2	4	5	191	187
-1	4	5	121	112
0	4	5	126	-129
1	4	5	147	-156
2	4	5	48	28
3	4	5	176	168
4	4	5	21	-6
5	4	5	114	-116
6	4	5	17	-2
7	4	5	75	70
9	4	5	46	-46
10	4	5	17	-18
11	4	5	26	12
-12	5	5	18	0
-11	5	5	21	-7
-9	5	5	21	25
-7	5	5	23	-27
-6	5	5	42	-57
-5	5	5	23	-25
-4	5	5	52	64
-2	5	5	68	-83
0	5	5	51	39
1	5	5	30	20
2	5	5	53	-43
3	5	5	41	-32
4	5	5	86	97
5	5	5	59	60
6	5	5	23	-22
7	5	5	37	-40
10	5	5	18	15
-12	6	5	20	10
-11	6	5	49	55
-9	6	5	47	-52
-8	6	5	31	-33
-7	6	5	47	53
-6	6	5	71	84
-5	6	5	82	-101
-4	6	5	84	-91
-3	6	5	47	54
-2	6	5	109	117
0	6	5	79	-85
2	6	5	79	88
3	6	5	36	37
4	6	5	18	-17
5	6	5	47	-58
6	6	5	20	35
8	6	5	21	15
-11	7	5	20	8
-10	7	5	21	18
-9	7	5	18	13
-8	7	5	28	-29
-7	7	5	17	-19
-6	7	5	18	7
-5	7	5	28	31
-4	7	5	32	-29
-3	7	5	23	-26
-1	7	5	23	22
0	7	5	30	-41
2	7	5	24	13
3	7	5	23	26
4	7	5	25	-13
5	7	5	27	-16
7	7	5	21	7
8	7	5	19	-16
-10	8	5	21	20
-8	8	5	28	-33
-6	8	5	39	43
-5	8	5	29	37
-4	8	5	70	-76
-3	8	5	41	-48
-2	8	5	59	62
-1	8	5	31	24
0	8	5	39	-47
1	8	5	63	-63
2	8	5	25	23
3	8	5	63	57
5	8	5	58	-54
6	8	5	30	-40
7	8	5	52	49
8	8	5	22	31
-9	9	5	27	14
-7	9	5	19	-19
-4	9	5	20	13
-3	9	5	31	-42
-2	9	5	18	-23
-1	9	5	39	53
0	9	5	21	24
1	9	5	26	-27
2	9	5	21	-36
3	9	5	24	16
4	9	5	32	39
6	9	5	26	-29
-9	10	5	28	-26
-7	10	5	34	34
-5	10	5	37	-37
-4	10	5	20	-17
-3	10	5	28	30
0	10	5	22	-10
3	10	5	22	14
-6	11	5	26	19
-4	11	5	20	-24
-3	11	5	20	-20
-2	11	5	24	19
1	11	5	24	-29
2	11	5	18	-6
-4	12	5	38	27
-3	12	5	22	17
-2	12	5	20	-16
-1	12	5	39	-29
1	12	5	31	17
2	12	5	22	12
-14	0	6	36	22
-13	0	6	48	42
-11	0	6	64	-63
-9	0	6	57	37
-8	0	6	23	16
-7	0	6	42	-37
-6	0	6	49	-50
-13	1	6	47	33
-11	1	6	50	-40
-10	1	6	30	-31
-9	1	6	79	72
-8	1	6	40	42
-7	1	6	68	-74
-6	1	6	35	-32
-13	2	6	46	32
-11	2	6	53	-30
-10	2	6	48	-38
-9	2	6	72	60
-8	2	6	107	88
-6	2	6	98	-80
-13	3	6	35	22
-12	3	6	22	10
-11	3	6	30	-22
-10	3	6	51	-48
-9	3	6	28	27
-8	3	6	107	109
-6	3	6	70	-74
-8	4	6	19	8
-7	4	6	17	-20
-6	4	6	27	-28
-11	5	6	21	-24
-10	5	6	22	-26
-9	5	6	16	20
-8	5	6	31	25
-6	5	6	66	-77
-11	6	6	23	3
-9	6	6	16	-6
-8	6	6	21	-21
-11	7	6	18	-31
-8	7	6	28	23
-6	7	6	16	-14
-6	9	6	18	-9
-8	10	6	37	-32
-7	10	6	19	13
-6	10	6	44	33
-7	11	6	18	-22

TABLE II.6

BOND LENGTHS AND THEIR E.s.d's (Å)

Rh	- Br(1)	2.54(1)		P(2)	- O(21)	1.61(2)	
Rh	- Br(2)	2.54(1)		P(2)	- O(22)	1.61(3)	
Rh	- P(1)	2.33(2)		P(2)	- O(23)	1.47(3)	
Rh	- P(2)	2.27(2)		O(11)	- R11C(1)	1.36(4)	
Rh	- N	2.04(4)		O(12)	- R12C(1)	1.41(3)	
N	- O(3)	1.26(9)		O(13)	- R13C(1)	1.41(3)	
P(1)	- O(11)	1.54(4)		O(21)	- R21C(1)	1.42(4)	
P(1)	- O(12)	1.59(3)		O(22)	- R22C(1)	1.33(3)	
P(1)	- O(13)	1.58(2)		O(23)	- R23C(1)	1.49(4)	

TABLE II.7

BOND ANGLES AND THEIR E.s.d's (DEGREES)

Br(1)	-	Rh	-	Br(2)	87.8(3)	Rh	- P(2)	- O(22)	117(1)
Br(1)	-	Rh	-	P(1)	93.1(6)	Rh	- P(2)	- O(23)	108(2)
Br(2)	-	Rh	-	P(1)	176.6(3)	P(1)	- O(11)	- R11C(1)	117(2)
P(2)	-	Rh	-	P(1)	87.7(6)	P(1)	- O(12)	- R12C(1)	127(2)
P(2)	-	Rh	-	Br(1)	165.7(3)	P(1)	- O(13)	- R13C(1)	130(2)
P(2)	-	Rh	-	Br(2)	90.7(4)	P(2)	- O(21)	- R21C(1)	125(2)
N	-	Rh	-	Br(1)	91 (2)	P(2)	- O(22)	- R22C(1)	128(3)
N	-	Rh	-	Br(2)	89 (1)	P(2)	- O(23)	- R23C(1)	119(2)
N	-	Rh	-	P(1)	94 (1)	O(11)	- R11C(1)	- R11C(2)	121(2)
N	-	Rh	-	P(2)	103 (2)	O(12)	- R12C(1)	- R12C(2)	123(3)
O(3)	-	N	-	Rh	109 (5)	O(13)	- R13C(1)	- R13C(2)	116(2)
Rh	-	P(1)	-	O(11)	109 (1)	O(21)	- R21C(1)	- R21C(2)	116(1)
Rh	-	P(1)	-	O(12)	114 (2)	O(22)	- R22C(1)	- R22C(2)	113(3)
Rh	-	P(1)	-	O(13)	116 (1)	O(23)	- R23C(1)	- R23C(2)	124(2)
Rh	-	P(2)	-	O(21)	120 (2)				

TABLE II.8

LEAST SQUARES PLANE AND TORSION ANGLES

The equation of the plane is expressed in orthogonalized space as PI + QJ + KR = S

Equation (13.054)I + (-2.067)J + (2.469)K = 4.001

Atoms included in calculation	Distance from Plane, Å	Atoms not included in calculation	Distance from Plane, Å
Br(1)	0.1065	Rh	-0.1822
Br(2)	-0.1103	N	-2.2088
P(1)	-0.1181	O(3)	-2.7386
P(2)	0.1219		

Torsion angles (degrees)

P(1) - Rh - N - O(3)	59.5
P(2) - Rh - N - O(3)	29.1

CHAPTER 2

Discussion of Results and Conclusions

In the preceding sections, it has been shown that

i. The synthesis of a five-coordinate rhodium nitrosyl complex $[RhX_2(NO)L']$, where L' is a ditertiary phosphine, cannot be accomplished by any of the conventional methods used to prepare the analogous monodentate phosphine complexes $[RhX_2(NO)L_2]$.

ii. The complexes $[RhX_2(NO)\{P(OR)_3\}_2]$, where R is an alkyl or aryl group, are all unstable with respect to compounds not containing a nitrosyl group. The most stable of the series is that in which R = Ph.

iii. The cationic complexes $[RhBr(NO)\{P(OPh)_3\}_3]^+$ and $[Rh(NO)\{P(OPh)_3\}_4]^{2+}$, which were not characterized apart from their mode of preparation, colour, and, in the case of $[Rh(NO)\{P(OPh)_3\}_4]^{2+}$ (and somewhat speculatively), by infra-red spectroscopy, appeared to form only as intermediates in reactions which progressed to give nitrosyl-free products.

iv. The five-coordinate rhodium nitrosyl complex $[RhBr_2(NO)\{P(OPh)_3\}_2]$ has a square pyramidal molecular configuration in which the basal ligands are *cis*-disposed, with a nitrosyl group coordinating at the apical position in a non linear manner. The plane defined by the Rh, N and O atoms approximately bisects the two Rh-P vectors: *i.e.* the nitrosyl group is 'staggered' with respect to the two Rh-P bonds. The Rh-N bond length is among the longest so far observed in a nitrosyl

complex, and, coupled with the unusually high ν(N-O) frequency of 1750 cm^{-1}, is consistent with the instability of this complex with respect to decomposition products not exhibiting a ν(N-O) band.

v. The physical properties of the series $[RhBr_2(NO)\{P(OPh)_xPh_{(3-x)}\}_2]$ show a systematic variation as x goes from 3 to zero and, on the basis of its colour and infra-red spectrum, $[RhBr_2(NO)\{P(OPh)Ph_2\}_2]$ appears to correspond to an intermediate point between the two limiting structures of *cis*-$[RhBr_2(NO)\{P(OPh)_3\}_2]$ and *trans*-$[RhBr_2(NO)(PPh_3)_2]$.

Traditionally, the coordinated nitrosyl group has been considered as NO^+ when found bonded to a metal atom in a linear manner and NO^- when the M-N-O angle is of the order of 120° [1,25]. The linearly bound nitrosyl group is isoelectronic with a carbonyl group, and pentacoordinate compounds containing such a group are characterized by a metal to nitrogen bond length in the range 1.57 - 1.77 Å, and a very variable ν(N-O) frequency, in the range 1770 - 1640 cm^{-1} [2,23]. A linearly bound NO group is usually associated with trigonal bipyramidal geometries *e.g.* $Mn(NO)(CO)_4$ [26] although $Fe(NO)(S_2CN(CH_3)_2)_2$ is square pyramidal with a linear apical NO [27,28]. However, there has been much speculation as to whether the nitrosyl group in this and in the related complexes $Fe(NO)(S_2CN(C_2H_5)_2)_2$ [29] and $Fe(NO)(S_2C_2(CN)_2)_2^{2-}$ [30,31] is in fact coordinated linearly since the nitrosyl oxygen atom exhibits very large thermal motion and models based on a disordered, bent nitrosyl group are also compatible with the X-ray data[27,28,30,31].

In contrast, metal complexes which contain a non-linearly coordinated nitrosyl group have a somewhat longer M-N bond length,

typically around 1.88 Å, and exhibit a nitrosyl stretching frequency in the ranges 1630 - 1654 cm^{-1} for neutral complexes (with, to the author's knowledge, the sole exception of $[RhBr_2(NO)\{P(OPh)_3\}_2]$ for which ν(N-O) is 1750 cm^{-1}) and 1680 - 1720 cm^{-1} for cationic complexes[2,23]. A bent nitrosyl group is usually associated with square pyramidal geometries although $[Ru(Cl)(NO)_2(PPh_3)_2]^+$ contains both a bent, apical nitrosyl and a linear, basal nitrosyl group[2].

However, the formalism of considering coordinated NO as either NO^+ or NO^- is of little use when the mode of bonding of NO in complexes with intermediate structures is discussed. For instance, $[CoCl_2(NO)\{PMePh_2\}_2]$ has a Co-N-O angle of 164.5° and a molecular geometry intermediate between trigonal bipyramidal and square pyramidal.[1,46] Its infra-red spectrum is complex and appears to depend on the method of preparation of the sample and on the sample temperature.

Enemark and Feltham[2] and, more recently, Hoffman, Chen, Elian, Rossi and Mingos[3], have considered the problem of the coordinated nitrosyl group in some depth, from a molecular orbital viewpoint. The approach of the former workers is based on the treatment of the M-NO moiety as a covalently bound entity, the relative energies of its molecular orbitals depending upon the various geometries observed for the complex under discussion. Their results show that the properties of nitrosyl complexes are primarily determined by the nature of the highest occupied molecular orbital.

In ascertaining the relative ordering of the molecular orbitals of the {MNO} moiety, Enemark and Feltham modify the approach

of Walsh[32] (applied initially to the study of triatomic species such as O-N-O^{m} (m = +1, 0, -1)) by replacing one of the oxygen atoms of O-N-O with a metal atom, M. They consider the effect, on this ordering, of placing the {MNO} group in fields of various symmetries. In the particular case of five-coordinate complexes, the possible symmetries are C_2, C_{4v} and C_s, corresponding to trigonal bipyramidal, square pyramidal with a linear apical NO and square pyramidal with a bent apical NO group, respectively. An orbital correlation diagram for these symmetries[2] is set out in Figure II.5. It can be seen

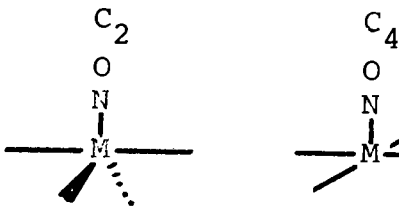

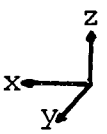

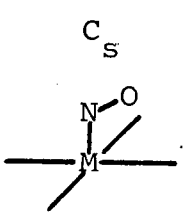

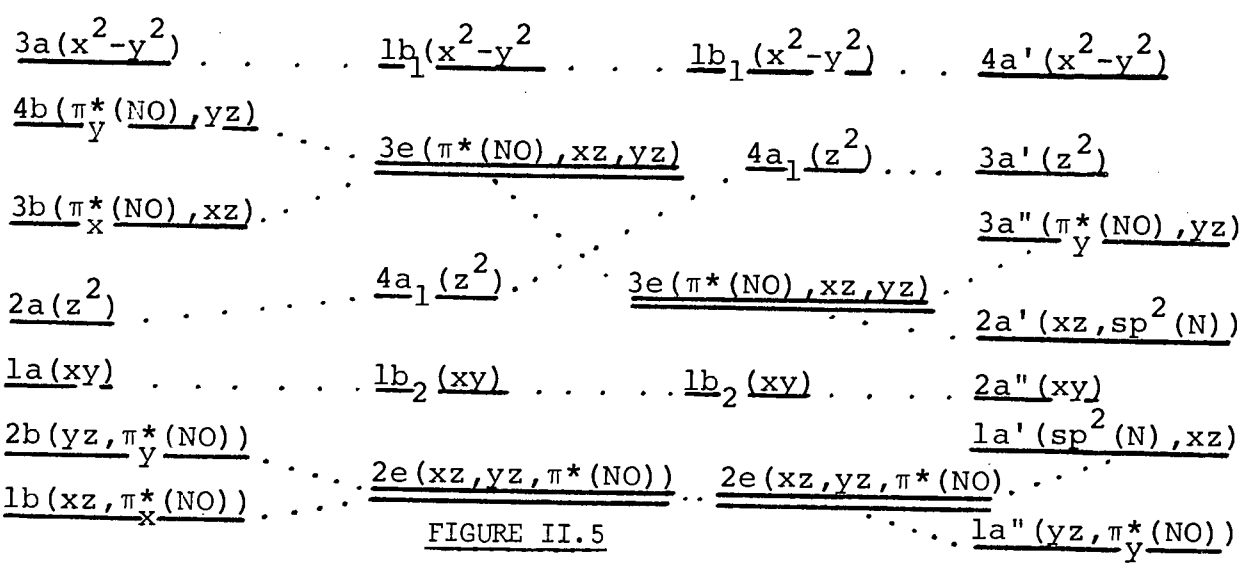

FIGURE II.5

that the nature of the highest occupied molecular orbital for a complex with eight d electrons available is highly correlated with the overall geometry of the molecule. Enemark and Feltham point out that when steric effects are minimal, the relative ordering of the $4a_1(d_{z^2})$ and $3e(\pi^*(NO),xz,yz)$ orbitals will determine, to some extent, the geometry of the molecule. Thus, if the $4a_1$ orbital is lower in

energy than the 3e orbital, a trigonal bipyramidal geometry with a linear NO group is expected; while population of the 3e orbital in preference to the $4a_1$ orbital will lead to a square pyramidal geometry with a bent {MNO} group. The complex $[CoCl_2(NO)\{PMePh_2\}_2]$ with an intermediate structure is thought to be near the crossing point of the $4a_1$ and 3e molecular orbitals. Ligands with good π-donating capabilities will tend to lower the energy of the 3e(xy, yz) orbital and give rise to square pyramidal configurations; *e.g.* $IrCl_2(NO)(PPh_3)_2$[12], whereas good π-acceptors, such as carbonyls, will increase the energy of the 3e orbital and a trigonal bipyramidal configuration will result. An example of such a complex is $Mn(NO)(CO)_4$[26].

Hoffman *et al*[3] base their more exhaustive treatment on the interaction of an ML_4 fragment of varying geometry with an NO group. Their conclusions are similar in principle to those of Enemark and Feltham but somewhat more detailed. The relevant points for square pyramidal {MNO} species in which there are eight electrons available for filling the molecular orbitals may be quoted as follows:

i. The better the σ- or π-donating capability of the basal ligands in a square pyramid, the more likely is the nitrosyl to bend.

ii. In compounds of the type $ML_2L'_2(NO)$, L *trans* to L', the nitrosyl group should bend in the plane containing the poorer bonors. iii. In a compound of the type $ML_2DA(NO)$, D = a π-donor group *trans* to A = a π-acceptor, if the NO group bends in the DMA plane, then it should bend towards the acceptor. iv. A nitrosyl ligand is less likely to bend in the equatorial position of a trigonal bipyramid than in the apical site of a square pyramid. v. Nitrosyl groups in axial positions

in a trigonal bipyramid and basal sites in a square pyramid should be linearly coordinated. vi. In ML_4NO species, if the ligands are strong π-donors, a range of geometries is possible from a strongly bent square pyramidal structure to a trigonal bipyramidal structure with a less-bent nitrosyl group. Finally, vii. a bent nitrosyl group will move its nitrogen atom off the coordination axis in the direction of π-coordination.

Within the framework of these findings, the structure of $[RhBr(NO)\{P(OPh)_3\}_2]$ and the possible structures of the cationic derivatives $[RhBr(NO)\{P(OPh)_3\}_3]^+$ and $[Rh(NO)\{P(OPh)_3\}_4]^{2+}$, as well as the observations mentioned at the beginning of this section, may be discussed.

At first glance, failure to synthesize $[RhBr_2(NO)(dppe)]$ by the methods employed to prepare the bis-triphenylphosphine derivative is inexplicable. However, consideration of the other five-coordinate structures where this ligand is present reveals a trigonal bipyramidal structure; *e.g.* $[Ru(NO)(dppe)_2]^+$ It would appear, therefore, that this tendency of dppe to give rise to trigonal bipyramidal structures in pentacoordinate complexes, opposes the tendency of such a complex to assume a square pyramidal geometry with a bent apical nitrosyl group, as found for $[IrCl_2(NO)(PPh_3)_2]$. This may reduce the thermodynamic stability of $[RhBr_2(NO)(dppe)]$ with respect to the nitrosyl-free complex $[Rh(dppe)_2]^+$ under the reaction conditions employed in efforts to prepare this complex. Thus, any such attempts, while possibly resulting in an intermediate $[RhX_2(NO)(dppe)]$, will usually produce the bis(dppe) rhodium cation.

The instability of the complexes $[RhBr_2(NO)\{P(OR)_3\}_2]$ is in the author's view, clearly correlated with the nature of R in these complexes. Thus, the attempted preparation of $[RhBr_2(NO)\{P(OMe)_3\}_2]$ resulted, initially, in a green solution of (presumably) the desired product which quickly decomposed to give nitrosyl-free compounds. However, green $[RhBr_2(NO)\{P(OPh)_3\}_2]$ is stable for many days in air at room temperature. The complexes $[RhBr_2(NO)\{P(OPh)_{(3-x)}Ph_x\}_2]$ (x = 1, 2) are correspondingly more stable than the triphenylphosphite derivative. Thus it would appear that the better the π-accepting capability of R, the more stable the complex $[RhX_2(NO)\{P(OR)_3\}_2]$ will be.

The effect on the nitrosyl stretching frequency in complexes such as $[RhBr_2(NO)(PPh_3)_2]$ of replacing the triphenyl phosphine groups with triphenylphosphite ligands is clearly to increase it. A similar increase is observed between the two complexes $[Ir(NO(PPh_3)_3]$ [33] (ν(N-O) = 1615 cm^{-1}) and $[Ir(NO)\{P(OPh)_3\}_3]$ [34] (ν(N-O) = 1715 cm^{-1}). This effect is due to the lesser π-donating capabilities (and concomitant depopulation of the π* orbital of the nitrosyl group) of triphenylphosphite as compared to triphenylphosphine. The instability of the cationic intermediates $[RhBr(NO)\{P(OPh)_3\}_3]^+$ and $[Rh(NO)\{P(OPh)_3\}_4]^{2+}$ may be rationalised in a like manner. The effect of replacing dppe in $[Rh(NO)(dppe)_2]^{2+}$ (ν(N-O) = 1750 cm^{-1}) with two $P(OPh)_3$ ligands will, on the above basis, be expected to increase the ν(N-O) frequency by some 100 cm^{-1} to give a complex with the remarkably high ν(N-O) frequency of about 1850 cm^{-1}. Since it appears that a high ν(N-O) band is correlated, in this class of complexes, with thermodynamic instability,

will be split, as d_{xz} and d_{yz} will not have the same energy, due to the *trans* arrangement of the basal ligands. The $\pi^*(NO)$ orbital will therefore interact differently with the d_{xz} and d_{yz} orbitals and bending of the NO group will take place preferentially in one plane - the plane containing the poorer donor ligands (in the above case, the PPh_3 groups). However, in *cis*-$[RhBr_2(NO)\{P(OPh)_3\}_2]$, the d_{xz} and d_{yz} orbitals will be degenerate and binding of the nitrosyl group will therefore take place in a plane where repulsions are minimised but where interaction of the $\pi^*(NO)$ orbital with metal orbitals of like symmetry will still be possible. Thus, it will bend, in a plane bisecting the Rh-P bonds, towards the poorer donor ligands, $P(OPh)_3$.

Finally, it is interesting to speculate on the structures of $[RhBr(NO)\{P(OPh)_3\}_3]^+$, $[Rh(NO)\{P(OPh)_3\}_4]^{2+}$ and $[RhBr_2(NO)\{P(OPh)Ph_2\}_2]$. The structure of the first-named complex may be discussed in the light of the known structures of $[IrX(NO)(CO)(PPh_3)_2]^+$ (X = Cl^{36} and I^{37}) and $[IrH(NO)(PPh_3)_3]^+$. In the first two complexes, the geometries are intermediate between square pyramidal and trigonal bipyramidal (P-Ir-P = 175.7° and 168.2°, Cl-Ir-C(of CO) = 161.3° and 158°) and the nitrosyl group bends in the plane defined by Ir, C and O - that is, towards the best π-acceptor ligand, as expected. Thus, the structures may be described as trigonal bipyramidal with axial PPh_3 groups and a bent, equatorial, NO group, although the X-Ir-C angles are greater than would be expected for this geometry.

The hydride ligand in $[IrH(NO)(PPh_3)_3]^+$ was not located in the structural study. The complex may be thought of as trigonal bipyramidal with the H and NO ligands occupying the axial positions

and the phosphine ligands occupying the equatorial positions. The M-N-O angle is 175°. In actual fact, if the presence of the hydride ligand is discounted, the geometry is closer to tetrahedral (P1-Ir-P2 = 118.4°, P1-Ir-P3 = 117.6°, P2-Ir-P3 = 110.4°, P1-Ir-N = 106°, P2-Ir-N = 99°, P3-Ir-N = 103°).

Thus, substitution of H for Cl, and of PPh_3 for CO, effects a change from a non-linearly coordinated NO group to a linear NO group in these two complexes. The structure of $[RhBr(NO)\{P(OPh_3\}_3]^+$ in which the halide ligand is retained but the CO and PPh_3 ligands replaced by $P(OPh)_3$, is likely to be intermediate between those of $[IrCl(NO)(CO)(PPh_3)_2]^+$ and $[IrH(NO)(PPh_3)_3]^+$.

The complex $[Ru(NO)(dppe)_2]^+$ is trigonal bipyramidal with an equatorial linear NO group[38]. The ν(N-O) frequency is 1673 cm^{-1}. The structure of $[Rh(NO)(dppe)_2]^{2+}$ [19] has not been determined but it is likely to be trigonal bipyramidal, also with a linear nitrosyl. Thus, it is probable that $[Rh(NO)\{P(OPh)_3\}_4]^{2+}$ will adopt a similar configuration.

The structure of $[RhBr_2(NO)\{P(OPh)Ph_2\}_2]$ is a matter for conjecture. It would appear that it has properties intermediate between those of $[RhBr_2(NO)\{P(OPh)_3\}_2]$ and $[RhBr_2(NO)(PPh_3)_2]$. *cis*-$[M(NO)L_2X_2]$ and *trans*-$[M(NO)L_2X_2]$ are related by a molecular distortion incorporating two Berry pseudorotations[39]. (Figure 11.6).

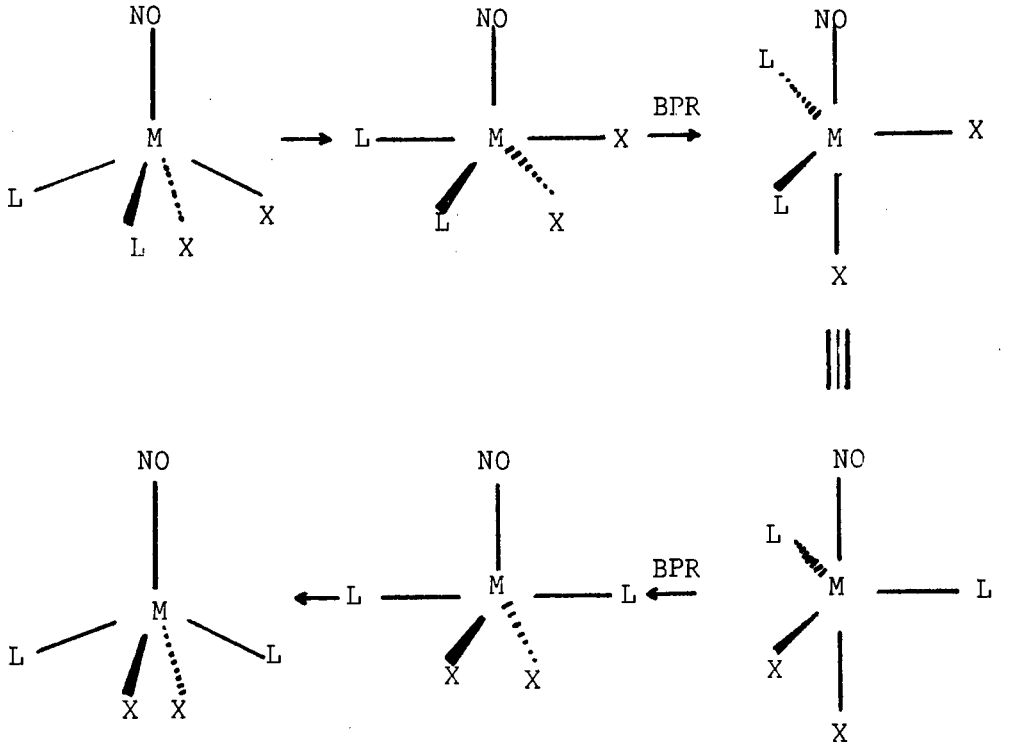

(BPR = Berry pseudorotation)

FIGURE II.6.

and the structure of $[RhBr_2(NO)\{P(OPh)Ph_2\}_2]$ may be akin to one of the intermediates depicted in the figure.

However, as pointed out previously, the infra-red spectrum of this complex suggests the presence of more than one isomer.

APPENDIX

LISTING OF THE PROGRAM 'MAP'

```
      DIMENSION FMAP(28,53),XCOORD(28),YCOORD(53),TITLE(40)
      JIN=11
      JOUT=12
      READ(8,3001)WID,HEI,NUM,ICTL,PSC,IPLT
      READ(JIN,100)TITLE
      READ(JIN,200)Z,ZZ,X,Y
      READ(JIN,300)SC
      READ(JIN,400)(XCOORD(J),J=1,28)
      DELX=XCOORD(28)-XCOORD(1)
      IF(XCOORD(28) .GT. XCOORD(1))GO TO 1
    1 IF (DELX .GT. 26) GO TO 2
      DELX=(100+DELX)
      XCOORD(28) = XCOORD(28)+100
    2 XINC=DELX/27
      READ(JIN,500)YCOORD(1),(FMAP(J,1),J=1,28)
      DO 10 K=2,53
      READ(JIN,501)YCOORD(K),(FMAP(J,K),J=1,28)
   10 CONTINUE
      DELY =YCOORD(53)-YCOORD(1)
      IF(YCOORD(53) .GT. YCOORD(1))GO TO 3
    3 IF(DELY .GT. 51)GO TO 4
      DELY=(100+DELY)
      YCOORD(53)=YCOORD(53)+100
    4 YSCALE=DELY/PSC
      YINC=DELY/52
      J=1
      K=1
      DO 150 J=1,28
      DO 250 K=1,53
      FMAP(J,K)=100*(FMAP(J,K)/SC)
  250 CONTINUE
  150 CONTINUE
      WRITE(JOUT,3002)IPLT
      WRITE(JOUT,1000)TITLE,Z,ZZ,X,Y
      WRITE(JOUT,2000)YSCALE,YSCALE,XCOORD(1),XINC,XCOORD(28),YCOORD(1),
     *YINC,YCOORD(53)
      WRITE(JOUT,3000)WID,HEI,NUM,ICTL
      DO 20 K=1,53
      DO 30 J=1,28
      XX=(XCOORD(1)+(J-1) XINC)
      YY=(YCOORD(1)+(K-1) YINC)
      WRITE(JOUT,4000)XX,YY,FMAP(J,K)
   30 CONTINUE
   20 CONTINUE
  100 FORMAT(26X,40A1)
  200 FORMAT(//1X,A1,2X,F5.2,5X,A1,12X,A1)
  500 FORMAT(/14X,F11.4)
  000 FORMAT(//4X,28F4.0)
  000 FORMAT(/1X,F2.0,1X,28F4.0)
  001 FORMAT(1X,F2.0,1X,28F4.0)
  000 FORMAT('JOB  ',40A1,1X,A1,2H =,F5.2,5X,A1,7H ACROSS,5X,A1,
     *5H DOWN)
  000 FORMAT('SIZE ',F5.0,F5.0,10X,F10.0,F5.0,F10.0,F10.0,F5.0,
     *F10.0)
  000 FORMAT('CNTL ',F5.2,F5.2,I5,I5)
  001 FORMAT(5X,F5.2,F5.2,I5,I5,F5.2,I2)
  002 FORMAT('TIME',1X,I2)
  000 FORMAT('CNTL ',F10.2,F10.2,F10.2)
      STOP
      END
```

REFERENCES : PART I.

1.1 R.W.F. Hardy and R.C. Burns, Ann. Rev. Biochem., 37, 311 (1968); K. Kuchynka, Catalysis Rev., 3, 111 (1970); L.E. Mortenson, Survey Progr. Chem., 4, 127 (1968); R.W.F. Hardy, R.C. Burns and G. Parshall, Adv. in Chem. Series, 100, 219, Amer. Chem. Soc. (1971).

1.2 See, *e.g.*, A.L. Lehninger, 'Biochemistry', p. 560, Worth Publishers, Inc., New York (1970).

1.3 J.R. Herriot *et al.*, J. Mol. Biol., 50, 391 (1970); T.V. Long *et al.*, J. Amer. Chem. Soc., 93, 1810 (1971).

1.4 R.C. Burns, R.D. Holsten and R.W.F. Hardy, Biochem. Biophys. Res. Comm., 39, 90 (1970).

1.5 D.O. Hall and M.C.W. Evans, Nature (London), 223, 1342 (1969).

1.6 B.B. Buchanan and D.I. Arnon, Advan. Enzymol. Relat. Subj. Biochem., 33, 119 (1970).

1.7 J.C.M. Tsibris and R.W. Woody, Coord. Chem. Rev., 5, 417 (1970).

1.8 G. Palmer and H. Brintzinger, 'Electron and Coupled Energy Transfer in Biological Systems', §9, 1B (1972), Marcel Dekker, New York.

1.9 a) J.R. Herriot, L.C. Sieker and L.H. Jensen, J. Mol. Biol., 50, 391 (1970).

b) K.D. Watenpaugh, L.C. Sieker, J.R. Herriot and L.H. Jensen, Cold Spring Harbour Symp. Quart. Biol., 36, 359 (1971).

1.10 C.W. Carter, Jr., S.T. Freer, Ng.H Xuong, R.A. Alden and J. Kraut, *ibid.*, 36, 381 (1971).

1.11 L.C. Sieker, E. Adman and L.H. Jensen, Nature (London), 235, 40 (1972).

1.12 B.A. Averill, T. Herskovitz, R.H. Holm and J.A. Ibers, J. Amer. Chem. Soc., 95, 3523 (1973) and references quoted therein.

1.13 A.F. Wells, Z. Kristallogr., Kristallgeometrie, Kristallphys., Kristallchem., 94, 447 (1936).

1.14 V. Albano, P. Bellon, G. Ciani and M. Manaserro, J. Chem Soc. Chem. Comm., 1242 (1969).

1.15 M. Poe, W.D. Phillips, C.C. McDonald and W. Lovenberg, Proc. Nat. Acad. Sci. U.S.A., 65, 797 (1970).

1.16 F.A. Cotton and G. Wilkinson, 'Advanced Inorganic Chemistry', 3rd Edn., Interscience (1972).

1.17 W. Hieber and G. Wagner, Z. Naturforsch., 136, 339 (1958).

1.18 R.E. Dessy, R. Kornmann, C. Smith and R. Haytor, J. Amer. Chem. Soc., 90, 2001 (1968).

1.19 R.E. Dessy and L. Wieczorek, *ibid.*, 91, 4963 (1969).

1.20 R.E. Dessy, J.C. Charkoudian, T.P. Abeles and A.L. Rheingold, *ibid.*, 92, 3947 (1970).

1.21 J.A. de Beer, R.J. Haines, R. Greatrex and J.A. Van Wyk, J. Chem. Soc. (Dalton) 2341 (1973).

1.22 P. Hydes, J.A. McCleverty and D.G. Orchard, J. Chem. Soc. (A), Part 3, 3660 (1971).

1.23 R.J. Haines, J.A. de Beer and R. Greatrex, J. Organometall. Chem. 85, 89 (1975).

1.24 G. Ferguson, H. Hannaway and K.M.S. Islam, J. Chem. Soc. Chem. Comm., 1165 (1968).

1.25 F.A. Cotton and C.S. Kraihanzel, J. Amer. Chem. Soc., 84, 4432 (1962).

1.26 F.A. Cotton, A. Musco and G. Yagupsky, Inorg. Chem., 6, 1457 (1967).

1.27 M. Clare, H.A.O. Hill, C.E. Johnson and R. Richards, J. Chem. Soc. Chem. Comm., 1376 (1970); See also J.A. de Beer, R.J. Haines, R. Greatrex and N.N.Greenwood, J. Chem. Soc. (A), 3271 (1971) and Ref. 1.21.

1.28 R.J. Haines, personal communication.

1.29 R. Mason, K.M. Thomas, K. Hardcastle, R. Greatrex, R.J. Haines and A.L. du Preez, being submitted.

1.30 L.F. Dahl, E.R. de Gil and R.D. Feltham, J. Amer. Chem. Soc., 91, 1653 (1969).

1.31 R.F. Bryan, P.T. Greene, D.S. Field and M.J. Newlands, J. Chem. Soc. Chem. Comm., 1477 (1969).

1.32 O.S. Mills, Acta. Crystallogr., 11, 620 (1958).

1.33 N.G. Connelly and L.F. Dahl, J. Amer. Chem. Soc., 92, 7472 (1970).

1.34 J.D. Sinclair, N.G. Connelly and L.F. Dahl, quoted in Ref. 1.30

1.35 R. Mason and D.M.P. Mingos, J. Organometallic Chem., 50, 53 (1973).

1.36 B.K. Teo, M.B. Hall, R.F. Fenske and L.F. Dahl, J. Organomettalic Chem., 70, 413 (1974).

1.37 N.G. Connelly and L.F. Dahl, J. Amer. Chem. Soc., 92, 7470 (1970).

1.38 J.L. Calderon, S. Fontana, E. Frauendorfer, V.W. Day and S.D.A. Iske, J. Organomettalic Chem., 64, C16 (1974).

1.39 F.A. Cotton and J.M. Troup, J. Amer. Chem. Soc., 96, 5070 (1974).

1.40 F.A. Cotton and J.M. Troup, J. Amer. Chem. Soc., 96, 1233 (1974).

1.41 H.B. Chin and R. Bau, J. Amer. Chem. Soc., 95, 5068 (1973).

1.42 R.J. Haines, A.L. du Preez and C.R. Nolte, J. Organometallic Chem., 55, 199 (1973).

1.43 F.A. Cotton, B.A. Frenz and A.J. White, J. Organometallic Chem., 60, 147 (1973).

1.44 F.W.B. Einstein and R.D.G. Jones, Inorg. Chem., 12. 1690 (1973).

1.45 F. Bonati and G. Wilkinson, J. Chem. Soc., 179 (1964).

1.46 J.E. O'Connor and E.R. Corey, Inorg. Chem., 6, 968 (1967).

1.47 N. Flitcroft, D.A. Harbourne, I. Paul, P.M. Tucker and F.G.A. Stone, J. Chem. Soc. (A), 1130 (1966).

1.48 See Ref. 1.47; also B.P. Bir'yukov, Yu.T Struchkov, K.N. Anisimov, N.E. Kolobova and V.V. Skripkin, J. Chem. Soc. Chem. Comm., 159 (1968).

1.49 B.P. Bir'yukov, Yu.T. Struchkov, K.N. Anisimov, N.E. Kolobova and V.V. Skripkin, *ibid.*, 750 (1967).

1.50 B.P. Bir'yukov, Yu.T. Struchkov, K.N. Anisimov, N.E. Kolobova and V.V. Skripkin, *ibid.*, 1193 (1968).

1.51 M.R. Churchill, B.G. Deboer and K.L. Kalra, Inorg. Chem., 12, 1646 (1973).

1.52 L. Pope, P. Sommerville, M. Laing, K.J. Hindson and J.R. Moss, J. Organometallic Chem., 112, 309 (1976).

1.53 See Ref. 1.52.

1.54 P. Braunstein and J. Dehand, J. Organometallic Chem., 88, C24 (1975).

1.55 See Ref. 1.54. D.M. Adams, J.B. Corell, J.L. Dawes and R.D.W. Kemmitt, Inorg. Nucl. Chem. Lett., 3, 437 (1967).

1.56 M. Ahmad, R. Bruce and G.R. Knox, J. Organometallic Chem., 6, 1, (1966).

1.57 T.S. Piper, F.A. Cotton and G. Wilkinson, J. Inorg. Nucl. Chem. 1, 165 (1955).

1.58 E.C. Johnson, T.J. Meyer and N. Winterton, J. Inorg. Chem., 10, 1673 (1971).

1.59 M.L.H. Green, 'Organometallic Compounds', 2, 3rd Ed., Chapman and Hall, London (1968).

1.60 R. H. Herber and Y. Goscinny, Inorg. Chem., 7, 1293 (1968).

1.61 M.R. Churchill and K.L. Kalra, Inorg. Chem., 12, 1650 (1973).

1.62 M.R. Churchill, B.G. Deboer, K.L. Kalra, Reich-Rohrwig and Wojcicki, J. Chem. Soc. Chem. Comm., 981 (1972).

1.63 M.D. Curtis and R.C. Job, J. Amer. Chem. Soc., 94, 2153 (1972).

1.64 R.J. Haines and C.R. Nolte, J. Organometallic Chem., 36, 163 (1972).

1.65 R.B. King and M.B. Bisnette, J. Organometallic Chem., 2, 15 (1964).

1.66 H.C. Clark and K.R. Dixon, J. Amer. Chem. Soc., 91, 596 (1969).

1.67 H.C. Clark and J.D. Ruddick, Inorg. Chem., 9, 1226 (1970).

1.68 P.M. Treichel and R.L. Shubkin, Inorg. Chim. Acta, 2, 485 (1968).

1.69 R.J. Haines and A.L. du Preez, J. Chem. Soc. Dalton, 944 (1972).

1.70 C.R. Nolte, Ph.D. Thesis, University of Pretoria, Republic of South Africa (1974).

1.71 J.A. de Beer, R.J. Haines, R. Greatrex and J.A. Van Wyk, J. Chem. Soc. (Dalton), 2341 (1973).

1.72 J.G. Bullitt, F.A. Cotton and T.J. Marks, Inorg. Chem., 11 671 (1972).

1.73 J.W. Dunker, J. Finer, J. Clardy and R.J. Angelici, J. Organometallic Chem., 114, C49 (1976).

1.74 M.A. Bush and P. Woodward, J. Chem. Soc. (A), 1833 (1967)

2.1 E.W. Abel and B.C. Crosse, Organometallic Chem. Rev., 2, 443 (1967).

2.2 W. Strohmeier, D. von Hobe, G. Schönauer and H. Laporte, Z. Naturforsch, 17b, 502 (1962).

2.3 R.E. Dessy, F.E. Stary, R.B. King and M. Waldrop, J. Amer. Chem. Soc., 88, 471 (1966).

2.4 R.E. Dessy, R. Kornmann, C. Smith and R.G. Hayter, *ibid.*, 90, 2001 (1968).

2.5 A.N. Nesmeyanov, G.G. Aleksandrov, A.B. Antonova, K.N. Anisimov, N.E. Kolobova, Yu. T. Struchkov, J. Organometallic Chem., 110, C36 (1976).

2.6 W. Strohmeier and J.F. Guttenberger, Chem. Ber., 97, 1871 (1964).

2.7 E. Klump, L. Markó and G. Bor, Chem. Ber., 97, 926 (1964).

2.8 C. Kowala and J.M. Swan, Aust. J. Chem., 19, 547 (1966).

2.9 A. Kay and P.C.H. Mitchell, J. Chem. Soc. (A), 2421 (1970).

2.10 C.G. Kuehn and H. Taube, J. Amer. Chem. Soc., 98, 689 (1976).

2.11 M.R. Churchill, B.G. Deboer and K.L. Halra, Inorg. Chem., 12 1646 (1973).

2.12 L. Pauling, 'The Nature of the Chemical Bond', 3rd ed., Cornell University Press, Ithaca, New York (1960).

3.1 G.M. Sheldrick, SHELEX program system (1976). To be published.

3.2 X-ray (1972). Program System, version of June 1972, Technical Report TR - 192 of the Computer Science Centre, University of Maryland.

3.3 P. Roberts and G.M. Sheldrick, (Cambridge). To be published.

3.4 W.D.S. Motherwell, (Cambridge). Unpublished.

3.5 C.K. Johnson, ORTEP. Report ORNL - 3794. Oak Ridge National Laboratory, Oak Ridge, Tennessee.

3.6 GPCP : A General Purpose Contouring Program, California Computer Products, Inc., California (1971).

3.7 D.T. Cromer and J.B. Mann, Acta Crystallogr., A24, 321 (1968).

3.8 R.F. Stewart, E.R. Davidson and W.T. Simpson, J. Phys. Chem., 42, 3175 (1965).

3.9 International Tables for X-ray Crystallography (1967 and 1968) Vols. I - III. Birmingham : Kynoch Press.

3.10 Molecular Structures and Dimensions (1935-1976). Utrecht : Bohn, Scheltema and Holkema, and a survey of references quoted therein.

3.11 See Chapter 2.

3.12

4.1 F. Bonati and G. Wilkinson, J. Chem. Soc., 179 (1964).

4.2 N. Flitcroft, D.A. Harbourne, I. Paul, P.M. Tucker and F.G.A. Stone, J. Chem. Soc. (A), 1130 (1966).

4.3 D.A. Symon and T.C. Waddington, J. Chem. Soc., Dalton, 78 (1974).

4.4 See Ref. 4.2.

4.5 J.D. Cotton and R.M. Peachey, Inorg. Nucl. Chem. Letters, 6, 727 (1970).

4.6 R.H. Herber and Y. Goscinny, Inorg. Chem., 7, 1293 (1968).

4.7 E. Giglio, Nature, 222, 339 (1969).

4.8 W.D.S. Motherwell, (Cambridge). Unpublished.

5.1 L.F. Dahl, E.R. de Gil and R.D. Feltham, J. Amer. Chem. Soc., 91, 1653 (1969).

5.2 G. Ferguson, H. Hannaway and K.M.S. Islam, J. Chem. Soc. Chem. Comm., 1165 (1968).

5.3 G.G. Summer, H.P. Klug and L.E. Alexander, Acta Crystallogr., 17, 732 (1964).

5.4 H.B. Chin, M.B. Smith, R.D. Wilson and R. Bau, J. Amer. Chem. Soc., 96, 5285 (1974).

5.5 F.A. Cotton and B.A. Frenz, Inorg. Chem., 13, 253 (1974).

5.6 R.D. Adams, M.D. Brice and F.A. Cotton, Inorg. Chem., 13, 1080 (1974).

6.1 L.F. Dahl and R.E. Rundle, Acta Crystallogr., 16, 419 (1963).

6.2 S.R. Finnimore, R. Goddard, S.D. Killops, S.A.R. Knox and P. Woodward, J. Chem. Soc. Chem. Comm., 391 (1975).

6.3 C. Barbeau and R.J. Dubey, Can. J. Chem., 51, 3684 (1973).

6.4 R.J. Doedens, W.T. Robinson and J.A. Ibers, J. Amer. Chem. Soc., 89, 4323 (1967).

6.5 M.J. Bennett and R. Mason, J. Chem. Soc. (A), 695 (1966).

6.6 G.J. Simon and L.F. Dahl, J. Amer. Chem. Soc., 95, 783 (1973).

6.7 K. Triplett and M.C. Curtis, J. Amer. Chem. Soc., 97, 5747 (1975).

6.8 R.M. Kichner, T.J. Marks, J.S. Kristoff and J.A. Ibers, J. Amer. Chem. Soc., 95, 6602 (1973).

6.9 H. Vahrenkamp, Chem. Ber., 107, 3867 (1974).

REFERENCES : PART II

1. B.A. Frenz and J.A. Ibers, MTP Int. Rev. Sci. : Phys. Chem., Ser. One, 11, 33 (1973).

2. J.H. Enemark and R.D. Feltham, Coord. Chem. Rev., 13, 339 (1974).

3. R. Hoffmann, M.M.L. Chen, M. Elian, A.R. Rossi and D.M.P. Mingos, Inorg. Chem., 13, 2666 (1974).

4. W.B. Hughes, E.A. Zuech, E.T. Kittleman and D.H. Kubceik, 23rd I.U.P. A.C. Congress, Boston, Abstract 566 (1971).

5. W.B. Hughes and E.A. Zuech, U.S. P., 3562178 (1971) (Chem. Abs., 75, 10868b (1971)); U.S. P., 3691253 (1972) (Chem. Abs., 78, 3657r (1973)).

6. W.B. Hughes and E.A. Zuech, U.S. P., 3558517 (1971) (Chem. Abs., 72, 99985w (1970)).

7. R.J. Haines and G.J. Leigh, Coord. Chem. Rev., 4, 155 (1975).

8. C.G. Biefeld, H.A. Eick and R.H. Grubbs, Inorg. Chem., 12, 2166 (1973).

9. J.X. McDermott, J.F. White and G.M. Whitesides, J. Amer. Chem. Soc., 98, 6521 (1976).

10. L.H. Jensen, Z. Anorg. Chem., 229, 237 (1936).

11. I.T. Millar and H. Heaney, Quart. Rev., 11, 109 (1957) and references quoted therein.

12. D.M.P. Mingos and J.A. Ibers, Inorg. Chem., 10, 1035 (1971).

13. Ref. 10 and J. Chatt and R.G. Wilkins, J. Chem. Soc., 2532 (1951).

14. P. Haake and R.M. Pfeiffer, J. Amer. Soc., 92, 4996 (1970).

15. J.P. Collmann, N.W. Hoffmann and D.E. Morris, J. Amer. Chem. Soc., 91, 5659 (1969).

16. W. Hieber and K. Heinicke, Z. Anorg. Allgem. Chem., 316, 321 (1962).

17. T. Bianco, M. Rossi and L. Uva, Inorg. Chim. Acta, 3, 443 (1969).

18. G.R. Crooks and B.F.G. Johnson, J. Chem. Soc. (A), 1662 (1970).

19. N.G. Connelly, M. Green and T.A. Kuc, J. Chem. Soc. Chem. Comm., 542 (1974).

20. C.R. Nolte, Ph.D Thesis, University of Pretoria (1974).

21. The 'cone angle' is the solid angle subtended at the metal atom by the ligand, and is discussed in two papers: C.A. Tolman, W.C. Seidel and L.W. Gosser, J.Amer.Chem.Soc, 96, 53 (1974)

22. C.A. Tolman, J. Amer. Chem. Soc., 92, 2956 (1970).

23. Molecular Structures and Dimensions (1935-1976). Utrecht: Bohn, Scheltema and Holkema.

24. L.M. Haines, Ph.D Thesis, University of South Africa (1970).

25. N.V. Sidgwick and R.W. Bailey, Proc. Roy. Soc., London, A144, 521 (1934).

26. B.A. Frenz, J.H. Enemark and J.A. Ibers, Inorg. Chem., 8, 1288 (1969).

27. G.R. Davies, J.A.J. Jarvis, B.T. Kilbourn, R.H.B. Mais and P.G. Owston, J. Chem. Soc. (A), 1275 (1970).

28. R.P. White, J.A. McCleverty and L.F. Dahl, quoted in J. Amer. Chem. Soc., 91, 1653 (1969).

29. M. Colapietro, A. Domenicano, L. Scaramuzza, A. Vaciago and L. Zambonelli, J. Chem. Soc. Chem. Comm, 583 (1967).

30. A.I.M. Rae, J. Chem. Soc. Chem. Comm., 1245 (1967).

31. D.G. van Derveer, A.P. Gaughan, Jr; S.L.Soled and R. Eisenberg, Abstracts. Amer. Cryst. Assoc., 1, 190 (1973).

32. A.D. Walsh, J. Chem. Soc., 2266 (1953).

33. L. Malatesta, M. Angoletta and G. Caglio, Angew. Chem. Internat. Edn., 2, 739 (1963).

34. D. Guisto and G. Cova, Gaz. Chim. Ital., 101, 519 (1971).

35. C.A. Reed and W.R. Roper, J. Chem. Soc. Chem. Comm., 155 (1969); D.M.P. Mingos and J.A. Ibers, Inorg. Chem., 10, 1035 (1971).

36. D.J. Hodgson, N.C. Payne, J.A. McGinnety, R.G. Pearson and J.A. Ibers, J. Amer. Chem. Soc., 90, 4486 (1968): D.J. Hodgson and J.A. Ibers, Inorg. Chem., 7, 2345 (1968).

37. D.J. Hodgson and J.A. Ibers, Inorg. Chem., 8, 1282 (1969).

38. C. Pierpont, A. Pucci and R. Eisenberg, J. Amer. Chem. Soc., 93, 3050 (1971).

39. R.S. Berry, J. Chem. Phys. 32, 923 (1960).

40. J. Chatt and L.M. Venanzi, J. Chem. Soc., 4735 (1957).

41. N. Calderon, E.A. Ofstead and W.A. Judy, Angew. Chem. Internat. Edn., 15, 401 (1976).

42. E.L. Muetterties, Inorg. Chem., 14, 951 (1975).

43. C.P. Casey and T.J. Burkhardt, J. Amer. Chem. Soc., 95, 5833 (1973); C.P. Casey and T.J. Burkhardt, J. Amer. Chem. Soc., 96, 7808 (1974).

44. J. McGinnis, T.J. Katz and S. Hurwitz, J. Amer. Chem. Soc., 98, 605 (1976); T.J. Katz, J. McGinnis and C. Altus, J. Amer. Chem. Soc., 98, 606 (1976); C.P. Casey, H.E. Tuinstra and M.C. Saeman, J. Amer. Chem. Soc., 98, 608 (1976).

45. P. Diversi, G. Ingrosso and A. Lucherini, J. Chem. Soc., Chem. Comm., 52 (1977).

46. C.P. Brock, J.P. Collman, G. Dolcetti, P.H. Farnham, J.A. Ibers, J.E. Lester and C.A. Reed, Inorg. Chem., 12, 1304 (1973).

ABBREVIATIONS

The following is a list of the abbreviations used in this Thesis:

Me	-	methyl
Et	-	ethyl
Pr^i	-	*iso*-propyl
Bu^t	-	*tert*-butyl
Ph	-	phenyl
cp	-	cyclopentadienyl
Mecp	-	methylcyclopentadienyl
py	-	pyridine
dipy	-	dipyridyl
en	-	ethylene diamine
dppm	-	bis(diphenylphosphino)methane
dppe	-	1,2-bis(diphenylphosphino)ethane
thf	-	tetrahydrofuran
cod	-	cyclo-octa-1,5-diene

Abbreviations used in describing infra-red and p.m.r. spectral peaks:

Infra-red bands:

s - strong, vs - very strong, ms - medium strong
m - medium, br - broad, w - weak, sh - shoulder

P.m.r. peaks

s - singlet, d - doublet, t - triplet,
q - quadruplet, mt - multiplet.